Dissertation for the degree of doctor of philosophy

Structural Analysis of Tectonic Lozenges in Anisotropic Rocks:

Fied Analysis and Experimental Modelling

Carlos Ponce Escudero

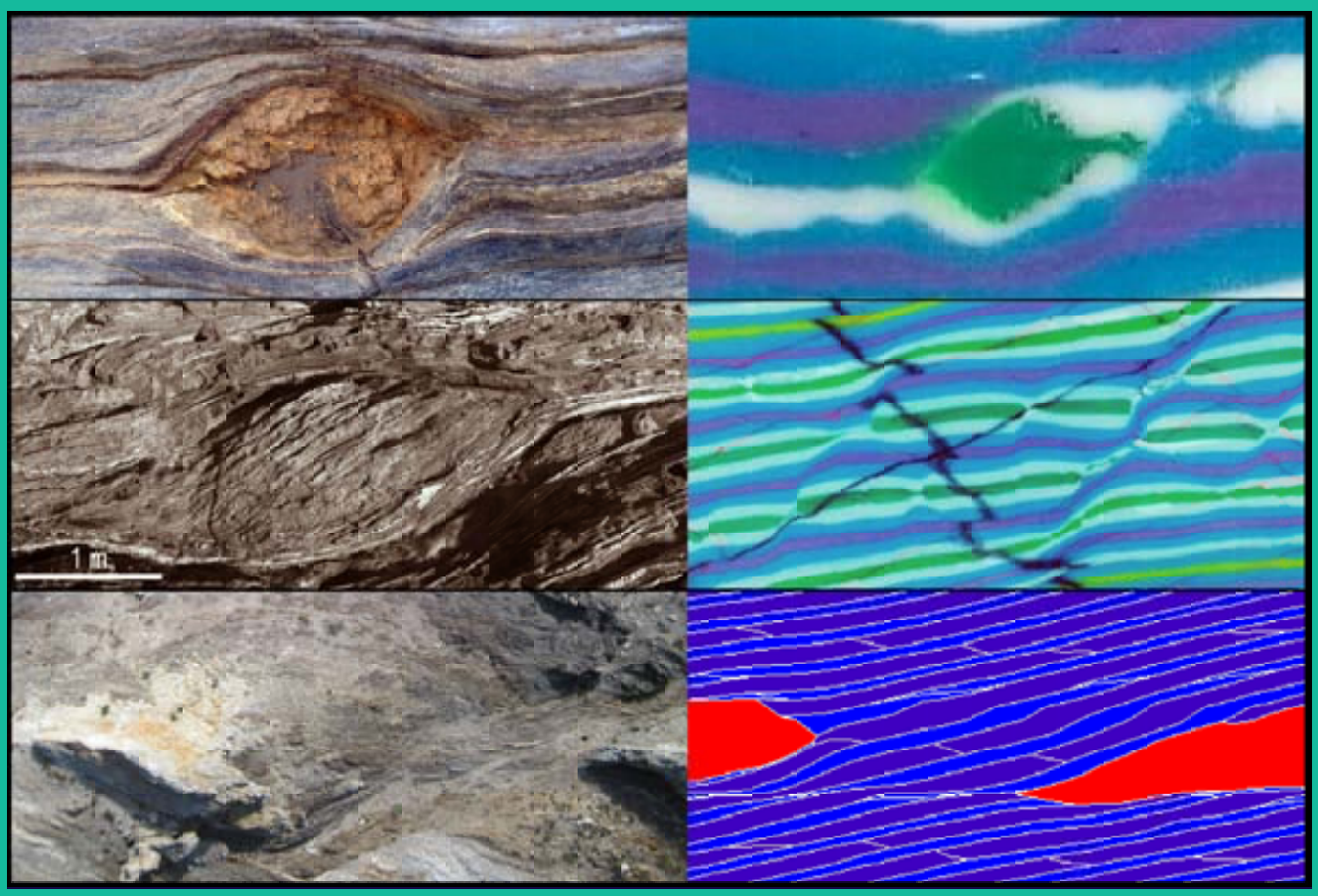

Chiefs:
Jordi Carreras
Elena Druguet

Universitat Autònoma de Barcelona

Barcelona, June 2014

Structural analysis of tectonic lozenges in anisotropic rocks:

field analysis and experimental modelling

Carlos Ponce Escudero

Chiefs:

Jordi Carreras Planells **Elena Druguet Tantiñà**

A dissertation submitted in
partial fulfillment of the requirements
for the degree of Doctor of Philosophy

Universitat Autònoma de Barcelona

Programa de Doctorat en Geologia
Gup de Modelització i Interpretació d'Estructures Tectòniques
Departament de Geologia
Universitat Autònoma de Barcelona

June of 2014

To the memory of my friend and father Lolo

AGRADECIMIENTOS

Quisiera reconocer el apoyo y la confianza recibidos por parte de los directores de este trabajo, Jordi Carreras y Elena Druguet. La formación científica que me han dado, la transmisión de conocimientos y las jornadas de campo compartidas es, además de un privilegio, algo que conservaré y de lo que les estoy muy agradecido. Su participación en este estudio les hace tan pártícipes como yo.

Los miembros y ex-miembros del Grupo de investigación (MIET) también han contribuido a este estudio con sus trabajos previos y ayudas durante este estudio. Especialmente es de reconocer la labor y contribución de Lina Marcela Castaño en la modelización analógia y Enrique Gómez-Rivas y Albert Griera en la modelización numérica. También agradezco la ayuda de los tutores de mis estancias en la Universidad de Tübingen y en la Universidad de Aberdeen, los profesores Paul D. Bons e Ian Alsop respectivamente.

Mis profesores de la Universidad de Granada, donde comencé mi formación en Geología allá por el año 2002 son también agradecidos, en especial Fernando Simancas, Antonio Azor y David Martínez-Poyatos pues fue con ellos con quienes me inicié en la investigación científica.

Alvar Pastor e Isaac Corral, amigos y compañeros de estos años de doctorado y de vida hicieron de este camino un viaje mucho más agradable.

Sin la referencia, el apoyo y la educación recibida de mi familia tampoco hubiera conseguido optar a este grado de Doctor. Es fácil llegar aquí habiendo crecido en una familia con una madre maestra y pedagoga, con un padre con tanta afición por el conocimiento y por su transmisión, y con un hermano tan sobresaliente en los estudios y ya doctorado. Gracias a ellos soy quien soy.

Todas aquellas personas cercanas a mí que de un modo u otro me apoyan y me quieren y que (por suerte) me es imposible de enumerar aquí, son igualmente agradecidas.

Por último, agradezco el apoyo financiero que vino del Ministerio de Ciencia e Innovación del Gobierno de España a través del subprograma de Formación de Personal Investigador. Las secretarias del Departament de Geologia Sílvia, Sara, Tere y Glòria, siempre tan eficientes y simpáticas, hicieron de la burocracia un trámite mucho más ameno.

PROLOGUE

One of the most ancient and wondered question made by human beings may be: "What do we do in here?" Although this question can have a metaphysical concern and analysis, it also has an empirical meaning, and that side of the question (inherent to human nature) has actually been the motivation for geologists: "Where we are?" "Why does the Earth exist?" "What is the Earth made of?" "Why are mountains, lakes or volcanoes there?" "What does yield earthquakes or volcanic eruptions and why do they take place?" This kind of questions, made by human curiosity, could lead some primitive people to observe the material those natural elements were made of and the processes controlling the changes on them. Just to find out any explanation. Perhaps using a rough method, if any, those people might be considered the first geologists, no matters the success of their "research".

It has been long time since then and now there is a huge international research community on geology that, by accumulating learning by the empirical and (later) the experimental methods through time, has driven itself to a more advanced knowledge in every step.

Although now there is a complex geological knowledge, the new research still comes from simple questions, although somewhat more specifics. This is the case of this Thesis since it was encouraged from one simple question: "what are these structures and why are they in there?" The structures are lozenges, and their settings are anastomosed networks of ductile shear zones. This is what this Thesis deals about: tectonic lozenges related to ductile shear zones. Such eye-catching structures appearing in the middle of anastomosing shear zone networks were the trigger for the research performed under this Thesis.

To do so, a previous deep view on shear zones is necessary to understand these structures. Once the geological frame is set, a detailed structural analysis is carried out on the geometry of the structure and the kinematics of the bounding shear zones defining the structure. By understanding the setting, the geometry and the kinematics, the origin of the structures and its geological implication are sought. The research has been focused on the metric scale although tectonic lozenges exist in all scales. It has been performed on different regions, although Cap de Creus shows the best outcrops.

This modest contribution aims to broaden the geological scientific knowledge by clarifying the origin and significance of ductile shear zone-related lozenges. However, since before this study only a few sentences in the literature were devoted to ductile lozenges, this work can be considered as an initial approach to these structures. Hopefully, it will contribute to develop a more advanced research on tectonic lozenges in the future.

ABSTRACT

Partitioning of ductile deformation in rocks produces low-strain domains wrapped around by shear zones. Such low-strain domains use to display a characteristic elongated, rhombus-like shape that usually stands out from the outcrop and that are named tectonic lozenges. The focus of this study is on the 2-D structure of tectonic lozenges developed during ductile shearing in rocks with a pre-existing mechanical anisotropy. They have been investigated through experimental modelling and mainly through field analysis in different locations and geological settings, among which Cap de Creus has proven to be the best area to investigate. Although lozenges exist at all scales (and they show self-similarity patterns), the studied structures are metric-sized lozenges. Thus, the fieldwork performed was detailed structural analysis up to the centimetric scale.

Lozenges are the less deformed domains (wall rock) bounded by comparatively more deformed domains (shear zones) and displaying an ellipsoidal shape. Consequently, there is no important internal deformation within them besides some mylonitization close to their rims, in the transition to the bounding shear zones. Since lozenges are defined by shear zones, they are strongly associated to them. In this sense, shear zone initiation, propagation and interaction have been also investigated in their relation to lozenges. The main part of this study is based on field analysis. It is combined to analogue and numerical modelling which have shown to support the field observations. Both the field and experimental research have shown that anastomosing shear zone networks in anisotropic rocks are appropriate settings for lozenge development since these networks are the result of shear zones interconnection and intersection and show characteristic romboidal morfology. Apart from Cap de Creus (Eastern Pyrenees), other reference field zones are the Laghetti area in Ticino (Swiss Alps), the Cabalón area in Cabo Ortegal (Galicia) and the Anti-Atlas of Morocco. The BCN-Stage at UAB has been used for the physical analogue experiments, and the platform *ELLE* for the numerical tests. The presence of strong anisotropy reveals to control the shear zone nucleation pattern, besides enhancing the anastomosing character of the network and therefore the presence of lozenges.

The geometry of the structure is analyzed and it is revealed not to have a straightforward relation to the vorticity of the deformation, but to depend on many other variables, such as the orientation of the rock anisotropy with regard to the kinematic axes and the interaction between shear zones. A typology on the internal geometry of lozenges in anisotropic rocks depending on the kinematics of the bounding shear zones is described. Some models for the formation of lozenges in anisotropic rocks are also proposed, and the evolution of lozenges with progressive strain is also analyzed. This study improves the knowledge on shear zone-related lozenges and clarifies the role and implication of lozenges in deformation.

RESUMEN

La partición de la deformación dúctil en rocas produce dominios de baja deformación envueltos por zonas de cizalla. Estos dominios de baja deformación suelen tener una morfología elongada romboidal, destacable a la escala del afloramiento y se denominan *lozenges*. El objetivo de este estudio es la estructura 2-D de *lozenges* tectónicos desarrollados durante cizallamiento dúctil de rocas con una anisotropía mecánica preexistente. Los *lozenges* se investigan en este trabajo mediante modelización experimental y principalmente a través del análisis de campo en diferentes lugares y ambientes geológicos, entre los que el Cap de Creus (Pirineos oriental) ha demostrado ser el mejor laboratorio para investigar. Aunque existen *lozenges* a todas las escalas (y muestran patrones de auto-similitud), las estructuras estudiadas son de dimensiones métricas. Por tanto, el trabajo de campo realizado se ha fundamentado en el análisis estructural detallado hasta la escala centimétrica.

Los *lozenges* son los dominios menos deformados (roca encajante) delimitados por dominios de alta deformación (zonas de cizalla) y que muestran una geometría elipsoidal. Por tanto, no hay deformación interna importante en su interior, a parte de algún grado de milonitización cerca de sus bordes y que es consecuencia de la transición hacia las zonas de cizalla envolventes. Los *lozenges* están fuertemente asociados a zonas de cizalla puesto que están definidos por estas. En este sentido, la iniciación, propagación e interacción entre zonas de cizalla en su relación con los *lozenges* han sido también objeto de investigación.

La parte principal de este estudio se basa en el análisis de campo. Éste es combinado con la modelización analógica y numérica, las cuales han corroborado positivamente las observaciones de campo. La investigación de campo y experimental han puesto de manifiesto que las redes anastomosadas de zonas de cizalla en rocas anisótropas son un escenario idóneo para el desarrollo de *lozenges* ya que estas redes son el resultado de la interconexión e intersección de zonas de cizallas y muestran una morfología típicamente romboidal. A parte de Cap de Creus, otras zonas de campo usadas como referencia en este trabajo son la zona de Laghetti en Ticino (Alpes suizos), el área de Cabalón en Cabo Ortegal (Galicia) y el Anti-Atlas de Marruecos. El aparato de deformación BCN-stage de la UAB se ha utilizado para los experimentos analógicos físicos, y la plataforma de simulación *ELLE* para los experimentos numéricos. La presencia de una fuerte anisotropía en las rocas demuestra que ejerce un control esencial sobre el patrón de nucleación de las zonas de cizallas, además de favorecer el carácter anastomosado de las redes miloníticas y por tanto de la formación de *lozenges*.

Se han analizado las estructuras desde el punto de vista geométrico, hecho que ha permitido confirmar la no existencia de una relación directa entre geometría y vorticidad de la deformación, pero sí la dependencia geométrica en otras variables, como la orientación de la anisotropía de la roca con respecto a los ejes cinemáticos y la interacción entre zonas de cizalla. Se describe una tipología de geometría interna de *lozenges* en rocas anisótropas en función de la cinemática de las zonas de cizalla envolventes. Se proponen modelos para la formación de *lozenges* en rocas anisótropas en función de la cinemática de las zonas de cizalla envolventes y se analiza su evolución con la deformación progresiva. Este estudio mejora el conocimiento sobre los *lozenges* relacionados con las zonas de cizalla y aclara su papel e implicación en la deformación cortical.

RESUM

La partició de la deformació dúctil en roques genera dominis de baixa deformació envoltats per zones de cisalla. Aquests dominis de baixa deformació que anomenem *lozenges* (literalment "pastilles"), acostumen a mostrar una morfologia elongada romboïdal destacada a escala d'aflorament. L'objectiu d'aquest estudi és l'estructura 2-D dels *lozenges* tectònics desenvolupats durant cisallament dúctil de roques amb una anisotropia mecànica preexistent. Els *lozenges* s'investiguen en aquest treball mitjançant la modelització experimental i principalment a través de l'anàlisi de camp en llocs geològica i geogràficament diversos, entre els quals el Cap de Creus ha demostrat ser el millor laboratori per investigar. Encara que els *lozenges* es desenvolupen a totes les escales (i mostren patrons d'auto-similitud), les estructures estudiades són de dimensions mètriques. Per tant, el treball de camp realitzat s'ha fonamentat en l'anàlisi estructural detallat fins a l'escala centimètrica.

Els *lozenges* representen dominis menys deformats (roca encaixant) delimitats per dominis de deformació elevada (zones de cisalla), i mostren una geometria 3-D el.lipsoidal. En conseqüència, no hi ha deformació interna important al seu interior, tret de cert grau de milonitització prop de les vores i que són un reflex de la transició cap a les zones de cisalla envoltants. Els *lozenges* es troben fortament associats a zones de cisalla, ja que són pròpiament definits per aquestes. En aquest sentit, la iniciació, propagació i interaccions entre zones de cisalla han constituït també objecte d'investigació d'aquesta Tesi.

La part principal d'aquest estudi es basa en anàlisis de camp, encara que de forma combinada amb la modelització analògica i numèrica, les quals han servit per corroborar positivament les observacions de camp. La recerca de camp i experimental ha posat de manifest que les xarxes anastomòtiques de zones de cisalla en roques anisòtropes són un escenari idoni pel desenvolupament de *lozenges*, ja que aquests, amb la seva morfologia típicament romboïdal, sorgeixen com a resultat de les interconnexions i interseccions de zones de cisalla. A part del Cap de Creus (Pirineu oriental), altres zones de camp emprades com a referència en aquest treball són la zona de Laghetti al Ticino (Alps suïssos), l'àrea de Cabalón al Cap Ortegal (Galícia) i el l'Anti-Atles del Marroc. L'aparell de deformació BCN-Stage de la UAB s'ha utilitzat per als experiments analògics físics, i la plataforma de simulació *ELLE* per a les proves numèriques.La presència d'una forta anisotropia a les roques exerceix un control essencial sobre el patró de nucleació de zones de cisalla, a més d'afavorir el caràcter anastomòtic de les xarxes milonítiques i per tant la formació de *lozenges*.

S'han analitzat les estructures des del punt de vista geomètric, fet que ha permès confirmar la no existència d'una relació directa entre geometria i vorticitat de la deformació, però si la dependència geomètrica en altres variables, com ara l'orientació de la anisotropia en relació als eixos cinemàtics i la interacció entre zones de cisalla. Es descriu una tipologia de geometries internes de *lozenges* en roques anisòtropes en funció de la cinemàtica de les zones de cisalla envoltants. Així mateix, es proposen alguns models per a la formació de *lozenges* en roques anisòtropes, i també s'analitza la seva evolució amb la deformació progressiva. Aquest estudi millora el coneixement sobre els *lozenges* relacionats amb zones de cisalla i aclareix el seu paper i implicació en la deformació cortical.

TABLE OF CONTENTS

1. INTRODUCTION, OBJECTIVES AND REFERENCE AREAS 1

1.1. State of the art 6
1.1. 1. Individual shear zones 6
1.1.2. Anastomosed networks of shear zones and related lozenges 14
1.2. Aims and methodology 20
1.3. Setting of the reference areas 27
1.3.1 Northern Cap de Creus shear belt (NE Spain) 27
1.3.2 Roses shear zones (Cap de Creus, NE Spain) 29
1.3.3. Laghetti area (Maggia Nappe, Helvetic Alps) 30
1.3.4. Cabalón area (Cabo Ortegal, NW Spain) 32
1.3.5. Zenaga and Kerdous inliers (Anti-Atlas, Morocco) 35

2. SHEAR ZONES AND LOZENGES: FIELD STUDIES 37

2.1. Geometry of individual shear zones 39
2.2. Initiation and development of shear zones 42
2.3. Interaction of shear zones 48
2.4. Shear zone networks 54

3. MODELLING LOZENGES IN ANISOTROPIC ROCKS 59

3.1 Modelling and representation of lozenges 66
3.1.1. Numerical modelling 66
3.1.2. Analogue modelling 71
3.1.3. Variations in the foliation angle through lozenges: Graphical representation 83
3.2. Lozenge typologies 88
3.2.1. Kinematic typology 88
3.2.2. Propagation typology 92

4. DISCUSSION AND CONCLUSIONS 103

4.1. Geometry of lozenges 105
4.2. Lozenge evolution and internal deformation 107

4.3 Lozenges modelling 110
4.3.1. Numerical modelling 110
4.3.2. Analogue modelling 111
4.3.3. Graphical representation 113
4.4. Disposition of internal foliation in lozenges and lozenge development in foliated rocks. Relations to the kinematics of the bounding shear zones 114
4.5. Role of anisotropy in foliated lozenges 116
4.6. Final remaks 124

5. REFERENCES 129

Appendix I. Numerical modeling videos DVD
Appendix II. Analogue modeling videos DVD

Chapter 1

INTRODUCTION, OBJECTIVES AND REFERENCE AREAS

1. INTRODUCTION, OBJECTIVES AND REFERENCE AREAS

"Nature gave us the knowledge seeds, not the knowledge itself"

Lucio Anneo Séneca (ca. 4 BC–AD 65), Roman Stoic Philosopher

The Earth is a geodynamic planet thanks to its internal heat: it causes the material to flow from hotter to cooler places and subsequently induces motion inside the globe. This leads to changes in material distribution in that part where the motion is taking place (Moores and Twiss, 1995). In Geology, such changes in material distribution are called deformation (roughly defined) and are the main focus for the research of structural geologists: the structures resulting from the constant internal dynamism of the Earth.

Deformation is a common and easy phenomenon in rocks if viewed at geological scales of time, space and energy (Ramberg, 1981). In fact, is not hard to find an outcrop with any deformation feature at any scale after its formation. Even if there were no tectonic stresses acting directly on the rock after its formation, it will undergo some changes due to the heat and the lithostatic load (gravity) in the case of burial, or will fracture by decompression in the way to the surface in the case of exhumation, or will experience the effects of hydrothermal fluids if stay in the same place. Indeed, if there is a stress system acting on the rock, no matter how hard the rock body is, if the stresses exceed the rock strength it will be deformed and any deformation structure will be recorded in it.

However, deformation in rocks is not only a stress vs. strain matter since the strength (the ability degree of the rock to strain under a certain stress) of the rock portion depends strongly on the conditions under which the deforming forces take places. The rheological evolution of earth materials is, in large part, controlled by changes in the physical and chemical state of the system. These physical and chemical factors are mainly the temperature, the hydrostatic and lithostatic pressures, the strain rate and the pore fluid pressure. They affect the ability of the rock to resist the stresses and therefore, the complex interaction between them determines whether a given system of forces acting on and within a given rock composition will or will not cause deformation and if will, whether the deformation is discontinuous (brittle deformation), continuous (ductile deformation) or contain evidences of both brittle and ductile deformation mechanisms (brittle-ductile deformation) (Hobbs et al., 1976).

This contribution deals with ductile deformation, whose main characteristic, besides being continuous, is that it generally takes place in the middle to lower crust and slow in time, over long periods of time by many small increments of deformation (Ramsay and Hubert, 1987). In ductile conditions, when the system of forces exceeds the rock strength, a permanent, no reversible deformation is achieved in the rock (unless the rock has elastic behaviour, something that only occur in the very first steps of deformation). When this occurs, the rock equilibrium state (initial state) is altered and then, a series of small increments of changes (progressive deformation) takes place gradually in the rock portion until a new equilibrium state (final state) is reached. During progressive ductile deformation, conditions are not statics all along the time and the space. At each point, temperature and confining pressure will change with time as

well as the crystalline atomic structure. Subsequently, the mechanical behaviour of any point will be changing with time along the progressive deformation, leading to hardening (if the stress needs to increase with time to cause the same strain) or softening (if less stress is needed with time to cause the same strain) (Passchier and Trouw, 2005). Therefore, the environmental conditions not only control the deformation type but also the deformation path. This means that many deformation paths exist for the same rock portion under the same stress state depending on the environmental conditions.

What we find in outcrops are the final states of one or more progressive deformations. Final states are the frozen record of the deformation evolution, like the end of a tale. And the geologist has to reconstruct the entire tale of deformation through tools as structural analysis techniques, geological evidences and previous knowledge. Although being the last stage in the Nature, final states are the starting point for structural geologists to infer the conditions and the evolution under the analyzing portion of rock was changed from the initial state. Unfortunattely, they are not the best information providers as they do not record the whole deformation evolution because every deformation increment is overprinted by the next one. Moreover, the final state could be reached departing from a number of different possible initial states and through a number of different paths (Davis and Reynolds, 1996). Of course, direct observation of the entire progressive deformation is a better information source; however this is not possible in nature since ductile deformation in rocks takes place at geological time scale and under confining conditions. Modelling can help us on this, although limited to the assumption of controlling factors and somehow simplistic apporaches.

Therefore, fieldwork becomes the most essential method of working to investigate and reconstruct the other states (and therefore the evolution) of structures in deformed rocks. Moreover, when researching on deformation structures -whether the aim of the research is the evolution of the structure or not-, it is extremely important to do a complete detailed structural analysis of the geometry of the final state found in the field, since it is there where we find all the primary information. If some information provided from the primary source is taking wrong, then all work performed upon that information is also wrong.

In the last years, the traditional field-based-*modus operandi* seems to have been forgotten by many researchers to the detriment of the new technologies. Of course, new technologies have provided a new powerful tool for researching, widening the research goals and becoming the main precursor of the huge advances on Geology in the last decades. However, modeling techniques should be applied upon consistent field information. If new techniques are applied to wrong field data or observations on a subject, no matter how convenient or sophisticated the new results are as they do not correspond exactly to the matter in question. Because of the novelty of modeling techniques or maybe the urgency for covering this new research field, fieldwork has somehow been left to a second level.

This Thesis stands for the importance of fieldwork. Actually, most of the research data were obtained through fieldwork. Numerical and analogue modelling is also used. However, it is not the main part of this contribution but it is aimed to check or strenghten field-based hypothesis. Once the primary information has been analyzed and interpreted, and the features of the structure is known better, further and more accurate modelling could be developed over it. Consequently, the modelling in this study should be considered as probationary.

The starting point of this Thesis is a final state: a geological structure related to ductile shear zones networks isolating lozenge-shaped bodies called tectonic lozenges or simply lozenges (Fig.1.1).

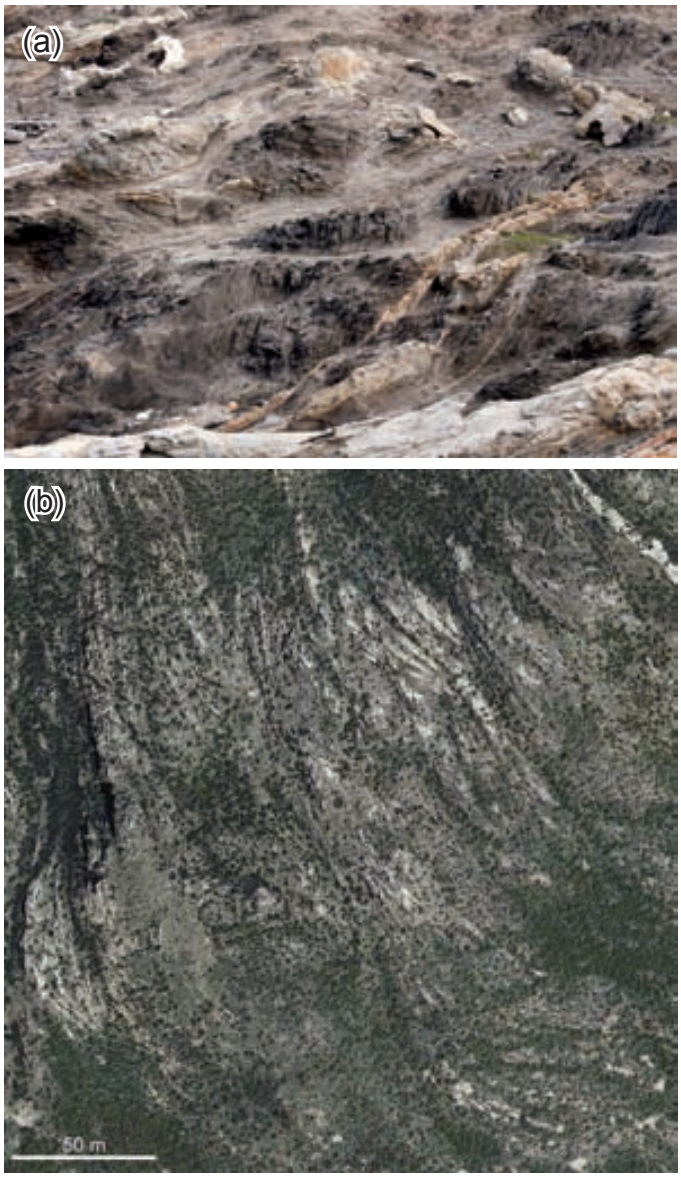

Fig. 1.1. Anastomosed network of shear zones isolating lozenge-shaped bodies of non-mylonitic schists. In (a) preserved foliation is a sub-vertivcal S_{1-2} foliation, Cala Culleró, Cap de Creus (width of view 20 m). In (b) aerial photograph showing a NNW-SSE anastomosed network of shear zones, Puig Alt Petit - Cap de Creus (Photo ICC).

No research was focused on lozenges prior to this dissertation and hence not too much has been written about them until now. If anything, they were mentioned, roughly described, showed in pictures and sometimes accompanied by a little interpretation concerning the geological environment where they were found and their possible implications in the deformation context; but never were the subject of any research. The research topic was other, and because tectonic lozenges are impressive, beautiful structures, some attention was paid on them, but they were never researched in detail. The lack of interest might be because lozenges are in the shadow of "real" deformation structures (shear zones). In fact, there is no important internal deformation inside them besides some mylonitization close to their rims, in the transition to the bounding shear zones. However, they can provide information about shear sense (taking care), shear zone interconnection or the chronology of different shear zone sets as it will be shown later.

It is important to finely set the structural framework of tectonic lozenges in order to understand their meaning and possible implications in Structural Geology. As they do not record strain related to the stresses they were formed by, it seems logic to concern on that structures recording such strain: ductile shear zones. Therefore, the introduction is not only concerning lozenges but also the shear zones they are related to and the arrays in which they are displayed.

1.1. STATE OF THE ART

Most lozenge-shaped bodies or lozenges appear in networks of anastomosed shear zones. Prior to introducing the geometry and development of tectonic lozenges, it is timely to introduce some concepts related to strain localization and the development of shear zones.

1.1.1. Individual shear zones

Shear zones have been extensively researched as they are a very common structure in the lithosphere. Consequently, their basic characteristics are well-known by geologists (e.g. Ramsay and Graham, 1970; Ramsay, 1980, Ramsay and Huber, 1983; Ramsay and Huber, 1987) and they can be easily found in any Structural Geology book. However, there are some issues concerning shear zones that are either, not well know by geologists or controversial, and these are the points in which this subchapter will focus.

The fascinating 2011 *Penrose Conference* hold in Cadaqués (Cap de Creus, Spain) under the name "*Deformation localization in rocks: new advances*" and organized by the same research group where this study has been performed, was a great chance for improving advanced knowledge on shear zones as well as it revealed some of those interesting and debatable aspects (Druguet et al., 2013). Consequently, this subchapter centres on these more advanced and currently debating aspects, although some common characteristics are also commented.

A shear zone is a tabular, planar or curvi-planar zone of intensely localized deformation relative to the surrounding rocks (e.g. Ramsay, and Graham, 1970; Ramsay, 1980; Simpson and Schimd, 1983; Lamouroux et al., 1994; Baird and Huddleston, 2007). They are a consequence of heterogeneous strain: the deformation concentrates on a relatively narrow planar zone when two relatively non-deformed rock blocks move relative to each other. The relatively rigid rock blocks are the shear zone walls and the space in between them is the shear zone. The amount of wall deformation depends on the degree of strain localization. Since the movement between the walls use to be dominantly lateral displacement with respect the each other, shear zones are localized deformation zone with a dominant component of non-coaxial strain (e.g. Passchier and Trouw, 2005); although many shear zones can depart slightly from heterogeneous simple shear (e.g. Carreras, 1997). In any case, shear zones achieve a high strain amount, a large number of deformation structures and their study is fundamental for investigating heterogeneous deformation and localization processes. This is why geologists are fascinated by these structures since decades ago, because they can be used as natural laboratories for intense deformation structures.

Shear zones are the result of the complex interaction between factors as P-T conditions and fluid pressure, and some parameters as partitioning of different deformation types (simple shear, pure shear, volume change), deformation distribution (i.e., degree of strain localization) and rheology (strain softening or strain hardening; Vitale and Mazzoli, 2010). They form in a wide variety of tectonic regimes, under many different conditions and from a variety of preexisting rock types, leading to a huge variety of shear zones. They have been classically divided by the dominant deformation mechanism that operated within the shear zone when it was formed (brittle or ductile shear zones). The operating mechanism depends on many intrinsic factors of the affected rock (e.g. mineralogy or grain size) and on the physical and

chemical conditions that prevailed during deformation (e.g. temperature or fluid pressure).

For the same rock type, brittle deformation mechanisms tend to dominate when temperatures and pressures are relatively low, strain rate is faster and fluid pressure is higher. When a shear zone is formed under brittle conditions it becomes a fracture and the contact between shear zone and shear zone walls is a geometrical discontinuity. This is called fault, the displacement is taken up by a network of closely spaced fractures (fault zone) and any passive marker will be cut when crossing the brittle shear zone. On the other hand, ductile deformation mechanisms become dominant when temperatures and pressures are higher, strain rate is much slower, and fluid pressure is lower. They are called ductile shear zones or simply shear zones and any passive marker will show continuity when crossing the ductile shear zone. Moreover, most ductile shear zones form under metamorphic conditions, so the deformation produces recrystallization inside the shear zone, forming a new foliation and sometimes a lineation, folds or other plastically deformed structures. All that give rise to a characteristic mylonitic foliation within ductile shear zones.

Nevertheless, this classical differentiation of brittle and ductile shear zones is not a division but a spectrum of which two end-members are faults and ductile shear zones. Shear zones formed under conditions that are intermediate between strictly brittle and strictly ductile deformation are called brittle-ductile shear zones. Although brittle and ductile shear zones are much more common than brittle-ductile, strictly brittle and strictly ductile are not very common neither. Brittle dominant and ductile dominant are much more frequent to find. This is because in polymineralic rocks some phases of the rock may deform by intra-crystalline plastic flow (as quartz or mica) and others may be deformed by micro-fracturing (as garnet, piroxene, hornblend or feldspar) (Grocott, 1977; Sibson 1977; Tullis et al., 1982; Ord and Hobbs, 1989). Moreover, the flow in polymineralic rocks can be homogeneous at the macroscopic scale, but inhomogeneous at the microscopic scale thus this division can be unclear. Consequently, when it is said ductile or brittle shear zone, it should be understood dominantly ductile or brittle shear zone at the scale of observation.

It has been classically assumed the temperature is the major control on the transition between dominantly brittle and ductile behaviour thus in a normal geothermal gradient this should occurs at 10-15 km depth. However, this should not be taken as a golden rule as the boundary from dominantly brittle to dominantly ductile behaviour depends on many other factors such as bulk strain rate, mineralogy, grain size, fluid pressure, relative orientation of the stress field and pre-existing micro-fabrics, metamorphic weakening reaction, LPO softening... (e.g. Ord and Hobbs, 1989). Although among all of them temperature and rock type are the major controls, the mix of all them will set the transition depth. Thus, it is possible to find ductile shear zones at shallow levels of the crust and brittle shear zones at deep levels, as for example rock units composed of halite, gypsum or clay will develop ductile shear zones under conditions in which quartz and feldspar will develop brittle shear zones (Alsop et al., 2000; Kim et al., 2010).

Besides, as it has been recently discussed in the Geotectonics listing mail, the term ductile shear zone is somewhat misleading since it is easy to deduce wrongly plasticity as the deformation mechanism implied in the formation of the shear zone (i.e, intracrystalline plastic deformation by dislocation gliding and climbing (Passchier and Trouw, 2005)). Although most ductile shear zones are formed by plasticity, some shear zones

formed by frictional flow can show continuity of a passive marker. This is the case, for example, of the ductile shear zones in the metasediments of the Mistaken Point Formation of SE Newfoundland, where maximum temperatures were around 200 to 250 °C and the "ductile shear" is accommodated by dissolution-precipitation (pressure solution); or some very low temperature ductile shear zones in olistostromal units (such as in the Apennines and Sicily; Pini, 1999) or in sandstones (e.g. Navajo Sandstone, in Utah) where the deformation was accommodated by granular flow while the sediments were unlithified (Fossen et al., 2011). Moreover, ductile deformation comprise elastic, plastic and viscous deformation, of which only the last two are permanent. Therefore, the term ductile shear zone should be taken as a field or geometric term, rather than a deformation mechanism-related one. All these misunderstandings should entail a revision of the nomenclature in which the main division might be done geometrically instead of the "dominant deformation mechanism". The new nomenclature could call shear zones (macroscopically) continuos and discontinuous instead of ductile and brittle shear zones.

Ductile (continuous) shear zones are generally formed in conditions in which the rocks are at T and P so high that they response to imposed stresses by ductile flow rather than by faulting and brittle fracture. For the vast majority of rocks this conditions take places at the middle to lower crust and in the astenosphere. In fact, ductile shear zones are the common way of rocks to accommodate deformation in mid and lower crustal levels and even in the mantle (Müntener and Hermann, 1996; Van der Wal and Vissers, 1996). Accordingly, ductile shear zones are generally developed in crystalline rocks formed at the middle crust and deeper such as schists, amphibolites, granulites, granites, pegmatites and plutonic intrusions, as well as in mafic and ultramafic rocks. They are associated to major tectonic events and occur in any tectonic regime and in any strain type. A nice paradox is shear zones are geometrically continuous structures with gradual strain gradients at the outcrop scale; however, at the tectonic scale, they can be considered as discontinuities in the displacement field, i.e., as slip surfaces.

When the deformational context is that of metamorphism and deep crustal levels, like in this study, to use shear zone is enough to understand predominantly ductile (or continuous) shearing. From now onwards, discussions about shear zones will be done on ductile shear zones (unless stated otherwise) and it will be used the term shear zone instead of ductile shear zone.

Shear zones are much longer and wider than thick. Ramsay and Huber (1987) established a 1:5 width/length ratio as the minimun ratio for a deformation structure to be considered as a shear zone. They exist at all scales. The largest are hundreds of kilometres long and tens kilometres thick, with displacement of tens to hundreds kilometres (e.g. Shear zones at Seridó, NE Brasil; Corsini et al, 1996). The smallest shear zones observable in outcrop are several centimetres long and about one milimeter thick and may have displacement of centimetric order. There is a width/displacement relation in shear zones that depends on the degree of strain localization and in his turn on ductility. For shear zones developed across granitoids under greenschist facies conditions the ratio is aproximately 1:10 (Carreras et al., 2004) but for higher temperature shear zones ratios of about 1:1 have been found (Mitra, 1979).

Shear zones are characterized by a transversal gradient of strain amount, increasing from border to the centre. As there are two borders, the strain gradient is a bidirectional gradient with a symmetry plane: the longitudinal section of the shear zone. While shear zones margins are subparallel,

the thickness is constant and the strain amount is also constant along the shear zone. When the margins converge at any point of their lengths, the shear zone thins and an increase of the strain amount can be observed. Alternatively, if margins are divergent, the shear zone widens and the strain amount gradient decreases. In fact, this is how shear zones use to end, by widening and spreading out the displacement and the strain in a wider zone until the displacement is gradually dropped to zero (horsetail splays) (Simpson, 1983).

Most common way of showing shear zones in books is that of a 2-D core high strain zone in a homogeneous isotropic host rock with straight and parallel margins and a symmetric fabric distribution within the shear zone (Ramsay and Huber, 1987; Davis and Reynolds, 1996; Ragan, 2009; Fossen, 2010). However in the field, shear zones depart from such description as they are much more complex as ascribed in theory. Complexities arise because the rock is heterogeneous (e.g. in composition and therefore in rheology) or anisotropic, because the flow may be no steady and no stable (Iacopini, 2011), there may be shear intersections with simultaneously active branching zones (zipper shear zones; Passchier, 2011), strain compatibility problems or lateral changes or different displacement profiles along different cross sections of the zone (Ramsay, 1980).

Actually, the most interesting contributions in the 2011 Penrose Conference at Cadaqués were those regarding the complexities on shear zones. These complexities were not only regarding geometric but also kinematic issues. For example, Iacopini pointed out that the most of the kinematic models for shear zones proposed in the literature assume steady and stable flow properties while in the field, most shear zones show heterogeneous and partitioned strain around boundary walls, specially in multilayered or anisotropic rocks. Of course, these models are done because of the sake of mathematical simplicity, but again it is evidenced that real structures are much more complex than they are treated in theory.

A more complex level appears when adding the third dimension. The 3-D configuration of a single shear zone in the field is difficult to decipher because of the lack of proper outcrops. We can not infer how shear zones are in 3-D from 2-D sections since any of the complexities said above could change either, their geometry or their kinematic characteristics in the next parallel cross-section. This makes highly tentative any 3-D representation from 2-D outcrops.

How shear zones nucleate is not really well know yet. However, for the evolution of shear zones the situation seems to be more clear. Fossen gathers the most widely accepted models in his book (Fig. 1.2; Fossen, 2010). These are:

- Type I or thickening shear zones. These are shear zones undergoing strain hardening in the central part while they are developing. The deformation migrates from the central part to the adjacent zones. Consequently the shear zone thickens and the central part records the first stages of the progressive deformation while the margins record the last stages.

- Type II or narrowing shear zones. Shear zones experiencing strain softening in their central part. They start with a certain thickness, but with progressive deformation strain migrates from the margins to localize in the central part. The margins become inactive leaving a narrower part of the shear zone as active. Contrary to Type I, Type II shear zones record the first stages of progressive deformation at the margins and the last stages at the core.

- Type III. Shear zones keep a fixed thickness along the progressive deformation, without broadening or narrowing. The entire shear zone

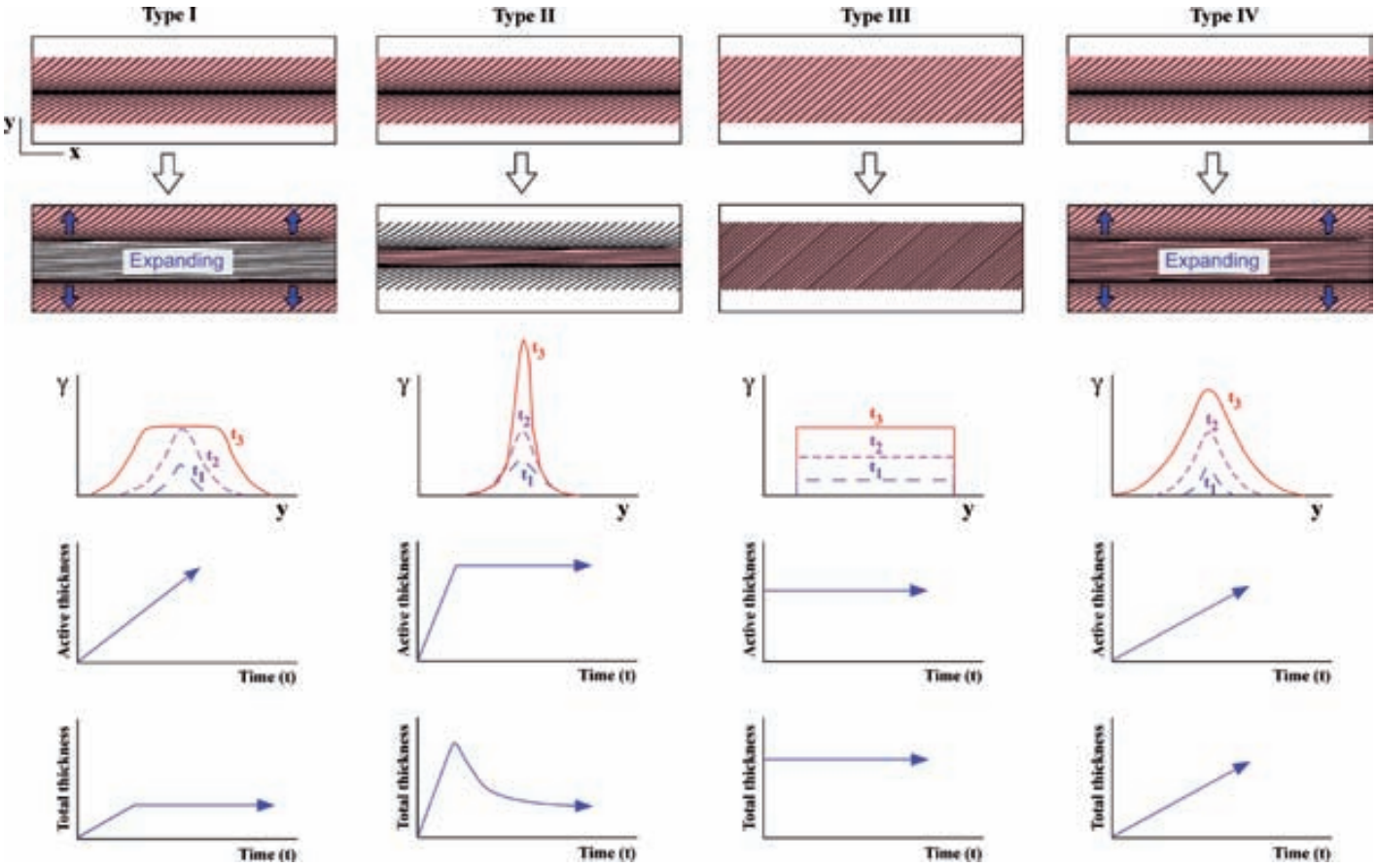

Fig. 1.2. Most accepted models of the growth of ductile shear zones (after Foosen, 2010). For every model, displayed in columns, it is shown: (i) drawing of a shear zone at an initial state of deformation, (ii) drawing of the same shear zone after some progressive deformation steps (red background denotes active shearing zone and no color denotes inactive shearing zone); (iii) graphic with the thickness of the shear zone and the shear strain in it for any three different time lapses, (iv) graphic of the active shear thickness through time and (v) the total shear thickness through time.

reflect the last deformation stage.

- Type IV. The strain keeps active at the central part of the shear zones and it spreads out to the adjacent zones. This is: shear zones grow in width and the strain decreases from the core to the margins. Thus, both the margins and the central part record the last deformation stage although the core experiences the entire deformation history and the margins does not.

The type of shear zone evolution would depend on the boundary conditions and the intrinsic properties of the affected rock during deformation. However, it seems type II and IV are the most common (and supported) models.

Some authors (Bowden, 1970; Poirier, 1980; White et al., 1980; Williams and Dixon, 1982; Gilotti and Kumpulainen, 1986; Hobbs et al., 1990) argued for progressive deformation leading to strain softening due to dynamic recrystallisation and the associated grain size reduction, the development of a LPO or the synkynematic minerals transformation (e.g, feldspar to muscovite and phyllonitization) as the reason for shear zone localization. Increasing deformation would cause weakening and increasing localization towards the central line of the shear zone, leading to a more spatially heterogeneous deformation with time (Mancktelow and Pennacchioni, 2005).

Other authors (Simpson, 1985, 1986; Segall and Simpson, 1986; Tremblay and Malo, 1991; Tourigny and Tremblay, 1997; Guermani and Pennacchioni, 1998; Pennacchioni, 2005) proposed a different model for localization of shear

zones in granitoids. In this model the localization is related to brittle precursors. The presence of pre-existing planes of weakening induce a strong localization and partitioning of the bulk deformation (Pennacchioni, 2005). Therefore, deformation would localize in pre-existing brittle structures (joints, veins, fractures…), first stages of displacements would take place through frictional flow and then it would change to plastic flow promoted by mineral transformation, what is induced by fluid flux through the precursor fracture. In this model, shear zones nucleate in brittle fractures and then develop by broadening during increasing deformation and subsequent ductile reactivation. Consequently, shear zones inherit the initial spatial distribution of brittle precursors (Mancktelow and Pennacchioni, 2005). This would explain parallel sets of shear zones (inheriting cooling extension joints) and is the microscale analogy to intracontinental range belts where stresses are transmitted from the plate boundary -where the collision takes place- towards the interior of the plate where there are previous discontinuities in the crust. Stresses are transferred among a rigid plate until they find a discontinuity where they concentrate (e.g. Atlas range belt in Marocco; Beuchamp et al., 1999).

There is currently an open debate concerning the nucleation of ductile shear zones. Some authors argue for brittle initiation and later evolution to ductile behaviour (e.g. Pennacchioni 2005; Mancketlow and Pennacchioni 2005; Fusseis, 2006). Fusseis (2006) claims for a brittle initiation of ductile shear zones in the Brittle-Ductile Transition, which evolve to ductile shear zones by broadening through crystal-plastic deformation and thanks to host rock weakening processes when the shear reach a critical point. On the same way, Mancketlow and Pennacchioni (2005) and Pennacchioni (2005) propose a similar model but they restrict it to granitoids.

Besides these authors considering preexisting instabilities as a major control on strain nucleation, others consider deformation nucleation as a matter of rheology-dependent parameters (e.g. Casey, 1980; Poirier, 1980; Jessell et al., 2005) like strain rate and/or strain softening (Mancktelow, 2002; Mancktelow, 2006) or strain softening associated to shear heating (Brun and Cobbold, 1980; Kaus and Podladchikov, 2006). Some authors have shown there is not need of a preexisting discontinuity for shear zone nucleation. For example, Paterson (2007) elaborated an analysis based on the linear perturbation analysis of Fressengeas and Molinari (1987) to assess the likelihood of localization in mono-mineralic rocks given either constant-stress or constant-strain-rate conditions. He showed that deformation subjected to constant -stress conditions always localizes, while deformation in materials subjected to constant-strain-rate conditions only localizes if preexisting heterogeneities produce large spatial variations in strength. Recently, the laboratory experiments performed by Hansen et al. (2011) testing this hypothesis, support the interpretation that deformation at constant stress will easily localize even if there are not any pre-existing structural heterogeneities. When regarding a polymineralic rock, the effect of localization without a brittle precursor becomes much easier. Instead of fractures, joints, veins or dykes, shear zones may nucleate from structures governed by buckling instabilities (Cobbold et al., 1976; Cosgrove, 1976; Carreras, 1997). This would be the case for shear zones nucleated from deformed foliated anisotropic rocks or at the weakest point or along the weakest layer in the rock, such as micaceous layers (e.g. Goodwin et al., 2011; Montesi, 2011), structural weakness zones like axial planes or inflection points in tight folds (e.g. Carreras, 1997), old shear zones (as they are easely reactivated; e.g. Passchier, 1990), zones with an LPO in which the slip planes are in a position relative to the local strain axis enhancing dislocation gliding and climbing (e.g. Ponce et al., 2012), partially molten zones (Rosenberg, 2004), rheological interfaces (Nabelek et al., 2001; Robert et al., 2013), etc.

With all those evidences, it seems obvious that these two nucleation models do not invalidate to each other. There are multiple combinations between all factors involved in boundary conditions, the initial internal properties of rock and their evolution through time. The brittle nucleation would fit better in an isotropic, homogeneous rock under strain-constant deformation and around the brittle-ductile transition and fluid-deficient conditions setting; and the ductile nucleation would fit better for stress-constant deformation, anisotropic and heterogeneous rocks in the ductile field with fluid-rich conditions. Also, as pointed above, some of the minerals composing the rock may deform brittle and others ductile, so the dominant deformation mechanism involved in the nucleation is a function of the combination of multiple factors.

Shear zone nucleation mechanism aside, what is a fact is shear zones are a consequence of strain localization. The localization range of strain is: no localization (homogenous strain, foliation), incipient localization (broad ductile shear zones), more localization (narrow ductile and ductile-brittle shear zones) and maximum localization (fractures). Hence, shear zones form because the deformation concentrates into a narrow plane rather than disperse throughout the entire rock mass. If once the deformation processes are operating on such narrow plane, the continuing deformation find easier to deform already deformed rocks than broaden to the wall rocks, this is called strain softening. And the processes by the rock weakens relative to the rocks outside the zone are called softening processes (White et al., 1980). There are many softening processes like softening metamorphic reactions, grain size reduction, textural softening or LPO, fluid-related softening or layers in polymineralic rocks with one of the mineral phases being either very weak or having a strongly non-Newtonian rheology like mica in the crust or serpentine in the mantle (Montesi, 2011). Shear zones undergoing strain softening would give rise to Type II and III shear zones.

All these crystalline processes of softening are temperature-controlled: observation of natural shear zones reveals that the efficiency of strain localization is inversely proportional to temperature: extreme in the brittle crust, still strong at the brittle ductile transition and considerably less efficient under “normal” middle crustal conditions (Vauchez, 2011). However, localization is not only an effect of decreasing temperatures, but also of increasing anisotropy (Cosgrove, 1976; Carreras, 1997).

Competing against strain softening is strain hardening. This latter is the responsible for shear zones to widens. Without its effect, strain only would concentrate on a very narrow plane and never would widens, what is a common phenomena in shear zones (e.g. Weijermars, 1987; Fusseis, 2006). For a shear zone to widen, there must be more difficult to deform the mineral rocks in the shear zone than in the surrounding rocks (wall rock). Strain hardening happens because the progressive strain has induced a high density of lattice defects (dislocations) in the minerals that different slip systems can act simultaneously. When this happens, migrating dislocations can become entangled impeding further dislocation glide. When a tangle is formed inside a grain, newly formed dislocations will pile up behind the blocked one, making the crystal harder to deform (Passchier and Trouw, 2005). Shear zones undergoing strain hardening would give rise to Type I and IV shear zones. The balance between strain softening and strain hardening is mainly controlled by temperature and strain rate, and this will determine if a shear zone widens or keep in the same narrow plane.

In the central parts of intracrystalline plastic deformed shear zones, the strain can be so high

that preexisting textures and structures are rotated and flattened. Accordingly, the rock becomes strongly foliated (and usually lineated) and is called mylonite. The fabric elements in mylonites use to show monoclinic symmetry (e.g. Hanmer and Passchier, 1991) and the mylonitic foliation induces a new mechanical anisotropy in the rock (e.g. Carreras, 2010). Mylonites are interpreted as exhumed, fossil ductile shear zone rocks and although they refer to a rock, it is a structural term and do not give any information about mineral rock composition.

As well as shear zones, mylonites can occur in any rock type and have been described from submillimetric scale to zones of several km wide (particularly in Precambrian shield areas and eroded collisional orogens) (Bak et al., 1975; Hanmer, 1988). In general, they are more fine-grained than their host rock and the contact of a mylonite zone and unaffected wall rock tends to be a gradual fabric transition.

The fabrics and mineral assemblages of mylonites reflect P-T conditions, flow type, movement sense and deformation history in the shear zone. As such, mylonites are an important source of geological information: shear sense, strain amount, vorticity number, pressure and temperature conditions, chemical and physical influence of fluids, etc… may be inferred from mylonites.

For example, the gamma value can be easily calculated through the angle between the mylonitic foliation and the shear zone margins (θ). For simple shears this initial angle is 45° and then, with progressive deformation θ decreases towards parallelism with the shear zone margin. This is because foliation initiates parallel to the instantaneous stretching axes (ISA_1) and rotates towards the fabric attractor (Passchier, 1997). For plane strain and no volume loss, this foliation represents the orientation of the XY-plane of the strain ellipsoid. The γ value of the simple shear at any point can be easily calculate through the θ value by this formula:

$$\theta' = 0.5 \tan^{-1} (2/\gamma)$$

Where θ' is the angle between the foliation and the shear zone at any point and γ is the value of the simple shear. This formula is only applicable for previously undeformed isotropic rocks and for sections perpendicular to the shear plane and parallel to the shear direction. This relationship is not applicable for anisotropic rocks as the initial angle γ does not start at 45° as it may be deflected by the previous anisotropy. As it will be shown in this Thesis, the previous layering or foliation has a major control on the arrangment of shear zones in previous anisotropic rocks.

Either in isotropic or anisotropic rocks, mylonites contain a rich variety of deformation structures such as foliations, lineations, shear bands, cleavages, folds, boudins, porphyroclasts, mica fishes… Tectonic lozenges, however, do not use to appear in mylonites but are wrapped by mylonitic foliation as they are shear zones-related structures.

1.1.2. Anastomosed networks of shear zones and related lozenges

Ductile shear zones can occur as relatively isolated single structures or as networks. Networks may occur in one set of subparallel shears, in which individual shears have changing directions and link to the others in an anastomosing pattern (e.g. Carreras, 1997; Carreras, 2001), may occur in two different orientated sets, crosscutting and displacing one another and linking together in an anastomosing network (e.g. Scheuber and Andriessen, 1990; Marquer et al., 1996; Holzer et al., 1998) or even in more than two sets giving rise to a more complex anastomosing and crosscutting pattern (e.g. Martínez et al., 1996; Garofalo et al., 2002; Brum da Silveira et al., 2009).

Shear zone networks use to develop anastomosed patterns. This is a well-established fact and well-illustrated in the literature by abundant examples (Arbaret et al., 2000; Bell, 1981; Bhattacharyya and Czeck, 2008; Burg et al., 1996; Carreras, 2001; Carreras et al., 2010; Choukroune and Gapais, 1983; Corsini et al., 1996; Czeck and Hudleston, 2003; Czeck and Hudleston, 2003; Hudleston, 1999; Mitra, 1979; Mitra, 1998; Ramsay and Allison, 1979; Ramsay and Graham, 1970). The anastomosing character of shear zone networks may appear in a wide variety of rocks, and does develop no matter the mechanical properties of pre-existing rocks (i.e., isotropy/anisotropy, homogeneity/heterogeneity, rheology…). Differences between anastomosed patterns developed across previously foliated (i.e. anisotropic) and those developed in low anisotropic or isotropic rocks arise from two main circumstances: (i) the role of anisotropy in the shear instabilities nucleation pattern and (ii) the structures developed in each individual shear considering that shearing of a pre-existing foliation causes additional instabilities at shear zone margins. A brief analysis of the role of each factor on the final geometry will be first introduced.

(i) No matter the bulk vorticity of the flow, the role of anisotropy is a crucial point in the initial pattern of instabilities arising from deformation of anisotropic materials (Williams and Price, 1990; Gomez-Rivas, 2008; Ponce et al., 2013).

(ii) Individual shear zones across foliated rocks cause complex relationships between geometry and kinematics (Carreras et al., 2012; Carreras, 2013). The marginal deflection might give apparent displacements that contradict the real shear sense. Moreover, the fact that the pre-existing foliation when sheared does not behave passively causes the development of buckling instabilities (e.g. folds) at the initial stages or marginal domains of the shear zones that in his turn become sheared as the result of shearing progression. This causes that shear related structures especially across pre-existing foliated rocks are far more complicated than ideal models. The fact that shear zones form anastomosed networks introduces an additional complexity of structural patterns.

In the common case of a shear zone network build up by two different oriented sets the pattern can be from regular conjugate pairs (Lamouroux et al., 1991), to sets with an octahedral arrangement (Mitra, 1979) to more complicated and less regular patterns (Bhattacharyya and Hudleston, 2001). In any of these patterns the network can have different degrees of anastomosing, the sets can be synthetic or antithetic, each set can have the same shear population or one set can be dominant over the other, one set can be dominant in displacement or width, sets can be coeval or asynchronous… In a coaxial deformation history same population of each set is expected, while in a non-coaxial deformation one dominant set over other

is expected (e.g. Choukroune and Gapais, 1987).

In networks of incipient shear zones the angle formed by individual shears can be close to 90º, while in highly evolved shear zone networks this angle increases up to the extreme that shear zones with opposite shear sense may trend nearly parallel (Carreras et al., 2010). It is generally assumed that anastomosed systems with coexisting nearly parallel shear zones with opposite shear sense is not an original feature but achieved as result of progressive deformation.

The networking of shear zones is of primary importance as it controls both strain accumulation (Hudleston, 1999) and deformation mechanisms (Fusseis et al., 2006). The strain distribution in and around the intersection point of shear zones is much more complex than in individual shear zones showing a much more complex kinematic history and structures (Carreras et al., 2010). Anastomosing exists at all scales as well as the shear zones, from grain size (phyllosilicates surrounding quartz or feldspars) to continental scale (crustal shear zones, e.g. the Patos-Seridó shear zone system in NE Brasil).

When shear zones are interconnected, displacement along them during progressive deformation may be altered by their interconnecting shear zones, with alternating active strands and a much more complex kinematics in individual shears (Carreras et al., 2010). Moreover, the relative spatial distribution of individual shears is also changing during progressive deformation.

Mancktelow (2002) shows that conjugate sets of shears zones initiate at approximate right angles and then rotate with increasing strain towards the instantaneous stretching axis. In the extensive field work of Carreras et al. (2010) it is showed that such a rotation is not achieved merely by passive rotation of the shears because strain compatibility requires the internal deformation of the bounded lenses of rock, the internal deformation of existing shears and the initiation of new ones. This would explain the anastomosing character of shear zone networks since the linkage of different generation of shears with different degrees of rotation gives rise to shear zone networks interconnected through different linkage angles. Bell (1981) addressed the anastomosing character of shear zones to variations in strain intensity. Rock bodies are highly heterogeneous on all scales, so an equally range of heterogeneity in strain intensity is expected. He argues that if the foliation orientation has to remain planar in average whatever the strain intensity is, that zones where the strain rate is higher must anastomosed back and forth to remain planar on average. A similar mechanism for anastomosing pattern development explanation is suggested in Bell and Hammond (1984). They proposed that the foliation anastomoses in the early stages of mylonitization and argued that ductility contrasts in the primary rock is the reason for anastomosing. Rheology differences in a homogeneous rock, at least on the grain scale, would cause the flow rate to be unequal at different parallel planes. Therefore, since not all planes parallel to the XY plane of the deformation ellipsoid have the same strain rate, the developed mylonitic foliation would anastomosed. Hudleston (1999) suggests that a component of differential stretching in X or Y leads to strain compatibility problems at the boundaries of the shear zones if deformation remains continuous. The only way to accommodate such stretching while maintaining compatibility strain is by linking individual shear zones in an anastomosing fashion. Iacopini (2011) points out that some works on microstructural deformation mechanisms suggest the anastomosing character, as well as the partitioning nature of the strain around boundary walls, are ascribed to intrinsically non steady deformation rate in some minerals which are controlled by the non linear viscous phase (Handy, 1994; Trepmann and Stockert, 2003) or simply to initial heterogeneities that

trigger non steady behaviour during strain localization (Jiang and Williams, 1999). Treagus (1988) also notes that in the case of multilayer or anisotropic rocks the networks of shear zones may have an anastomosing character because of flow refraction due to alternating rheologies.

Shear zone networks also anastomose in YZ in a similar fashion to XZ (e.g. Bell 1981). This makes the 3-D analysis a complex matter, moreover when outcrops -as well as for individual shear zones- do not provide large 3-D views.

A coaxial history can preserve symmetric patterns during progressive deformation and result in symmetric conjugate shear zones (Choukrane and Gapais, 1983; Gapais et al, 1987). In contrast, experiments (Hoeppener et al., 1969; Tchalenko 1970; Mandl et al., 1977; Logan et al., 1981), numerical models (Priour, 1985) and field examples (Berthé et al., 1979; Platt and Vissers, 1980; Carreras, 2001) all show that non-coaxial deformation histories result in asymmetric shear zone patterns with predominance of one set of shear zones over the other set.

In all cases, anastomosing networks reveal a high strain partitioning with a 3-D strain heterogeneity and they show a strain distribution with high deformation domains (shear zones) bounding undeformed or less deformed domains (Ramsay and Graham, 1970; Mitra, 1979; Mitra, 1998; Ramsay and Allison, 1979; Bell, 1981; Choukroune and Gapais, 1983; Gapais et al., 1987; Burg et al., 1996; Corsini et al., 1996; Hudleston, 1999; Arbaret et al., 2000; Carreras, 2001; Czeck and Hudleston, 2003; Czeck and Hudleston, 2004; Bhattacharyya and Czeck, 2008). When the less deformed domain has an ellipsoidal shape it is called lozenge (e.g. Ramsay, 1980; Carreras et al., 2005). In fact, anastomosing networks of shear zones are more likely to develop lozenges since these latters are associated to curvilinear shear zones and their interconnections.

Partitioning of ductile deformation in rocks produces low-strain domains wrapped around by shear zones (Fig.1.1; Simpson, 1983; Reston, 1989 ; Carreras, 2001). Such low-strain domains use to display a characteristic elongated, rhombus-like shape that usually stands out from the outcrop (Figs. 1.3; 3.9). These main features (shape, shear zone-wrapped and outstanding arrangement) make of those low-domains a geological structure entity, which has been named “tectonic lozenge” or simply referring to its geometry. Therefore, lozenges are not truly deformation structures hosting deformation localization but the space between deformation localization bands when these are arranged in a particular way enclosing non-equiangular parallelograms of material, i.e., lozenges.

The term lozenge has been used since the late 1800s to refer to the shape of diverse geological features. In structural geology, the term lozenge refers to elongate rock masses bounded by fractures or shear zones (Graham, 1980; Simpson, 1983; Naruk, 1986; Woodcock and Fisher, 1986; Carreras, 2001; McClay and Bonora, 2001; Weinberg et al., 2004; Carreras et al., 2005; Fusseis et al., 2006; Baldwin et al., 2007; Kuiper et al., 2011). Lozenge is also used as an adjective to describe the geometry of some structures, such as the also called mica-fishes (e.g. ten Grotenhuis et al., 2003; Marques et al., 2007; Duguet et al., 2007), veins deformed into lozenge shapes (Maeder et al., 2009), lozenge-shaped crenulation domains (Aerden et al., 2010); slivers (Tilke, 1986), boudins (Aitchison et al., 1988), horst blocks (Boud, 1987) and strike-slip stepovers (McClay and Bonora, 2001). In fault tectonics, the term “horse” is more widely used with equal meaning (Butler, 1982).

It is proposed a definition of “tectonic lozenge” as a scale-independent, 2-D generally elongate

structure of rock (or mineral) bounded by relatively more deformed rocks (or minerals) when the long axis of the structure forms an acute angle (generally <30°) to the mean trend of the main bounding shear zones.

As defined here, and used in most of the existing works, the term lozenge is a 2-D feature. The

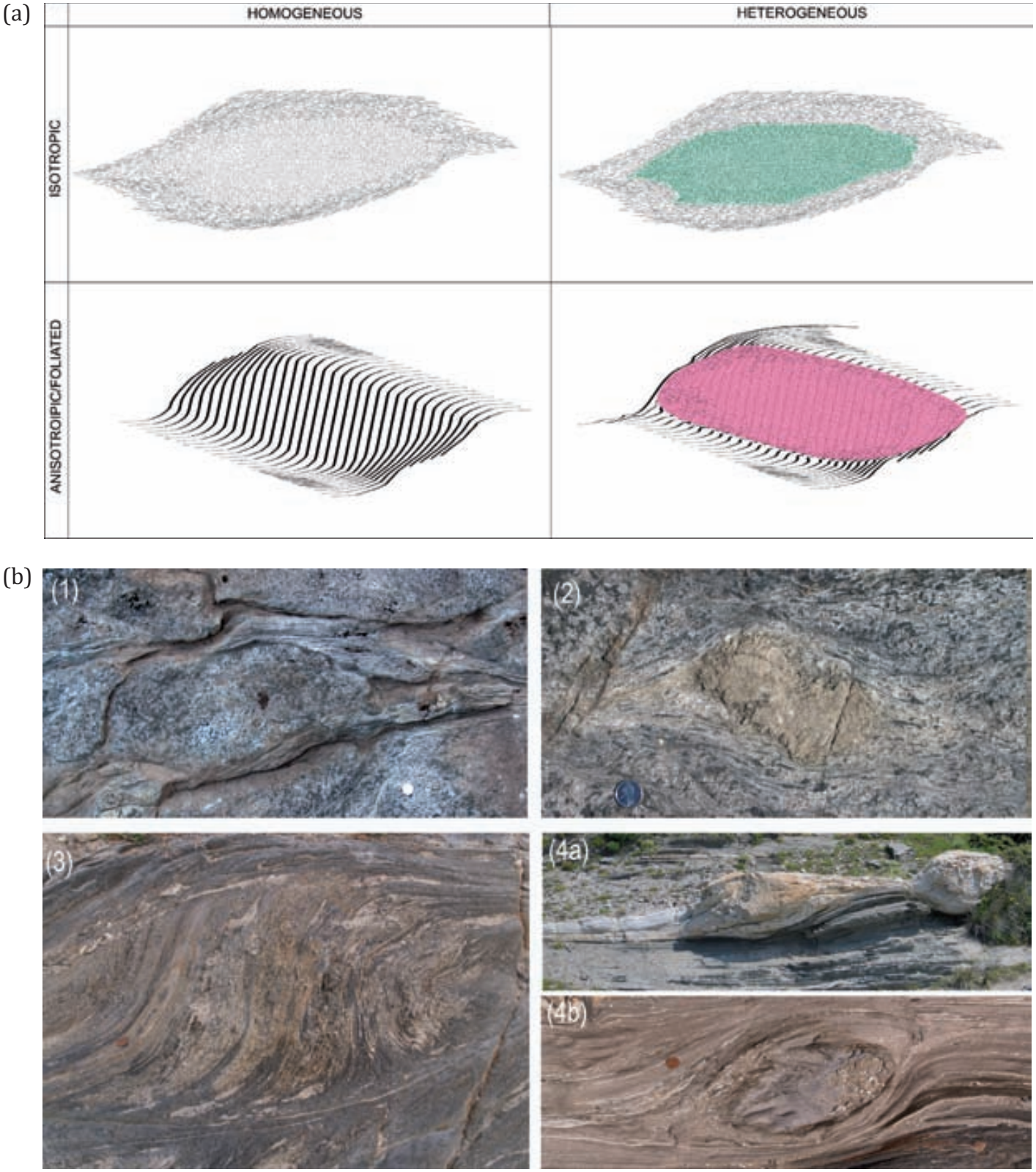

Fig. 1.3. Typology of lozenges depending on rock properties. (a) Fourfold types based on rheological homogeneity / heterogeneity and on mechanical isotropy / anisotropy. (b) Examples of types shown in (a): type(1), lozenge forming in an heterogeneously deformed gabbro (Rainy Lake, Ontario); type (2), lozenge developed in anorthosite bearing gabbros where anorthosites are deformed into a lozenge shape (Rainy Lake, Ontario); type (3), milipede-shaped lozenge developed in an homogeneous foliated schists (Cap de Creus); type (4), two examples of lozenges in heterogeneous and foliated rocks, (a) pegmatites and (b) calc-silicate rocks appear as competent material developping sigma-shaped lozenges (Cap de Creus).

few studies that mention an equivalent 3-D geometry either give the lozenges a 3-D fusiform shape (Bell, 1981; Carreras 2001; Chardon et al., 2009) or interpret them as as having a prismatic shape with a lensoid or rhomboidal transversal section (e.g. Choukroune and Gapais, 1983; Hudleston, 1999).

An overview will be given to the 2-D geometry of tectonic lozenges in Figure 4.1. The parameters considered are the aspect ratio (ratio of lozenge length to width normal to the long axis), the symmetry and the straight vs. curvilinear character of the lozenge sides. Four main types are depicted: rhombic, lensoidal, rhomboidal and sigmoidal lozenges. A wider variety of lozenge shapes can be found, among which lensoidal and sigmoidal lozenges are the most characteristic. It is important to notice that this typology is only geometrical and thus not suitable to establish connections to formation mechanisms, neither from a mechanical nor a kinematical sense.

The fact that lozenges are scale-independent structures is well documented in the literature, with reports at the regional scale (Tilke, 1986; Bickford et al.,1994; Corsini et al., 1996; Czeck and Hudleston, 2003; Chardon et al., 2009; Delcaillau et al., 2011), at the meso-scale (Bell and Rubenach, 1980; Bell, 1981; Simpson, 1983; Choukroune and Gapais, 1983; Carreras et al., 2005; Fusseis et al., 2006), at the micro-scale (e.g. Ross and Wilks, 1996; Vollbrecht et al., 2006; Bédard et al., 2009) and at multi-scale (Carreras, 2001; Schrank et al., 2008).

Tectonic lozenges have been classically regarded from two different perspectives or approaches:

(1) Lozenges in rheologically heterogeneous rocks that are generated by rheological/lithological contrasts, where the lozenge is formed by a relatively competent material surrounded by a more deformed incompetent material (Figs. 1.3(2), (4a) and (4b); Cobbold, 1983; Bell and Rubenach, 1980; Passchier and Trouw, 1996; Treagus and Lan, 2000; Czeck et al., 2009; Jessell et al., 2009; Fagereng, 2011). The more competent material adopts a lozenge shape after deformation because strain partitioning amongst the phases leads to strain localization at the boundaries (Treagus and Sokoutis, 1992; Handy ,1994) . It causes stretching of the rims and this may result in lozenge shape and in a more strain concentration at the edge of the structure. This is a phenomena of ductile deformation and therefore heterogeneous lozenges only arise in ductile flow as the shapes achieved by deformation in brittle flow are due to cataclasis and there is not plastic deformation of grains rising up lozenge shapes. This extensively documented type of lozenges is therefore exclusive of lithologically heterogeneous rocks. This is the case, for instance, of many lozenges of sheared pegmatite in less competent mylonitic schists from the field area in the Northern Cap de Creus. However, they are not the object of the present investigation since they are ascribed to rheological contrast instead of kinematics and shear zone networks.

(2) Lozenges which rheological properties are similars to that of the surrounding at the lozenge scale. They are formed by the interconnection of curved or straight, but non-parallel, sets of shear fractures or ductile shear zones (Figs. 1.3(1) and (3)). In this case the deformation localizes to produce sets of brittle or ductile shear zones that isolate less deformed domains forming lozenges. They have been studied and modelled by mostly considering the simplest scenarios of heterogeneous brittle to ductile deformation of homogeneous isotropic materials, and several mechanisms have been suggested for their development. The most common consists in the confluence of pairs of conjugate shears (Choukroune and Gapais, 1983; Gapais et al., 1987; Lamouroux et al., 1991; Hud-

leston, 1999; Mancktelow, 2002; Mahan and Williams, 2005; Pennacchioni and Mancktelow, 2007; Schwarz and Kilfitt, 2008; Aerden et al., 2010). Lozenges can also develop in deformation zones by intersection of different fractures of the Riedel shear zone system, as R- and R'-shears (e.g. Davis et al., 1999; Ahlgren, 2001; Carreras et al., 2010), R- and P-shears (e.g. Swanson, 2005, 2006) or R-, P-, and Y-shears (Tchalenko, 1970). They can also form by the linkage of pairs of sub-parallel stepped propagating shear fractures through their curving tips (Pollard and Aydin, 1984; Walsh et al, 1999; Pennacchioni, 2005; Mann, 2007; Tentler and Amcoff, 2010). In all situations tectonic lozenges of either contractional or extensional geometry may form. However, as stated by Woodcock and Fisher (1986), these different modes may operate simultaneously and/or can be indistinguishable from the observed final geometries. This is often the case in ductile shear zone networks. In this sense, Simpson et al. (1982) and Simpson (1983) related lozenges to a general anastomosing arrangement. Bell (1981) and Choukroune and Gapais (1983) point to strain heterogeneities that make shear zones vary strongly in direction and link isolating lozenges.

All these "simplest" cases referred above illustrate the complex interplay between several factors controlling the geometries of the generated lozenges, such as the initial geometry, orientation and relative proportion of different sets of bounding shears, the propagation mechanisms and the ability of the rock to internally deform. But the situation becomes even more complex when layered and/or foliated rocks are considered. There is abundant literature on the progressive development of lozenges and duplexes in stratified rock sequences under different tectonic regimes (e.g. Boyer & Elliott 1982; Childs et al., 1996; Walsh et al., 1999; McClay and Bonora, 2001; Nicol et al., 2002), with particular attention being payed to the effect of layering on fault morphology (Swanson, 1990; Peacock and Sanderson, 1992). Deeper in the crust, shear zones are typically developed in crystalline rocks, such as plutonic intrusions, gneisses, but also in mid to high-grade schists and migmatites (Carreras, 2001). In this last case where the rocks are previously foliated ± layered, the arrangement of shear zones and their related lozenges is thought to be mainly controlled by the orientation of the previous foliation relative to the deformation/kinematic framework. The presence of previous anisotropies can strongly influence the orientation, propagation and interconnection of shears (Donath, 1961; Cobbold et al., 1971; Williams and Price, 1990; Carreras et al., 2000; Carreras, 2001; Fusseis et al., 2006; Gomez-Rivas and Griera, 2012). However, the development of this type of lozenges in foliated rocks is at present less understood than all other types.

1.2 AIMS AND METHODOLOGY

The aim of this dissertation is to improve the knowledge on shear zone-related lozenges and to clarify their significance in Structural Geology by means of establishing a clear typology and setting the structural framework of each type.

Shear zone-related lozenges have been a topic of consideration in the structural geology literature since the 1980's (Bell and Rubenach, 1980; Bell 1981, Simpson, 1983; Choukroune and Gapais, 1983; Hudleston, 1999; Carreras, 2001; Fusseis et al., 2006; Culshaw et al., 2011). These studies focus on various aspects of lozenges and some have attempted to infer strain and kinematic (e.g. Hanmer, 1986; Gapais et al., 1987; Lacassin, 1988; Fernández, 1993) or mechanical (e.g. Gerbi et al., 2010) attributes from their geometry. However, all these studies are not specifically focused on tectonic lozenges, but either on shear zone geometry, strain compatibility at shear zone networks, or a regional study of an area where lozenges appear. Therefore, all references to lozenges are shallows and even tentative, although various mechanisms for their development or their kinematic significance have been suggested. They have been simply geometrically described or related to the anastomosing character of shear zone networks (Choukroune and Gapais, 1983), related to the strain ellipsoid (Fernández, 1993), to the strain path (for both, coaxial (Bell, 1981) and non-coaxial strain (Gapais et al., 1987; Huddleston 1999; Fusseis, 2006)), to strain compatibility maintenance (Huddleston 1999; Bhattacharyya and Huddleston, 2001) to kinematic sense (Fusseis, 2006), or explained as ductile duplexes in strike-slip shear zones (Woodcock and Fischer, 1986; Corsini et al, 1996). However, there are many lozenge types (Fig. 1.3), and every type has different implications to deformation. Therefore, prior to seek into their significance and value for Structural Geology, a clear and concise classification in tectonic lozenges is indispensable for understanding this structure. Once lozenges are properly structurally differentiated, the implications of each type on deformation is analyzed. For such a purpose, detailed structural analysis has been performed upon these structures together with some modelling to understand them better (Fig. 1.4). In such a context, the main objectives are:

1) To set better the structural framework of tectonic lozenges.

2) To establish a tectonic lozenge classification.

3) To analyze their geometry and define their main geometric characteristics.

4) To relate their geometry to kinematics and Wk.

5) To assess their kinematic value, specially as shear sense indicators.

6) To unravel development models.

7) To seek their implications in deformation and their possible application on Structural Geology.

The procedure followed in this dissertation to attain these objectives has been to apply the three main aims of Structural Geology upon lozenges (Davis and Reynolds, 1996). These main aims are:

1) Describing the geometry of rock bodies.

2) Analyzing the kinematics (and dynamics) of such geometries.

3) Developing models that explain the occurrence of the structures.

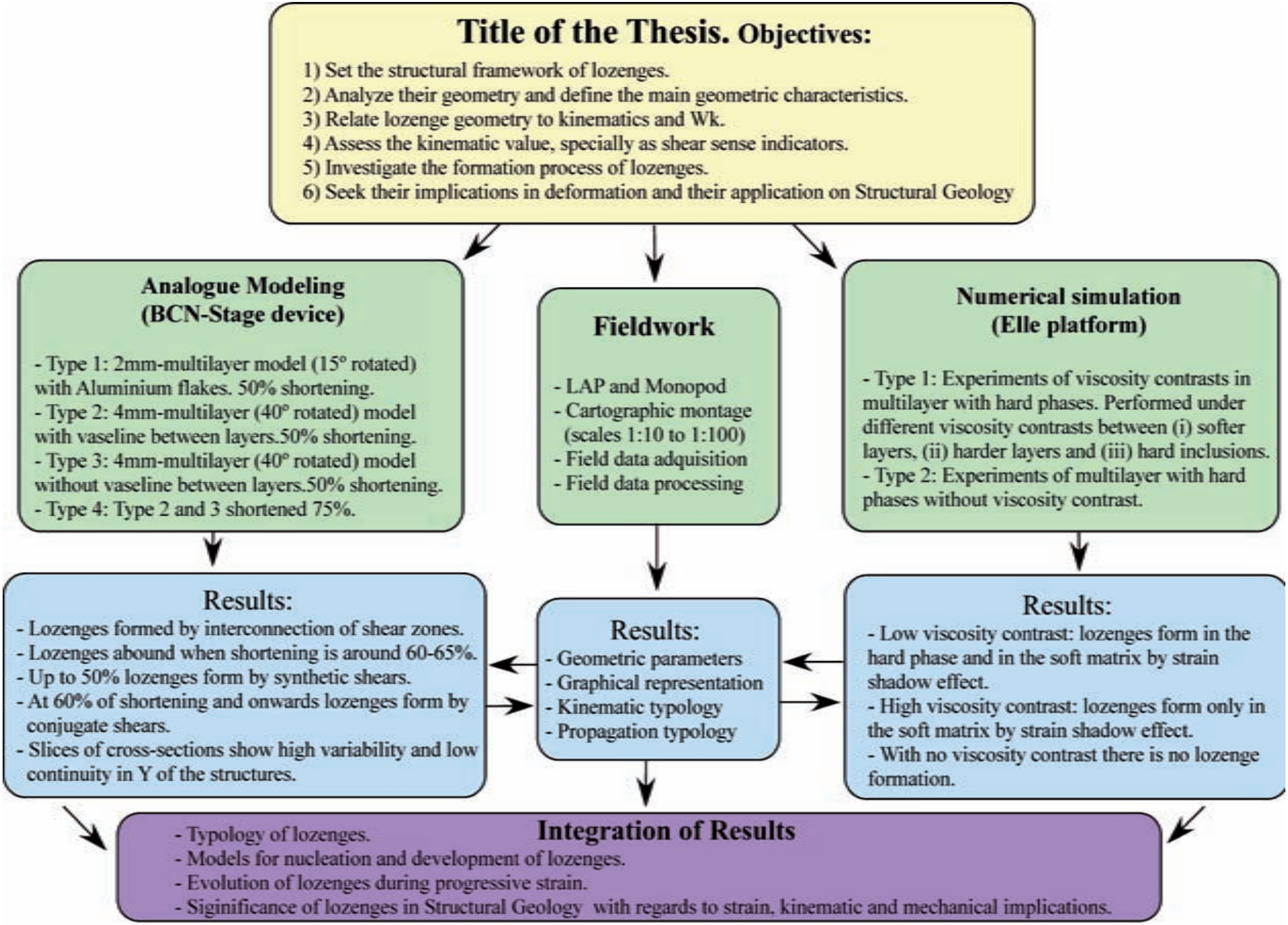
Title of the Thesis. Objectives:
1) Set the structural framework of lozenges.
2) Analyze their geometry and define the main geometric characteristics.
3) Relate lozenge geometry to kinematics and Wk.
4) Assess the kinematic value, specially as shear sense indicators.
5) Investigate the formation process of lozenges.
6) Seek their implications in deformation and their application on Structural Geology
Analogue Modeling (BCN-Stage device)
- Type 1: 2mm-multilayer model (15° rotated) with Aluminium flakes. 50% shortening.
- Type 2: 4mm-multilayer (40° rotated) model with vaseline between layers.50% shortening.
- Type 3: 4mm-multilayer (40° rotated) model without vaseline between layers.50% shortening.
- Type 4: Type 2 and 3 shortened 75%.
Fieldwork
- LAP and Monopod
- Cartographic montage (scales 1:10 to 1:100)
- Field data adquisition
- Field data processing
Numerical simulation (Elle platform)
- Type 1: Experiments of viscosity contrasts in multilayer with hard phases. Performed under different viscosity contrasts between (i) softer layers, (ii) harder layers and (iii) hard inclusions.
- Type 2: Experiments of multilayer with hard phases without viscosity contrast.
Results:
- Lozenges formed by interconnection of shear zones.
- Lozenges abound when shortening is around 60-65%.
- Up to 50% lozenges form by synthetic shears.
- At 60% of shortening and onwards lozenges form by conjugate shears.
- Slices of cross-sections show high variability and low continuity in Y of the structures.
Results:
- Geometric parameters
- Graphical representation
- Kinematic typology
- Propagation typology
Results:
- Low viscosity contrast: lozenges form in the hard phase and in the soft matrix by strain shadow effect.
- High viscosity contrast: lozenges form only in the soft matrix by strain shadow effect.
- With no viscosity contrast there is no lozenge formation.
Integration of Results
- Typology of lozenges.
- Models for nucleation and development of lozenges.
- Evolution of lozenges during progressive strain.
- Siginificance of lozenges in Structural Geology with regards to strain, kinematic and mechanical implications.

Following this, after a geometrical description, the kinematics aspects are analyzed and then some development models are proposed to unravel those objectives listed above. Finally, some conclusions regarding the lozenge relevance in deformation are made upon those results.

To reach such objectives two complementary approaches have been carried out: the structural analysis of field observations and data from the structures (fieldwork) and the performance of experimental methods upon those observations and data (experimental work). Figure 1.4 shows a sketch of the methodology performed in this Thesis. However, as it has been already pointed out, both approaches have not the same relevance in the achievement of the objectives of this Thesis, since the fieldwork is considered much more important for being the primary source of information and concerning the current state of the art in tectonic lozenges.

FIELD METHODOLOGY AND CARTOGRAPHY

As the studied structures are metric-sized lozenges, the fieldwork performed upon them was detailed structural analysis up to the centimetric scale. Fieldwork was done in different stages:

The already existing maps of the studied areas were not detailed enough to work metric structures in detail, so the first stage of the research was to create a proper cartographic information for the objectives by downing scales up to 1:10. Therefore, the scale range of the cartographic work was from 1:10 to 1:100. To do so, pictures were taken with a reflex digital camera of high resolution (14.7 Megapixels). All pictures were taken with the optical axis perpendicular to the pictured surface. For avoiding lens distortion in pictures and get a better resolution for the cartographic base, sets of contiguosu, overlapping pictures were taken for each interested area. They were systematically taken along different parallel lines at regular intervals and with an approximate overlapping of 30% for the later montage. Some of the outcrops were cleaned prior to the picture acquisition. Little rock blocks upon the outcrop were easily removed by hands, and a brush was used to remove the gravel and sand covering the outcrop surface.

For vertical outcrops there was no need for any special technique or help of any device when taking the pictures: they were simply taken by the photographer, moving his location and placing the camera in the right angle to point the lens camera axis to the normal to the outcrop surface (Fig. 1.5a). However, for horizontal outcrops different techniques were used according to the different size of the research subject: for individual (metric) lozenges a monopod was enough to cover the entire area (generally less than a dozen of square meters) with a few pictures. The monopod allows to locate the camera at a vertical distance between two and three meters, the camera lens was set perpendicular to the outcrop plane with the help of a bubble level and it was triggered with a remote control; for the studied horizontal reference areas (up to hectometric areas) other different technique was used. The need of locating the camera at a higher vertical distance becomes the monopod unuseful. So, a slightly different technique to KAP (Kite Aerial Photograp) was used. KAP consists in flying a single lined kite (such type allows very long lines lengths and steady stability), hanging a lightweight camera on the kite line and triggered it remotely from the ground. The device used for such purpose is a DuneCamTM system. This is a low power wireless remote camera system capable of driving a pan/tilt platform, controlling remotely the platform movements and sending real time video to a base unit. It consists of a lightweight aluminium platform (where the camera is placed on) bearing a circuit board that controls three radio control servo mo-

tors: one for pan movement, other for tilt one and the third for triggering the shoot button. The circuit is also connected to the camera to capture the real time video and send it to the base unit (Fig. 1.5b). As said above, this platform is hanged on the line kite and the line is released till getting the desired vertical distance.

However, this technique requires constant wind blow direction and medium intensity (number 3 in Beaufort force wind scale = 12-19 km/h). This characteristic was not easy to find in the areas of interest and thus a different technique was developed to avoid the wind requisites. This technique consists in setting two parallel lines from one high point to another. The two parallel lines work as a railway where a wooden platform (working as vehicle) passes by with the remote camera system placed on it. The wooden platform is moved along the lines, pulled by other line connected to it, and is stopped at regular intervals to take the pictures with approximate 20-30% of overlapping between one and another. The interested horizontal area is located at a lower level in between the two ends of each line. By moving the lines working as railways, different parallel tracks are gotten and a large wide horizontal area can be photographed in detail. The vertical distance is set depending on the relative distance between outcrop plane and the high points. Pictures taken for this Thesis through this technique were taken between 20-30 metres. This technique has been called LAP (Line Aerial Photograph).

PROCESSING IMAGES

Cartographic montage. To assemble the pictures, the photomontages were performed through two softwares: *PhotoStitch 3.1* (software of *Canon Inc.*) to merge pictures horizontally and *Photoshop cs4* (software of *Adobe Systems Ltd.*) to merge pictures vertically. Once all the pictures were assembled, the whole final picture was printed on A3 sheets. Depending on the size of the final picture and the required scale, the whole picture was splitted into several A3-size sheets and then printed.

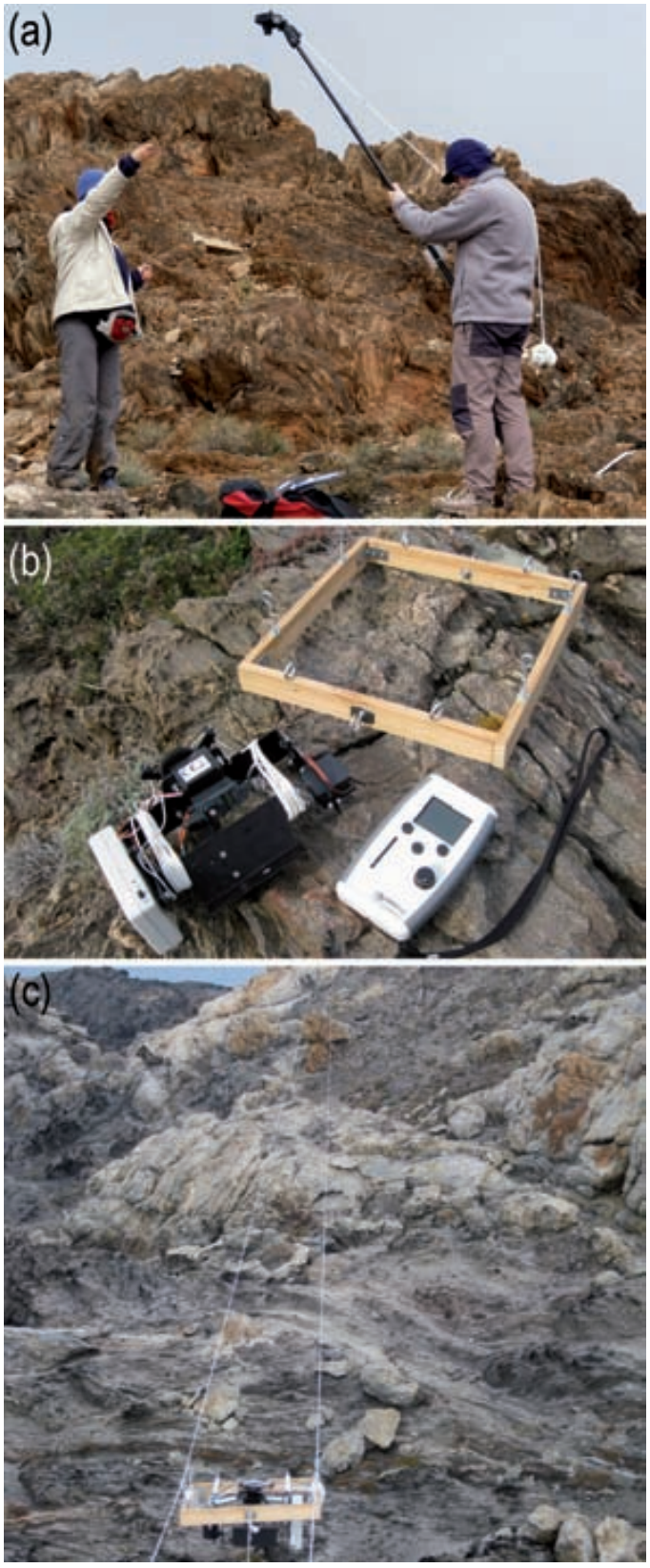

Fig. 1.5. Acquisition of low altitude photogrpahs: (a) Monopede (b) Dune Cam c) Line Aerial Photograph

FIELD DATA ACQUISITION AND PROCESSING

When the large-scale cartographies are prepared, the next step is the field data acquisition. With those A-3 sheets pictures stick on wooden boards, the work consisted in going to the field area, drawing the foliation trace in the interested areas to see where the foliation trace goes (especially in, around and out the lozenges and the shear zones) and taking structural measures with the compass (mainly orientation and dip measures of the regional and mylonitic foliation and lineations) as well as many observations as possible. Each measure were located on the cartography.

Field data processing involves: databases creation, data introduction, data processing and interpretation. When the cartography is filled with the field information, all data on it are separated in groups according to the foliation generation (S_1, S_2, S_3...) and/or nature (mylonitic or regional foliation). The data were projected on a plot using the indepent software *Stereonet 7*. The foliation traces were digitally drawn on *Canvas X* software, thus the changes of the foliation orientation in and around lozenges and the bulk shear zone pattern and network of the area could be clearly observed. Through *SURGE* software, scale color maps of the changes in orientation of the foliation traces along a tectonic lozenge were performed. They were made upon metric lozenges with different foliation orientation relative to the bounding shear zones. The lozenges were photographed through the monopod and its foliation direction was carefully measured in around 40 points. Once the field data are obtained, the graphical representation is gotten through a combination of four softwares: (i) *Canvas*, to draw the bounding shear zones of the lozenge and the measure points in it and to export the files as two text files with GIS properties, (ii) *Microsoft Excel*, to organize the data in columns and add the value 0 to the third dimension, (iii) *TextEdit*, to change the filename extension and finally (iv) *SURGE*, to overlay both files and calculate the grid through interpolation of data and finally to get the map. This representation combined with the stereoplots allows a better interpretation.

ANALOGUE AND NUMERICAL MODELLING

Experimental work is a powerful complement to field work, which is assumed to be performed after the field work for supporting and reinforcing the field observations. However, as it has been previously stated, field work on lozenges was very scarce prior to this study and therefore the experimental work in this research was not deeply developed and may be somehow undetermined. Moreover, the difficulty of modelling the formation of such structures involving shear zone interconnection and interaction according to the the present day development of the techniques (especially in the platform used for numerical modelling) stopped further research in these experiments. A brief explanation of the techniques are presented:

Analogue modelling. This was carried out at the *Laboratori de Deformació* of the *Universitat Autònoma de Barcelona* (UAB) through the BCN-Stage device (Fig. 1.6). This is a press machine for deforming crystalline rock analogue materials. It consists of a parallelogram deformation cell (where the model is introduced) of which one parallel side pair moves closer while the other pair moves away at the same rate (thus they keep constant volume) through a double piston axis connected to an electric motor which, at the time the experiments were conducted, were controlled by LabView 3.1 software (Fig. 1.6). The device allows controlling the strain rate and the kinematic vorticity number (Wk, Truesdell, 1954; Astarita, 1979; Means et al., 1980) by the rotation of one

of the axis (Y axis) induced by a third motor (Z motor; Fig. 1.6). It is also provided with an air-conditioner and a fan device with some sensors to control the temperature. The geometrical and kinematic basis of this deformation device are explained in Carreras and Ortuño (1990).

The top of the cell has a transparent glass cover which allows semi-confined experimental conditions and the direct observation of the top of the model while the experiment is working. A high-resolution digital camera with a timer intervalometer shutter is placed above the cell, thus it takes pictures at regular time intervals of different deformation states. The montage of the picture sequence lets to create a video of the deformation process.

The deformation conditions were (i) sub-simple shear (gamma (γ) value = 0,27 (Φ =15°) and shortening = 50%) and pure shear (shortening = 50% and 75%), both at a constant strain rate

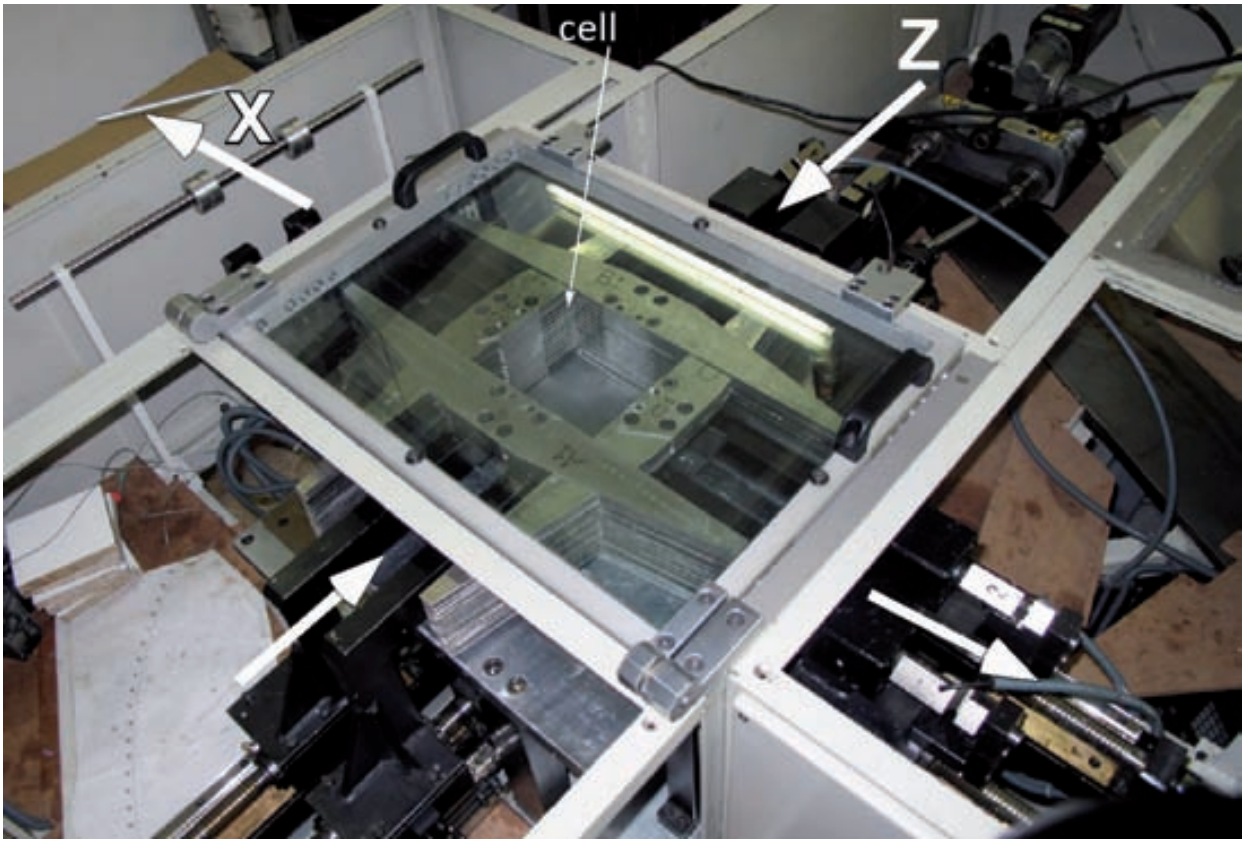

Fig.1.6. BCN-deformation stage. : extension axis, Z: shortening axis.

of 2.5 x 10^{-5} s^{-1}. The compression was along the direction of the longer axis of the initial model (Z) and the extension along the direction of the initially shorter axis (X). The deformation experiment duration was between 8 and 10 hours and the pictures were taken every 10 minutes.

The analogue materials used for the experiments were plasticine of different colours, aluminium flakes and vaseline. All experiments were performed upon multilayer models. Models had a dimension of 30x15x10 cm^3 (see Fig. 3.15, 3.18 and 3.21). The plasticine is used as an analogue of middle/low crust deforming rocks (McClay, 1976; Sofuoglu and Rasty, 2000; Schöpfer and Zulauf, 2002; Druguet and Castaño 2010) since they have a non-Newtonian visco-elastic behaviour under room temperature deformation. The plasticines used for these models have a stress exponent around 4 (Gómez-Rivas, 2008) with a slightly different viscosity according to the colours (probably induce by the colouring product;

Gómez-Rivas, 2005). This fact enhances the anisotropy effect and the possible stress refraction. The aluminium flakes simulate the phylosillicates and were added to some layers at a proportion of 10% in weight. The vaseline was used as lubricant between layers in some of the experiments. Detailed explanation on the procedure of building up similar models can be found in Castaño (2010)

Numerical modelling. The simulation platform used for numerical modelling was *ELLE,* that is a compilation of independent softwares that can be combined according to the experiment specifities. It allows microdynamics simulation of metamorphic and deformation processes (e.g. nucleation and subgrain formation, Grain Boundary Migration (GBM), diffusion creep, localisation of deformation or visco-elastic and brittle deformation) and analysing the influence of variables controlling those processes by changing their values.

An experiment consists in the calculation of a set of defined driving forces and boundary conditions upon a framework, calculated for small time steps. The framework describes the distribution of physical and chemical properties and it is in an *Elle* data file which values are changing after every calculation in every time step or loop (a complete sequential cycle of the process is called time step or loop; Fig. 1.7).

Existing codes can be used as a micro-process (e.g. the non-linear viscous deformation program Basil of Barr and Houseman, 1996) and run upon any framework of interest. Only Conversion Utilities may be needed to translate the *Elle* data structure into the appropiate input format for the algorithm and incorporate the output back into the data structure (Bons et al., 2008).

Simulations were performed by the several repetition of a sequence of three processes (loop): i) viscous deformation through the Finite Element method; ii) repositioning and iii) viscosity update.

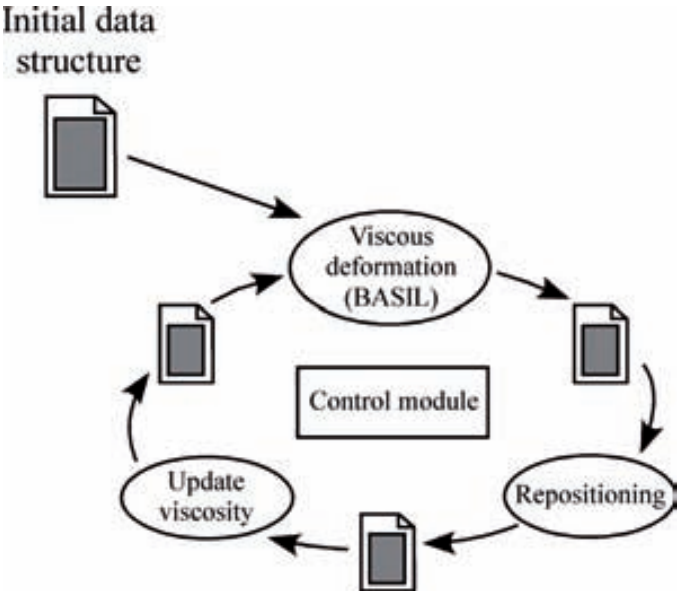

Fig. 1.7. Flow diagram showing the simulation process by repetition of the sequence of processes (loop). The initial framework (initial geometry and properties) is described in the Initial Data Structure file, and this is submited, every time step, to the control module consisting of thse three processes: viscous deformation, reposicioning and viscosity update.

1.3. SETTING OF THE REFERENCE AREAS

Ductile and brittle-ductile shear zone belts abound in mid- and low crustal crystalline domains deformed under any deformation regime, from compressional to extensional. They are more common in exhumated orogenic belts affected by compressional, transpressional or wrench tectonics. In the present study the Northern Cap de Creus shear belt (Carreras, 2001) has been taken as the main reference area because of the quality of structures and outcrops. However in order to enable comparisons, examples from other areas have also been analyzed.

Reference areas are:

- Northern Cap de Creus shear belt (Eastern Pyrenees)
- Roses shear zones (Southern Cap de Creus shear belt)
- Laghetti area (Maggia Nappe, Helvetic Alps)
- Cabalón area (Galicia, NW Iberian Massif)
- Zenaga and Kerdous inliers (Anti-Atlas, Morocco)

1.3.1 Northern Cap de Creus shear belt (NE Spain)

This belt consists of a network of dominantly NW-SE trending shear zones with moderate to steep dips to the NE (Figs. 1.8 and 1.9). Associated stretching lineation plunges shallow to the NNW. Dominant kinematics is dextral/reverse although shear zones with associated normal/dextral are also present. The shear zones are associated to a late Variscan deformation event, labelled D_3. The belt cuts across medium to high grade metasediments (mainly metapelites and metapsammites) with associated pegmatites and localized migmatite complexes, those associated to quartz-diorites, tonalites, granodiorites and leucogranites (Druguet, 1997).

The Northern Cap de Creus shear belt evidences a high heterogeneity of deformation, with domains consisting of wide shear zones made of anastomosing shear zones coexisting with domains with no relevant D_3 shearing and only isolated and smaller shear zones. This fact makes the area specially appropriate for the aim of this study because it allows to compare settings were only isolated shear zones are present with domains where there is an interplay of different shear zones that isolate lozenges. This shear belt evidences a self-similarity pattern with the presence of lozenges of different size from kilometric to centimetric (Carreras, 2001). For the purpose of the work, analysis will be concentrated in metric to decametric sized lozenges because these are the most adequate to perform the analysis of the whole body.

To achieve the goals, analyses have been concentrated into the geometry and kinematics of: i) individual shear zones (those found in domains with low D_3 deformation) and ii) the intersections of shear zones displaying coalescences and branching that isolate non-sheared or less sheared domains.

The fact that sheared rocks bear previous strong foliations (either S_1, S_2 or a composite $S_{1/2}$ fabric) makes a significant difference with other shear belts where commonly shear zones develop on isotropic or low anistotropic rocks (e.g granitoids and/or gneisses). A relevant fact of this belt

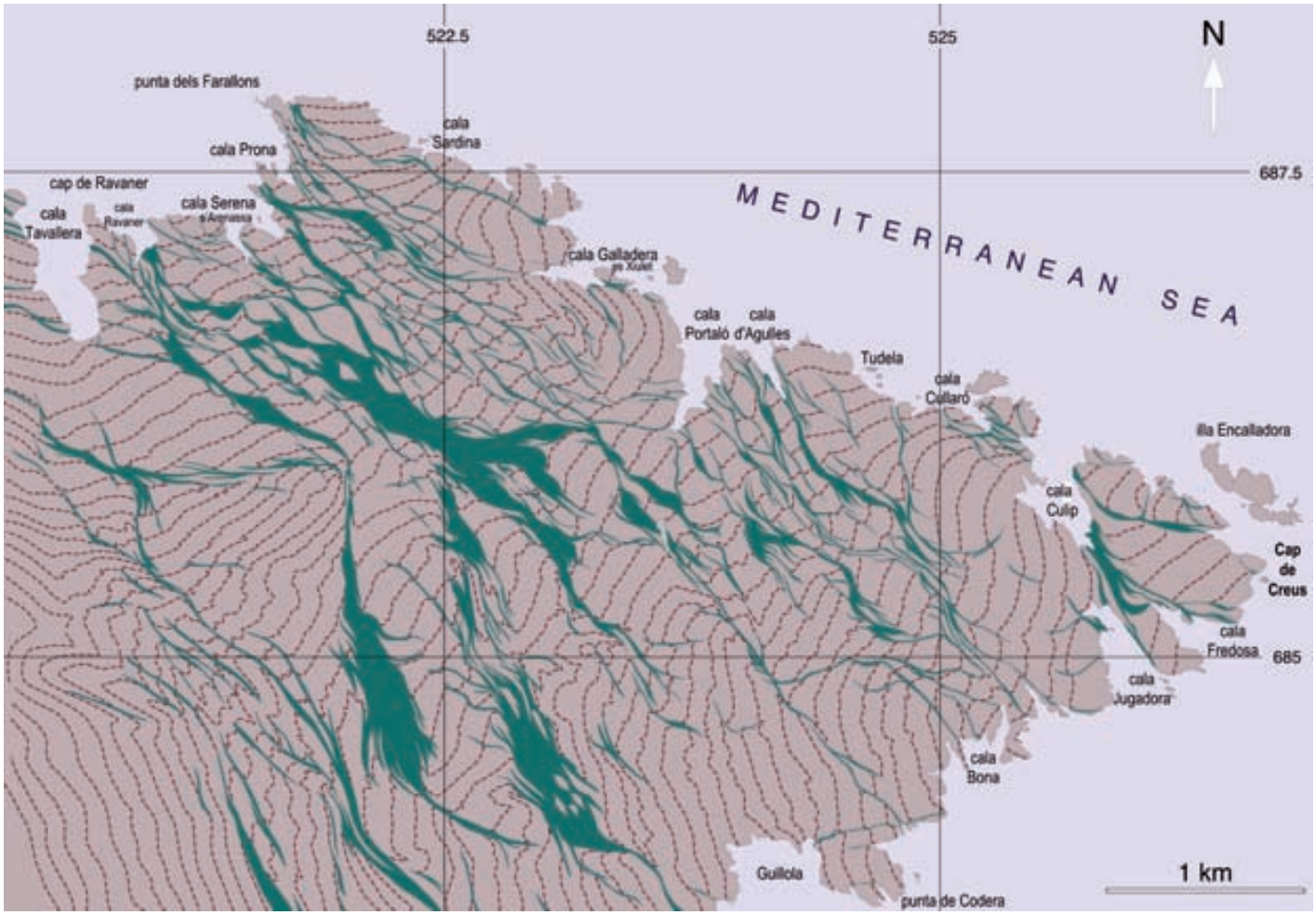

Fig. 1.8. Structural map of the Northern Cap de Creus shear belt evidencing anastomosed character of shear zones isolating different sized lozenge-shaped domains (after Carreras and Druguet 2013).

and other belts developing across foliated rock concerns the complex relations between geometry and kinematics of each individual shear zone. There, the vorticity axis bears a variable angular relationship with the kinematic axes (i.e. the stretching lineation, which is closely parallel to the shear direction; Fig. 1.9). In consequence it has to be taken into account that some of the deflections of the previous foliation at the margins of an individual shear zone or an isolated lozenge is an apparent feature that must be analyzed in 3-D, otherwise some mistaken conclusions can be reached. This is well illustrated in the example shown in (Figs. 10.3 and 10.5 in Carreras, 1997) where a lozenge wrapped by dip-slip shear zones show highly contradictory deflection and shear related marginal folds.

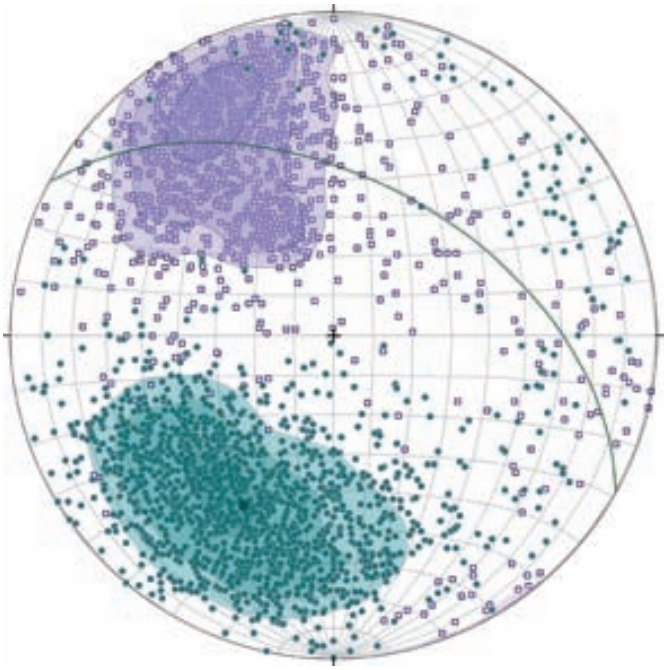

Fig. 1.9. Lower hemisphere stereoplot of poles to mylonitic foliation and associated stretching lineation (after Carreras and Druguet, 2013).

1.3.2 Roses shear zones (Cap de Creus, NE Spain)

These shear zones belong to the Southern Cap de Creus shear belt, affecting both the Rodes and the Roses granodiorite massifs. These shear zones are also associated to the late Variscan D_3 deformation event. Due to the overall Alpine overturning of the structures in the Cap de Creus massif these shear zones are predominately sinistral (Carreras and Losantos, 1982; Simpson et al., 1982; Carreras et al., 2004). They develop across a slightly foliated granodiorite containing microquartz-diorite enclaves and aplite-pegmatite dykes (Figs. 1.10 and 1.11).

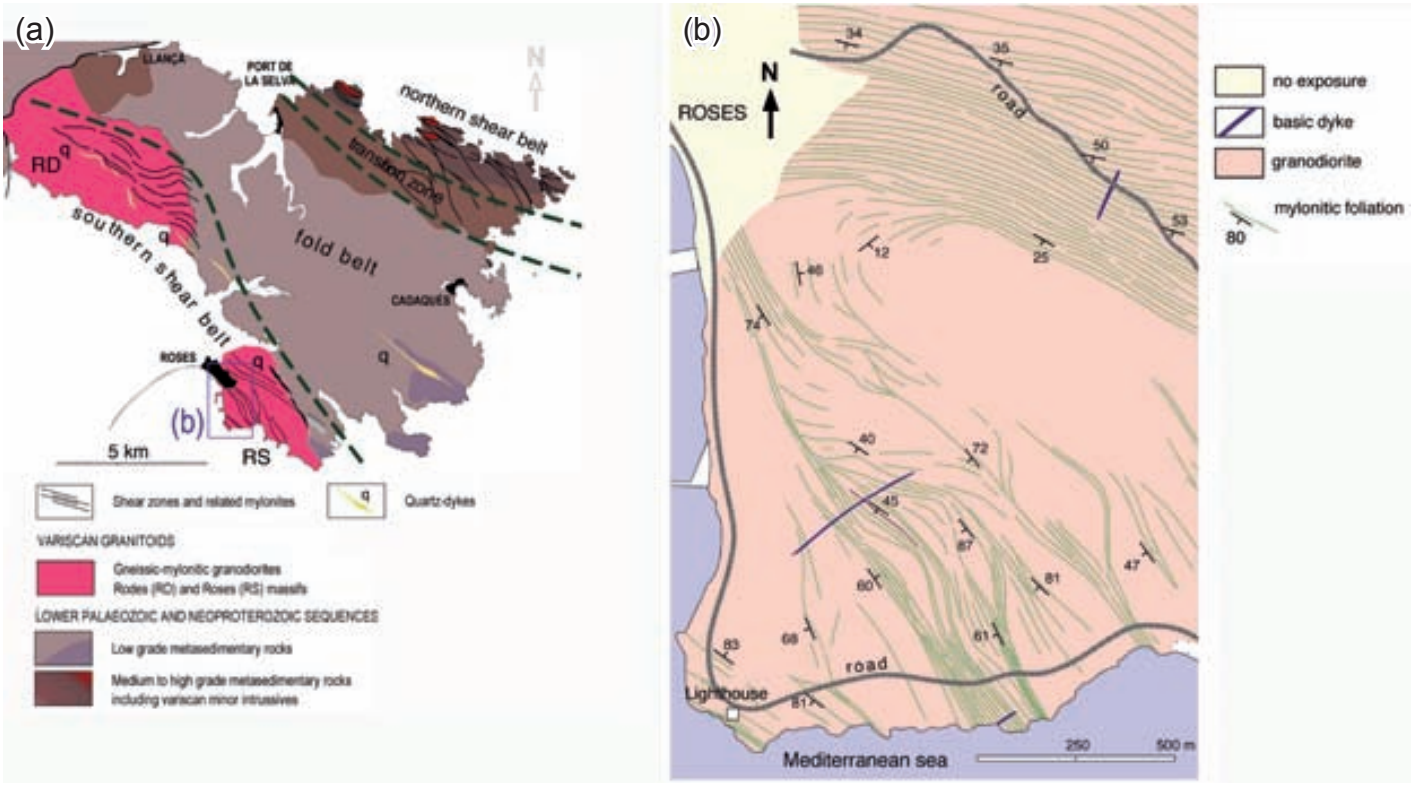

Fig. 1.10. Structural map of the Cap the Creus shear belts and detail map (b) of the Roses shear zones close to the lighthouse (after Carreras and Druguet, 2013).

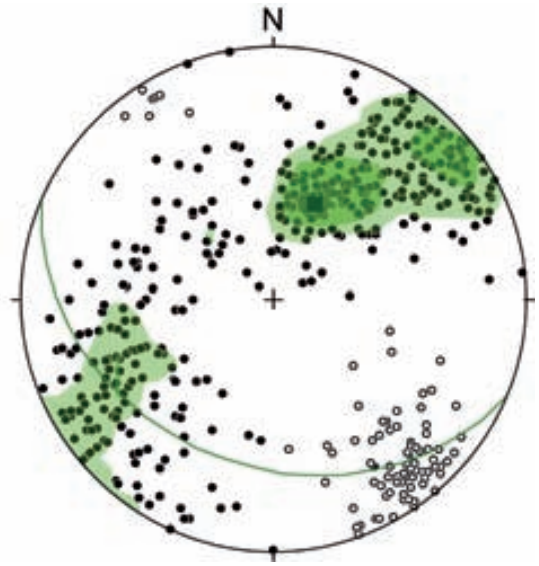

Fig. 1.11. Stereoplot of poles to mylonitic foliation (dots) and associated stretching lineation (open circles) from the area shown in Fig. 1.8 (after Carreras and Losantos, 1982).

1.3.3. Laghetti area (Maggia Nappe, Helvetic Alps)

The Laghetti area consists of Variscan granites and quartz-diorites (Matorello group) involved in a recumbent fold (Maggia Nappe) of the Helvetic Alps (Fig. 1.12). The Maggia Nappe consists on a Penninic recumbent fold including the pre-Triassic crystalline basement. The basement is mainly made of granitoids that show the effects of Alpine polyphase deformation that generated an anastomosed network of ductile shear zones (Ramsay and Allison, 1979). Shear zones in the crystalline basement formed contemporaneously with the folds of the cover sequence (Grujic and Manckte-low ,1996).

Shear zones (Fig. 1.13) are of Alpine age and form an anastomosed pattern in plane view and also in vertical sections (Fig. 1.14) .

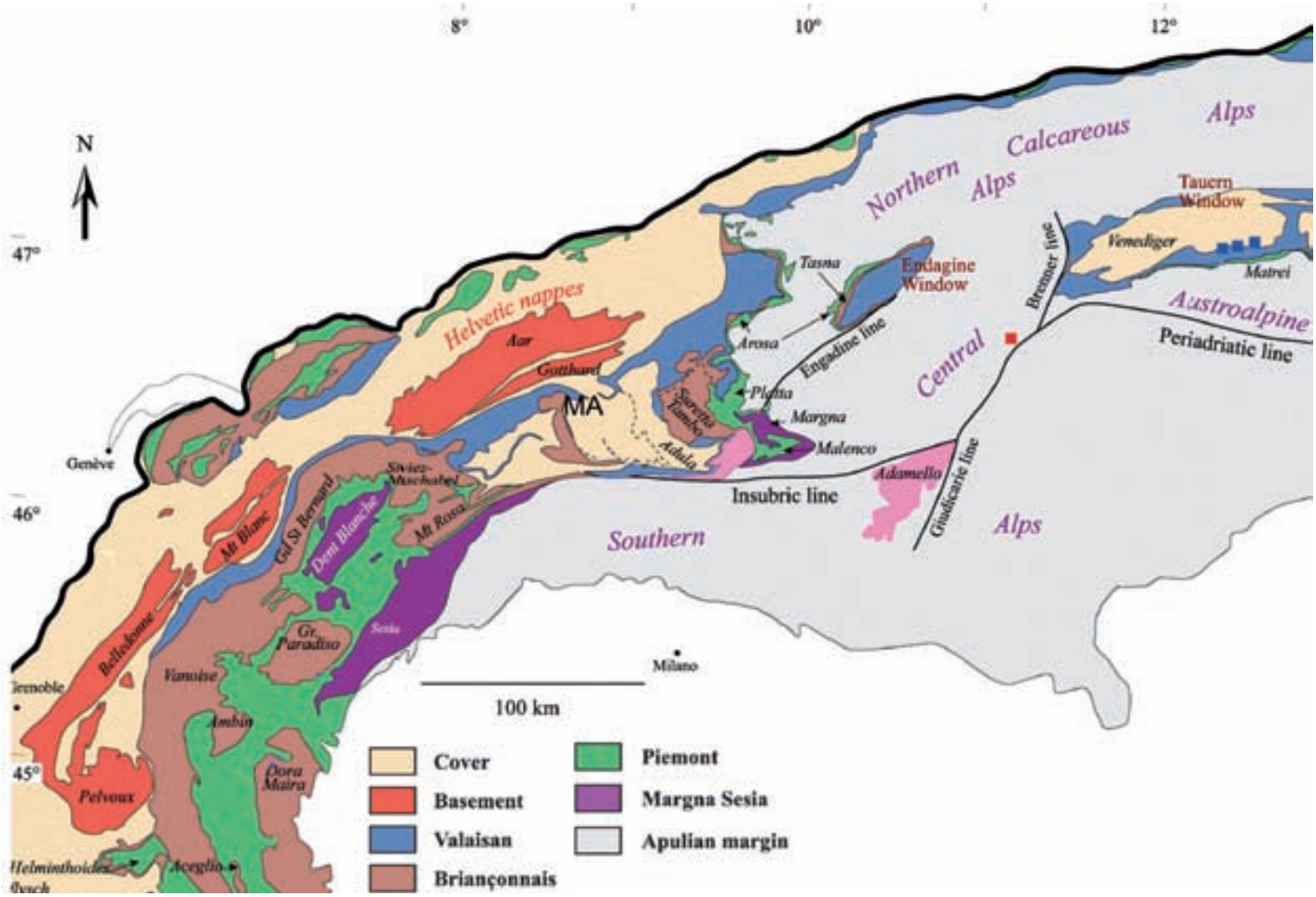

Fig. 1.12. Setting of the Maggia Nappe (MA) in the Alpine unites (from Froitzheim et al., 1996 modified).

Fig. 1.13. Dextral shear zone in plane view affecting granites and an associated leucocratic vein.

Fig. 1.14. Detail of the shear zone arrangement in a vertical section. Width of view: 30m.

Shear zone poles distribute along a great circle. It must me noted that similar to the Roses shear zones, the stretching lineation lies close to the pole of the great circle (Fig. 1.15).

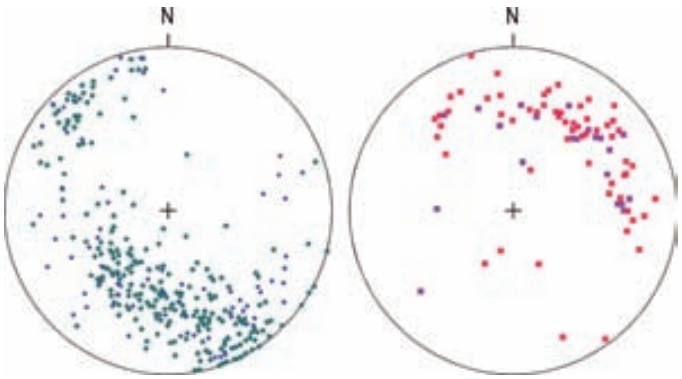

Fig. 1.15. Stereoplots of poles to mylonite foliation (left) an associated stretching lineations (right). Green circles and magenta squares are data from Ramsay and Allison (1979), blue circles and red squares are own data.

1.3.4. Cabalón area (Cabo Ortegal, NW Spain)

Studied shear zones are located in the Cabo Ortegal complex (Vogel, 1967) which is a metamorphic nappe that is a part of the Allochthonous Complexes made of mafic and ultramafic rocks of the northwestern Iberian Peninsula (Arenas et al., 1986; Fig. 1.16a). Three of these complexes, Ordenes, Cabo Ortegal and Malpica-Tuy, are located in Galicia (NW Spain), and two, Braganca and Morais, are in Trás-os-Montes (NE Portugal). These complexes represent fragments of variably deep subducted continental and oceanic lithosphere that were subsequently exhumed and thrusted over the Gondwana edge during the Variscan orogeny, (e.g. Ries and Shackleton, 1971; Bard et al., 1980; Bastida et al., 2000; Iglesias et al., 1983; Vogel, 1984; Arenas et al., 1986; Matte, 1991). Three main structural elements may be correlated on a regional scale within the complexes. From bottom to top these are: a Basal Unit or Lower Allochthon, an Ophiolitic Unit, and an Upper Allochthon Unit (Fig. 1.16a). The Basal and Ophiolitic units correspond to the passive margin of Gondwana and outboard oceanic sequences related to this continent (van Calsteren et al., 1979; Peucat et al., 1990; Dallmeyer and Gil Ibarguchi, 1990; Dallmeyer et al., 1991; Santos Zalduegui et al., 1995; Ordóñez Casado et al., 2001). The Upper Allochthon is the most distinctive element that constitutes a composite nappe pile displaying inverted metamorphism and containing a basal, migmatitic, high-pressure paragneiss, and mafic (eclogite and granulite) and ultramafic (metaperidotite) high-pressure rocks on top.

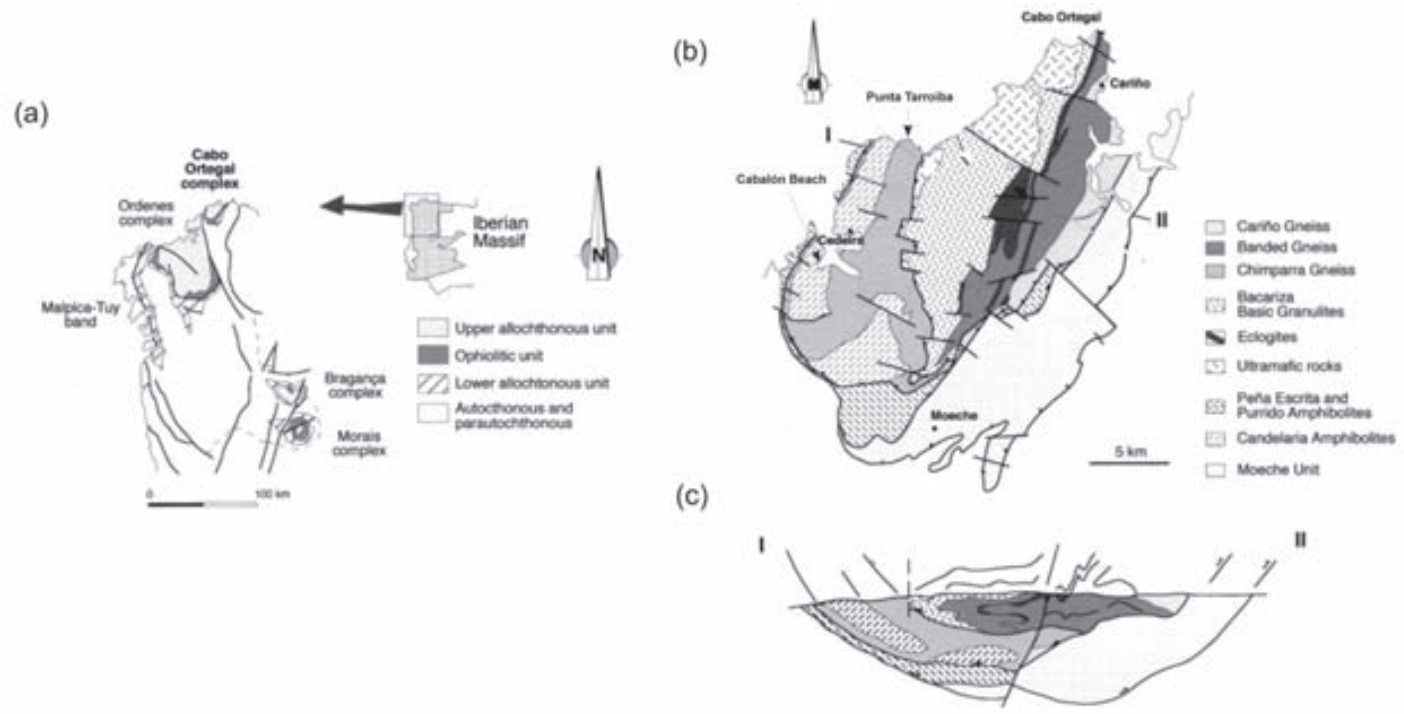

Fig. 1.16. (a) Allochthonous complexes within Iberian Massif (after Arenas et al., 1986). (b) Simplified geological map of the Cabo Ortegal complex (modified from Arenas et al., 1986) with the investigated locations and the trace of the cross section (I–II); (c) Simplified geological cross-section (after Bastida et al., 1984; Arenas et al., 1986)

The Cabo Ortegal complex is a synform (Bastida et al., 1984; Fig 1.16b, c) whose tectono-metamorphic evolution is clearly different from that of the low-grade Silurian metasediments and metavolcanic rocks where the complex lays. The complex is composed of internally imbricated units that mainly belong to the regional Lower Allochthon, Ophiolitic and the Upper Allochthon

Fig. 1.17. Strongly deformed Gneisses at Punta Tarroiba cliff (a, b and c) showing different degrees of mylonitization, anastomosing pattern (a) and sheat folds (b and c); and at Cabalon cove (d) showing a sheat fold of 180° hinge curvature (Alsop and Carreras, 2007).

Units. This nappe complex comprises, from bottom to top, the following thrust-bounded major tectonic units (Gil Ibarguchi et al., 1990, Ordóñez Casado et al., 2001): (a) amphibolites, metagabbros and metaplagiogranites of the Purrido-Peña Escrita and Candelaria formations; (b) medium- to high-grade, locally eclogite-bearing gneisses of the Cariño, Banded and Chimparra formations; (c) eclogites of Concepenido; (d) HP mafic to acid granulites of the Bacariza formation; and (e) ultramafic bodies, mainly harzburgites with abundant pyroxenites.

Investigated rocks are from the Upper Allochthon: the amphibolites of Candelaria formations at Cabalón boulder beach and the Chimparra gneiss at Punta Tarroiba, both on the west side of the complex (Figs. 1.16 and 1.17). The rocks at Candelaria formation are intensely deformed and

amphibolitized metagabbros, displaying a banded and inhomogeneous aspect (Fernández, 1993). The most common type of gneiss at Chimparra gneiss formation are flattened gneiss displaying mylonitic or blastomylonitic textures (Vogel, 1967).

The widespread, heterogeneous mylonitic foliation is superimposed to the high grade metamorphic textures (amphibolite facies) and shows a lineation very close to the regional lineation (Fernández, 1993; Fig. 1.18). Therefore, interconnections of shear zones were not found and individual, mesoscipic shear zones consits of bands showing a higher mylonitic texture and a slightly higher strain than their walls (Fig. 1.17b and c).

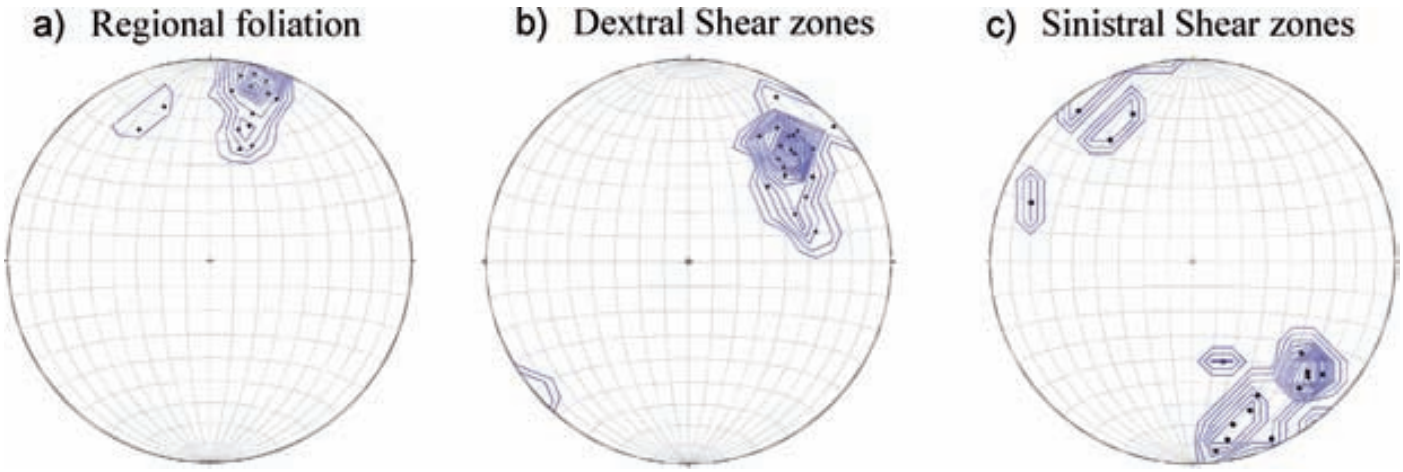

Fig. 1.18. Poles to (a) regional foliation, (b) dextral shear zones and (c) sinistral shear zones at Punta Tarroiba (Cabo Ortegal, NW Spain).

1.3.5. Zenaga and Kerdous inliers (Anti-Atlas, Morocco)

The Zenaga and the Kerdous plain consists of an inlier (or *boutonnière*) made of crystalline rocks belonging to the Eburnian basement (North border of the West African Craton), mainly consisting of metasediments, gneisses and granites. These rocks are affected by localized shear zones associated to Pan-African deformation. In addition, a basic (diabase) dyke swarm is emplaced into the Eburnian Rocks. Basic rocks are also locally affected by shear zones (Fig. 1.19).

Strain localization is controlled by the presence of the dykes and some shear zones nucleate parallel or sub-parallel to the dykes preferentially along their margins (Carreras et al., 2006; Castaño, 2010). Other dykes exhibit strain localization along the dykes which is not parallel to dyke walls, but slightly oblique. Most common basic dykes exhibit penetrative foliations at the margins, while are less deformed or undeformed at the central domains. This strain localization and the irregular shape of the dykes cause shear zones to anastomose and to develop lozenges (Fig. 1.20).

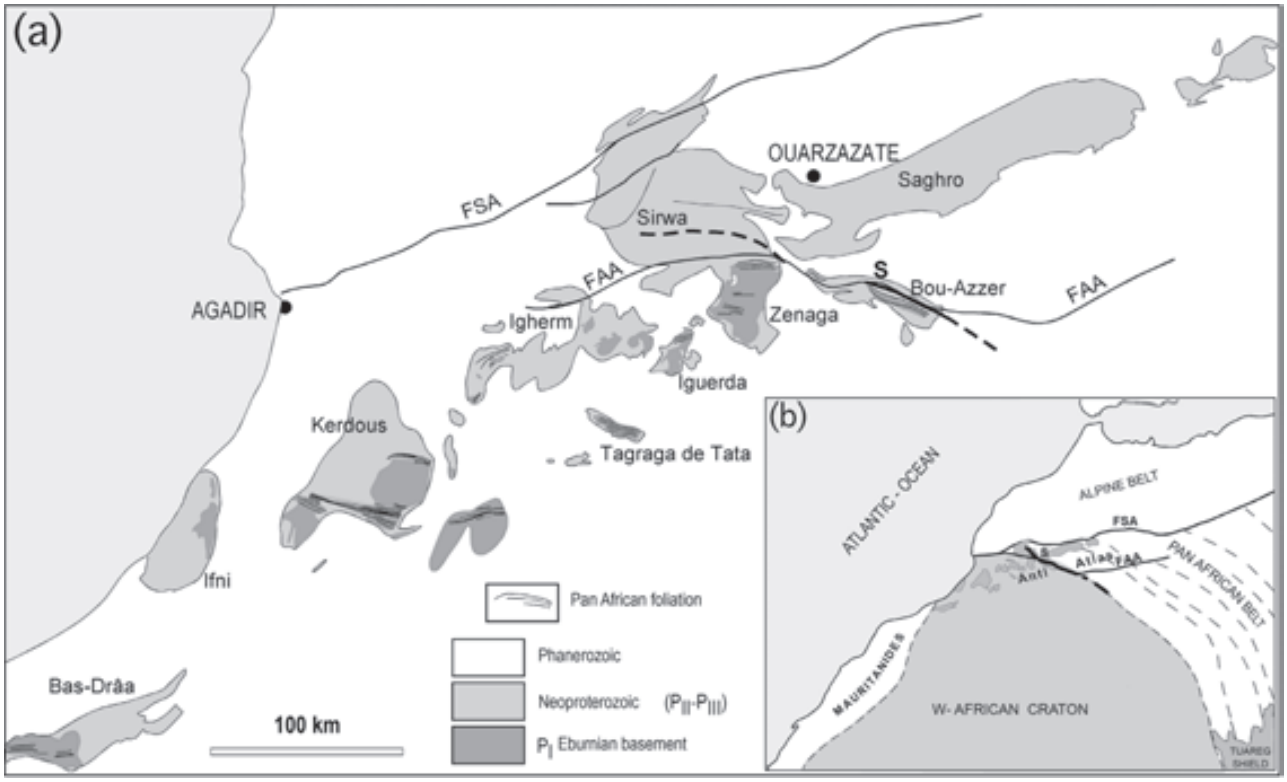

Fig. 1.19. Map of the Anti Atlas inliers (a) Setting of NW Africa. geological units. (b) Anti-Atlas inlayers and their relation with the Pan African belt (after Carreras et al., 2006).

Fig. 1.20. Lozenge consisting of a segment of a basic dyke exhibiting a less deformed core and strongly mylonitic margins. Width off view: 5 m.

Chapter 2

SHEAR ZONES AND LOZENGES: FIELD STUDIES

2. SHEAR ZONES AND LOZENGES: FIELD STUDIES

The understanding of the development of lozenges requires the following steps:

1. Geometry of individual shear zones.
2. Initiation and propagation of shear zones.
3. Interaction of shear zones.
4. Lozenge morphology and their internal structure.

The section dealing with these points will be presented on the basis of detailed studies of structures performed in the areas of reference.

2.1. GEOMETRY OF INDIVIDUAL SHEAR ZONES

The geometry of ideal ductile shear zones corresponds to heterogeneous simple shear. This is assumed to occur if no volume loss is associated to the deformation or if the shear zone and no homogeneous strain is superimposed (Ramsay and Graham, 1970). Assuming heterogenous simple shear, structural differences in shear zones depend on the isotropy or foliation/bedding condition of the sheared rock. In isotropic rocks, a new foliation forms with a sigmoidal-shaped pattern. At low sheared marginal domains, the foliation is oblique to the shear zone trend. Under increasing shear strain, the foliation tends to parallelism with the shear zone (Fig. 2.1).

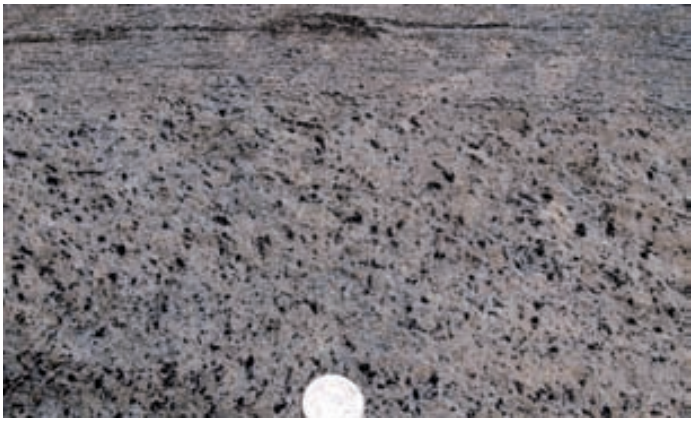

Fig. 2.1 Shear zone affecting granite. Note the obliquity of the incipient mylonitic foliation (Laghetti, Helvetic Alps)

In 3-D, the foliation adopts a sigmoidal-cylindroidal shape (Fig. 2.2a). The shear direction is normal to the cylindroidal axis, i.e. the pole of the cylindrical best-fit circle of the foliation planes (Fig. 2.2b).

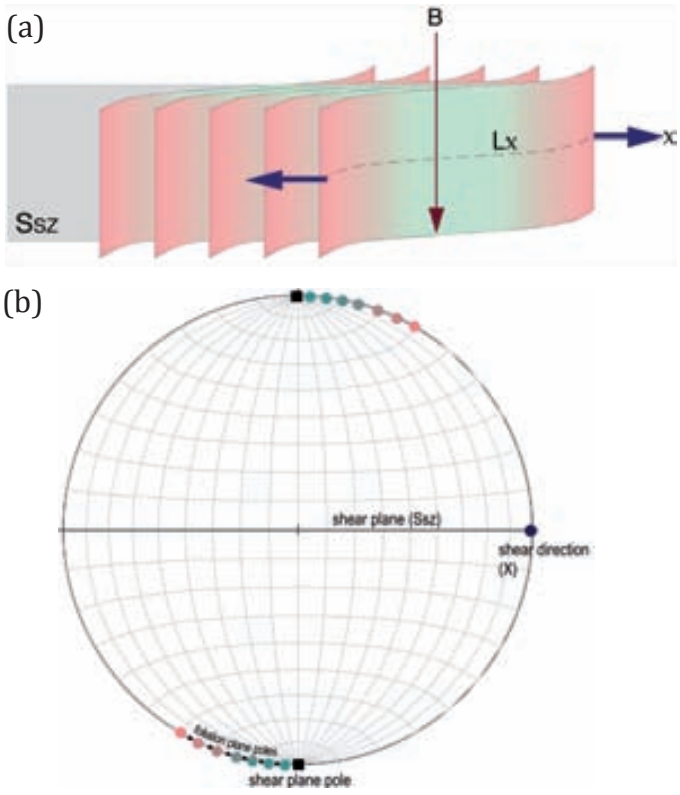

Fig. 2.2. Ideal shear zones by heterogeneous simple shear in isotropic rocks (after Carreras 1997, modified). (a) 3-D disposition of the shear-related foliation and relation with shear plane and shear direction; (b) stereoplot of the elements involved in the shear zone shown in (a).

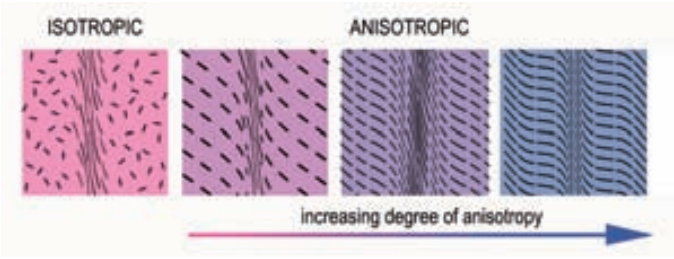

Fig. 2.3. Transition from ductile shear zones in anisotropic rocks to deformation bands associated to buckling instabilities (asymmetric folds with sheared limbs). The transition depends on the variable degree of mechanical anisotropy what in his turn depends on rock the crystallinity (after Carreras et al. (1980) modified).

Shear zones across anisotropic (foliated and/or banded) rocks are less common because deformation is accommodated by structures arising from mechanical anisotropy like folds or boudins. However, under increasing crystallinity the mechanical effect of ductility contrast and anisotropy decreases and a gradation from those structures to shear zones exists. Experimental based studies (Cobbold, 1976; Cosgrove et al., 1971; Cosgrove, 1976) and field based studies (Carreras et al., 1980) show these transitional structures (Fig. 2.3).

Additional differences between shear zones across isotropic or foliated rocks are:

(i) While in shear zones in isotropic rocks the mylonitic foliation tracks the XY plane of the finite strain ellipsoid associated to the shearing event, this is not the case for foliated rocks since the shear zone orientation is controlled by the relative orientations of the ISAs and the foliation. The obliquity between the XY plane of the finite strain ellipsoid and the sheared foliation decreases under increasing shear strain. If the foliation is passively deformed, the foliation at the shear zone margins track the orientation of a deforming plane (Carreras, 1975). However, as a result of shearing, a foliation plane inducing mechanical instabilities minor structures (involving extension and or shortening) may often form. Thus, at shear zone margins of shear zones affecting foliated rocks crenulations are common (Carreras, 2001).

(ii) Another significant difference concerns the relation between kinematic axes and structural elements. As shown in Figure 2.2, the vorticity

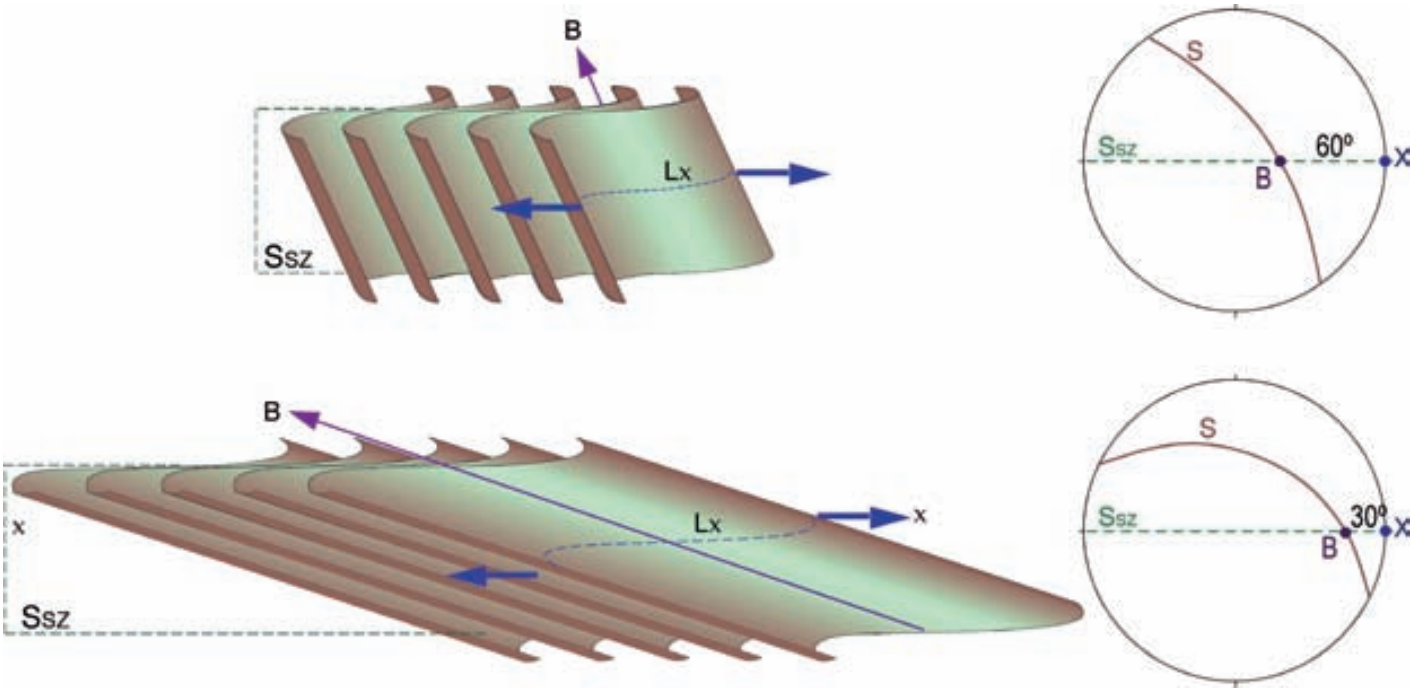

Fig. 2.4. Schema and coprresponding stereoplots showing the variable relations between the vorticity axis (B = axis of the foliation "S" flexure) and the shear direction (X). Ssz: Shear plane, Lx: shear-related stretching lineation on the S plane (after Carreras et al., 1987 modified)

axis of the sigmoidal structure developed in shear zones across isotropic rocks is contained in the shear plane and normal to the shear direction. In foliated rocks it is also contained in the shear plane but the angle with respect to the shear direction might vary between 0° and 90° (Figs. 2.4 and 2.5; Carreras and Casas, 1987; Carreras, 1997). This is because the vorticity axis in foliated rocks is the intersection line between shear and foliation planes which is acting like a hinge during foliation rotation. The histogram in Figure 2.5 shows the diversity of this angle based on 83 pairs of measures of shear zone plane and foliation orientation in Cap de Creus . It shows a wide range of the angle value, although wider angles (>50°) are more common than narrower angles (<50°). The variability in the angle of the vorticity vector is a relevant consequence as there is not fixed relation between geometry and kinematics.

Related to this fact, it has to be taken into account that marginal deflections at shear zone margins may show apparent deflections in contradiction with the real shear sense (Carreras and Casas, 1987; Passchier and Trouw, 2005).

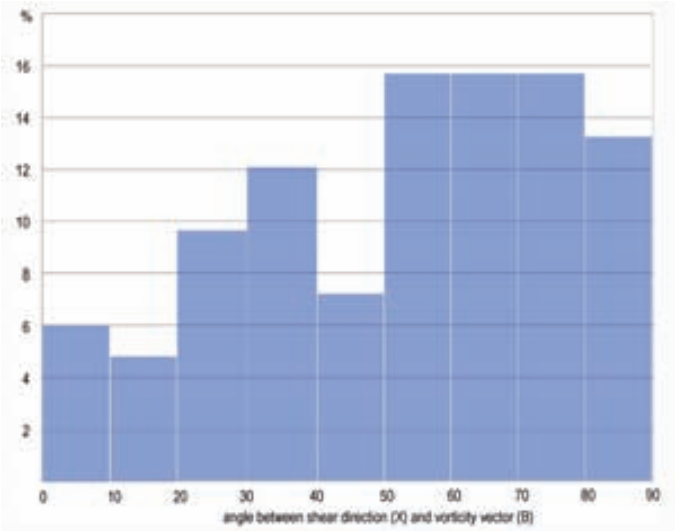

Fig. 2.5. Histogram showing the frequency of the vector of the vorticity angle, based in 83 pairs of measures. Although there is a high distribution , there is more frequency for angles higher than 50°.

2.2. INITIATION AND DEVELOPMENT OF SHEAR ZONES

As exposed in Chapter 1, the rheological aspects of the initiation and propagation of ductile shears zones (especially when the conditions are brittle-ductile) is a topic of current debate. The use of field evidences does not help much because same structures can be interpreted in different ways as illustrated in the Cap de Creus Northern shear belt (Carreras, 2001; Fusseis, 2006). Some authors argue for a ductile initiation and propagation while others, based on some brittle tips at ductile shear zones, suggest that the initiation and the propagation of the shear may be brittle and then, with progressive strain, they evolve to ductile.

The difficulty of solving this problem on field analysis rises from the fact that only the finite states are available. Different approaches have been used to solve the problem. Due to the fact that shear zones are confined and have a limited length, shear zone tips can be regarded as an analogous to a shear zone initiation. However, this is a debatable approach because tips of shear zones correspond to propagation zones with likely differences in strain distribution, strain rate and stress trajectories. An alternative and less questionable approach regards on focusing in isolated and confined shear zones with relatively low shear values at the central domains.

Works analyzing ductiles shear zone tips evidenced that these consist of splays of micro fractures (Segall and Simpson, 1986; Fusseis, 2006). This has been reported in both the Cap de Creus Southern belt affecting granodiorites (Fig. 2.6a) and the Northern belt affecting foliated schists. Accepting this assumption, shear zone initiation is (Fig. 2.6b) governed by fracture criteria and thus brittle fractures are the precursors of ductile deformation. This can be explained as the terminations, with less finite strain, show brittle deformation while the central part, more sheared and with more finite strain, shows mylonitic fabric achieved by dynamic recrystallisation as an effect of strain softening induced by the increasing strain and fluid circulation along the fracture.

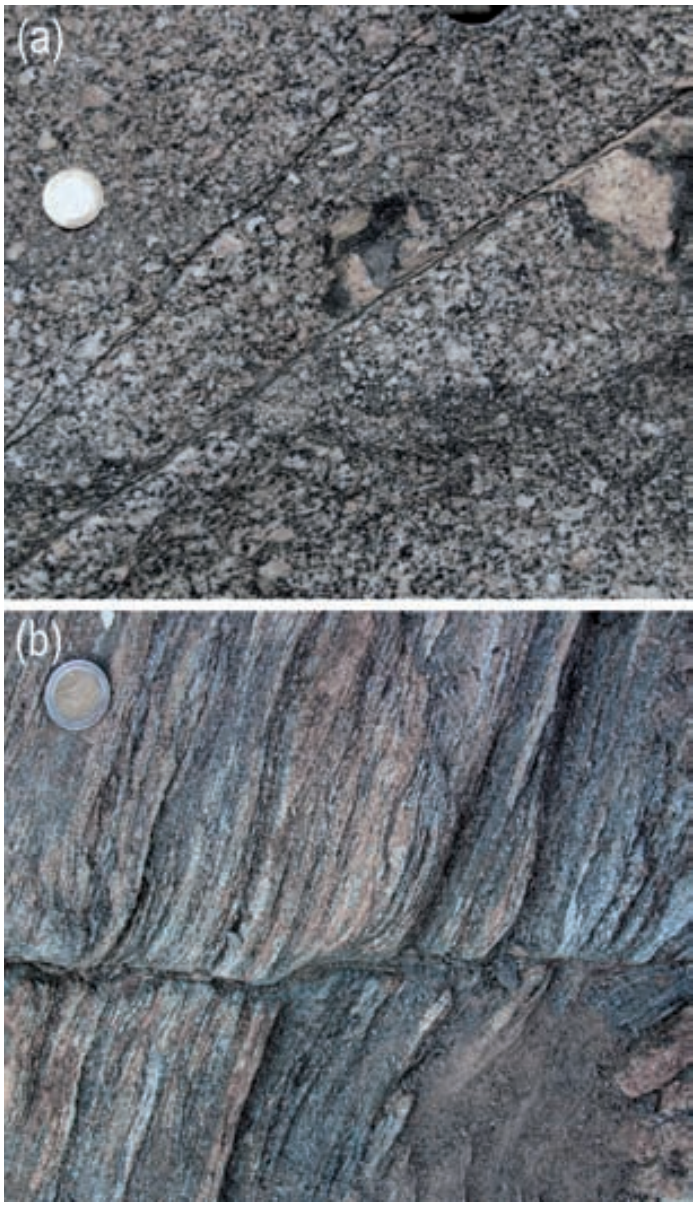

Fig. 2.6. Shear zone tips (a) corresponds to a shear zone across Roses granodiorite; (b) shear zone termination across schists (cala d'Agulles).

Alternatively, incipient isolated shear zones do represent equivalent to initial stages of the development of a shear zone. Examples of these abound in the Northern Cap de Creus shear belt. In such settings, deflection of the foliation rather resembles the buckling instabilities generated by defor-

mation of layered anisotropic materials (Cobbold, 1976; Cosgrove, 1976). Thus it can also be assumed that shear zones nucleate as instabilities governed by the buckling principles. This alternative, proposed for the Cap de Creus shear zones (Carreras, 1975; Carreras and Casas, 1987; Carreras, 2001), is also supported by the fact that in the shear zone marginal domains where the preexisting foliation is deflected, the geometry does not fulfil the heterogeneous simple shear model (dip isogons should remain parallel) but evidence a small amount of shear zone normal shortening generating a type 1B fold type geometry (Fig. 2.7).

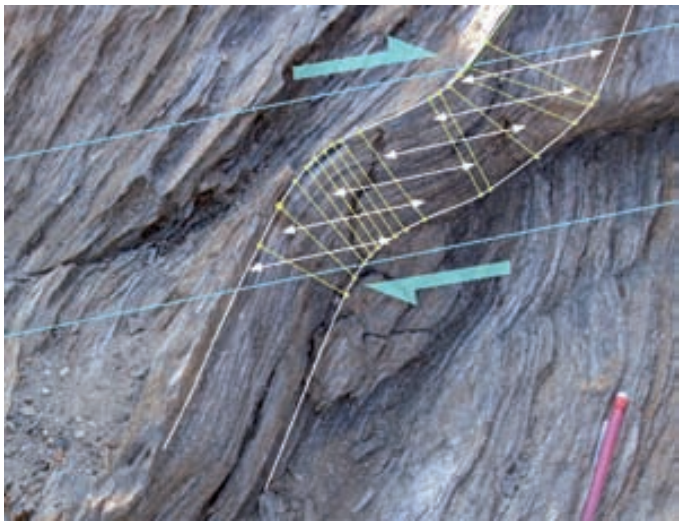

Fig. 2.7. Shear zone geometry of a isolated inceptive shear zone. Yellow lines correspond to dip isogons. White arrows correspond to the theoretical parallel thickness if the shear zone would obey heterogeneous simple shear (Cap de Creus).

Assuming the initial ductile initiation of shear zones, the presence of brittle tips in some ductile shear zones in low metamorphic grade conditions would be explained because both ductile and brittle deformation mechanisms may coexist in the same shear zone during initiation and propagation. In this way, some minerals deform by microfracturing (e.g. Feldspar), whereas others deform by dynamic recrystallisation (e.g. Chlorite and Muscovite). Even a same mineral (quartz), for low metamorphic conditions (low greenschists facies conditions) may deform either brittely or ductilely depending mainly on the temperature and the strain rate (Passchier and Trouw, 1996; Bernet and Bassett, 2005). Thus, for low metamorphic conditions, in both the central part and the tips of shear zones there are some minerals deforming by brittle mechanisms and others deforming by ductile mechanisms at the same time. The reason because the central part shows mylonitic fabric and the tips show microfracturing may be that in the central, initially deformed part the minerals susceptible of deforming by crystal-plastic deformation under the given conditions achieve more finite strain and hence these minerals recrystallize and start to develop a proto-mylonitic fabric. However, at the tips, these minerals achieve much less deformation; they do deform internally but do not recrystallize and thus they do not give rise to a proto-mylonitic foliation. At the tips, only the microfractures are observed at the outcrop scale. The direct observation of the minerals in the tips at the microscope could give more detailed information, however no samples were taken in order to preserve the integrity of the outcrops and their Geological Heritage values.

Another important factor controlling the initial orientation of shear zones concerns the role of the preexisting foliation. It is well established that mechanical heterogeneities, particularly a planar anisotropy, play an important role in the nucleation of deformation instabilities. This applies to both brittle (Donath and Parker, 1964; Cobbold et al., 1971; Platt and Vissers, 1980; Price and Cosgrove, 1990; Williams and Price, 1990; Weijermars, 1992; Gomez-Rivas and Griera, 2012) and semi-ductile or ductile deformation (Cosgove, 1976; Carreras et al., 2000; Carreras, 2001; Fusseis et al., 2006; Carreras et al. 2013).

In homogeneous isotropic or nearly isotropic rocks and under coaxial ductile deformation two sets of conjugate shear zones should form. The initial angle between the two sets is not well established. Following the Coulomb criteria, and with

material properties with a frictional angle close to zero, the initial angle between conjugated sets should be close to 90°. This angle can be modified under increasing deformation if the bulk deformation is also partly accommodated by homogeneous deformation (Fig. 2.8). Alternative interpretations (Zheng et al., 2011) propose the MMS criteria and state that initial angle should approach a value of 110°. An analysis of shear zones in nearly isotropic gabbros from Rainy Lake area (Norther Ontario) indicates that in this particular case under a sequential development, older shears exhibit an obtuse angle with respect to the main shortening direction while the later sets form angles close to 90° (Fig. 2.8a). This indicates that obtuse angles facing the shortening direction are not necessarily a primary feature but achieved under progressive or sequential deformation (Fig. 2.8b). However it must be stated that this can not be presented as a general rule. Examples from Roses show incipient conjugate shear zones with large obtuse angles facing the shortening direction (Fig. 2.9).

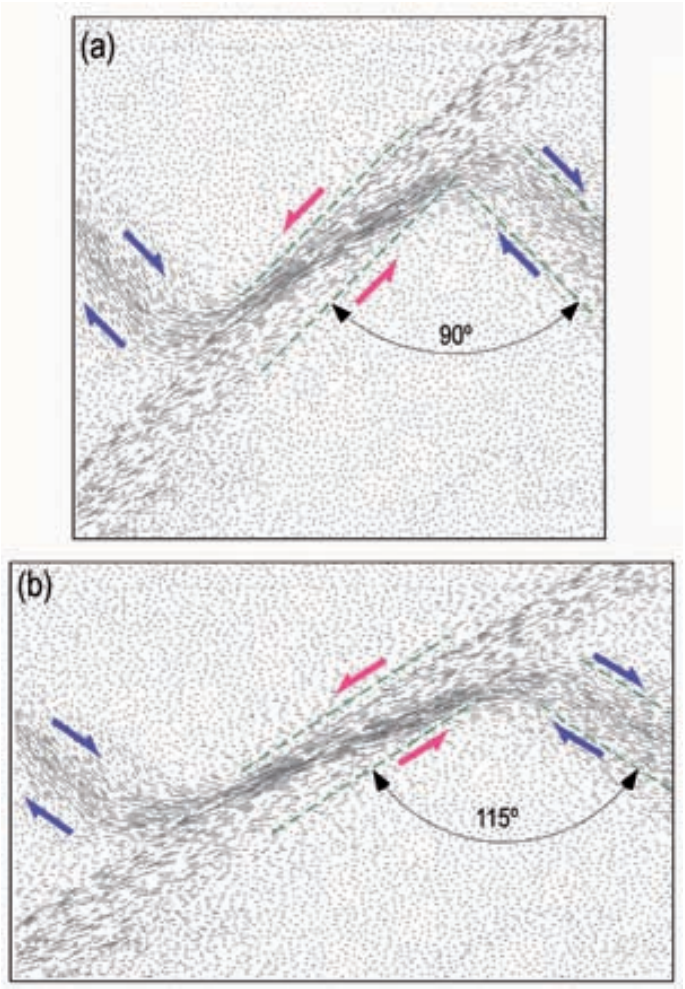

Fig. 2.8. Schema showing the development of obtuse angle facing the bulk shortening direction achieved by combination of deformation localized on conjugate, centimetric wide shears and bulk superimposed homogeneous deformation. (a) All deformation is accommodated in the shear zones. (b) shearing plus homogeneous deformation cause the gradual angle opening.

It has to be taken into account that the explanation illustrated in Fig. 2.8 is adequated if the bulk strain is coaxial. In the more common settings where bulk deviation is non-coaxial, although the initial angle is close to 90°, under increasing shear one set (the synthetic one) prevails over the other and angles between both change depending on the orientation of each sets with regard to the ISAs. Thus in isotropic rocks ductile shear zones form conjugate sets with obtuse angles facing the bulk shortening direction.

In anisotropic/foliated rocks the initial orientation of shear zones is far more complex because the degree of anisotropy and/or viscosity contrasts and the relative orientation of the anisotropy plane with regard to the ISAs are the most important factor. This concept has been already presented in the introductory chapter, and field evidences highlighting this point will be presented in this section. Carreras (2001) proposed that the initial prevalent orientation of shear zones along the Cap de Creus Norther shear belt is strongly influenced by the orientation of the preexisting dominant foliation relative to the regional strain axes. Different areas have been chosen to test this idea. Best adequated places are those where shear zones are discrete and isolated. The conjugate sets of shear zones from North of cala Prona are presented (Fig. 2.10). The absence of significant shear-related deformation outside the shear zones and the low shear values associated to each shear zone suggest that the initial angular relationships between foliation and shear zones represent initial stages. From the data presented in Figure 2.10 it follows that: (i) shear zones already nucleated

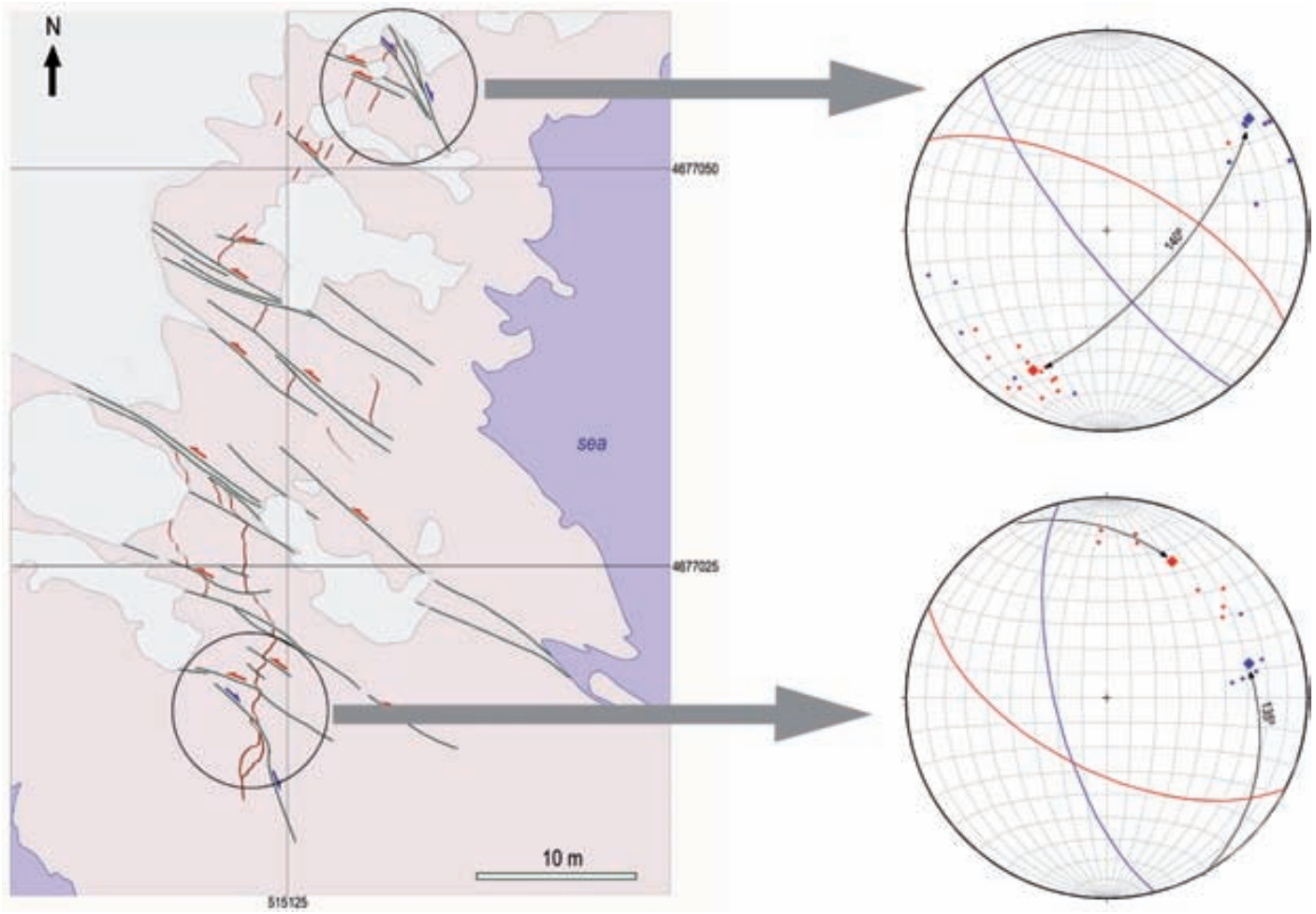

Fig. 2.9. Conjugate shear zones in Roses. Local conjugate set of shear zones are present on a dextral strike-slip shear belt. Circles correspond to areas where conjugate sets are present. Stereoplot show the mean attitudes of shear planes (blue: dextral set, red: sinistral set). Values of obtuse angles facing the regional shortening are given.

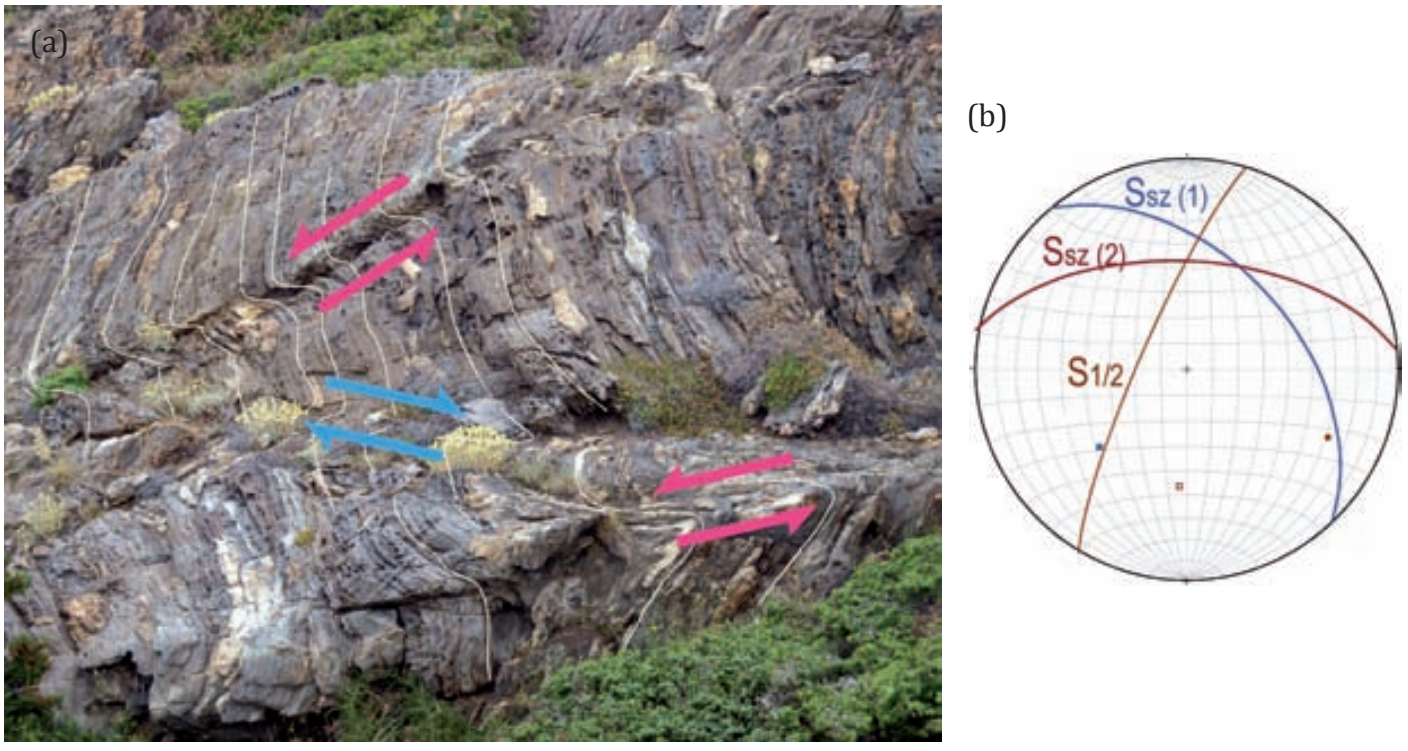

Fig. 2.10. Incipient conjugate shear zones affecting schists (Punta dels Farallons, Cap de Creus). (a) Drawing of the foliation traces and arrows indicating the incipient shear zones. Width of view: 6 m. (b) Stereoplot of the shear zones orientation showing how the obtuse angle is facing the shortening direction and the pre-existing foliation is bisecting such angle.

with obtuse angles facing the main shortening direction; (ii) this angle is roughly bisected by the preexisting foliation; (iii) individual shear zones display a fold-like geometry. These facts are in agreement with experimental works (Cosgrove, 1976; Williams and Price, 1997) suggesting that the shear zones development are governed by similar principles as shear bands, crenulations or kinks in foliated materials. In this particular setting the bulk ISA's are aligned closely parallel to the rock anisotropy planes causing the appearance of conjugate sets.

Along the cala Serena valley (Cap de Creus) shear zones abound. There, shear zones form a prevalent dextral set. At the margins of the main shear zone, incipient shear zones with restricted displacement can also be observed. The relationships between shear zones and previous foliation have been analyzed in a small area (Fig. 2.11).

The analysis of this area reveals that the orientation of the dominant foliation determines the presence of a single set of dextral shear.

A consequence of the presented field data is that initiation of shear zones is controlled by the preexisting anisotropy of the rocks. This is in apparent contradiction with the interpretations where shear zone initiation depends on the presence of preexisting fractures (Pennacchioni, 2005) or shear-related brittle fractures. The first hipothesis can not be ruled out because in a similar way that foliation controls the orientation of nucleating shear zones, the presence of brittle fractures (e.g. joints) can also controls the localization and orientation of the forming shear zones. In the analysed areas this is not the general situation, but can be the case in local situations where: (i) there is a widespread sets of pre-shear joints and (ii) where this joints are favorably oriented to accommodate shear strains. The presence of joints normal to foliation is specially developed in some ar-

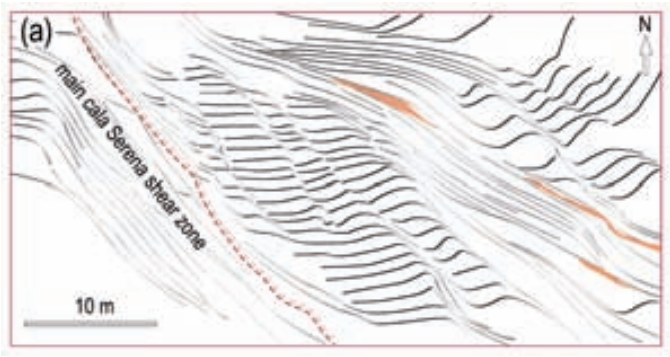

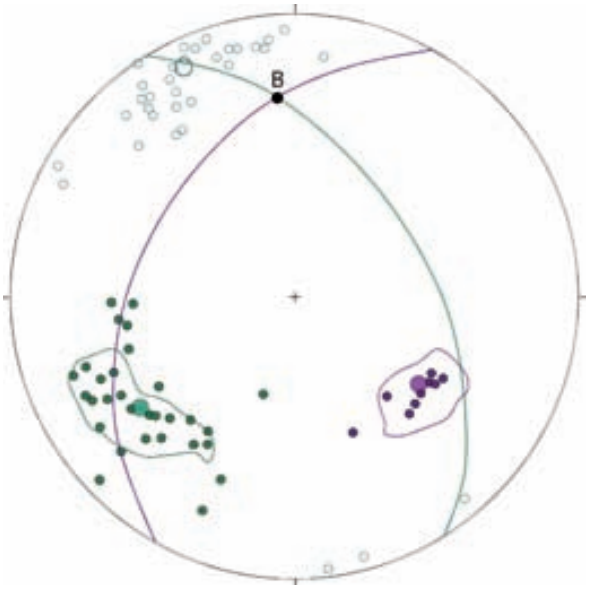

Fig. 2.11. (a) Sketch of the minor shear zones formed at the NE margin of the cala Serena shear zone. (Dashed line correspond to the trail. (b) Stereoplot of 40 mylonitic foliation (Sm) planes (green circles) and 33 associated stretching lineations (open circles). The attitude of the dominant foliation (Sd) is shown by 9 poles (violet circles). Great circles represent the mean attitudes of Sm and Sd planes. In this particular case the angle between Vorticity Axis (B) and the shear direction is < 30°. 5% contours are shown.

Fig. 2.12 Incipient shearing along preexisting joints formed normal to the foliation. Width of view: 3 m (Punta des Noraix, coastal cliffs north of the Cap de Creus lighthouse).

eas like north of the Cap de Creus lighthouse. There is some evidence of shearing localizing parallel to this joints (Fig. 2.12).

The alternative hypothesis for the existence of brittle precursors is more debatable. Although minor fractures abound at the margins and tips of shear zones, these can be interpreted as contemporaneous to the shear zone development in small domains of high stress concentration and higher strain rates. It is a common fact that most folds are associated to fractures and joint development (Fig. 2.13). On the contrary there is strong evidence of brittle deformation following ductile stages.

Fig. 2.13. Fold-related shear zones (D3) show late embrittlement stages associated to veining. Width of view: 1 m (Es Camell, Cap de Creus).

2.3. INTERACTION OF SHEAR ZONES

Once a shear zone is initiated, propagation proceeds under progressive deformation. At this stage, initially confined shear zones approach each other and stress perturbations interfere. Thus, as result of stress perturbations, shear zones deflect generating an anastomosed pattern. The different causes for stress perturbation and hence anastomosing were outlined in subchapter 1.1.2. Anastomosing pattern is the basis of tectonic lozenge formation. When there is a high density of shear zones in an area, it is very common to find shear zones crosscutting one another. If the shear zones involved in the crosscutting are inactives, the younger does not only predates the older one but drag the mylonitic fabric formed by this towards its kinematic sense, developing a wedged coalescence (Fig. 3.42; Duebendorfer and Christensen, 1998; Passchier and Coelho, 2006; Druguet et al., 2009, Carreras et al., 2010). However, if they are actives when the crosscutting is taking place, then the kinematics at the junction become much more complex as there is kinematic interplay between both shears (Lamouroux et al., 1991; Harris, 2003; Pennacchioni and Mancktelow, 2007). Experimental data show that when active shear zones interconnect, not all individual shears are simultaneously active (Williams and Price, 1990; Mancktelow, 2002; Carreras et al., 2010). Thefore, there is a big spectrum of kinematic situations at the shear zone intersection, being very common to find kinematic indicators of both senses when the crosscutting shear zones are antithetic and very difficult to deduce the sequence of shear pulses at the junction.

Propagation is controlled by different factors, among them the rock properties (homogeneous/inhomogeneous, isotropic/anisotropic). The propagation of a shear zone also approach lithological boundaries associated to competence contrasts. The diversity of factors involved in shear zone propagation originates a wide range of shear zone interaction patterns.

Detail maps showing different examples of shear zone interaction will be presented on the basis of different original properties of the sheared rocks.

(i) *Lithology is homogeneous and isotropic with shear zones having same kinematic sense.*

Under this setting, although situations with parallel propagation with no interaction can be observed (Fig. 2.14), curvatures are commonly formed (Fig. 2.15) giving rise to sheaz zone interconnections.

Fig. 2.14. Two parallel shear zones across a granodiorite. Shear zones are almost parallel, the upper one show strain perturbations at the tip of the shear zone (C: compressional domain) but no deflection is observed in spite of the nearness of both shear zones. Lower shear zone width: 2 cm (Roses lighthouse, Cap de Creus).

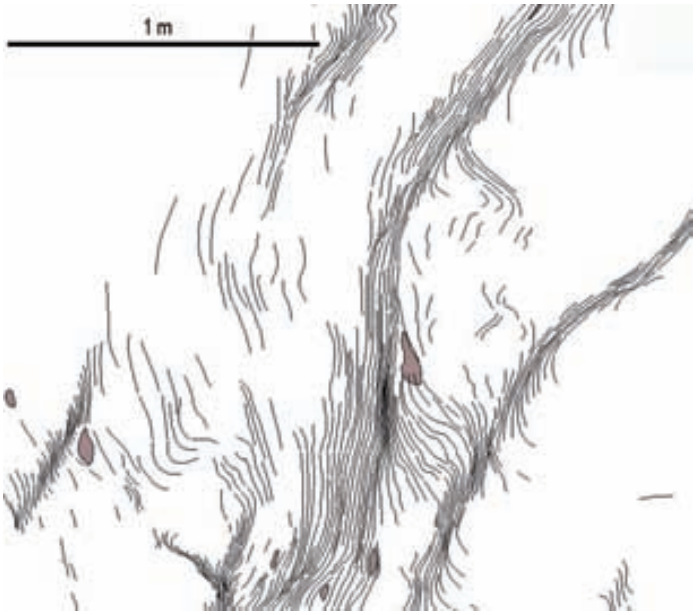

Fig. 2.15. Set of dextral shear zones. The curvatures of the shears enhance interactions (Laghetti area in the Maggia Nappe, Helvetic Alps).

Fig. 2.16. Sets of conjugate shear zones. Conjugate shears enhance high angle intersections (Laghetti area, Helvetic Alps).

(ii) *Lithology is homogeneous and isotropic with shear zones forming kinematically conjugate sets.*

Under this setting, the propagation of the initial differently orientated conjugate sets will necessarily lead to shear zone interferences. Although both sets are roughly coeval, the observation of a shear zone being displaced by the conjugate one is quite common (Fig. 2.16). However, the relative chronology in interfering spots of conjugate shear zones is not always easy to determine, and a complex damage zone forms. The angular relationship is also highly variable while in the example shown in Figure 2.16 is close to 90°, in the example shown in Figure 2.17 it is obtuse and close to 140°. This angular relationship will control the initial shape of the resulting lozenges.

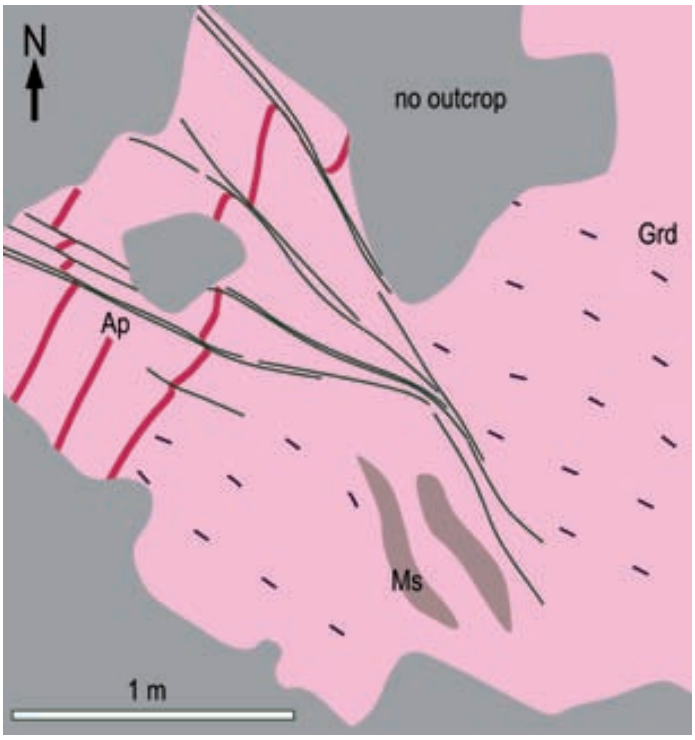

Fig. 2.17. Low angle conjugate sinistral and dextral shear zones in the Roses granodiorite (Grd). The fact that shear zones involve minor displacement and aplite dykes (Ap) are not deformed outside the sheared domains, suggests that the angle between both sets is not due to superimposed deformation and is rather a primary feature (Ms: metasedimentary enclaves; E of Roses Lighthouse).

(iii) *Lithology is inhomogeneous*

Crystalline rocks often include bodies of irregular shape that result from intrusions and/or partial

melting. In such a setting, propagation of shear zones is strongly influenced by the presence of ductility contrasts. Only non-systematic inhomogeneities like intrusive bodies will be considered here, systematic planar inhomogeneities like bedding or foliation will be analyzed ahead. Two situations have been observed. When the propagation of the shear zone faces a more competent rock body, shear zone tends to deflect an localize along the boundary if this is in the appropriate orientation (Fig. 2.18a). This is not the case when shear zone reaches the lithological boundary at a high angle. There, the shear zone is forced to propagate across the rigid body (Fig. 2.18b), initially generating a narrowing of the shear zone when crossing the rigid body. Once the rigid body has been split by the shear zone, the shearing also affects the competent body and a narrow high strain zone can be observed at the boundary of the rigid body (Fig. 2.19).

Fig. 2.18. Propagation of a shear zone affecting pegmatite dykes. (a) The shear zone is parallel to the trend of the dyke boundary thus the shear zone splits into two shears bounding the pegmatite (Cala Culleró, Cap de Creus); (b) the shear zone strikes normal to the pegmatite walls. The shear zones localizes along a very narrow zone cross-cutting the dyke. Width of view: 6 m (Clot de la Vellosa, Cap de Creus).

Fig. 2.19. Shear localizes mainly in the schists (dark) and affects only a few centimetres wide zone of the pegmatite border producing a drastic grain refinement (Cala Francaló, Cap de Creus).

A second situation arises when the existence of less competent bodies control the propagation of a shear zone. This can be the case where, e.g. fine grained phyllosilicate-rich rocks are located inside a more competent feldspar-rich rock. No general rules can be given because, e.g. the relative competence between basic and granites rocks depends on temperature. A second possibility arises when magmatic rocks emplace syntectonically and then the strain tends to localize on the hot intrusion. Examples showing shear localization along basic rocks emplaced in granites occur often in the Pan-African dyke swarm emplaced in the Eburnean basement in the Anti-Alas inlayers. In this particular case shear localization can be interpreted as the result of deformation occurred during cooling of the dykes (Carreras et al., 2006) or the result of later localization because of alteration and fine grain textures of the dykes (Figs. 2.20 and 2.21).

Under these rheologically inhomogeneous settings, the propagation and interaction of shear zones will be strongly influenced by the initial shape and distribution of rock heterogeneities. In general, where more competent rocks form irregularly or lensoid-shaped bodies, the shear zones

will adopt an irregular anastomosed pattern with shear zones bounding lozenge-shaped bodies of competent rock (Fig. 2.22).

Fig. 2.20. Shear zones localize sub-parallel to basic dykes. Shear related foliation forms obliquely to the dyke. Shear localizes preferentially at the margins of the dyke in contact with undeformed granites. Width of view: 1 m (E of Tazenakht, Zenaga Inlier, Anti-Atlas, Morocco).

Fig. 2.21. Shearing is localized on a basic dyke (B.D) giving rise to a oblique mylonitic foliation. Dyke cross-cuts schist bearing a prevous foliation (Sd). Outcrop surface is horitzontal (Azerbi, Kerdous Inlier, Anti-Atlas, Morocco).

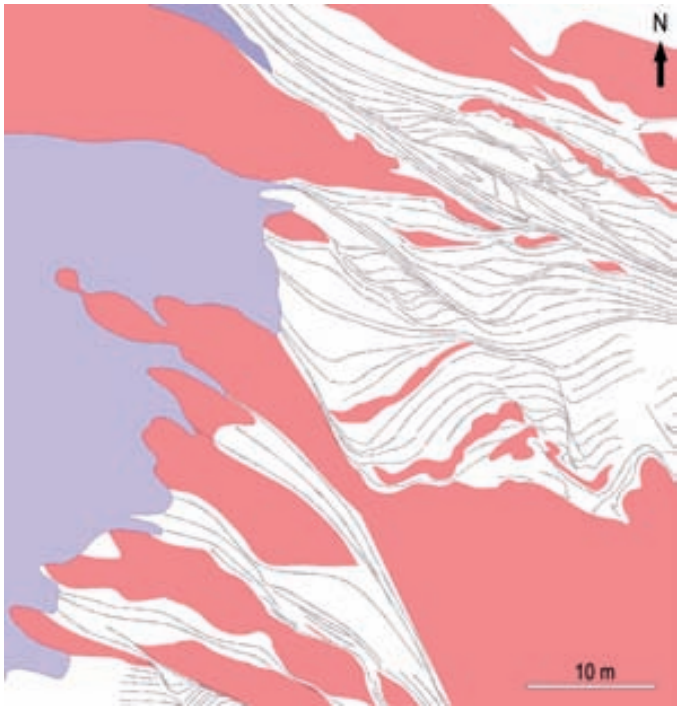

Fig. 2.22. Complex anastomosed pattern where the shear zone distribution is strongly influenced by the irregular shapes of the pegmatite layers (red). While pegmatite boundaries oriented at high angle to the dominant NE-SE trending shear zones impede the propagation of shear zones, boundaries sub-parallel to the shear zones exhibit strongly mylonitic borders. Cala Cullero (Cap de Creus).

(iv) *Lithology is anisotropic and or banded*

This is the most common situation analyzed in this work. There are two aspects where anisotropy plays an important role: (1) the initial pattern of nucleating shear zones and (2) the propagation of shear zones. Where conjugate systems form, the patterns arising from interactions share similarities with those described for isotropic rocks but with complex folding generated due to drag foliation where conjugate shears meet (Figs. 2.23 and 2.24).

Alternatively, and depending on the orientation of the preexisting anisotropy, a prevalent set of shear zones may form. Although initially theymay form sub-parallel (Fig. 2.25), propagation generates interconnection and intersection. Some of this arise from stress perturbations when two tip zones approach. However, in anisotropic/banded rocks there is a possibility of shears occurring parallel to the preexisting surfaces. In cases where shear zones initiate oblique to anisotropy it can be assumed that it occurs because of the

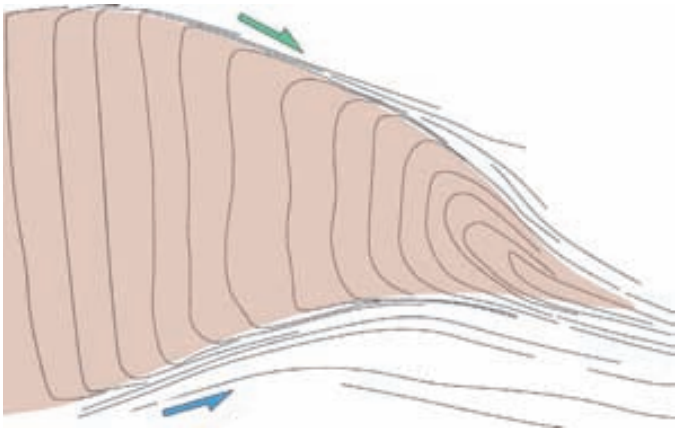

Fig. 2.23. Coalescence of conjugate shear zones (green arrow: dextral/reverse; blue: sinistral normal). Sketch corresponds to an inclined section dipping towards the front. Width of view: 4 m (Cala d'Agulles shear zone, Cap de Creus).

Fig. 2.24. Complex folding at the coalescence of conjugate shear zones. Sub-horitzontal outcrop (Cala Serena shear zone, Cap de Creus).

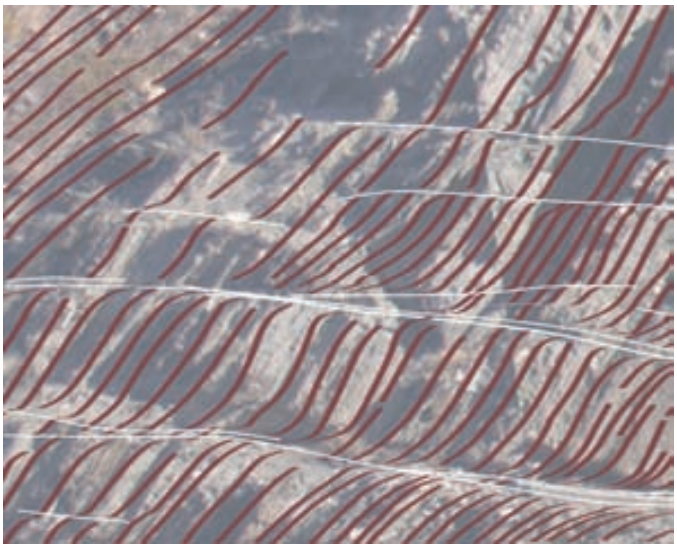

Fig. 2.25. Set of parallel dextral shear zones with low interaction between individual shears. Subvertical section. Width of view: 5 m (Cala d'Agulles shear zone, Cap de Creus).

non-favourable orientation. However, stress perturbations during shear zone propagation and strain compatibility requirements cause shearing parallel to the anisotropy/layering to occur (Fig. 2.26-2.28). This is a common situation that can be recognized by the presence of wedges, and it can be observed along many shear zones.

Fig. 2.26. Layering/foliation-parallel antithetic shear on a dextral shear zone originating a wedge structure in the main shear zone. Outcrop surface is sub-vertical. Width of view: 3 m. (Cala Prona, Cap de Creus).

Fig. 2.27. Wedge structures arising from the interaction of layer/foliation parallel shear (pink) and secondary shears (blue) crosscutting the previous foliation. Width of view: 2 m (Clot de la Vellosa, Cap de Creus).

For particular orientations of layering/foliation, shear zones can nucleate and propagate parallel to the lithological boundaries and foliation. This is the case when two conditions are fulfilled: (1) appropriate orientation and (2) low competence. An example of this setting is analyzed in detail in Druguet et al. (2009). In such a situation, the bulk deformation is accommodated by main shears parallel to the lithological boundary and secondary shears oblique to the layering/foliation. The results is also the development of wedge structures (Fig. 2.27). Figure 2.28 shows a comparison of the two types of wedge structures arising from interaction of shear zones developed in layered/foliated materials.

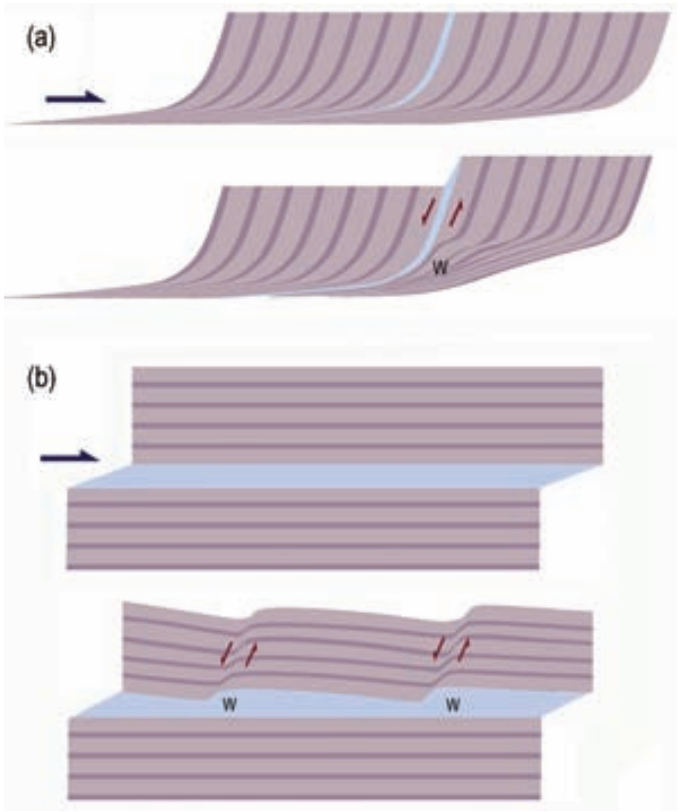

Fig. 2.28. Two models of secondary shears. (a) Main shear is oblique to previous foliation while antithetic secondary shear develops parallel to foliation/bedding. (b) Main shear is parallel to bedding/foliation while antithetic secondary shears form oblique to the previous foliation. W: wedges.

2.4. SHEAR ZONE NETWORKS

Propagation of shear zones under progressive deformation leads to increase of shear zone interactions generating anastomosed networks typical of shear belts.

These belts define self-similarity frameworks. The most common situations are (i) the network is built by two sets of conjugated, differently orientated shear zones, the initial arrangement is that of dextral and sinistral shears intersecting at nearly right angles, and the angles progressively open towards the extension direction as a result of increasing strain (Baumann, 1986; Baumann and Mancktelow, 1987; Ildefonse and Mancktelow, 1993; Mancktelow 2002, Carreras et al., 2010); and (ii) the network is set up by one set of synthetic shears but with different orientations. The different orientation of shears of same kinematic sense is achieved by the rotation of the older shear zones towards the bulk shear direction and the formation of new shears with the original orientation of the older ones. The new forming shear zones interconnect to the rotated older ones making a network, which would also rotate and would incorporate new forming shear zones generating an anastomosing network.

These belts allow to analyze the shear zone arrangement from unsheared domains to domains with isolated shear zones to highly sheared domains displaying anastomosed patterns. Tectonic lozenges abound in anastomosing shear zone net-

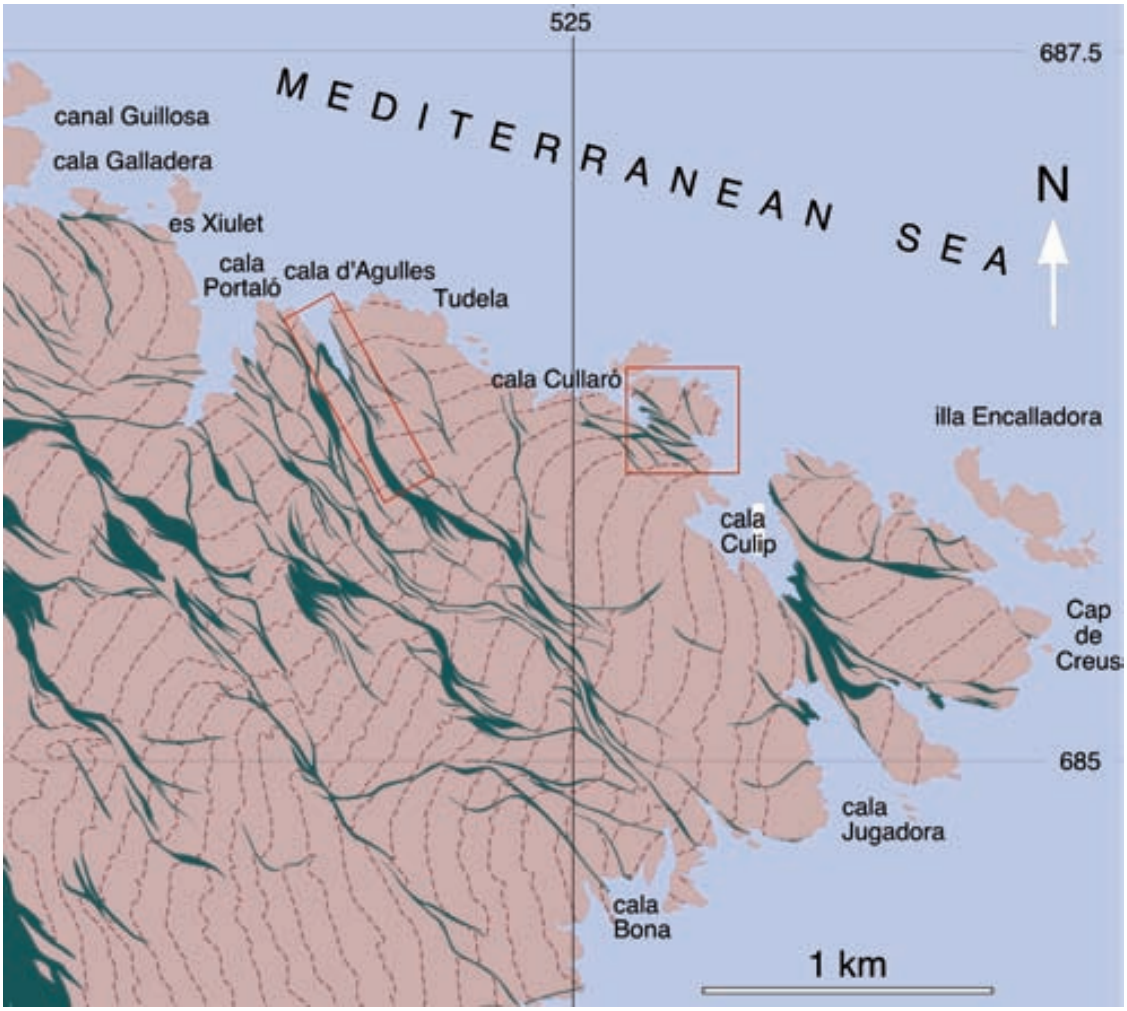

Fig. 2.29. Shear zones (dark green) on the NE part of the Cap de Creus peninsula. Dashed lines correspond to the trace of the previous dominant foliation. Red rectangles indicate location of the areas described in this section. (Redrawn from Carreras, 2001).

works (Figs. 2.31, 2.32, 3.1, 3.8, 3.26 and subchapter 3.1.2). Two areas from Cap de Creus have been selected to examine this arrangement (Fig. 2.29). The Cala d'Agulles shear belt has been studied on a sub-vertical section, while the Cala Culleró belt has been analyzed on a detailed map view. Both enable to focus on the transition from low to high shear domains.

The Cala d'Agulles shear zone

Is a NNW-SEE trending main shear zone on the NE part of the Cap de Creus peninsula. Bulk kinematics of this shear zone is dextral strike-slip, although some sinistral shear zones forming the anastomosed belt have been recognized. The shear zone cuts at high angle a previous foliation that in this area corresponds to the S_2 transposition foliation. The attitude of the S_2 foliation ranges from moderately- to steeply dipping and has a dominant WSW-ENE trend (Fig. 2.30). Pegmatites abound, most of them irregularly shaped, causing deflections of the shear zones due to its competent behaviour. In the northern part of the section, pegmatites are scarce and S_2 foliation has a quite regular attitude (Fig. 2.31). Shear zones at the margin of the belt are quite regular in orientation, and interactions between shear zones are almost absent (Fig. 2.25 and 2.31). Towards the central part of the shear belt the pattern become anastomosed (Fig. 2.31). Three main reasons account for this: (1) the presence of abundant pegmatites, (2) the presence of conjugate shear zones and (3) the interaction between shear zones of identical kinematics. This area is specially adequate because of the well-exposed transition from unsheared domains to an anastomosed shear belt.

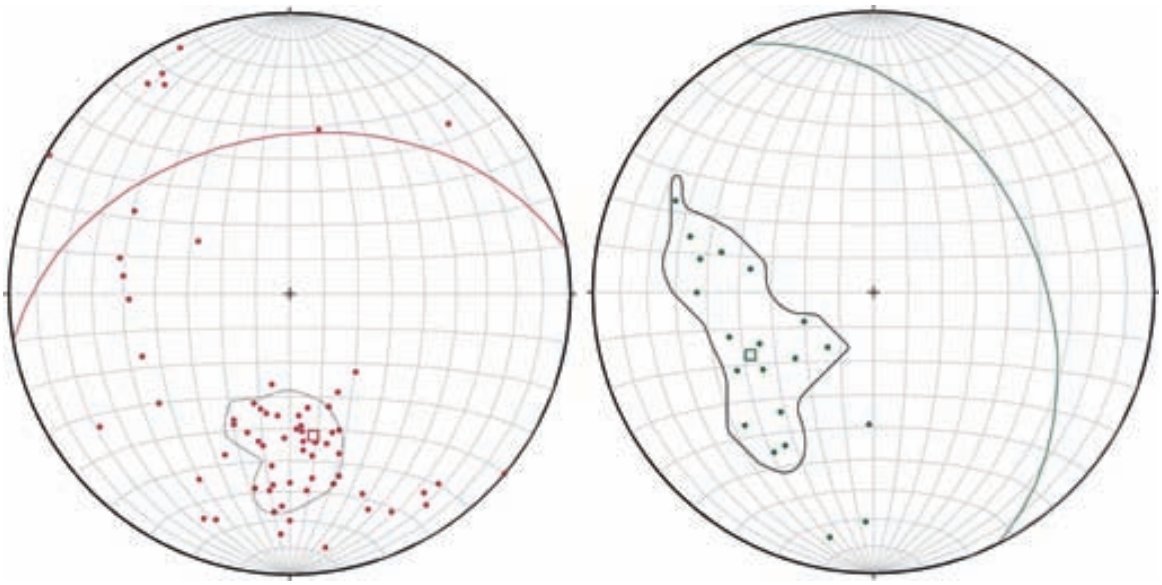

Fig. 2.30. Stereoplots of the attitude of the S2 foliation (left) and mylonitic foliation (right) in Cala d'Agulles. Contours represent 6%(left) and 4% (right). In both plots the great circles represent the main planes.

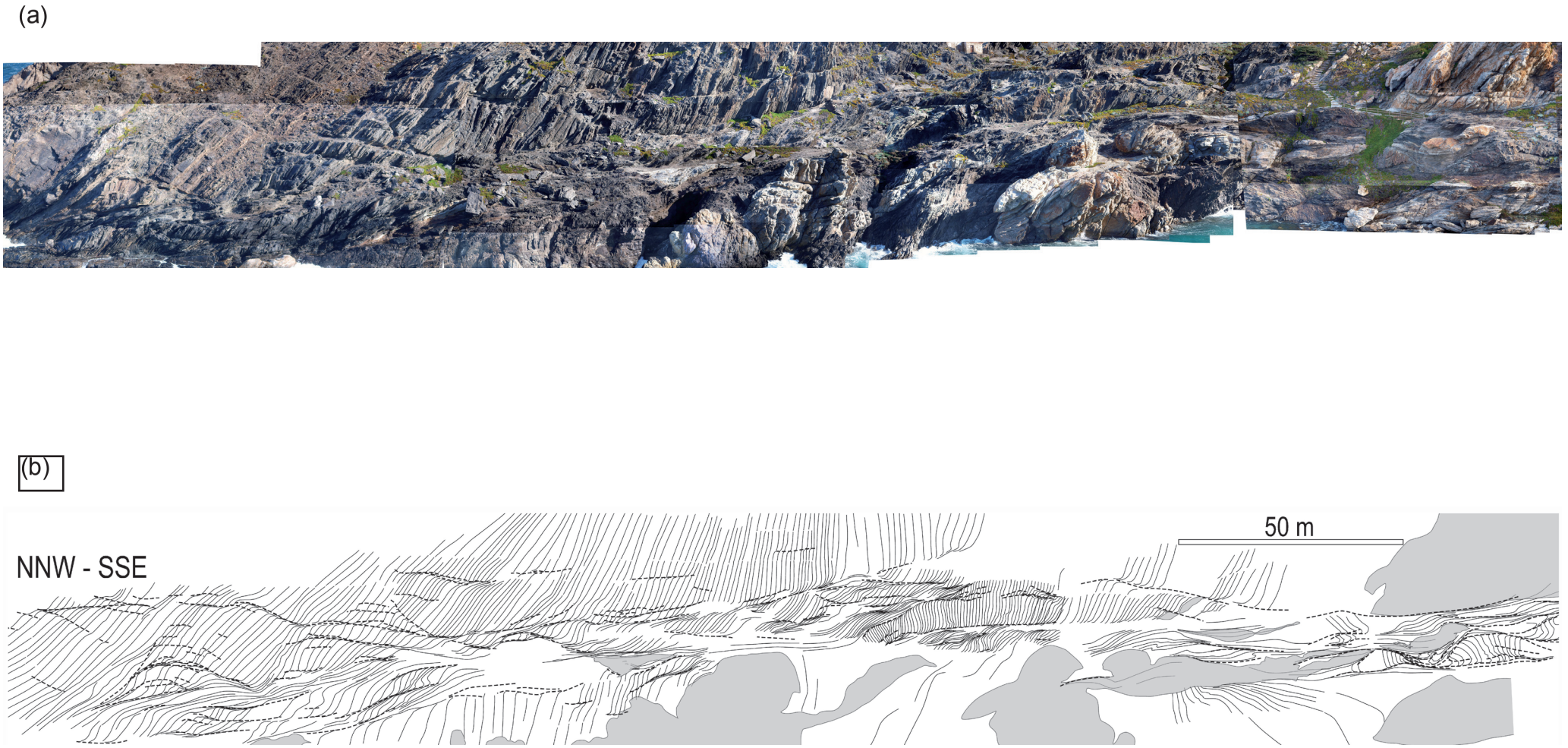

Fig. 2.31. Cala Agulles anastomosed shear belt. The complex pattern is controlled by two factors: (i) the lithological /rheological heterogeneity induced by the presence of irregular-shaped pegmatite bodies and (ii) the presence of minor conjugated sinistral shears.

The Culleró shear zone

This is a NW-SE trending main shear zone located on the NE part of the Cap de Creus peninsula (Fig. 2.32). Dominant kinematic is dextral although conjugated sinistral shear zones can be observed at the northern margin of the belt. In addition dextral NNW-SSE trending shear zones can also be observed. This area furnishes a complementary view of an anastomosed belt in map view that can be compared with the Cala d'Agulles section. The most relevant feature of the Culleró belt is the different attitude of the previous foliation. Along the southern part of the belt previous foliation is a E-W trending $S_{1/2}$ composite foliation while along the northern margin foliation is a N-S trending $S_{s/1}$ foliation. The different attitude of the foliation is a D_2 feature thus previous to the D_3 shearing. This setting enables to study the effects of the orientation of previous anisotropy on the initial orientation and subsequent evolution of the shear zones.

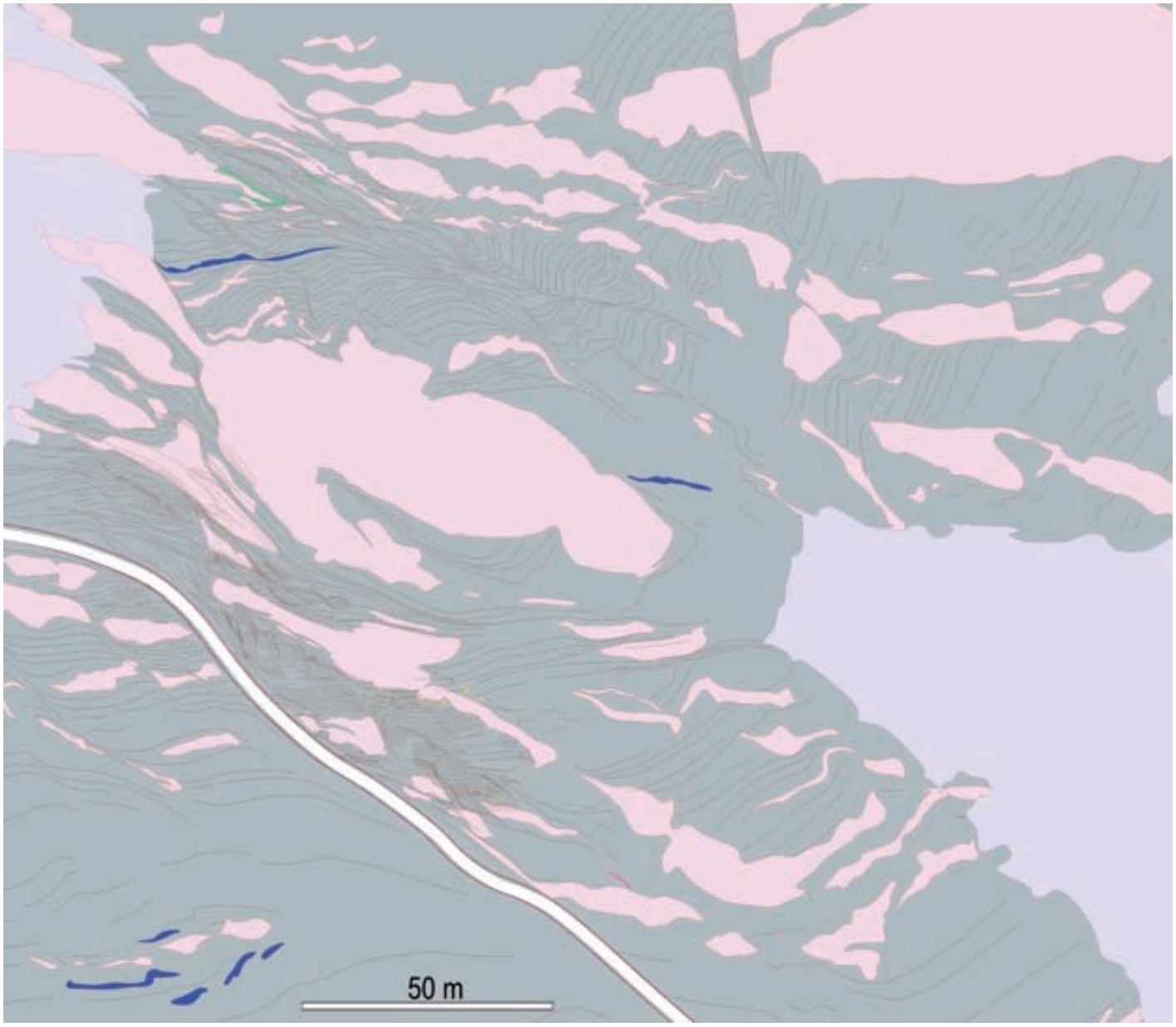

Fig. 2.32. Map of the Culleró shear belt. Traces of dominant foliation (S1/2 outside the shear zones, Sm in the shear zones). Pink: pegmatites; blue: quartzites; green: calc-silicate rocks.

Chapter 3

MODELLING LOZENGES IN ANISOTROPIC ROCKS

3. MODELLING LOZENGES IN ANISOTROPIC ROCKS

According to field observations carried out along the years of this study, the modelling performed and the literature (Carreras, 2001; Fusseis et al., 2006, Le Pourhiet et al., 2012), it can be stated that the best setting for lozenges development is an anisotropic, strongly-foliated rock developing an anastomosing shear zone network (Fig. 3.1).

In non-foliated or weakly foliated rocks few isolated lozenges may form by shear zone intersection (Fig. 3.2a) or lozenges can develop in a harder phase as a sigma-like lozenge within shear zones (Fig. 3.2b, subchapter 1.1.2).

Fig. 3.1. Picture of an appropriate domain for the presence of lozenges: strongly-foliated rocks with harder inclusions (pegmatites) and high heterogeneous deformation developing anastomosing shear zones (Culleró, Cap de Creus, NE Spain).

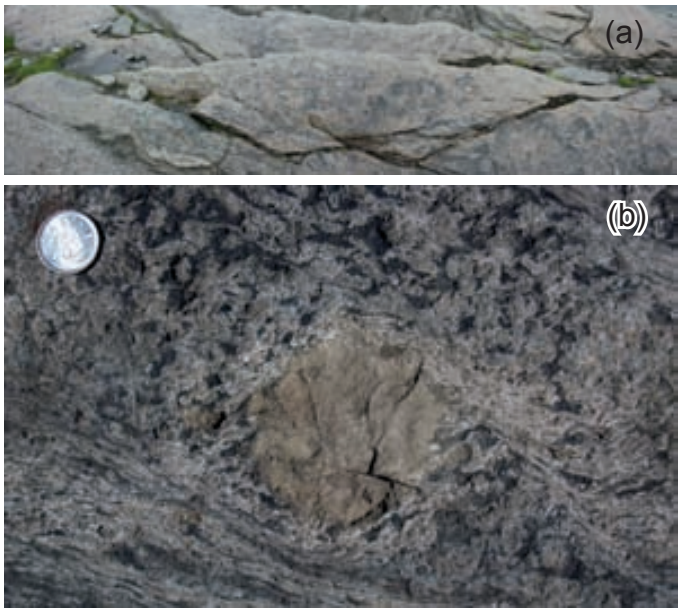

Fig. 3.2 .- (a) Lozenge formed by intersection of two paired narrow shear zones in granite (Laguetti, Switzerland); (b) Sigma-like lozenge consisting on an anorthosite inclusion in weakly-foliated gabbro (Rainy Lake, Canada)

However, not all well-foliated rocks with shear zones develop lozenges. The shear zone system has to be evolved, with a high shear zone concentration forming an anastomosing network with differently orientated shears intersecting and interconnecting (Carreras et al., 2010). Geological settings of strongly foliated rocks having an incipient shear zone system do not give rise to lozenges formed by shear zones interconnections (e.g. North and upper part of Cala D'Agulles; Fig. 2.31b). This is the case of the Chímparra gneiss (Cabo Ortegal, NW Spain; subchapter 1.3.4), that are well foliated rocks but the two sets of conjugate shear zones developed in them do not form a network since both sets are sub-parallel to the foliation (Fig. 1.18), being difficult to find shear zones interconnections or either cross-cutting or dragging the gneissic foliation. In such a highly deformed area, isolated shapes similar to lozenges may be found, either outlined by changes in the foliation orientation or by a cross-section of a sheath fold (Fig. 3.3), rather than by shear zones interconection and intersection.

Moreover, disturbances in the strain field induced by rheology contrasts in the rock favour the nucleation of shear zones (e.g, Rowe, 1962; Wawersik and Brace 1971; Rice, 1976; Ildefonse et al., 1992; Ildefonse and Mancktelow, 1993; Groome et al, 2006), and therefore the later propagation and interconnection of them. This leads to high shear zone concentration and the formation of a shear zone network where lozenges can occur.

Therefore, the best scenario for tectonic lozenge formation is that of an anisotropic, strongly foliated rock with some hard inclusions and an anastomosing shear zone network develops

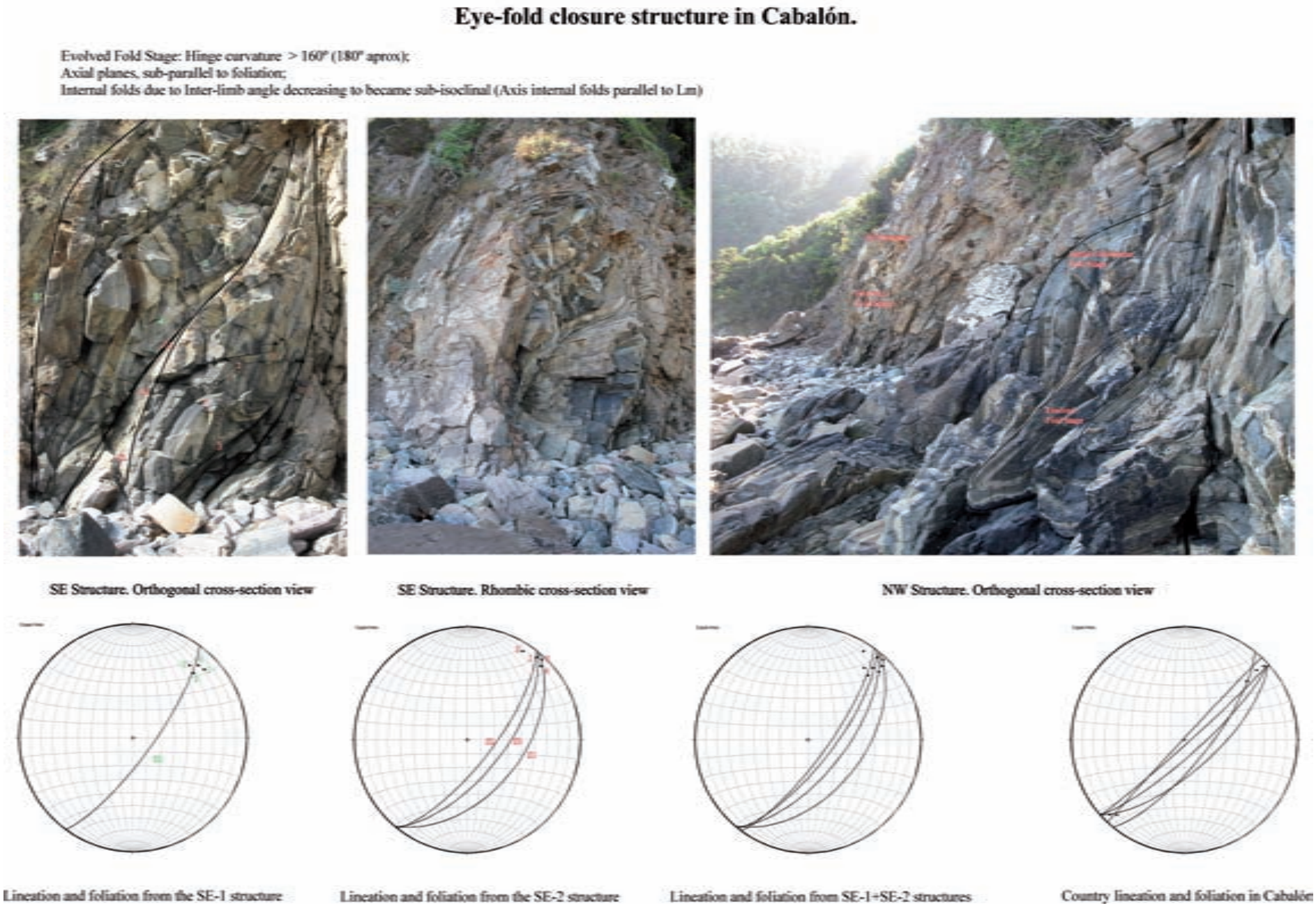

Fig. 3.3. Lozenge shapes at Cabalón (Cabo Ortegal, NW Spain); (a) Pictures of sections of sheath folds showing lozenge shapes; (b) Stereographic representation of the foliation and lineation of the sheath folds and the regional foliation.

Fig. 3.4.- (a) Detail profile drawing of part of the Cala d'Agulles shear belt (sub-vertical profile). This belt affects high-grade schists and pegmatites. In the upper part shear zones are isolated and discrete, whereas in the lower part they anastomose and lozenges abound; (b) Lozenge developed by the intersection of two sub-parallel ductile shears; (c) Lozenges developed by intersection of two differently oriented sets of ductile shears. (b) and (c) are details shown in (a).

throughout (Figs. 3.1, 3.4 and 3.5).

According to this, the geological setting of Cap de Creus is very suitable to produce lozenges. Effectively, from all the field reference areas studied, Cap de Creus is the one displaying more outcrops with lozenges and having the best quality outcrops. Especially, in Nothern Cap de Creus shear belt there are domains with high concentration of lozenges. Two of these domains were selected and worked in detail: Cala de Agulles (Fig. 3.4) and Culleró (Figs. 3.5 and 3.6). The high concentration of lozenges in these two zones made of Cap de Creus the main reference field area for this study.

In other reference areas shear zone-related lozenges are present but scarce. However, the study of lozenge examples from other geological

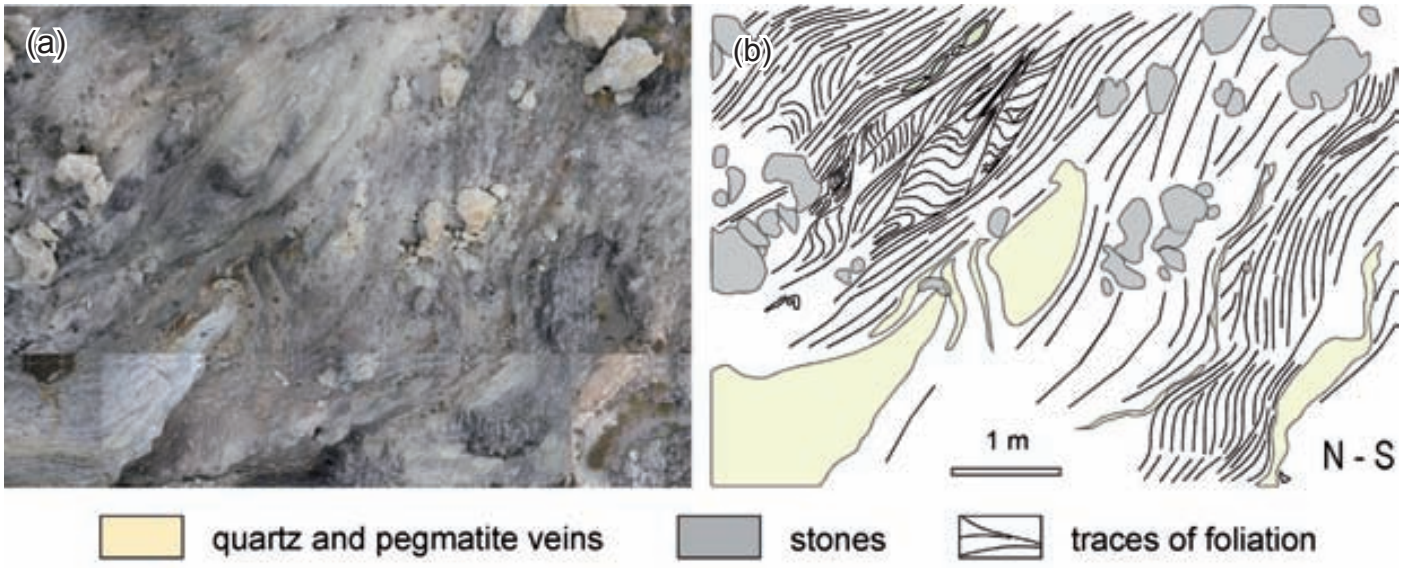

Fig. 3.5. Horizontal section of a part of the Culleró shear belt (Cap de Creus). This domain gives rise to different lozenge types. (a) Picture of the section; (b) drawing of the section.

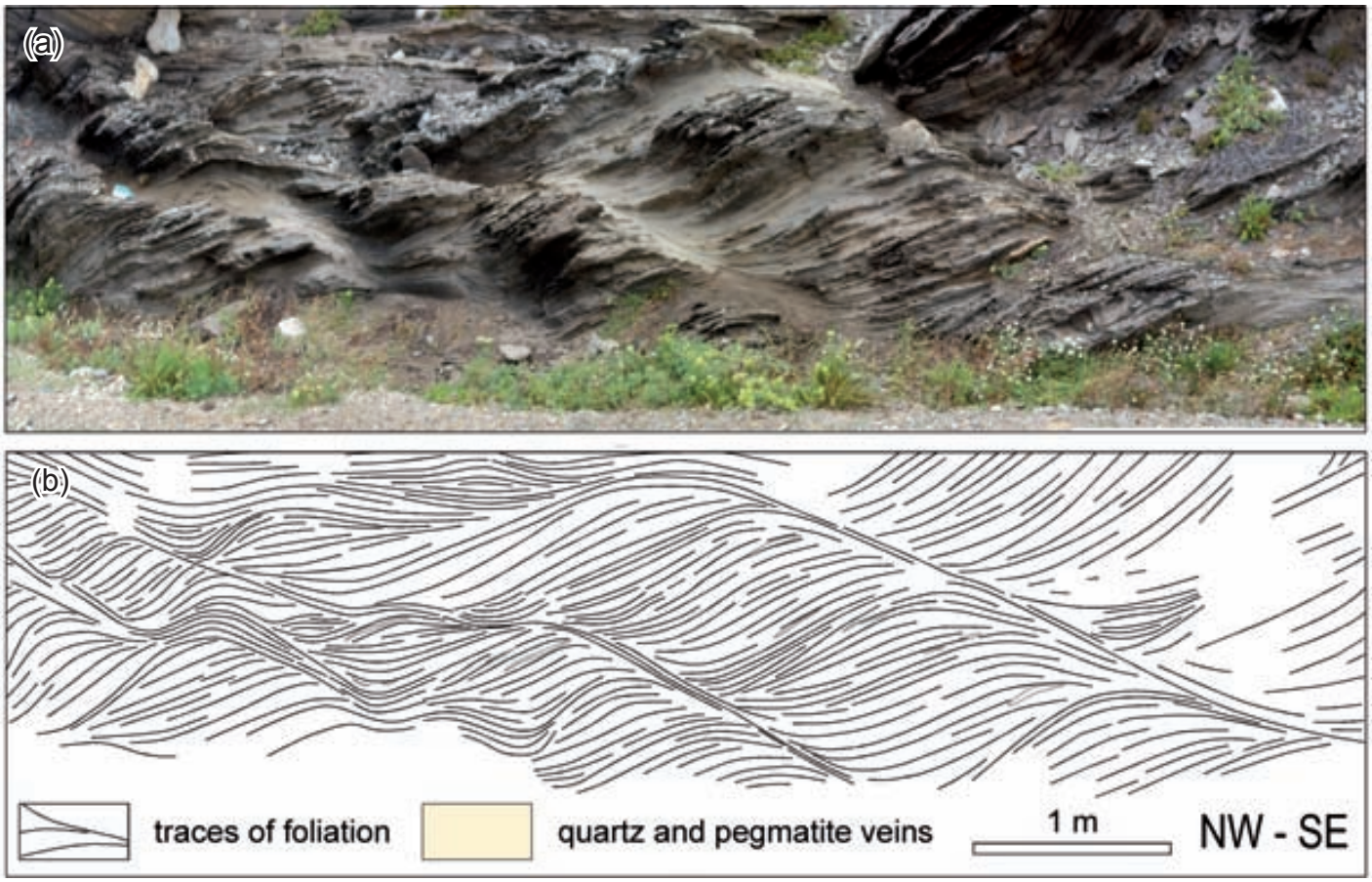

Fig. 3.6. Picture (a) and drawing (b) of a sub-vertical profile of an area with high lozenge concentration in Culleró.

settings has become necessary to build a broad setting for lozenge formation. Figure 3.7 shows some shear zone-related lozenges found in the field areas. These and other lozenges showed in

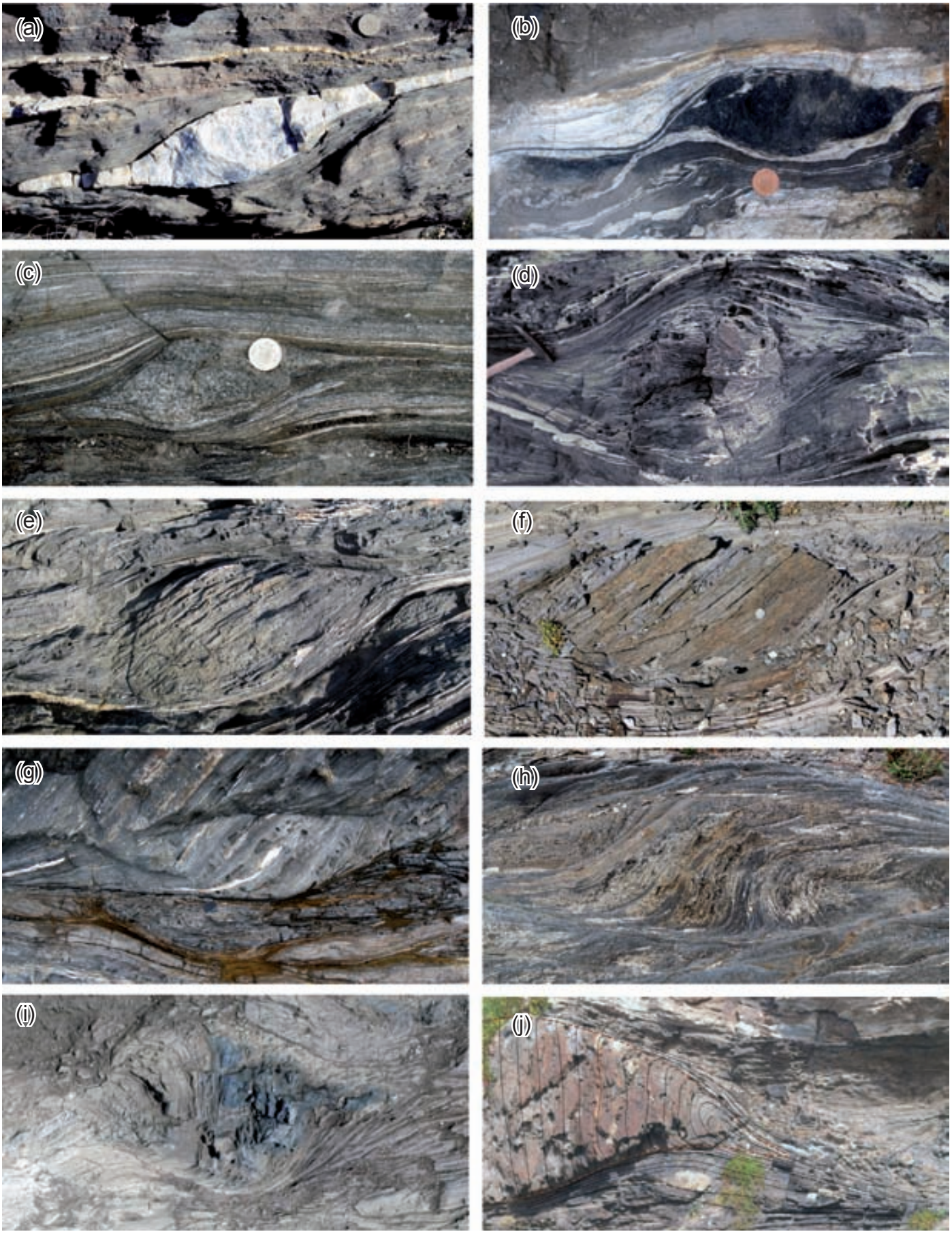

Fig. 3.7. Examples of lozenges from Cap de Creus. (a) Lozenge-shaped quartz vein in mylonitic schists; (b) ; (c) lozenge of granitoid in mylonitic schists ; (d) lozenge in schists preserving previous folds (Cala Prona, Cap de Creus); (e)-(h) lozenges formed by dextral shear zones cross-cutting metasedimentary rocks (different locations at Cap de Creus); (i) and (j) lozenges formed by conjugate shear zones in schists (Cala Prona and Cala d'Agulles, Cap de Creus).

3.1 MODELLING AND REPRESENTATION OF LOZENGES

The results of modelling and graphical representation of lozenges are shown in this subchapter. Since the interpretation from the modelling results will be coupled to the previously presented field information, discussion and conclusions referring to this issue are reserved for Chapter 4.

3.1.1. Numerical modelling

A set of experiments was carried out at Tübingen University through the *Elle* simulation platform (Bons et al, 2008) under the supervision of Post-doc Enrique Gómez-Rivas and Prof. Paul D. Bons. The making up of the experiments was done at the user level, however. A user can simply run precompiled *Elle* binaries over new structures: the user creates a new structure according to the aim of his experiment and change the parameters of an existing process; then, one can run the processes on his own-made structures with his own parameters, but it is not able to create new processes.

The process used for these experiments was the already existing simple shear deformation with dextral kinematic. However, when the experiments were performed (during a 3-months stay in 2010) there was not a suitable localization law in the deformation localization script of this process. The problem of that localization law was that it drastically changed up and down the viscosity values of the flynns (the polygons of the simulated structure, which are defined by bnodes and straight boundary segments connectining the bnodes) in the first time steps. The impossibility of finding a better localization law led to perform the experiments without any localization law. Instead, a structure with strength heterogeneities was created to induce some strain localization (e.g, Rowe, 1962; Wawersik and Brace 1971; Rice, 1976; Ildefonse et al., 1992; Ildefonse and Mancktelow, 1993; Groome et al, 2006). Therefore, the experiments point to the effect of hard phases in a softer anisotropic, multilayer media on the strain distribution, and therefore they are set to analyze lozenges formed in rheological heterogeneous rocks; instead of pointing to the initiation and propagation of shear zones to analyze lozenges in rheological homogeneous rocks, which are more interesting for the aims of this study. For this reason, only a selection of the most relevant experiments are shown, instead of the whole set.

A structure of an anisotropic, equal-thickness multilayer media with two embedded elliptic bodies was created. A similar setting of this structure is North Cap de Creus, which consists of a multilayer of meta-pelites and meta-sammites with harder pegmatites inclusions. By changing the viscosity values of these elements, it was possible to analyze, for different shear strain values, the effect of (i) contrasting viscosity between the multilayer and the inclusions and (ii) contrasting viscosity between layers on (a) the formation of lozenges in rheological heterogeneous rocks and (b) the perturbation of the strain field induced by the competent elliptical inclusions and the competence contrast between layers. The shear strain value was set by the amount of time steps: the higher the number of steps, the higher the shear value.

The frame of the experiments is a square, and it keeps as a square during all the deformation experiment. The frame is not sheared but the flynns inside it. As the flynns are dextrally sheared and displaced away from the fixed squared frame, they are displayed on the left side of the frame. Thus, the structure is sheared and completely

showed inside a fixed square (Videos in Appendix I). All the experiments shown in this report are run without any localization law, thus any strain localization is due to the viscosity contrast. When there is viscosity contrast in the elements of the experiment, the viscosity value of each element is denoted by the colour. the colder the colour, the higher the viscosity. Thus, incompetent materials are in cold colours and competent materials in warm colours.

First experiment to show (Fig. 3.8; Video M1_ isotropic.avi in Anppendix I) is the simulated structure with equal viscosity value in all the elements (hence, no viscosity colour scale), i.e., the multilayer and the inclusions have the same viscosity value and therefore the experiment behave as a rheologically isotropic media:

It can be observed that there is no strain localization and thus the deformation is homogeneous throughout the system.

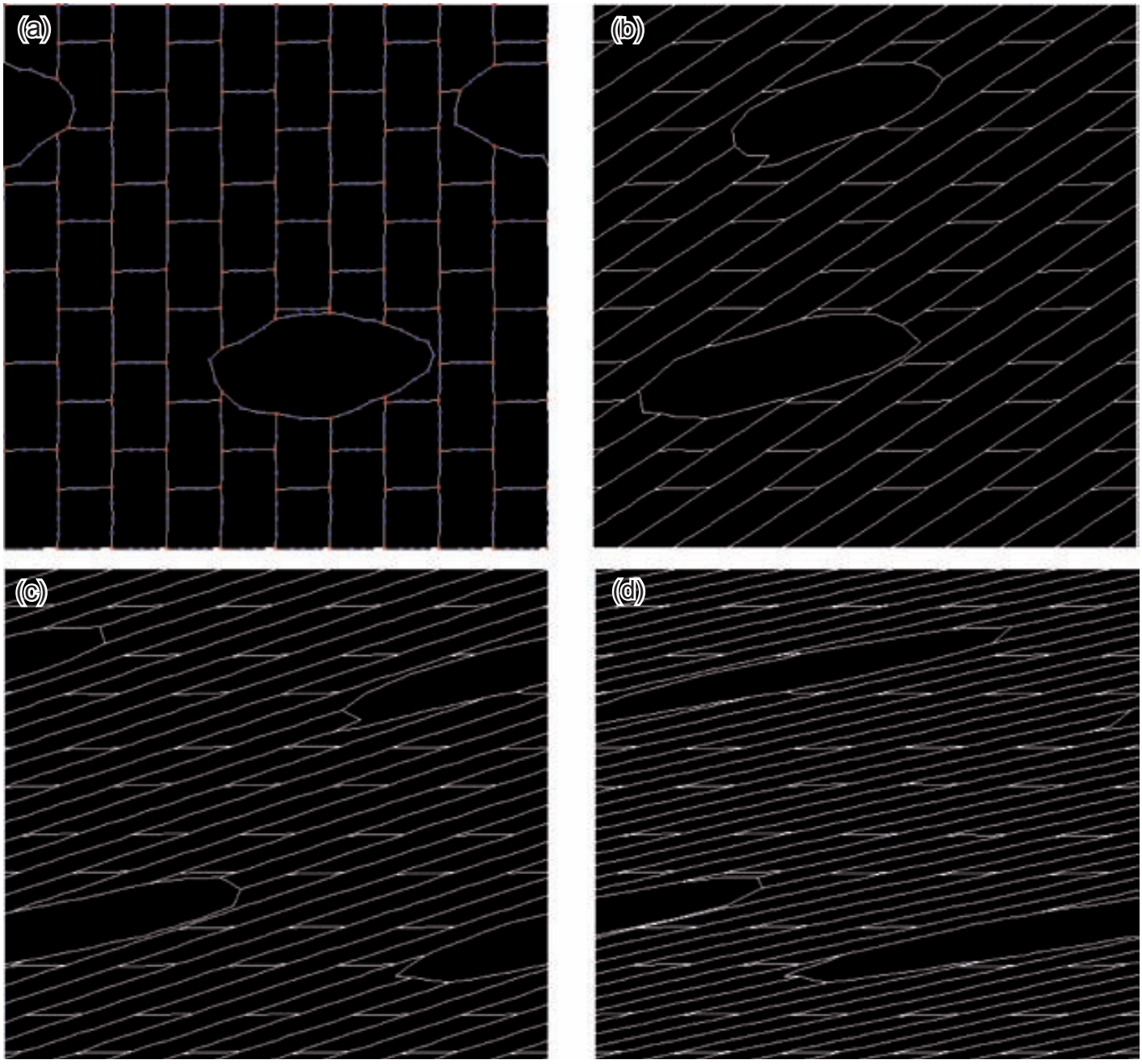

Fig. 3.8. Pictures of an simulation experiment consisting in a structure with equal viscosity value in all the elements (no viscosity colour scale), i.e., the multilayer and the inclusions have the same viscosity value and therefore it behaves as a rheologically isotropic media; (a) time step = 0; gamma = 0; (b) time step = 30; gamma = 1,5;(c) time step = 60; gamma = 3; (d) time step = 90; gamma = 4,5.

Next experiment consist on the same structure with viscosity values set to perform an alternating 'competent' and 'incompetent' multilayer with low viscosity contrast between them and higher viscosity contrast between the elliptical bodies and the multilayer (competence relations 1:2:5, Fig. 3.9; Video M1_1_2_5.avi). The differential strength between the elliptical bodies and the multilayer elements induces perturbations in the strain field and the result is (i) the elliptical bodies deform in a lozenge shape and (ii) there is a strain shadow effect that gives rise to a lozenge shape besides the lower inclusion: the left and right sides of the lozenge are outlined by the inclusions and the up and down sides are outlined by the more strained matrix out of the shadow effect (Fig. 3.9c and d). Other lozenge formed by the strain perturbation produced by the hard phase can be observed right to the upper inclusion (this is more evident in Fig. 3.9 (c) than in (d) because the lozenge in (d) is split by the border frame and is not continuously shown as in (c)).

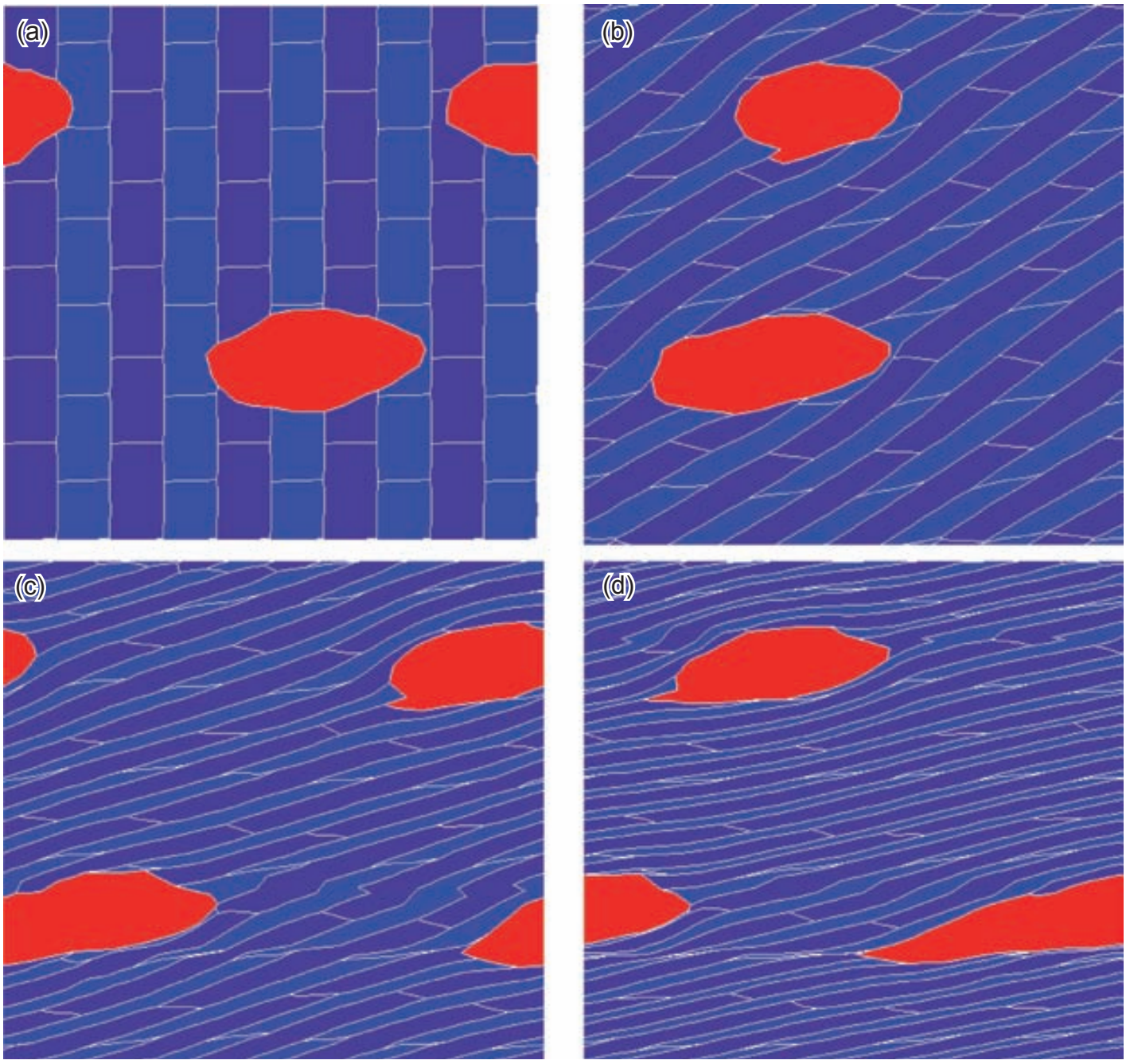

Fig. 3.9. Pictures of an *Elle* experiment consisting on an alternating competent and incompetent layers and two harder elliptical bodies embedded in the multilayer. The competence relations are 1:2:5; (a) time step = 0; gamma = 0; (b) time step = 30; gamma = 1,5;(c) time step = 60; gamma = 3; (d) time step = 90; gamma = 4,5.

Fig. 3.10. Field example of a lozenge formed by shadow effect. The shear zone (dashed line) surrounds a more competent pegmatite body (left side of the lozenge, pink colour in (b)) that makes the shade for the lozenge shape.

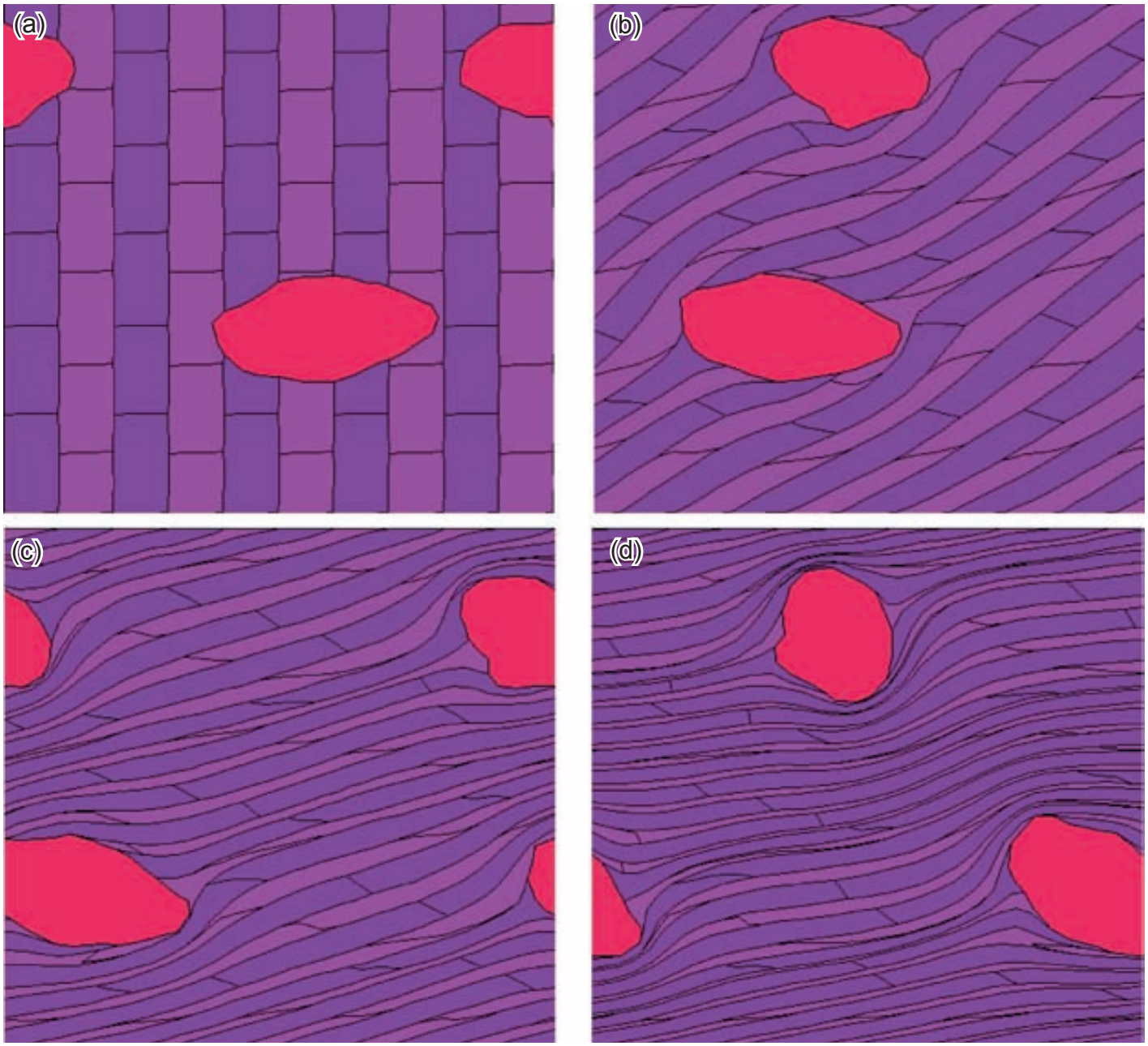

Fig. 3.11. Pictures of an *Elle* experiment consisting on an alternating competent and incompetent layers and two harder elliptical bodies embedded in the multilayer. The competence relations are 1:2:50; (a) time step = 0; gamma = 0; (b) time step = 30; gamma = 1,5;(c) time step = 60; gamma = 3; (d) time step = 90; gamma = 4,5.

Lozenges formed by the strain shadow of a harder phase can be observed in Cap de Creus (Fig. 3.10).

If the viscosity contrast between the inclusions and the multilayer is increased by setting the hard phase more competent (competence relations 1:2:50, Fig. 3.11 and Video M1_1_2_50.avi), the competent inclusions rotate within the much softer matrix instead of deforming. However, the lozenge shape is still achieved as the rotation is added to the shadow effect and thus the right and left sides of the lozenge are more visibles (Fig. 3.11).

Not only the viscosity contrast between the multilayer and the inclusions have effect on the field strain distribution: the viscosity contrast between the layers also influences. Figure 3.12 shows this effect with different viscosity contrasts between incompetent and competent layers (1:2 and 1:1,5; Video M1_1_1'5_5.avi). For the same viscosity contrast between the incompetent layer and the harder phase (1:5), if the viscosity contrast between the layers is higher, then both the strain shadow effect and the hard phase deformation into lozenge shape are enhanced (Fig. 3.12a and b).

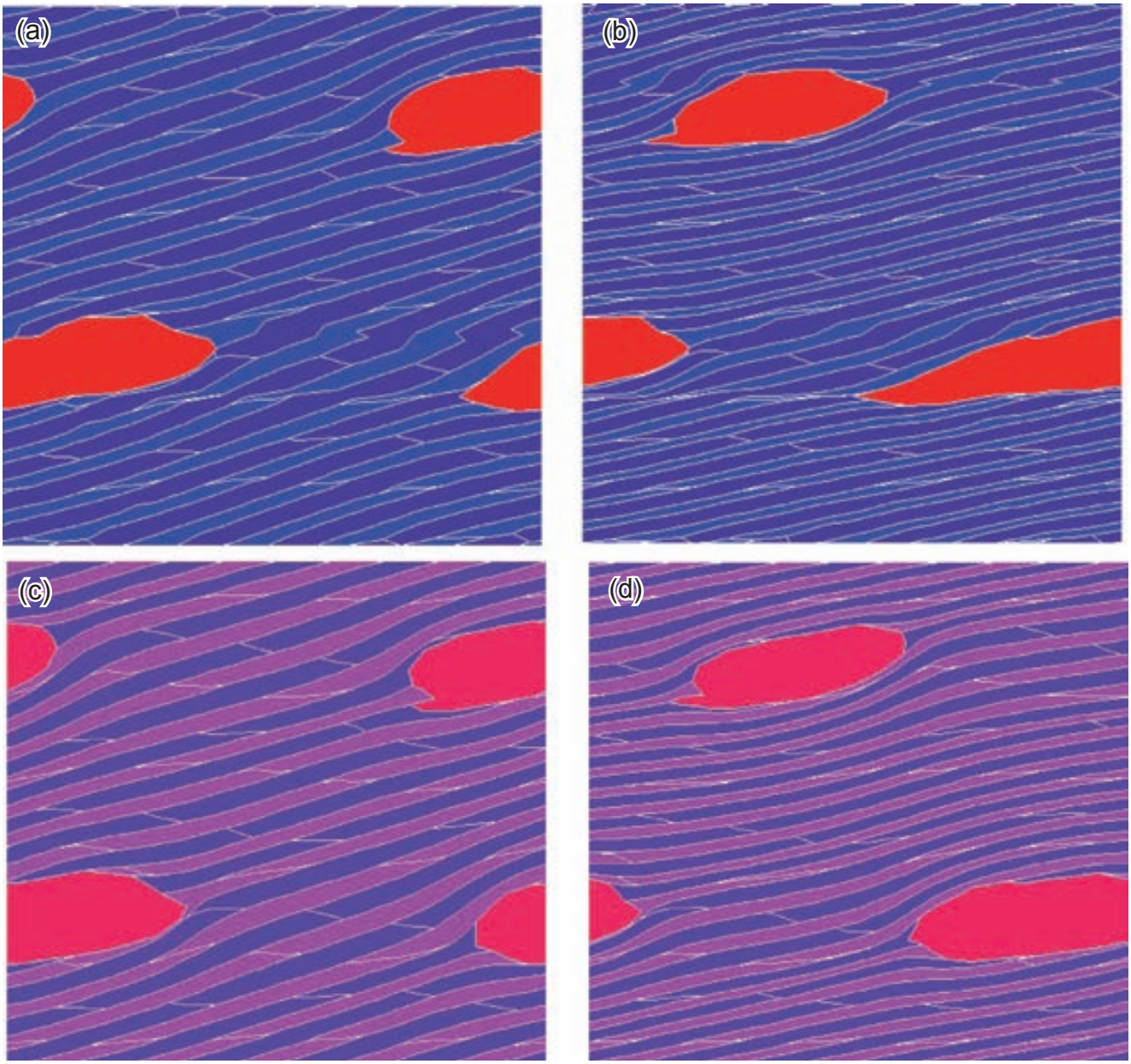

Fig. 3.12. Comparison of two experiments with different competence contrasts in the multilayer (competence contrast of (a) and (b) = 1:2:5; competence contrast of (c) and (d) = 1:1,5:5) and same competence contrast between incompetent layer and hard inclusion to show the effect on the lozenge generated by the shadow effect and by the hard inclusion. (a) time step = 60; gamma = 3; (b) time step = 90; gamma = 4,5. (c) time step = 60; gamma = 3; (d) time step = 90; gamma = 4,5.

3.1.2. Analogue modelling

Analogue modelling was carried out through the BCN-Stage deformation device (Fig. 1.6) at the Universitat Autònoma de Barcelona with the aim of (i) modelling shear zones developing in an anisotropic media, (ii) analyze their interaction and (iii) check the role of shear zone networking in giving rise to lozenges. For such a purpose, several models consisting of a multilayer media were made up and then subjected to deformation under bulk coaxial stress.

Figure 3.13 shows the experiment 14.01. It consists of a plasticine multilayer of four colours: white, purple, yellow and blue. The colours, with slightly different rheologies, have been listed with increasing ductility (see Gómez-Rivas (2005) for the mechanical properties). Layers have a dimension of 15x0.2x10 cm^3 (Fig. 3.13), and aluminium flakes were added at a proportion of 10% in weight to simulate phyllosilicates, since the natural anisotropic rocks from the main field area are metapelites and metapsammites. The multilayer block was built up by the addition of one layer upon another. Layers were added in a systematic order making packs of the four colours, piled up with increasing ductility. They were stuck together by pressing one onto another. The multilayer has a dimension of 15x15x10 cm^3 and a block of 15x7.5x10 cm^3 was added at each side. Thus, the model is 15x30x10 cm^3. The multilayer has a total thickness of 15 centimetres instead of 30 because such thin layers were tedious to create. Thus, these

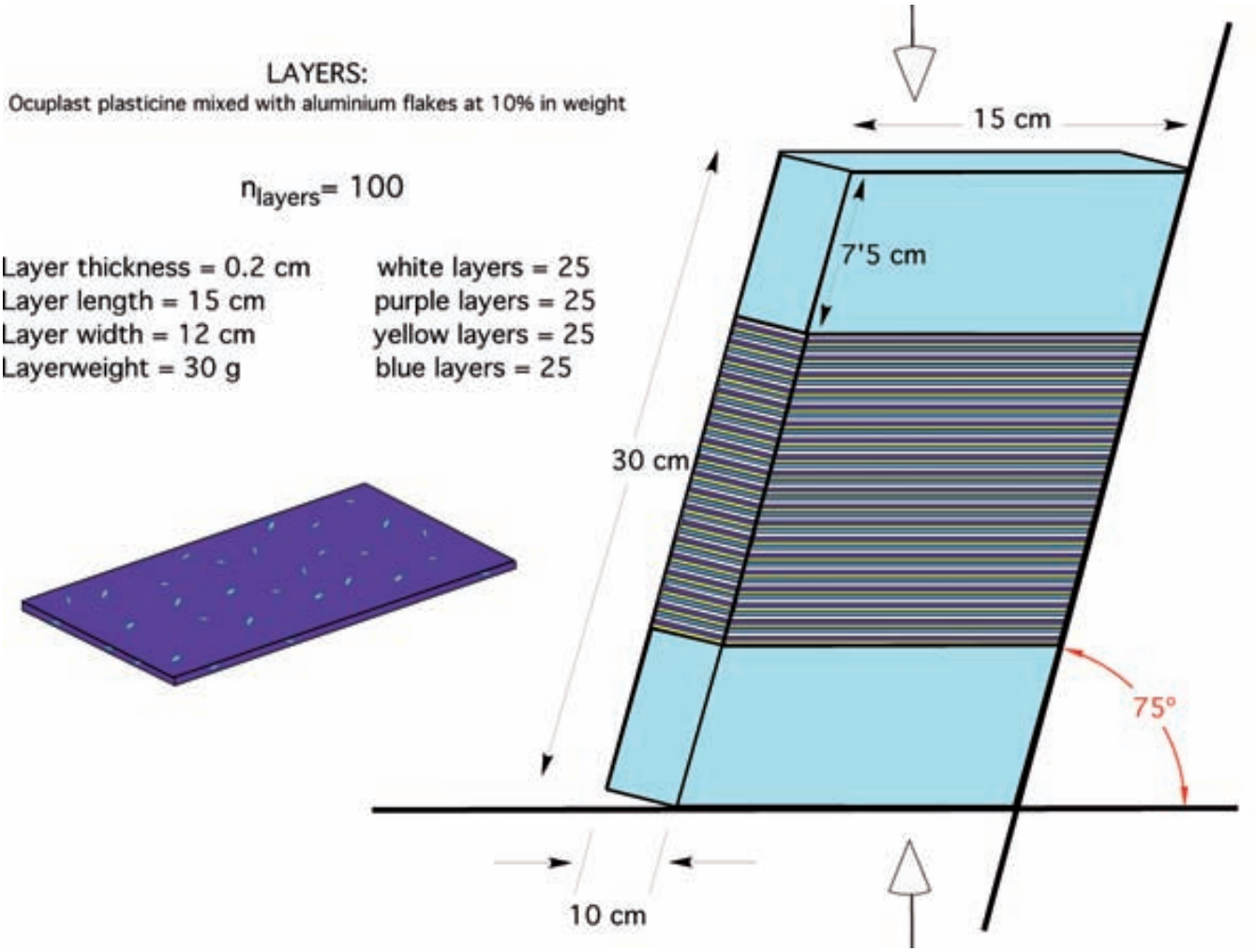

Fig. 3.13. Drawing of model 14.01, made up by 100 layers containning 10% of aluminium flakes in weight and two blocks made by mixing each plasticine type in an equal proportion.

two blocks were made of an equal proportion of each plasticine and were added to the model to get a 30 centimetres block thickness. The base of the model is parallel to the stretching axis but its longest side (thickness) is 15° counter-clockwise inclined relative to the shortening axis in order to add a small component of non-coaxiality to the induced shortening (Fig. 3.13). However, the multilayer is perpendicular to the shortening axis. The experiment was shortened up to 50% (Video Experiment_1401.mov in Appendix II).

Figure 3.14 shows the initial and final states of experiment 14 and Figure 3.15 shows the traces of the shear zones on the final state (Fig. 3.15a; detailed in Fig. 3.15b). Two sets of antithetic shear zones can be observed: sinistral (in red) and dextral (in yellow). The sinistral set is more populated than the dextral one. This may be because one of the eigenvectors (ξ_2) is dextrally rotate with respect to the eigenvector parallel to the flow plane of the simple shear component (ξ_1) or because the strain is localized at the corners while the central part behaves as a solid-rigid, thus the

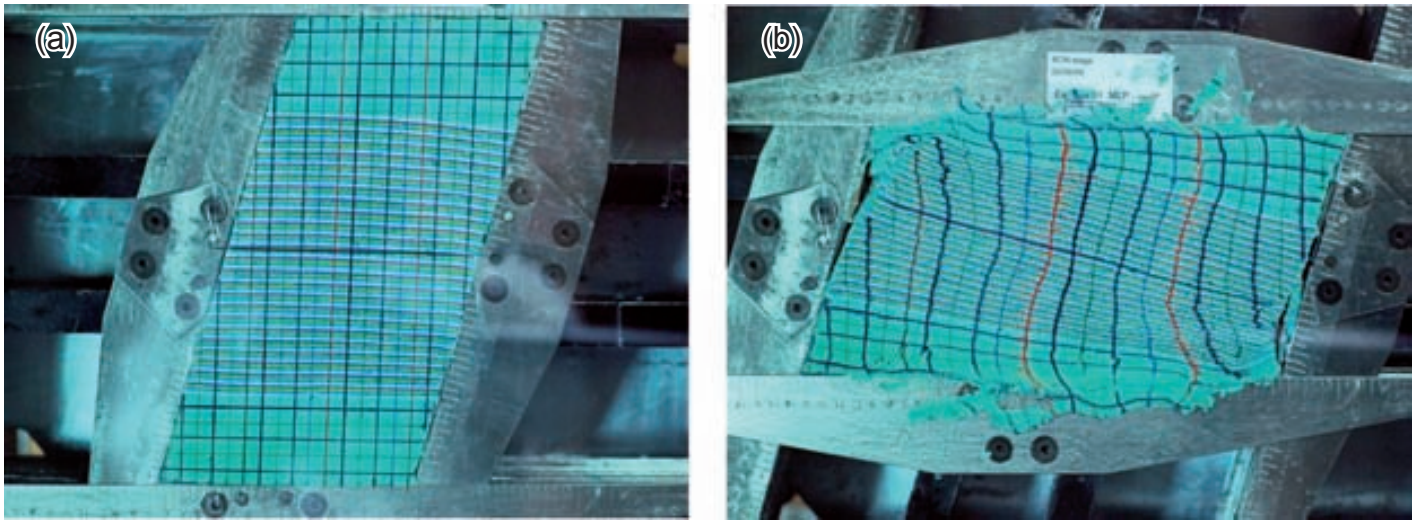

Fig. 3.14. Initial state (a) and final state (b) of model 14.01 after 50% of shortening.

coaxial shortening is achieved through anithetic shears like bookshelf shears at the corners. Three small lozenges are formed by interconnection of small shear zones, all them with sinistral kinematics. Both sides of each shear zone outlining the lozenges end in the less competent layer (blue colour). The lozenges body, therefore, are formed by small portions of the other three layers in between (Fig. 3.15b and c).

After this experiment, that was not really successful in shear zone development and related lozenges, a set of experiments with thicker layers was tested. This new set consists of two subsets, each one made of two experiments with the same structure. The only difference in each subset is that one experiment has vaseline in between the layers and the other has not. The four experiments of this set were submitted to coaxial shortening up to 50%.

Figure 3.16 shows the structure of the first set: experiments 15.01 (the one with vaseline in between the layers) and 15.02. It is a 15x30x10 cm^3 structure with their sides parallel to the shortening and stretching axis thus there is not non-coaxial component in the strain. The multilayer, however, is counter-anticlockwise inclined 50° from the shortening axis (Figs. 3.16 and 3.17). It consists of alternating blue layers (most incompetent material in the model) and the other colour layers. All layers are 0.4 centimeters wide and in

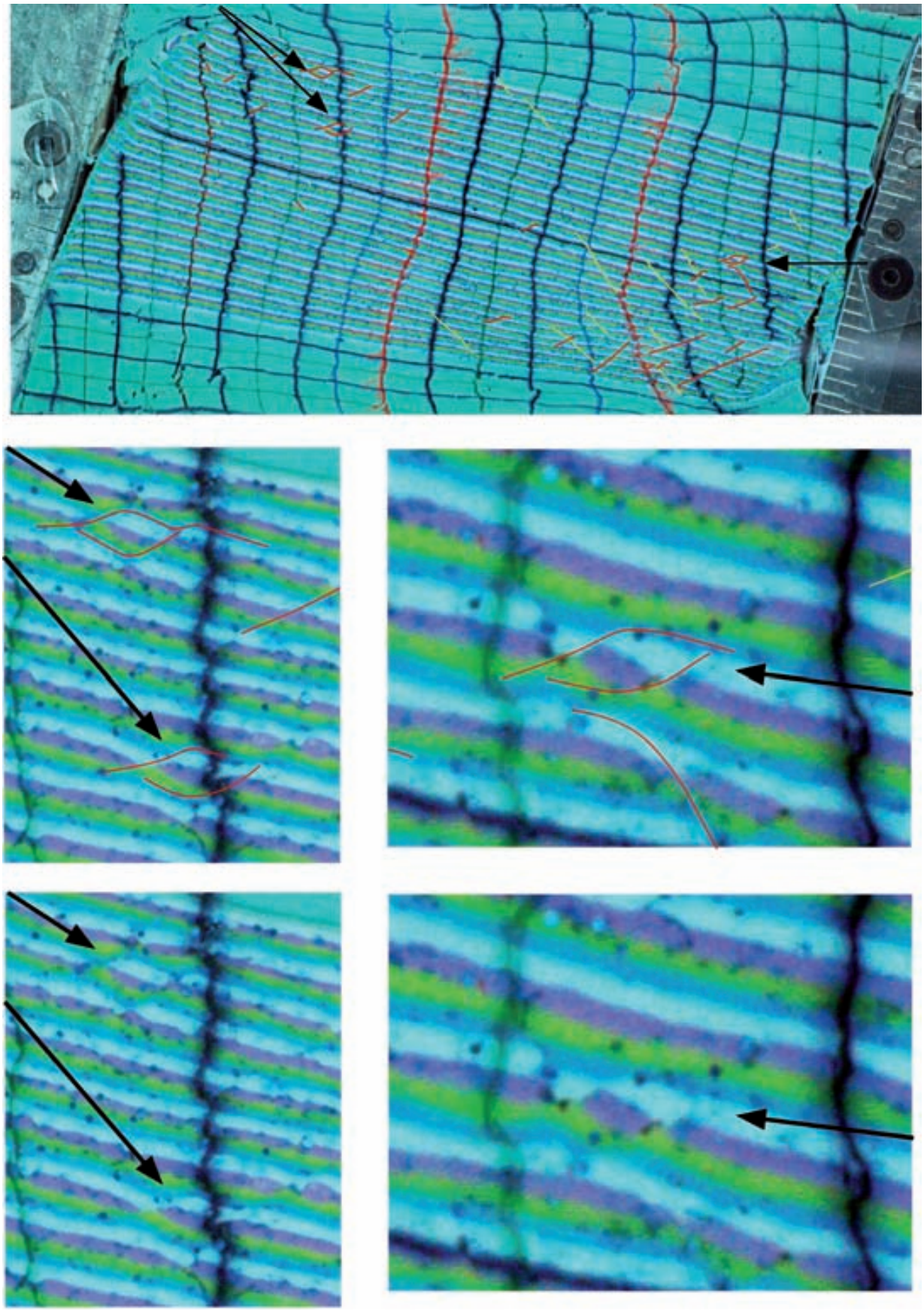

Fig.3.15. Traces of the shear zones (a, dextral in yellow and sinistral in red) and detail of the lozenges formed in the model (b and c).

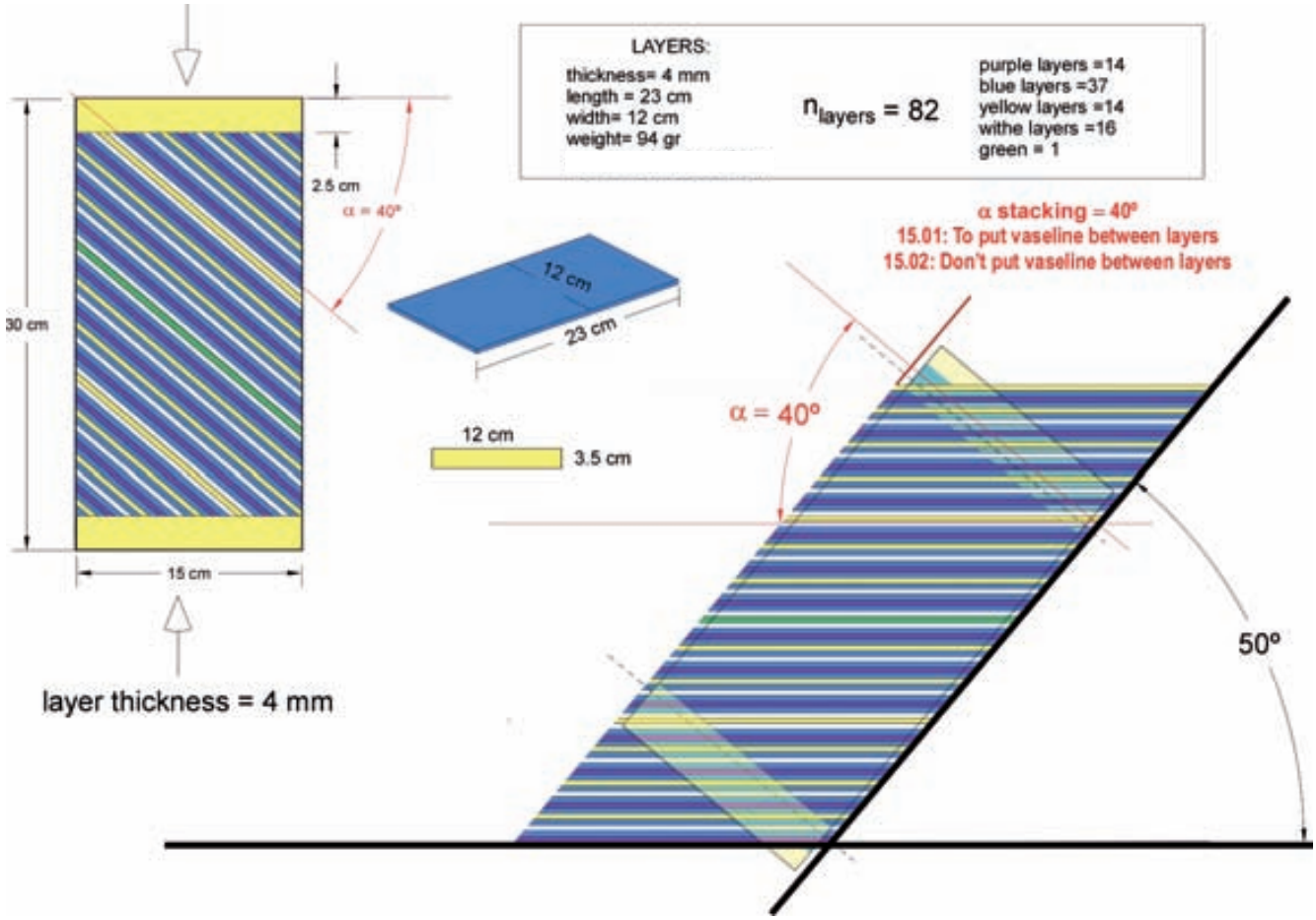

Fig. 3.16. Drawing of models 15.01 and 15.02 both having the same structure with the difference of adding vaseline between layers in model 15.01. The central part of the figure shows the layer dimensions, the right side shows the multilayer pack, and the left side shows the initial state and the features of the models prior to deformation.

the middle of the multilayer there is a green layer (the most competent material in the model) bordered by two white layers.

Experiments 15.01 and 15.02 did not develop lozenges but boudins in the green, most competent layer (Figs. 3.17 and 3.18; Videos Experiment_1501.mov, Experiment_1502part1.mov and Experiment_1502part2.mov in Appendix II). Experiment 15.01 developed some small shear zones while experiment 15.02 did not develop any shear zone (Fig. 3.18). Although the boudin shape is amplified in the surrounding layers giving aspect of lozenge (black dashed lines in Fig. 3.18), there is no formation of lozenges by interconnection or intersection of shear zones but the lozenge-shaped boudins are due to competence contrast.

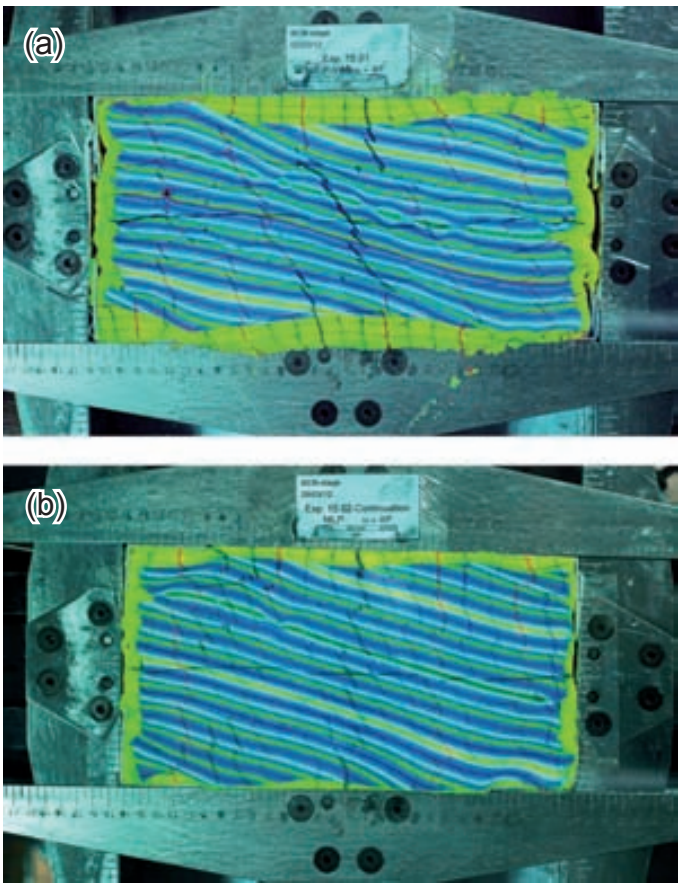

Fig. 3.17. Final states of model 15.01 (a, vaseline between layers) and model 15.02 (b) after 50% of shortening.

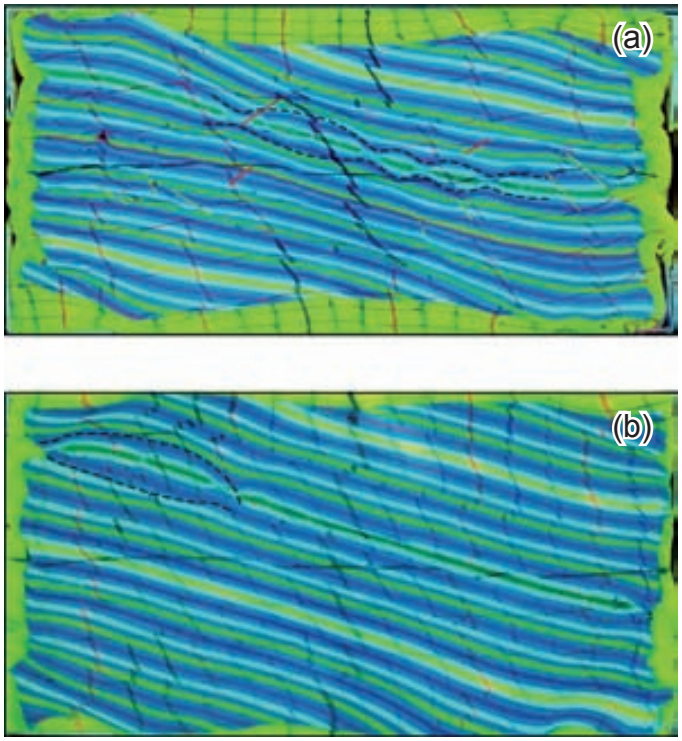

Fig. 3.18. Traces of shear zones (dextral in yellow and sinistral in red) and outline of the lozenge shapes formed (black dashed lines) in model 15.01 (a) and 15.02 (b).

The other subset, experiments 15.03 (vaseline between layers) and 15.04 has the same size and structure than experiments 15.01 and 15.02. The difference to the former set is the composition of the multilayer since this set has 4 stiff layers in the middle: two central green layers made of green Jovi plasticine (most competent layers) and two lateral bright green layers made of Jovi and Ocuplast plasticines (Fig. 3.19). This difference was made to create a more rheologically heterogeneous media that could generate a more heterogeneous strain distribution and therefore give rise to more shear zones and yield lozenges by the interconnection and intersection of them (e.g, Rowe, 1962; Wawersik and Brace, 1971; Rice, 1976; Ildefonse et al., 1992; Ildefonse and Mancktelow, 1993; Groome et al., 2006).

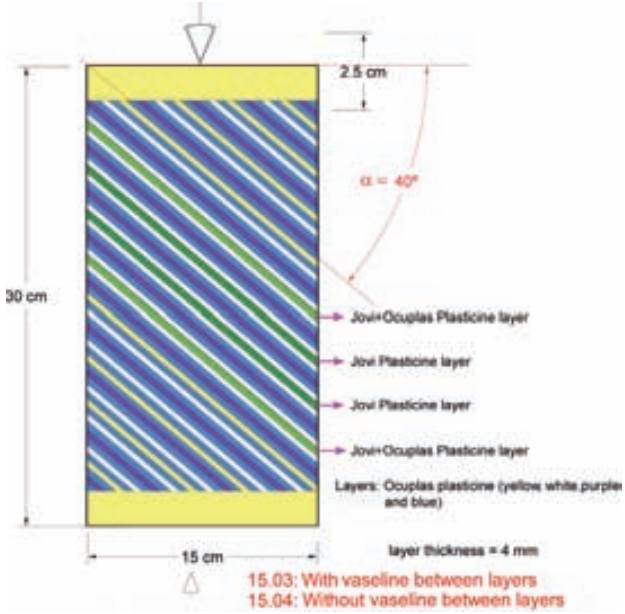

Fig. 3.19. Drawing of models 15.03 and 15.04 both having same structure except the difference of 15.03 has vaseline between layers.

Effectively, experiments 15.03 and 15.04 give rise to more shear zones (Figs. 3.21 and 3.22; Videos Experiment_1503.mov and Experiment_1504.mov in Appendix II). Since the structure of the models is similar to that of experiments 15.01 and 15.02, the formation of these shear zones is ascribed to the increase of the competence contrast in the multilayer. The strain is localised around the competent layers, especially around the two

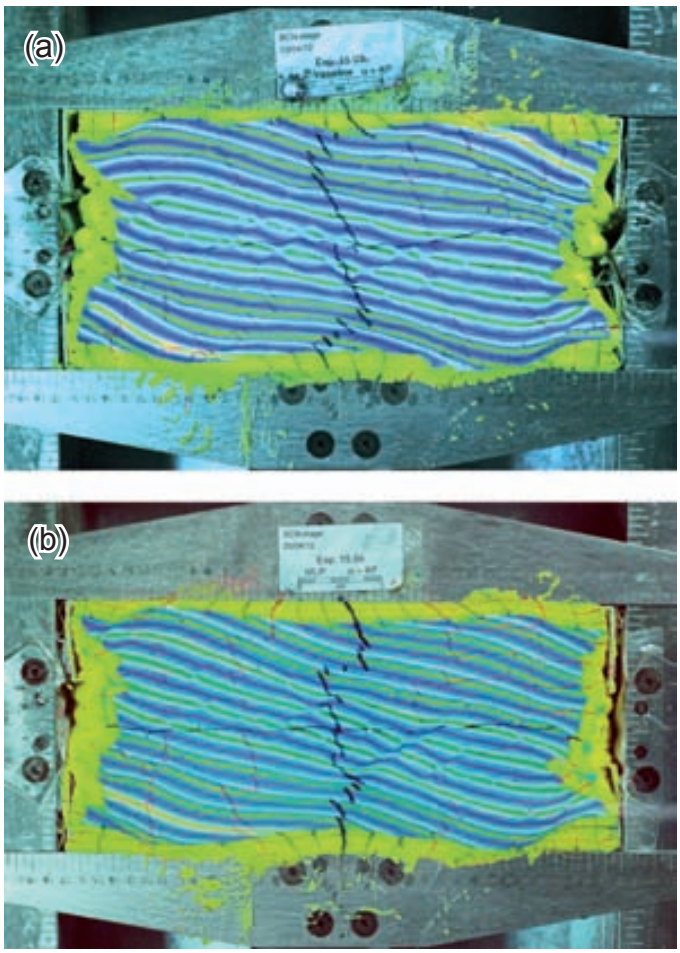

Fig. 3.20. Final states of model 15.03 (a, vaseline between layers) and model 15.04 (b) after 50% of shortening.

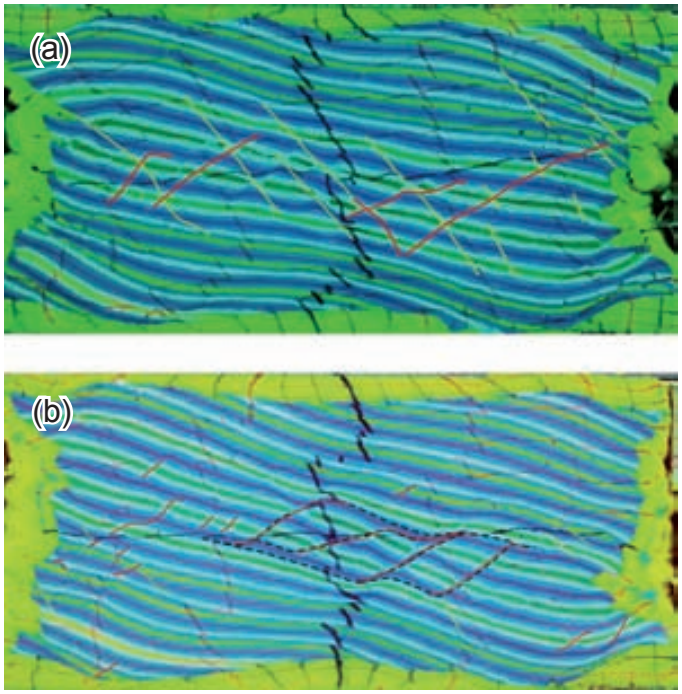

Fig. 3.21. Traces of shear zones (dextral in yellow and sinistral in red) and outline of the lozenge shapes formed (black dashed lines) in model 15.03 (a) and 15.04 (b).

most competent layers (green Jovi layers, in the central part) inducing shear zone nucleation in the surrounding.

Therefore, it seems the heterogeneous rheology of these models is high enough to cause important perturbations in the strain distribution along the model (for 50% of shortening). Such a perturbation in strain distribution induced by a hard phase, is also achieved in the experiments performed under the *Elle* platform.

Experiment 15.03 (vaseline) develops more shear zones but they do not join together to form lozenges. In experiment 15.04, however, some shear zones join together and give rise to a couple of lozenges (Fig. 3.21b), although less shear zones are formed in this experiment. In experiment 15.03 the dextral shear zone family is more populated than the sinistral one, while in experiment 15.04 the sinistral family is the most populated (Fig. 3.21). A common occurrence in both experiments is all shear zones ends in the most incompetent material (blue plasticine).

As this last set gave rise to many shear zones

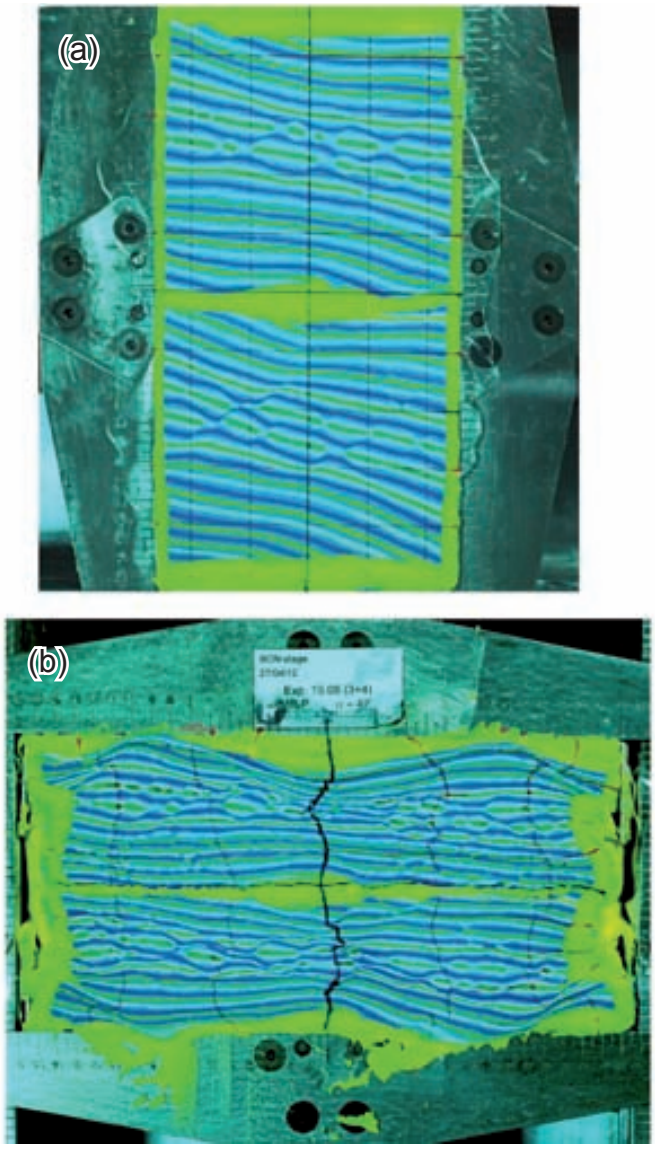

Fig. 3.22. Initial state (a) and final state (b) of model 14 after 50% of shortening.

and some lozenges, the final state of each model was deformed another 50% in experiment 15.05 (Fig. 3.22) to check out if more shear zones and lozenges were developed. Therefore, the total shortening achieved from the first initial state (i.e., the undeformed state) is 75%. As expected, a higher population of shear zones is formed in both models (Fig. 3.23) by the initiation of new shear zones and the propagation of the former ones (Video Experiment_1505.mov in Appendix II). Model 15.03 develops more sinistral shear zones up to the situation in which both families are approximately equally populated. Same situation occurs in model 15.04: more dextral shear zones develop, balancing the population of both families in accordance to the imposed coaxial deformation.

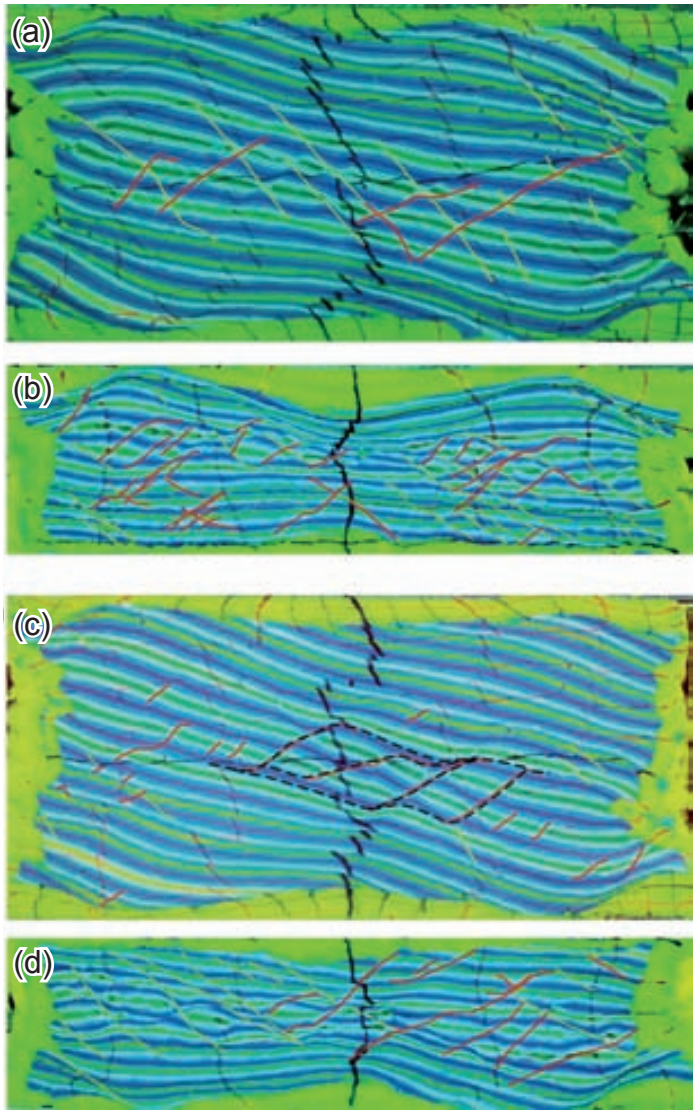

Fig. 3.23. Comparison of shear zones at the initial states -(a), model 15.03 shortened 50% and (c), model 15.04 shortened 50%- and at the final states -(b), model 15.03 shortened 50% and (d), model 15.04 shortened 50%- in experiment 15.05. Shear zones have been traced (dextral in yellow, sinistral in red).

Both models developed lozenges formed by interconnection and intersection of shear zones, which end in the blue plasticine. Each model displays (i) lozenges formed by interconnection of dextral shear zones, (ii) lozenges formed by interconnection of sinistral shear zones, (iii) lozenges formed by intersection of sinistral and dextral shear zones (Fig. 3.24b) and lozenges formed by competence contrast since the boudins evolved to sigma-like structures.

As experiment 15.05 gave rise to interconnected shear zone networks and some related lozenges, the model was cut into 1 cm thick slices to view different sections of the XZ deformation plane. Pictures of these sections of models 15.03 and 15.04 shortened up to 75% (experiment 15.05) are shown in Figure 3.25 and Figure 3.26, respectively. From the sections, it can be inferred that shear zones and related structures are highly changing from one section to another. In Figure 3.25 four areas have been highlighted by one red square and three ellipses. The square shows an area with many small shear zones that appear or disappear from one section to another. The biggest ellipse shows a group of boudins or sigma structures that are also changing their arrangement. The other ellipses show a small shear zone and a boudin that either exists or does not exist from one section to another. Figure 3.26 shows two areas with high concentration of boudins and shear zones, and their arrangement is changing through the sections. Although only these areas have been highlighted, such changes happen in almost any structure of the model. This reason makes the 3-D interpretation of lozenge geometries from 2-D sections really tentative.

These experiments also may give information on the rheological aspect of shear zone initiation and propagation. Although the shear zones of the analogue models do not develop any mylonitic fabric, the geometric continuity or discontinuity along the shear zones, as a simile to ductile and brittle deformation mechanisms respectively, can shed some light on the brittle or ductile nucleation debate. The black ellipses in Figure 3.25a and 3.26a indicate shear zones having both, continuity and discontinuity along their length as the shear zone cross-cuts different layers with different rheological behaviour, thus the stiffer layers behave brittlely while the softer layers behave ductilely (decreasing competence of the colours is: green, white, purple, yellow and blue). These experiments support the fact that different deformation mechanisms may coexist along a same shear zone depending on the deforming material.

One fact that should be taken into account is

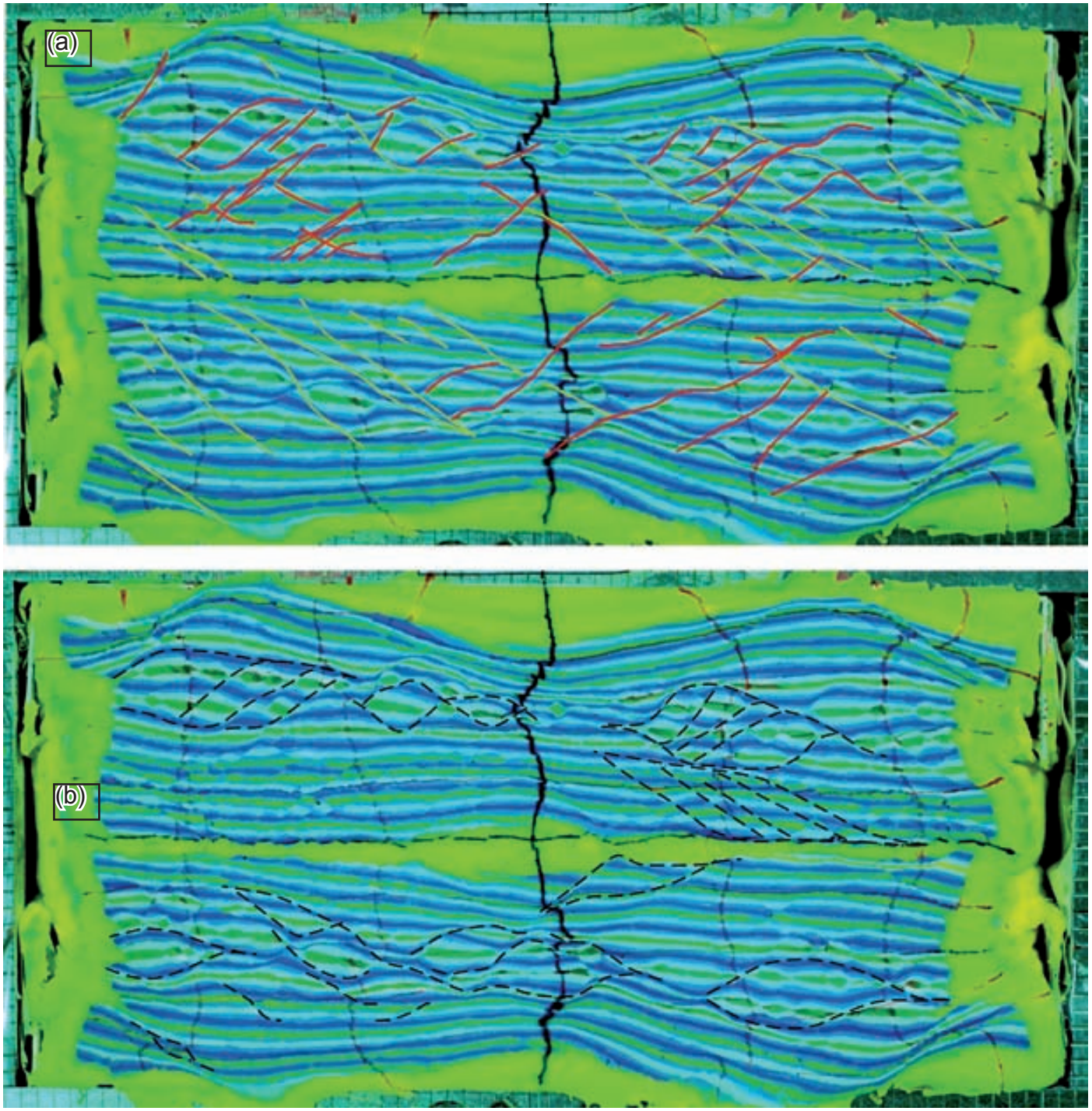

Fig. 3.24. Final state of experiment 15.05 with traces of the shear zones (a, dextral in yellow, sinistral in red) and traces of the lozenges (b, black dashed lines).

that observations from natural shear zones likely gives information about shear zone termination, and this may differ from the initiation mechanism. However, the modelling may give some information on the shear zone initiation process. In the performed analogue modelling, all the layers stretch and show geometric continuity at the first strain increments. As the strain increases and the layers keep stretching, the stiffest layers (green ones) start to pull apart, showing discontinuity, whilst the more ductile layers do not break. With increasing strain, new fractures appear in the green layer and the other stiff layers start to break (yellow and white layers). However, the most ductile layers (blue and purple) never break (videos in Appendix I). Thus, initially all layers deform internally and then, with further strain only the stiffer layers start to fracture. This observation

supports the fact that under the same deformation conditions some materials may deform ductilely while others do it brittlely (black ellipses in Fig.325a and 3.26a).

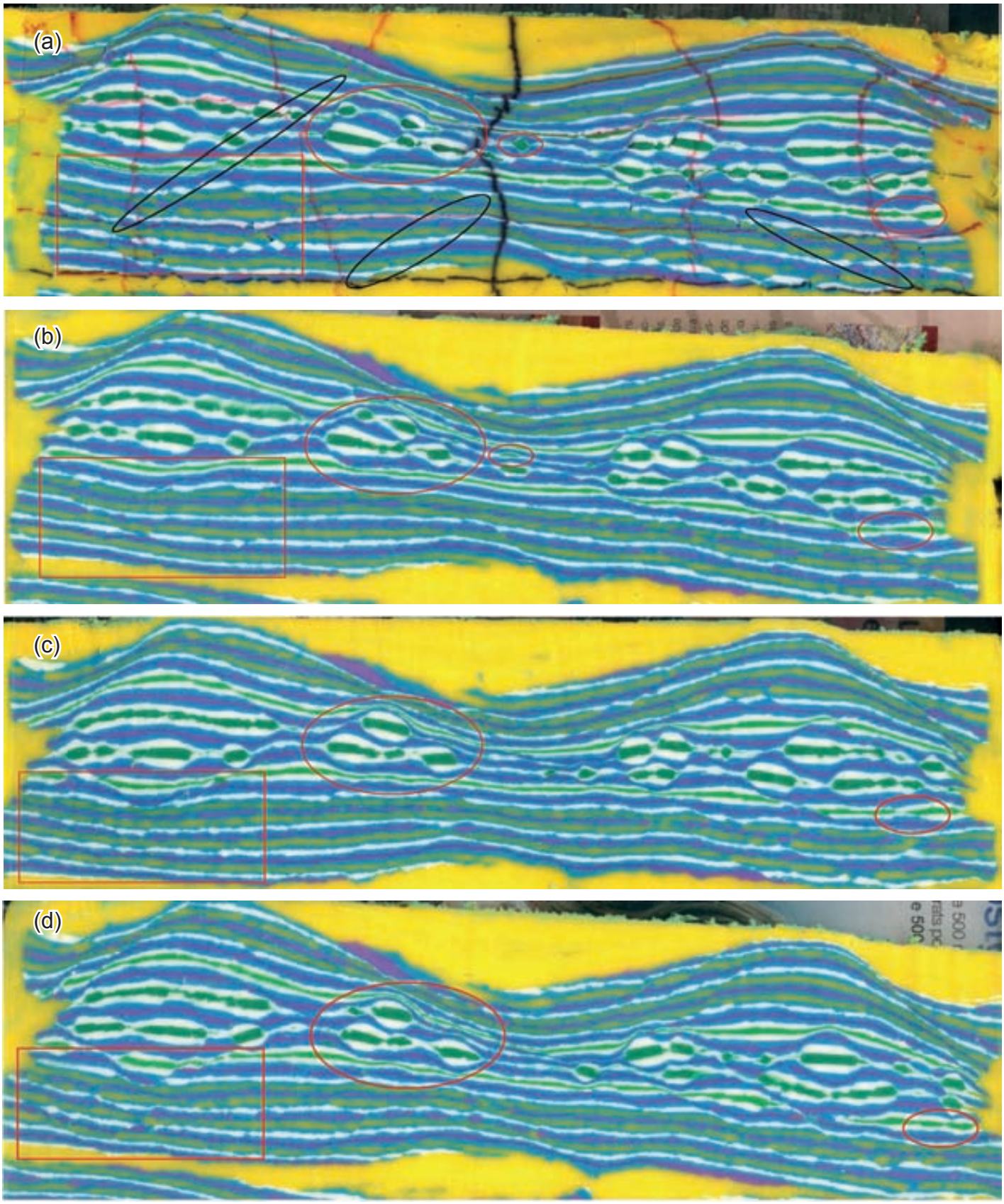

Fig. 3.25. Scanned sections of model 15.03: (a) top section; (b) 1 cm-deep section; (c) 2 cm-deep section; (d) 3 cm-deep section

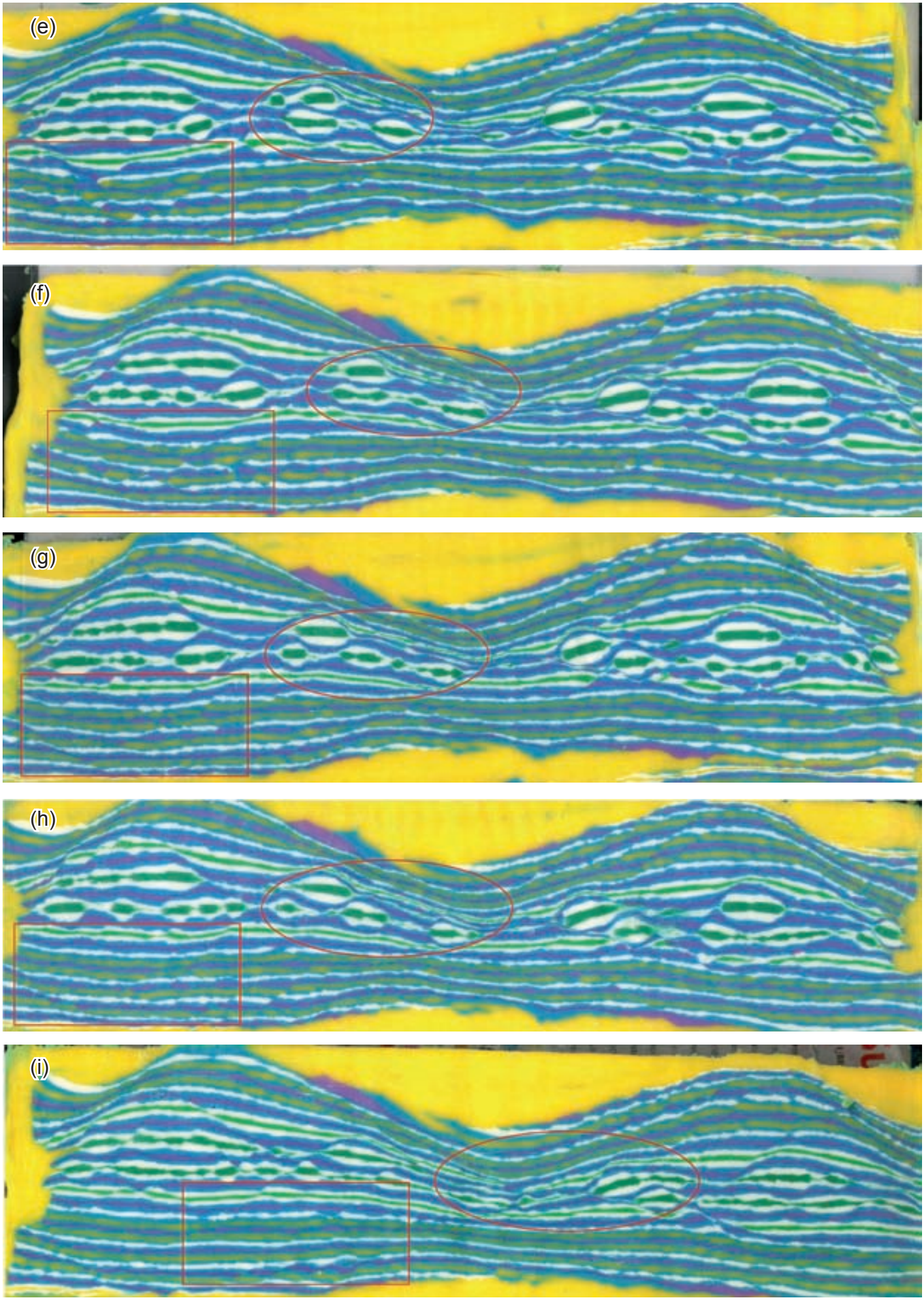

Fig. 3.25 (continuation). Scanned sections of model 15.03: (e) 4 cm- deep section; (f) 5 cm-deep section; (g) 6 cm-deep section; (h) 7 cm-deep section; (i) 8 cm- deep section.

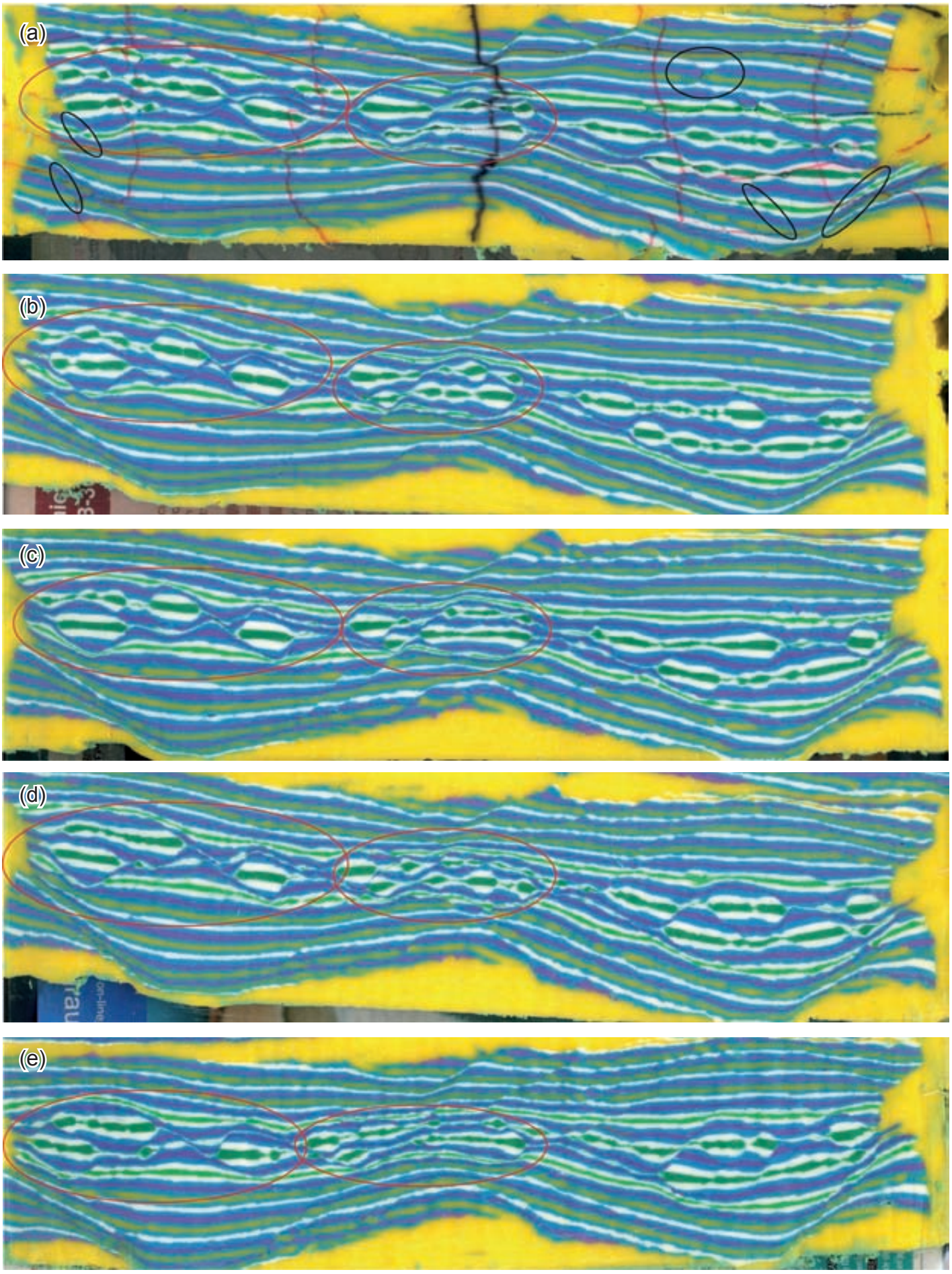

Fig. 3.26a. Scanned sections of model 15.04: (a) top section; (b) 1 cm-deep section; (c) 2 cm-deep section; (d) 3 cm-deep section; (e) 4 cm- deep section.

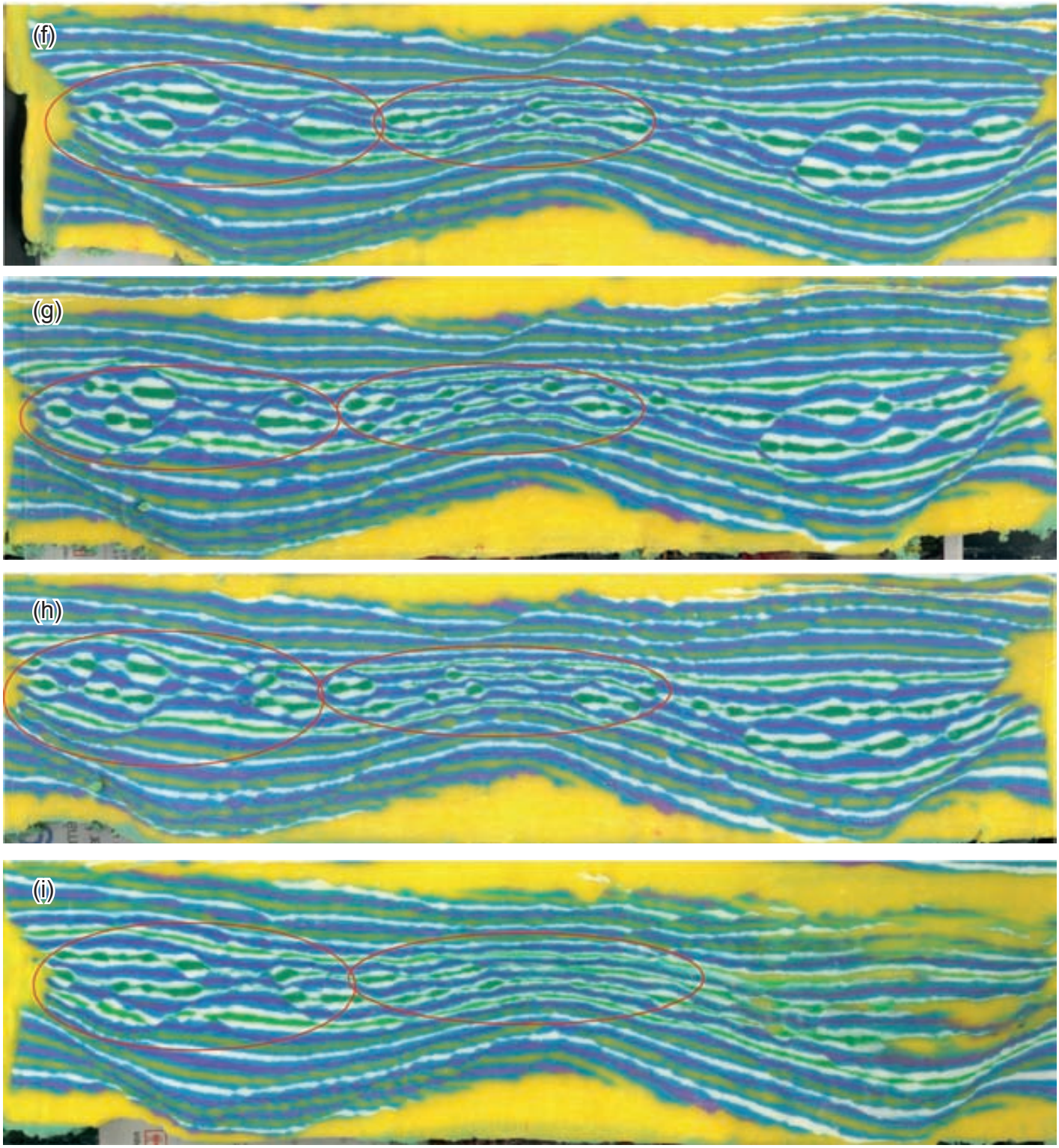

Fig. 3.26 (continuation). Scanned sections of model 15.04: (f) 5 cm-deep section; (g) 6 cm-deep section; (h) 7 cm-deep section; (i) 8 cm- deep section..

3.1.3. Variations in the foliation angle through lozenges: Graphical representation.

For lozenges in anisotropic rocks, their internal foliation is a good source of information. By knowing how a foliation plane changes its orientation along its path through the lozenge, information on the local kinematics and the strain distribution can be obtained.

In order to have a proper understanding on "where the lines go" through lozenges (i.e., how the orientation of the foliation is changing), a 2-D graphical representation of the changes in the orientation of the foliation traces has been performed (Fig. 3.27). It has been done through the independent software SURGE, and the procedure has been already explained in subchapter 1.2.

Although this is only a 2-D graphic method, it gives a spatial distribution of foliation traces which cannot be depicted in stereographic 3-D projections. Moreover, in a graphical representation the observer can track a single foliation trace all along its path through the lozenge, thus providing more information besides a quick and better view.

The graphical representation consist of the picture of a lozenge upon which has been taken as many measures on the foliation orientation (white dots in the picture, black dots in the representation) as possible. Then, the change in the foliation trend through the lozenge is easily calculated by the difference between the value (in degrees) of the measured point and the value of the mean trend of the regional foliation in the area where the lozenge is located. These new values (the difference between regional foliation and measured point orientations) are input in *SURGE* and the color map is created upon these values through interpolation. Those points with higher change in orientation (higher rotation) would have greater

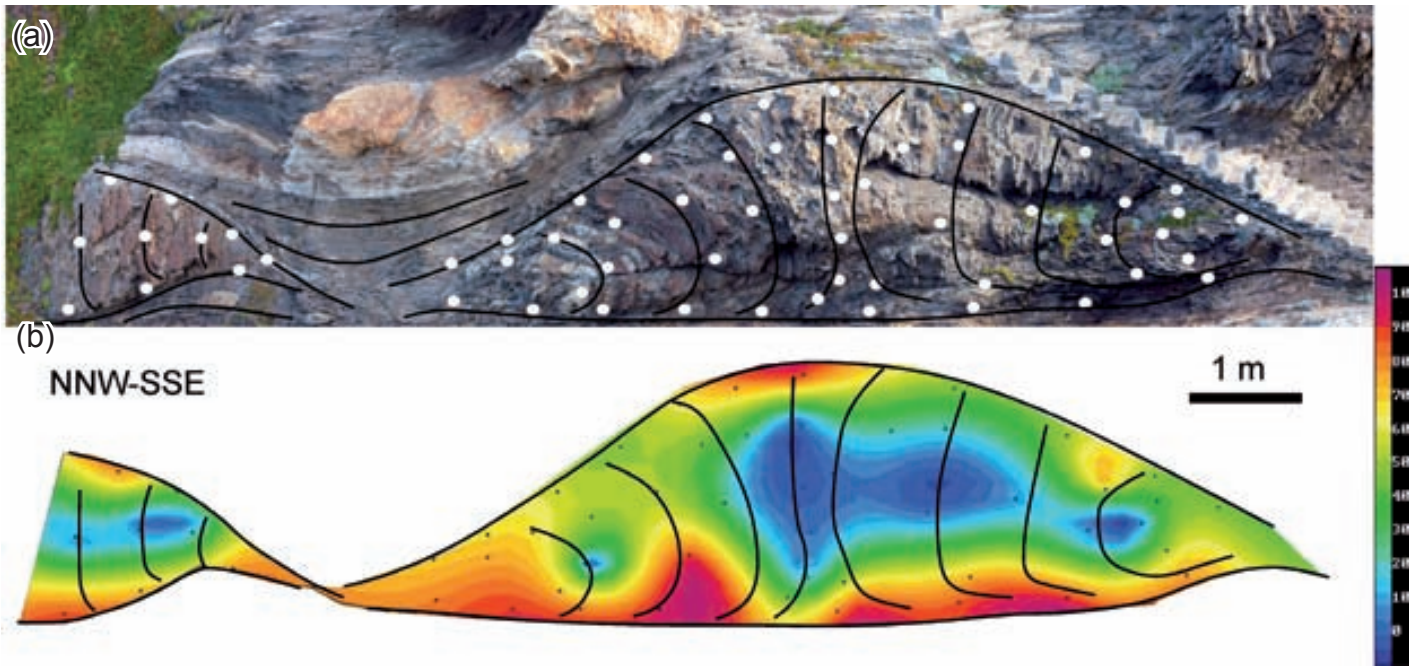

Fig. 3.27. (a) Picture of a millipede-type lozenge (profile view) in Cala d'Agulles (Cap de Creus) showing the drawing of the outline and the traces of the internal foliation (black lines) and the measure points (white dots). In (b), the map of the degree of angular variation in the trend of the foliation through upon the same lozenge is shown, depicted by colour scale. The coldest blue colour shows no angular variation relative to the regional foliation (0°), and the hotter the colour, the higher the angular variation.

value than those having rotated less, and therefore would be coloured in a warmer colour by the software. The scale colour can be seen at the right of the graphical representations.

Therefore, the track of the foliation inside the lozenge can be easely seen and thus the change in the orientation also, allowing a qualitative evaluation of the kinematic and the strain distribution inside the lozenge.

Figure 3.27 shows a millipede-type lozenge from Cala d'Agulles (Cap de Creus). The colour map shows that the internal foliation in the lozenge is more rotated close to the borders and less rotated in the interior, where it shows some areas with no rotation. Thus, the kinematics and the strain are localized at the rims and decrease towards the interior, where there may be areas not affected by the kinematics and the strain of the deformation event that gave rise to the shear zones defining the lozenge.

Figures 3.28 and 3.29 show two sigmoidal lozenges from Cala Culleró (Cap de Creus) and Tazenakt (Morocco) respectively. The distribution of the angular variation in the lozenge from Culleró is somewhat different. It also shows the higher strain and kinematic change at the borders, although not in all of them but only next to the main border shear zones. This is because it is a domino-type lozenge (see subchapter 3.2.2) and thus the secondary antithetic shears that propagate sub-parallel to the pre-existing foliation show smaller rotation than

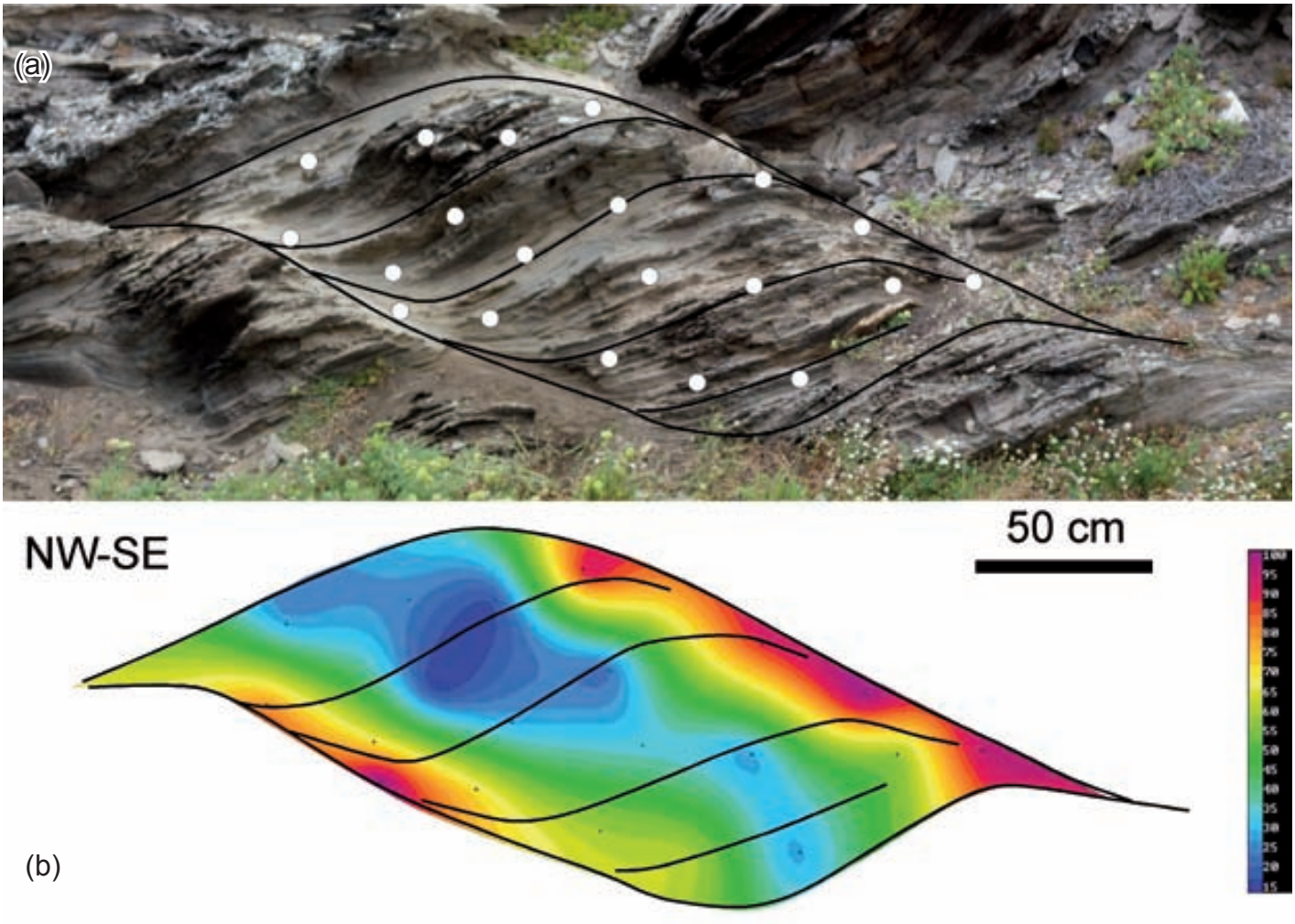

Fig. 3.28. (a) Picture of imbricated domino-type lozenges in Cala Culleró (Cap de Creus) showing the drawing of the outline and the traces of the internal foliation (black lines) and the measure points (white dots); (b) map of the degree of angular variation in the trend of the foliation through upon the same lozenge.

the main shears. It can be observed how the foliation-parallel antithetic shears show more rotation at their junction with the main shears (Fig. 3.28b).

The lozenge from Tazenakt (Fig. 3.29) also displays less rotation at the interior in agreement with the formers. However, its interpretation is not so clear since the foliation angular variation map is not as coherent as the others.

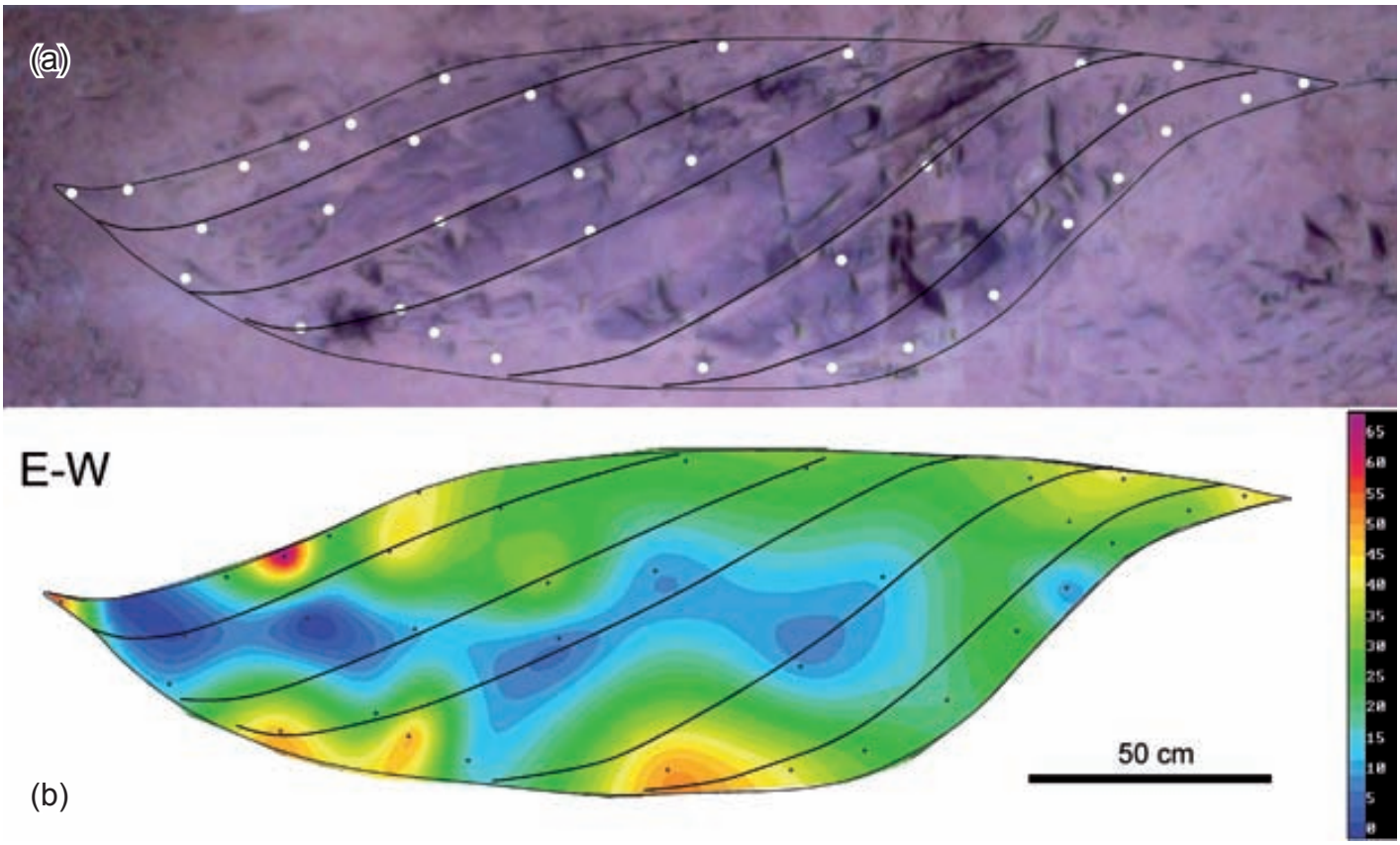

Fig. 3.29. (a) Picture of a lozenge in Tazenakt area (Zenaga Inlier, Marocco) showing the drawing of the outline, some traces of the foliation and the measure points; (b) the map of the variation in the trend of the foliation.

3-D representations of the internal foliation from outcrops of lozenges were attempted, but the fact that the cross-sections from experiment 15.05 show high variability in geometry and low continuity of the structures from one section to another prevented to make the 3-D representation. The initial steps for this representation were done. An outstanding sigmoidal lozenge (angle δ=105° and aspect ratio L1/W=6m/2.5m=2.4; Fig. 4.1b) from Cap de Creus was chosen (Fig. 3.30). The aim was to do several cross-sections from field data (measures of dip and direction taken every 50 cms), like parallel slices, thus they could be joined later through a Computer Aid Design (e.g., AutoCAD or Rinhoceras) and the 3-D geometry of the lozenge could be obtained. To take the field data for the cross-sections, a reference E-W line was fixed and placed closely parallel to the lozenge long axis, and a perpendicular, N-S line was moved in 50 cms intervals along the reference one (Figs. 3.30a and 3.30b). The N-S moving line had marked signs every 20 cms thus measures were taken systematically. For every measure point, besides the dip and the direction of the foliation, the distances from the sign in the moving, N-S line to the reference, E-W line (Fig. 3.30c) and the distance from the sign in the moving line to the measure point (Fig. 3.30d) were measured with a tape measure thus an invisible, moving 3-D grid over the lozenge was set, what would allow to locate any measure point and to connect different cross-sections. The cross-sections were initiated but not finished (Fig. 3.31) and

thus neither the 3-D representation. It could not be finished since it was impossible to know how the anastomosed bounding shear zones behave in dip and attitude with deep. The anastomosing shear zones bounding the lozenge may change their orientation in decimeters, thus a huge component of guessing would be needed to finish the cross-sections. This is why the cross-sections are made only for the next decimeters to the measure point and do not go beyond.

Fig. 3.30. Performance of the measures of the lozenge chosen for 3-D representation. (a) Picture showing the reference and the moving lines; (b) displacement of the moving line on the reference line to obtain several parallel cross-sections; (c) marked signs, measure points and distance from the measure point to the reference line; (d) measuring the distance of the measure point to the moving line (z value).

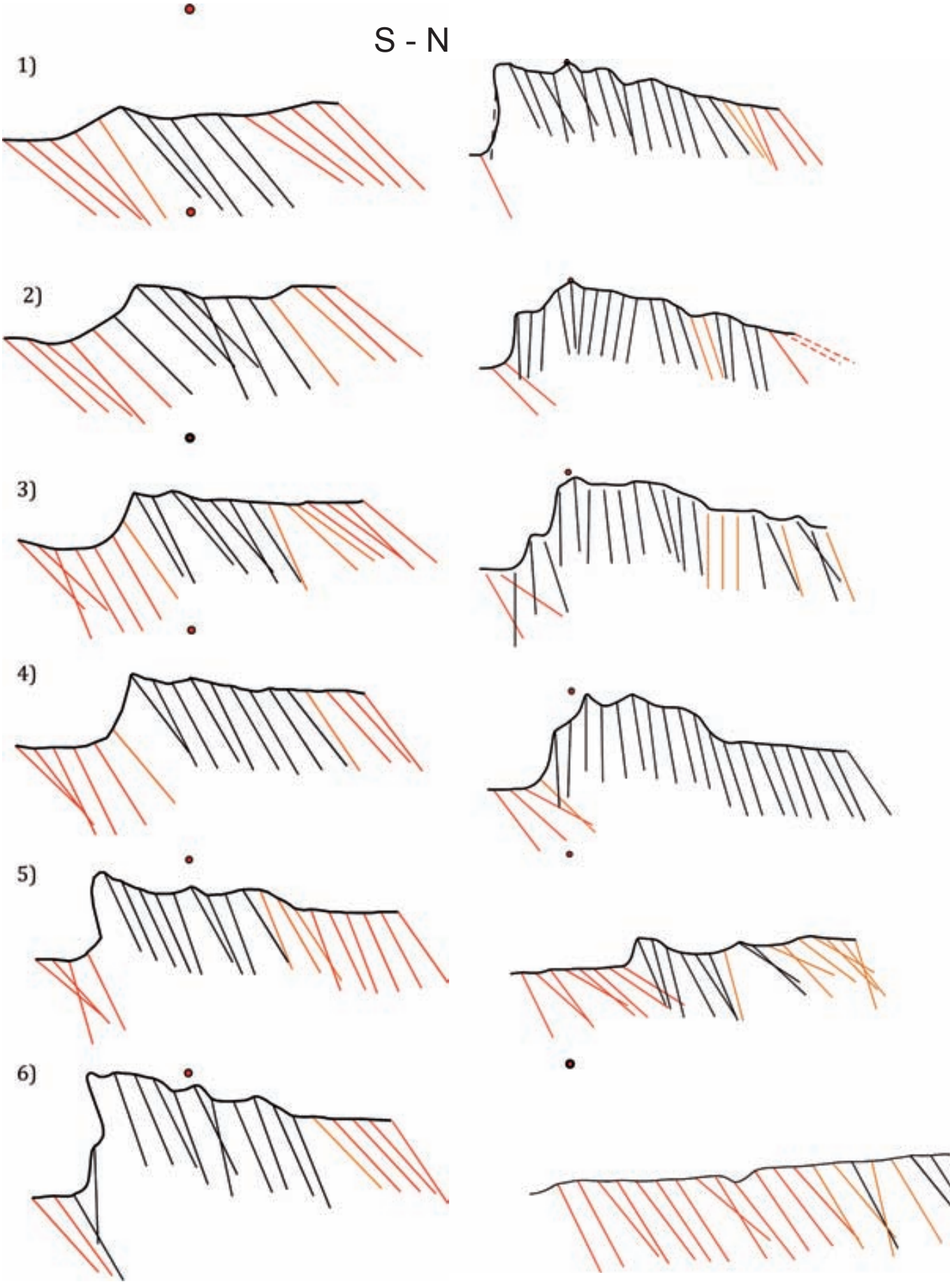

Fig. 3.31. Cross sections of every moving line position. Separation between cross-sections is 50 cms. Mylonitic foliations are coloured in red lines (boundary shear zones), internal foliations of the lozenges in black (rotated regional foliation), foliation planes with orientations between the mean mylonitic foliation trend and mean non-mylonitic trend in yellow lines. Every cross-section shows (i) the topographic profile, (ii) d dip and orientation of the foliation and (iii) the position of the cross-section relative to the reference line (red point).

3.2 LOZENGE TYPOLOGIES

3.2.1 Kinematic typology

For the case of lozenges developed by intersection of shear zones in homogeneous anisotropic rocks, a two-dimensional typology on the internal geometry has been proposed. Although a complete understanding of the internal geometry of tectonic lozenges in anisotropic rocks and their relation with kinematics requires a deeper three-dimensional analysis, in most available natural examples two-dimensional outcropping prevails and analyzed patterns show map of sectional patterns (e.g. Figs. 3.4-3.6).

This typology, defined in profiles normal to the mean shear plane and parallel to the shear direction, consider different lozenges 2-D patterns arising as result of the following main variables: (i) the relative orientation of the anisotropy with respect to the existing shears, and (ii) the initial pattern of the intersecting shear zone systems (Fig. 3.32). Two end members will be considered (i) shear zone intersection consisting of a prevalent shear sense and (ii) shear zone intersection consisting of conjugate shear systems. In both cases, for the sake of simplicity, differently oriented shear zones will not be simultaneously active but sequentially activated as this is the generally accepted common behaviour (Williams and Price, 1990; Mancktelow, 2002; Carreras et al., 2010) This is a typology on the internal geometry of tectonic lozenges in anisotropic rocks with regard to those variables, and it does not take into account (i) the effect of the anisotropy (foliation) orientation may have in the arrangement or kinematics of the bounding shears and (ii) wether the different angular relationships between the previous foliation and the bounding shears are original features or achieved during shear progression as the result of strain affecting the shape of the lozenge. The typology considers that the bounding shear zones make an acute angle to the lozenge long axis and that each individual shear zone satisfies the simple shear model (Wk=1). In any case, the final structure of a tectonic lozenge is independent of the bulk deformation, whose kinematic vorticity number is variable ($0 \leq Wk \leq 1$) as it is discussed in Chapter 4.

For conjugate systems an initial angle close to 90° is assumed (Baumann, 1986; Baumann and Mancktelow, 1987; Ildefonse and Mancktelow, 1993; Mancktelow 2002) although similar patterns would arose if initial obtuse angles (Zheng et al., 2011) were considered. For synthetic shears and initial angle of 30° is assumed based on Riedel pattern geometry (Riedel, 1929).

The arising spectrum of lozenge patterns is shown in Figure 3.32. It shows initial shapes of lozenges however, with progressive deformation, the angles between shears would progressively open towards the extension direction as a result of increasing strain. This is achieved by the combined effects of continued shearing on the shears and internal deformation of the lozenges by foliation rotation and the origin of new shears inside the less deformed lozenge (Carreras et al., 2010). The effect of the increasing strain for conjugate shears is shown in Fig. 3.33. The angle between shears has been opened 30° and the internal foliation of the lozenge has rotated consistently with the closest shear zone. Real examples of some types of this kinematic typology in lozenges (Figs. 3.32 and 3.33) are shown in Figure 3.34. It is a relevant fact that complex structures giving apparent contradictory shear senses often arise as the result of coalescent conjugated shears and the

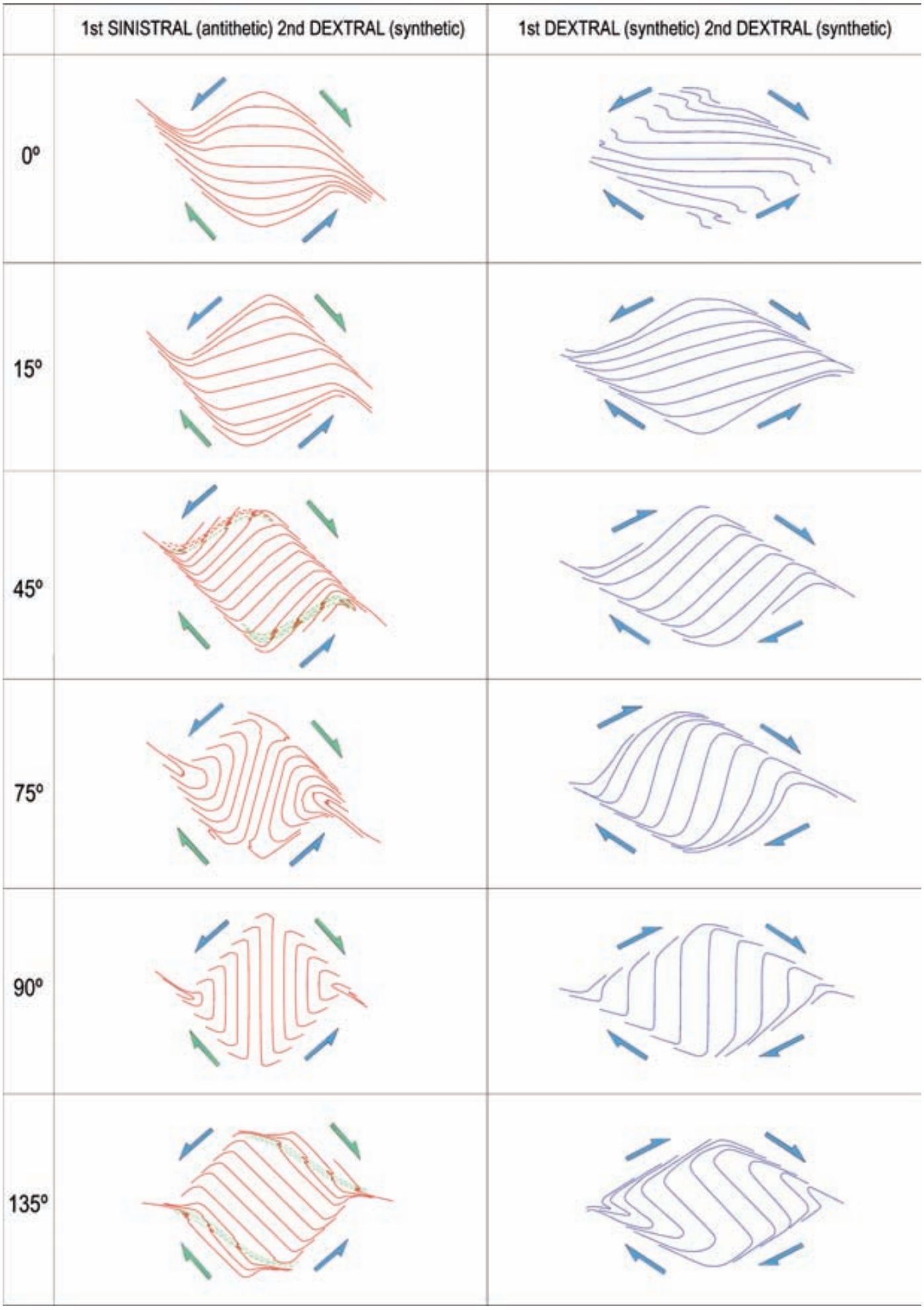

Fig. 3.32. 2-D Typology on the internal geometry of lozenges developed in hoomogeneous anisotropic rocks by intersection of shear zones. See explanation on the text.

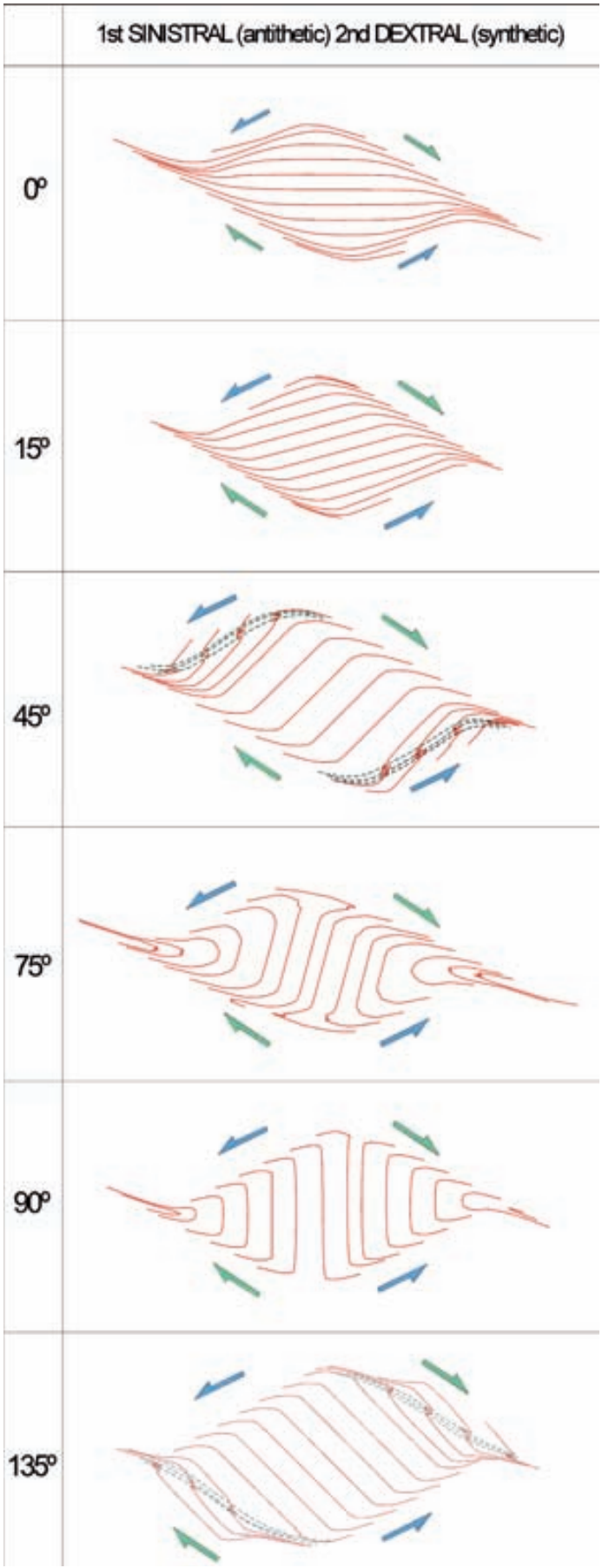

Fig. 3.33. Effect of increasing strain along the shears for the case of conjugate shears. The obtuse angle between shears opens and the internal foliation rotates syntethically towards the closest bounding shear.

presence of associated buckling instabilities nucleated at the margins and subsequently sheared. It is an important point that the presence of millipede-like geometries (Bell, 1981) does not have any implication on the bulk strain regime (regional vorticity) because the presence of one or two sets and the prevalence of one over the other is the result of a complex relation between orientation of the ISAs, anisotropy and progressive deformation. Examples of lozenges developed in a prevalent dextral shear regime abound in the Northern Cap de Creus shear belt (Carreras, 2001; Ponce et al., 2013; Fig. 3.7 and others).

There is less information on the 3-D external geometry of lozenges because the scarcity of outcrops enabling this approach. In addition, existing modelling is restricted to 2-D approaches. The slices of analogue modelling (Figs. 3.25 and 3.26) showed high variations in the arrangement of shear zone networks and lozenges in the third dimension, giving some insight into the 3-D shape of the analogue structures. However, the deduced non-cylindrical geometry of the experimental structures is probably influenced by distribution of boudin partitions at a more detailed scale. From the 1 cm-spaced slices it can be stated that lozenge-shaped boudins are not longer in Y than in X direction and lozenges formed by interconnection or intersection of shear zones are longer in Y than in X (Figs. 3.25 and 3.26). The three-dimensional shape of the lozenge depends also on various factors, among them: the initial shear patterns, the orientation of anisotropy with regard to the shear system and the internal deformation undergone by the lozenges as the strain increases in the shear zones. Observations of lozenges in different sections relative to the shear planes and the shear directions point that, in general, the final shape tend to be spindle-shaped bodies with the long axis contained in the bulk shear plane. It has to be taken into account that in high strain anastomosing systems with co-existing conjugate shears the stretching lineation

of both systems tends to parallelize. This fact, together with the existence of the previously quoted factors, causes the fact that the bulk shape of the lozenges cannot be univocally related with shear strain type or amount (Bell, 1981; Choukroune and Gapais, 1983; Gapais et al. 1987).

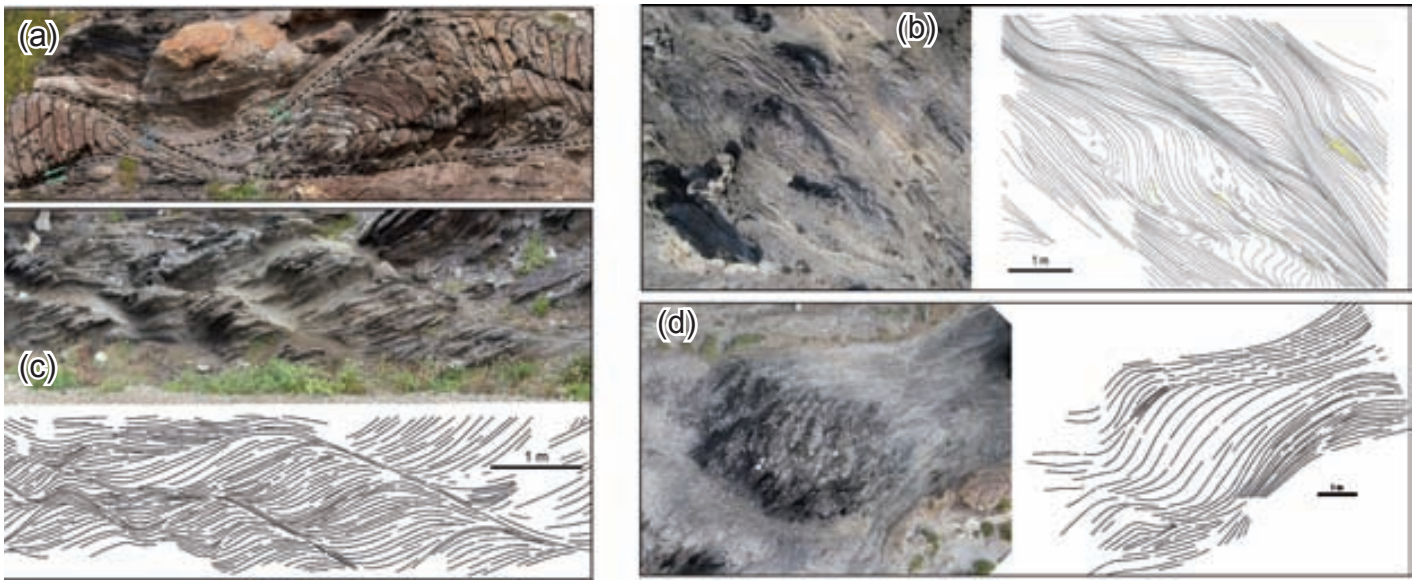

Fig. 3.34. Field examples from the typology shown in Fig. 3.35. (a) and (b) lozenges formed by conjugate shear zones and (c) and (d) lozenges formed by a dextral synthetic shears. Note the similarities to some of the drawings from Fig. 3.35.

3.2.2 Propagation typology

In this section, several mechanisms that can be involved in the generation and evolution of shear zone-related lozenges in highly foliated rocks (Fig. 3.35) are described. They have been ascertained through detail mapping and analysis of shear zones from the Northern Cap de Creus area (Figs. 3.36-3.43). All these shear zones and their corresponding lozenges have been analyzed on sections sub-parallel to the overall shearing direction. Any single mechanism is dominant within a range of orientations of the previous foliation with regard to the bulk shear direction, which in the study area has a NW-SE trend (Carreras, 2001). This way, several mechanisms can be involved in a particular initial setting over which one generally prevails. This is because the orientation of the previous anisotropy is a main control on the initiation and evolution of a shear zone pattern.

The investigated lozenges are considered to develop in multi-layered mechanically anisotropic rocks. Although the metasedimentary rocks consist of two alternating lithologies, the psammitic and the pelitic schists, the competence contrast between them is small, being the metapsammites slightly stiffer (Druguet and Carreras, 2006). The marked planar mechanical anisotropy (the schistosity) seems to exert a major control on such partitioning and localization (Williams and Price, 1990; Carreras, 2001), to which the likely small effect of competence contrast can be added. The formation of lozenges is therefore related to the bulk mechanical anisotropy of the metasedimentary layering, as a multilayer in the sense of Price and Cosgrove (1990). However, the angular relation between previous anisotropy and shear zone is suitable for initial stages of lozenges and bounding shear zones, since such angular relationship are changing as the strain increases. With increasing strain the shears rotate towards the extension direction and this opens the angle between the shears, which display the acute angle containing the lozenge long axis. This change is achieved by the combined effects of continued shearing on the high strain domains bounding the lozenge (shears zones) and also by deformation inside the lozenge through rotation of the foliation within the lozenge and the formation of new shears in it. Thus, the angular relations should take into account for initial stages of lozenges.

The following mechanisms, labelled as models L1 to L5, are ordered by the angle α, which indicates the initial orientation of the previous foliation with regard to the bulk shearing direction (Fig. 3.35). The models are drawn assuming bulk simple shear deformation (as D_3 shear zones in Cap de Creus), and different patterns arise on the basis of the analysis of natural lozenges in foliated rocks. These models are also in agreement with the results from modelling of shear zones in anisotropic materials under simple shear (Williams and Price, 1990).

Model L1: Millipede type lozenges

In domains of the study area where the initial angle α was between 45° and 90°, deformation partitioning gives rise to two sets of conjugate shear zones oriented symmetrically with regard to S_1. The space between the shear sets intersection may form a millipede-type lozenge (Fig. 3.37). This mechanism takes place in domains where the dominant previous foliation (bedding/S_1) is close to N-S, which in turn is sub-parallel to the instantaneous shortening direction. This observation is in agreement with the experiments performed with anisotropy angles of $40°\leq\alpha\leq70°$ by Williams and Price (1990). In these situations bedding/S_1 lies in

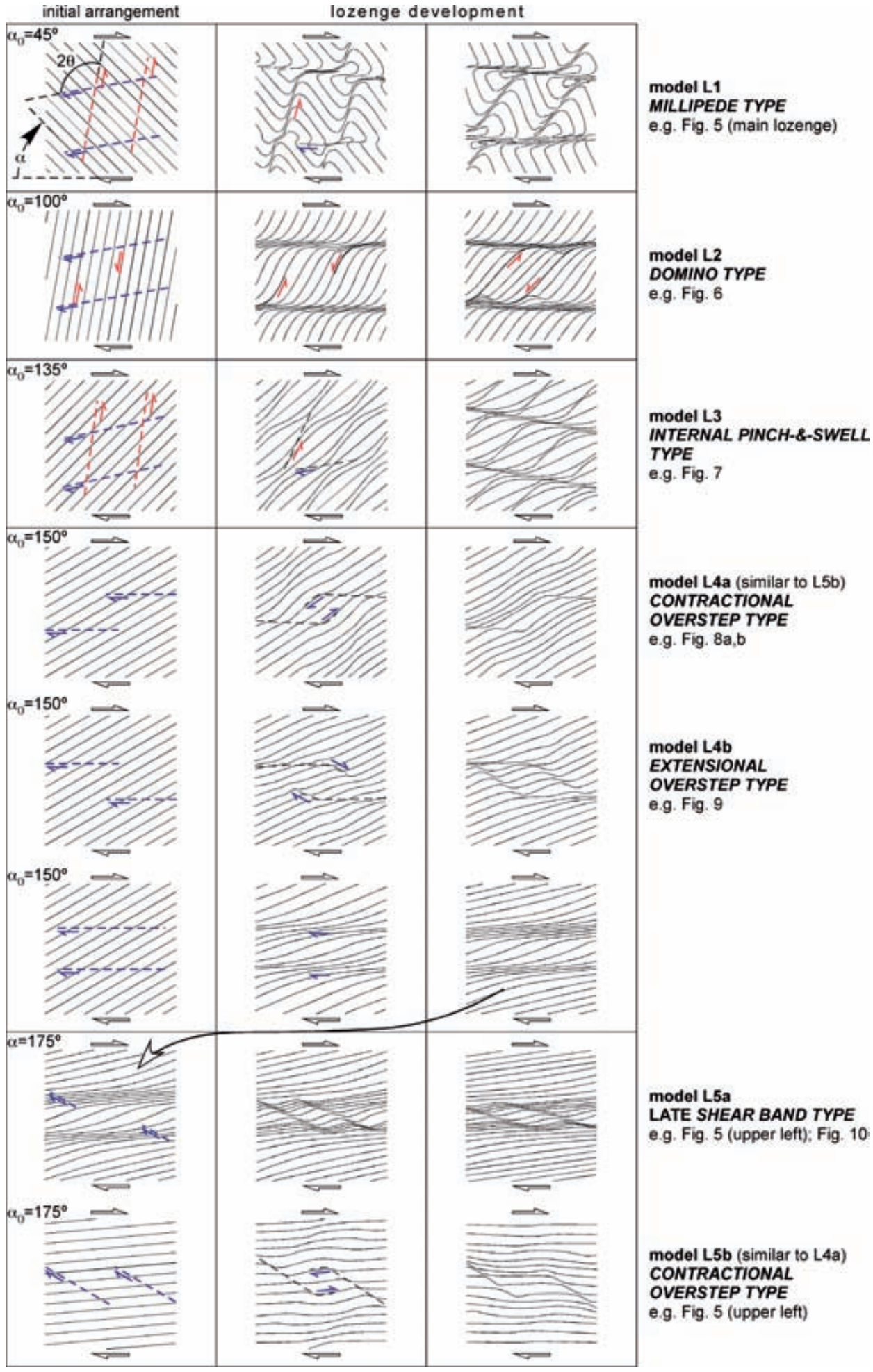

Fig. 3.35. Basic models for the initiation and development of shear zone-related lozenges in foliated rocks under a (dextral) simple shear-dominated regime.

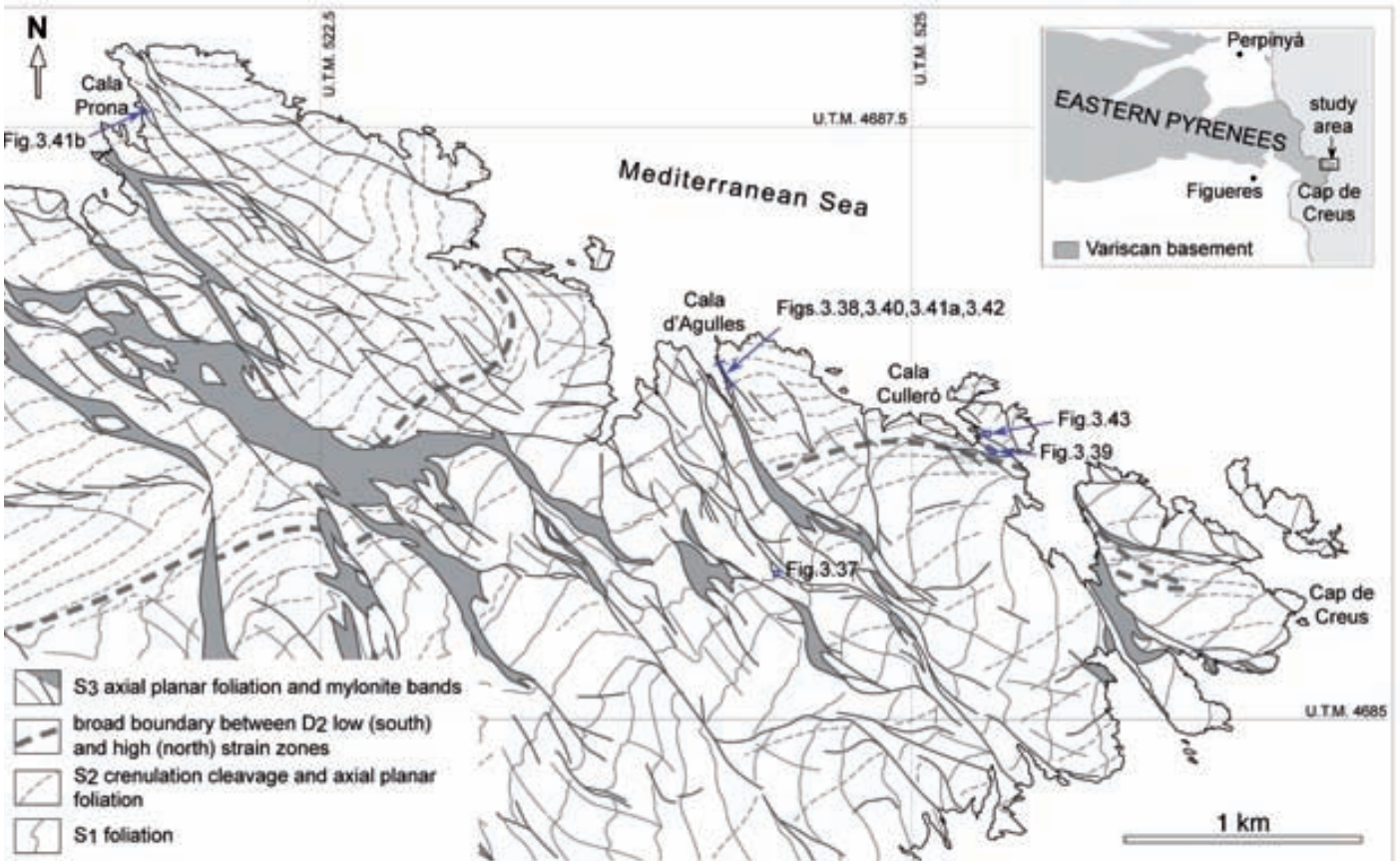

Fig. 3.36. Location of the examples used to investigate the different forms through lozenges the northeast Cap de Creus peninsula (modified from Druguet, 2001).

the shortening field during D_3. Thus, the layering/foliation embedded by the conjugate shears drags and shortens to form oppositely concave microfolds (Johnson and Moore, 1996) that resemble the typical millipede structures described by Bell and Rubenach (1980) and Bell (1981), such in the example shown in Figure 3.37.

The angle 2θ between dextral and sinistral shears is bisected by the regional shortening axis and is always larger than 100°, even for incipient lozenges. This fact, the instantaneous shortening axis bisecting the obtuse angle between conjugate shears, has been reported for networks of ductile shear zones in both nature and experiments (Cosgrove, 1976; Carreras, 2001; Mancktelow, 2002; Aerden et al., 2010; Carreras et al., 2010; Gomez-Rivas and Griera, 2012). It is also important to notice that, despite the overall regional dextral kinematics, at this range of α values there is no prevalence of one set over the other, and lozenges initially display symmetric (rhombic to lensoidal) shapes.

The crosscuts observed around millipede type lozenges indicate that dextral shears commonly overprinting the sinistral ones. With progressive dextral rotation of the bounding shears, imposed by the bulk regional kinematics, lozenges deform

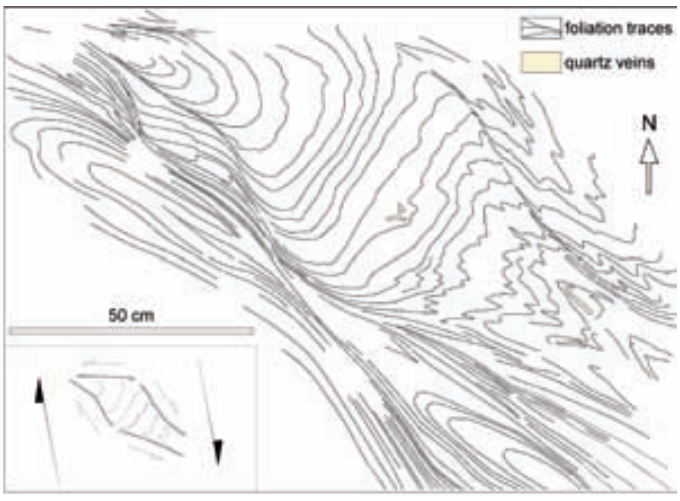

Fig. 3.37. Structural sketch of a millipede type lozenge from Coll de ses Portes. See Fig. 3.36 for location. Note on the upper left side another smaller lozenge of the contractional overstep type.

internally developing very complex folding patterns and achieving sigmoidal shapes.

Model L2: Domino type lozenges

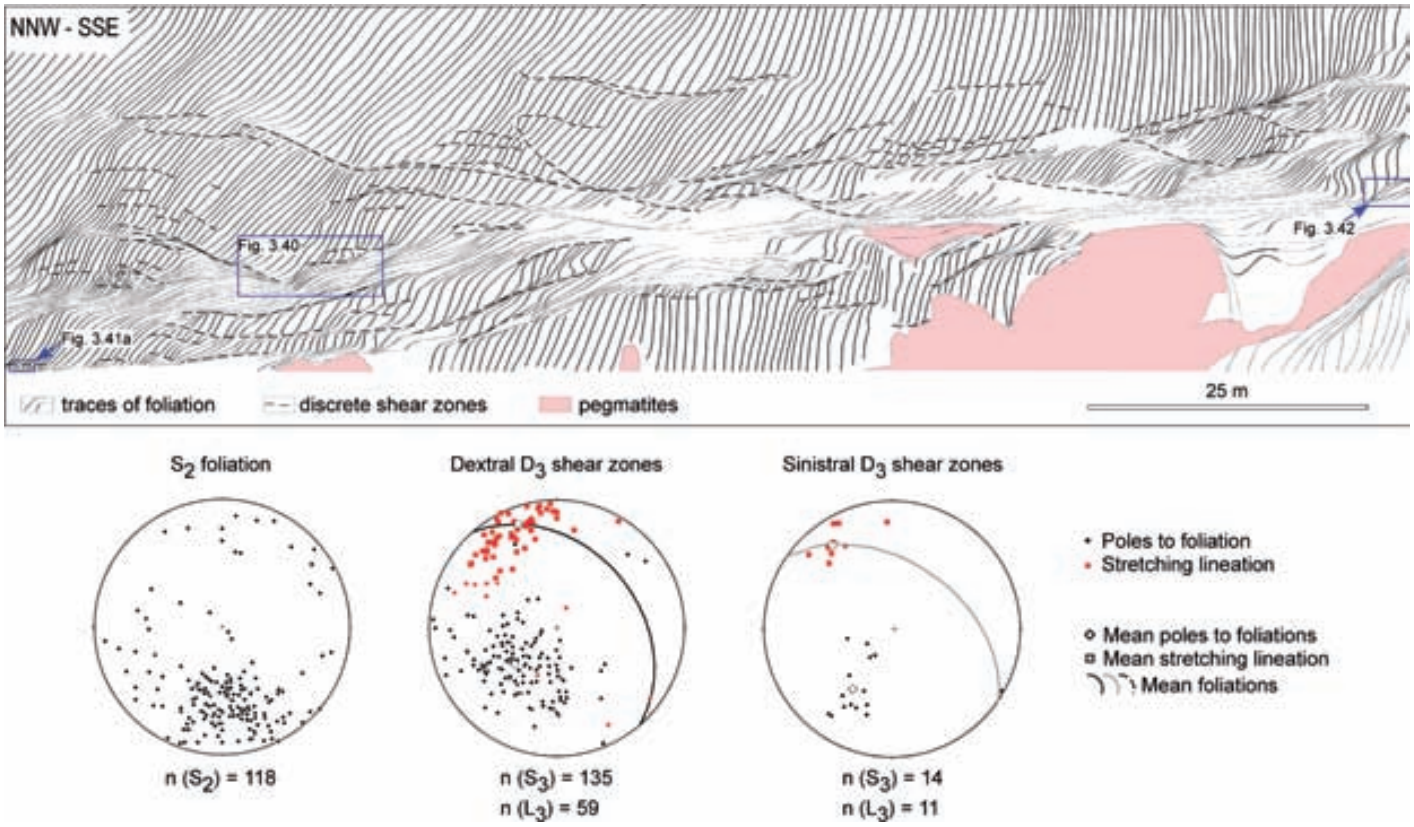

Fig. 3.38. Cross-section and equal area lower hemisphere projections of structural elements of the Cala d'Agulles shear zone array, centimetric to metric scale overstep type lozenges (models L4) abound towards the central part of the profile. See Fig. 3.36 for location. The three boxes indicate location of Figs. 3.41, 3.42a and 3.43.

In this model, the previous host foliation is subjected to progressive extension, being oriented close to a plane of maximum shear strain. In this case, lozenges preferentially initiate by linkage of individual principal synthetic shear zones throughout secondary antithetic shears that propagate sub-parallel to the pre-existing foliation (Lister and Williams, 1979; Carreras, 2001). The mechanism is analogue to the domino or bookshelf mechanism (Mandl, 1984) in which bulk shearing is partly accommodated by synthetic rotation of blocks through antithetic shears, that in our case study are parallel to the foliation and have sinistral sense. Domino type lozenges have a sigmoidal shape and tend to form imbricated arrays (Fig. 3.39). Another feature characteristic of this type of lozenges is the progressive development of wedge-shaped coalescences (Carreras et al., 2010) that result from deflection of the principal shear zones by the secondary antithetic shears (two of them highlighted with the red squares in Fig. 3.39).

The foliation-parallel antithetic shears may form as in the depicted sketches (Fig. 3.35) or as splays or oversteps between stepped synthetic shears. The last mechanism would likely correspond to the one suggested by Fusseis et al. (2006) and Schrank et al. (2008) to explain the anastomosing geometry of the Cap de Creus shear zones. The shear zones they analyzed mostly correspond to localities (Cala Culleró and Cala Prona; Fig. 3.36) where the previous S2 foliation have an ENE-WSW orientation, which is optimal for the generation of domino and/or overstep type lozenges.

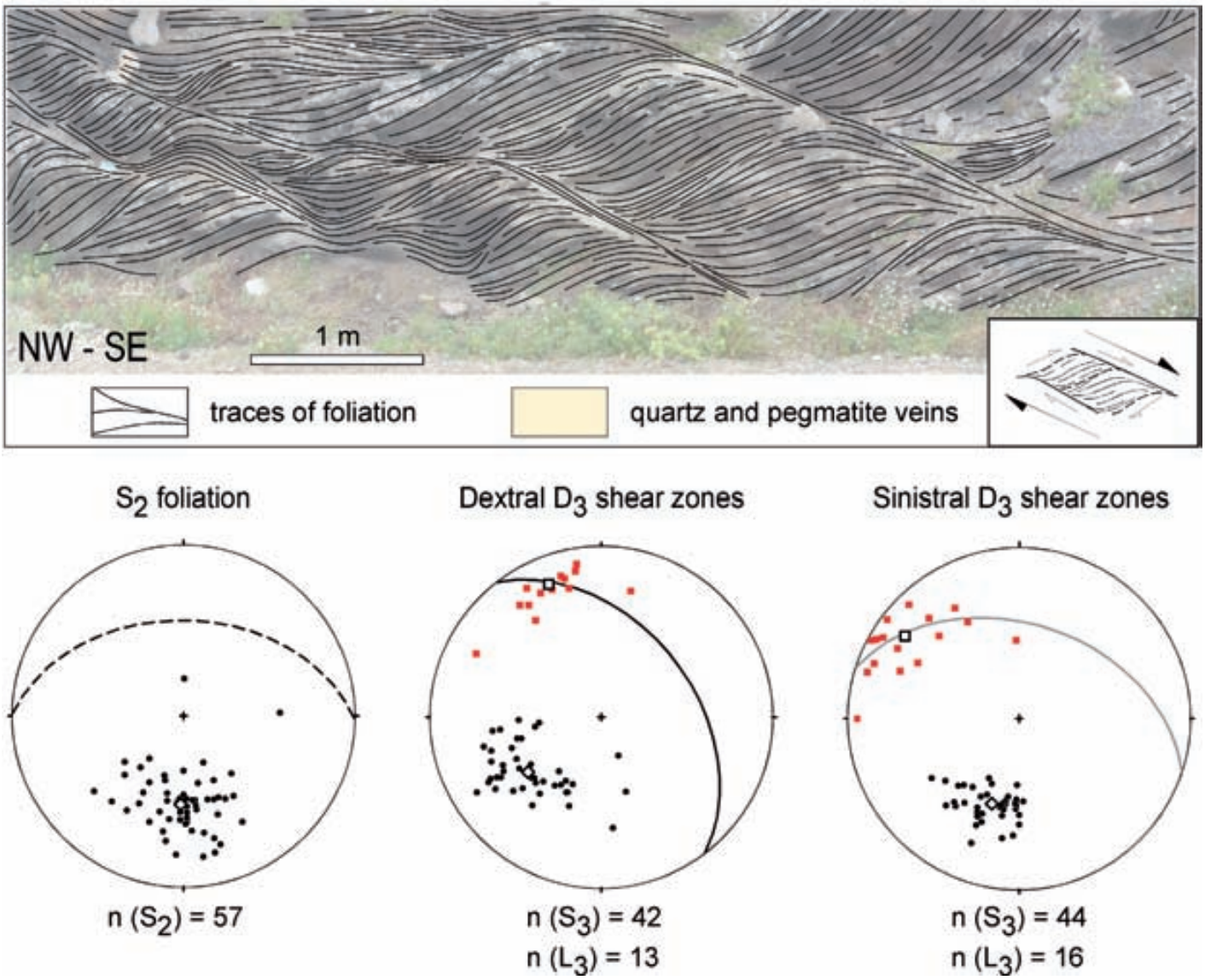

Fig. 3.39. Structural sketch and equal area lower hemisphere projections of structural elements of lozenges of the domino type from Cala Culleró. See Fig. 3.36 for location. Legend for the stereoplots as in Fig. 3.38.

Model L3: Internal pinch-and-swell type lozenges

Those settings with α around 135° are characterized by the presence of two sets of equally dominant conjugate shear zones that are, like in model L1, oriented symmetrically with regard to the previous foliation, which in this case is subparallel to the instantaneous extension direction. The intersection of dextral and sinistral shears gives rise to lensoid lozenges with the preserved internal foliation laying in the extensional field and matching the lozenge long axis (e.g. Fig. 3.40). The resulting structure correspond to the so called internal pinch-and-swell (Cobbold et al., 1971; Cosgrove, 1976), internal boudinage (Ramsay and Huber, 1987), normal kink bands (Cobbold et al., 1971; Kidan and Cosgrove, 1996) or foliation fish (Hanmer, 1986), where internal ductile instabilities grow in foliation planes during progressive foliation-parallel extension. Like in the millipede type, the pinch-and-swell type lozenges may become asymmetric (sigmoidal) with progressive non-coaxial deformation.

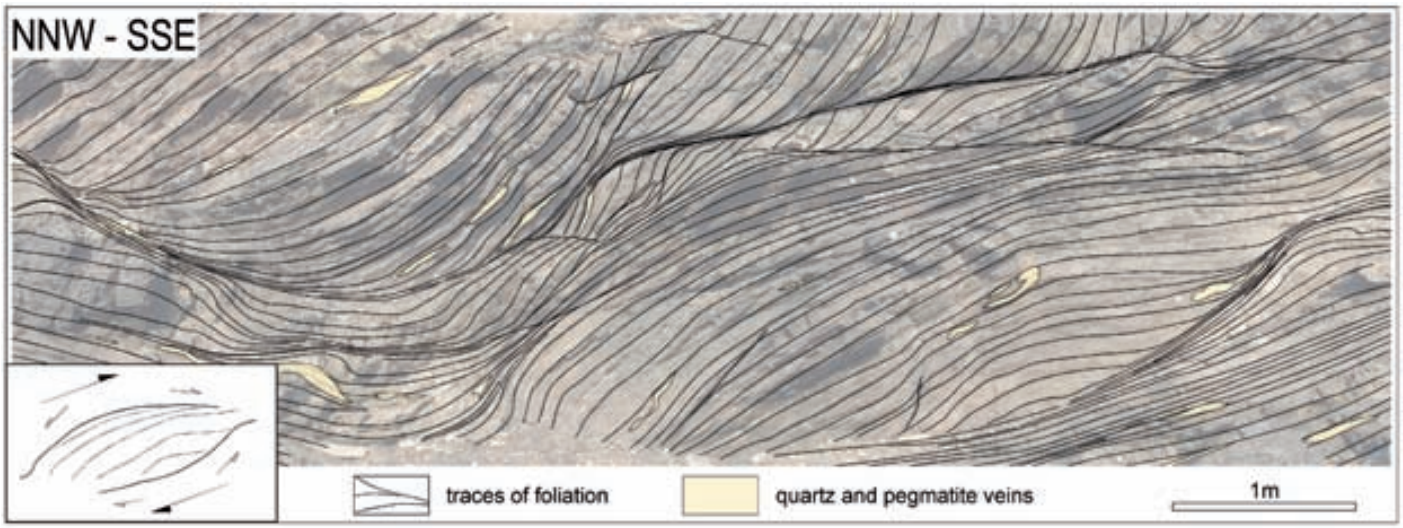

Fig. 3.40. Structural cross-section of lozenges of the pinch-and-swell type from Cala d'Agulles. See Figs. 3.36 and 3.38 for location.

Models L4: Overstep type lozenges

In the study area, for α around 150°, i.e., in domains where the previous foliation strikes ENE-WSW, there is prevalence of synthetic (dextral) shear zones. In these settings, and in areas of isolated shear zones where lozenges are scarce, dextral shear zones form a relay pattern consisting on quasi-straight, overlapping or underlapping subparallel discrete shears. This is well illustrated in the upper part of the Cala d'Agulles cross-section (Fig. 3.38). Towards domains of more widespread shearing, these shear zones are progressively mutually connected through their curved propagating tips, causing the development of lozenges in the transfer zones, such in the central part of the Cala d'Agulles section. The linkages can give rise to contractional or extensional oversteps (following the nomenclature of Peacock et al., 2000), depending on the initial left- or right-stepping of the principal shears, respectively. Lozenges developed by this mechanism use to have a sigmoidal shape due to the stepped geometry of the initial shear zones. The asymmetry may be "S", as in model L4a, or "Z", as in model L4b (Fig. 3.35), depending on the stepping sense (left and right, respectively). Sometimes, lozenges of very similar geometries can be interpreted as formed by coalescence of principal and secondary shears or splays (as it could be inferred from geometries in the central part of the section shown in Figure 3.38), rather than by overstep linkage. However, it is often difficult to infer the precise lozenge forming mechanism. For the sake of simplicity, the sketches in Fig. 3.38 only show the overstep types.

Models L4a: Contractional overstep type

In this model, left-stepping shears intersect, curving asymptotically towards parallelism with the host foliation until merging with the opposite shear (e.g. Fig. 3.41). Shear sense along the transfer zones is generally apparently synthetic (dextral). However, since this type of overstep has to be accommodated by contraction, a minor component of reverse movement associated to dextral shearing is implied.

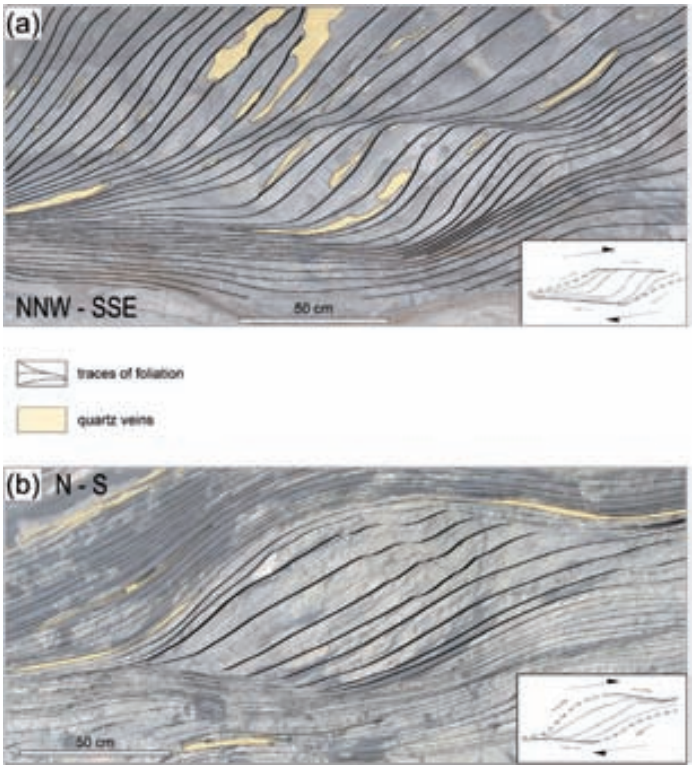

Fig. 3.41. Structural sketch of lozenges of the contractional overstep type. (a) Northern Cala d'Agulles, see Figs. 2and 4 for location. (b) Vicinities of Cala Prona. See Fig. 3.39 for location. Note the more isolated lozenges surrounded by pronounced mylonitic fabrics in (b).

dated by extension, implying a component of normal movement.

In Cap de Creus, lozenges of the type L4a are more common than those of type L4b, likely because shearing is initially more favourably partitioned into left-stepping, en-echelon arrays, giving rise to contractional steps. This prevalence of contractional over extensional steps was also observed by Pennacchioni (2005) in shear zones developed in tonalites from the southern Alps. In anisotropic rocks, as in our case, the L4a type lozenges would also be easier to develop because shear propagation along foliation becomes preferable. The overstep type lozenges described here using examples from the Cap de Creus shear zones are considered analogous to the releasing and restraining oversteps in strike-slip fault systems (e.g. Woodcock and Fisher, 1986; Swanson, 1990; McClay and Bonora, 2001; Mann, 2007).

Models L4b: Extensional overstep type

This model results from the linkage of two right-stepping shears through their curved propagating tips (Fig. 3.42). The overstep shears also show a predominant dextral movement but, contrarily to the previous case, the curved tips abut against the host foliation and deformation has to be accommo-

Models L5: Late shear band and contractional overstep type lozenges

As shown in the previous section (models L4), those settings with α around 150° are characterized by the prevalence of a single set of synthetic (dextral) shear zones. In this situation, lozenges

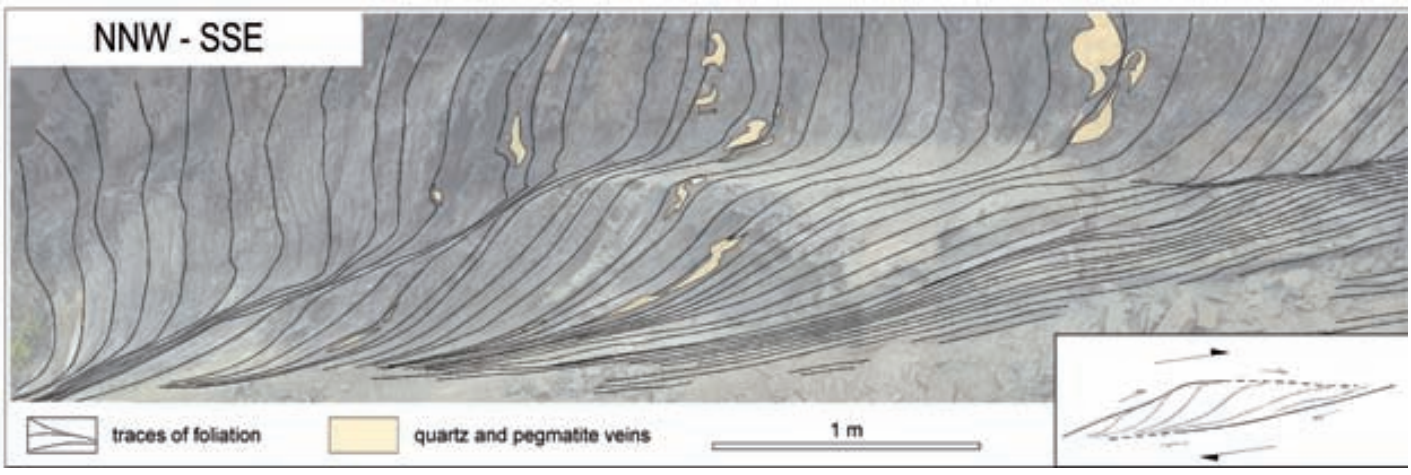

Fig. 3.42. Structural sketch of a lozenge of the extensional overstep type. South of Cala d'Agulles section, see Figs. 3.36 and 3.38 for location.

would not form unless, as in models L4, the main shear zones have a stepped geometry or have associated non-parallel subsidiary shears, bifurcations or splays. If this is not the case but the host foliation continues stretching and rotating towards the bulk shear direction, domains of mylonitic foliation can develop at a around 175°. Instabilities generated by shearing of these mylonitic foliations, originate secondary synthetic shears at about 30° to the bulk shear direction (late shear bands, e.g. White et al., 1980; Agard et al., 2011). The new arising geometry of mylonitic bands being obliquely sheared leads to formation of a type of sigmoidal lozenges, here named "late shear band type" (model L5a, Figs. 3.35; 3.37, upper left side; 3.43).

Finally, we can also consider the situation where the prevalent previous foliation is close to parallel to the mean shear plane (α angles around 175°). Under this orientation, oblique shear bands (analogous to the R-shears in brittle deformation) will preferentially develop as left-stepping, en-echelon, arrays that may give rise to contractional steps. This type of lozenges is geometrically identical and genetically similar to the contractional overstep type (model L4a), being difficult to distinguish from the late shear band type of lozenges. This is the case, for instance, of a lozenge shown in Figure 3.37 (small lozenge on the upper left side).

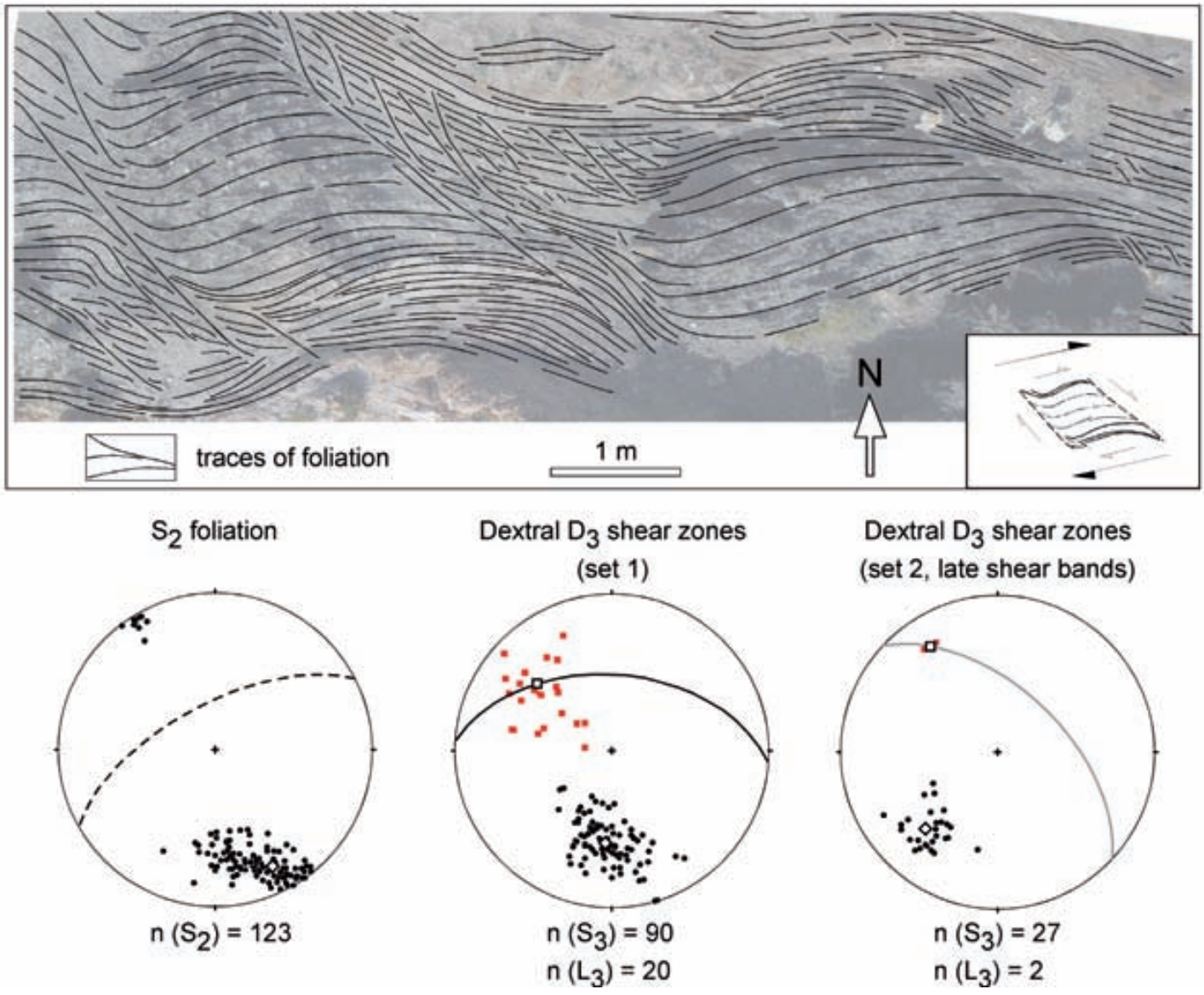

Fig. 3.43. Structural sketch and equal area lower hemisphere projections of structural elements of lozenges of the late shear band type from Cala Culleró. See Fig. 3.39 for location. Legend for the stereoplots as in Fig. 3.41.

Taking these development models, an assessment on the formation mechanism of a lozenge developed in foliated rocks can be done through careful observation and detailed analysis of the bounding shear zones: their kinematics, their interconnections and mainly their angular relations with the foliations in the host, less deformed rocks. The initial angle α_0 may also be extracted from the surrounding less deformed rocks. However, caution should be taken when analysing lozenge shapes in terms of extracting general strain and kinematic inferences.

Only if the precise mechanism of lozenge initiation is determined, the bulk shear sense can be inferred from the shape of some rhomboidal and sigmoidal lozenges. This is reliable for domino and for shear band type lozenges (models L2 and L5, respectively). Inferences from millipede and internal pinch-and-swell types lozenges (models L1 and L3, respectively) may be done if their shapes have been asymmetrized by non-coaxial progressive deformation. Reliability of the overstep type lozenges (model L4) as shear sense indicators is only warranted if contractional and extensional stepping can be discriminated from the lozenge internal and marginal structures (see Fig. 3.35).

Local variations in foliation orientation at metric to centimetric scales due to the pre-shearing structural arrangement can lead to lozenges of different mechanisms coexisting at the same outcrop (e.g. Fig. 3.38). Furthermore, lozenge initial shapes can be modified, as both the bounding shear zones and the lozenges are able to progressively deform (see subchapter 4.2). The structural evolution with progressive deformation may obliterate initial structures.

Indeed, with progressive rotation of the former anisotropy new shears can initiate, propagate and interconnect according to the changing foliation orientation, i.e., as the initial angle α_0 changes (Fig. 4.1c). This often bears to very complex structures, so that it is difficult to relate an individual lozenge or group of lozenges to a single development model. Sigmoidal asymmetric shapes may superimpose on previous millipede or internal pinch-and-swell types (e.g. Fig. 3.37).

Chapter 4

DISCUSSION AND CONCLUSSIONS

4. DISCUSSION AND CONCLUSIONS

4.1. GEOMETRY OF LOZENGES

Tectonic lozenges are important structures as they may form under many different scales and geological and tectonic contexts (vorticity number, strain type, hosting rock type, metamorphic conditions at which the involved shears form…). They are rather common in highly heterogeneous ductile deformed domains, where shear zones abound and anastomosed shear zone networks form. Ths is because strain tends to localize along rheologically contrasting boundaries and within the weaker materials. Lozenges formed in these type of settings are analogous to the sigma micro-structures in minerals (Passchier and Simpson, 1986). Natural examples (Coward et al., 1976; Passchier and Williams 1989; Passchier and Coelho, 2006) as well as analogue and numerical modeling abound (subchapter 3.2.1; Tullis, 1990; Mancktelow, 2002; Jessell et al., 2009). However, anastomosed patterns are not exclusively associated to deformation of heterogenous media and are also common in isotropic/anisotropic homogeneous media. Lozenges in this type of networks represent domains of less deformed rocks bounded by anastomosing and interconnecting shears. There are also numerous examples documented of lozenges formed by shear zone interconnection in the literature (Boyer and Elliott 1982; Choukroune and Gapais, 1983; Pollard and Aydin, 1984; Gapais et al., 1987; Lamouroux et al., 1991; Childs et al., 1996; Walsh et al., 1999; Davis et al., 1999; Hudleston, 1999; Ahlgren, 2001; McClay and Bonora, 2001; Nicol et al., 2002; Mancktelow, 2002; Carreras et al., 2005; Mahan and Williams, 2005; Pennacchioni, 2005; Fusseis et al., 2006; Pennacchioni and Mancktelow, 2007; Mann, 2007; Schwarz and Kilfitt, 2008; Tentler and Amcoff, 2010: Carreras et al., 2010; Ponce et al., 2013). The subject of this Thesis is restricted to anastomosing and associated lozenges formed in relatively homogeneous foliated rocks, although in the presented examples the role of some minor rheological contrast cannot be completely neglected.

Lozenges developed in homogeneous media basically are ellipsoidal structures outlined by shear zones enclosing less deformed rocks than the milonites they are surrounded by. I.e., the boundaries of the lozenges have underwent recristallization, been actively involved in a deformation event giving rise to shear zones, while the interior has not been directly involved into this new shear zone deformation event, although it may be affected by some shearing, folding or undergo solid body rotation as a consequence of strain partitioning. In sections parallel to the shear direction, shear zone-related lozenges are tipically elongate, with the long axis sub-parallel or at a low angle to the shear direction.

An overview is given to the 2-D geometry of tectonic lozenges in Figure 4.1a. The lozenge variety is displayed considering the aspect ratio (ratio of lozenge length to width normal to the long axis; Fig. 4.1b), the symmetry (anticlockwise angle between long axis and mean shear plane: δ; Fig. 4.1b) and the straight vs. curvilinear character of the lozenge sides. Four main types are depicted: rhombic, lensoidal, rhomboidal and sigmoidal lozenges. A wider variety of lozenge shapes can be found, among which lensoidal and sigmoidal lozenges are the most characteristic. Actually, the external geometry of lozenges can be thought of

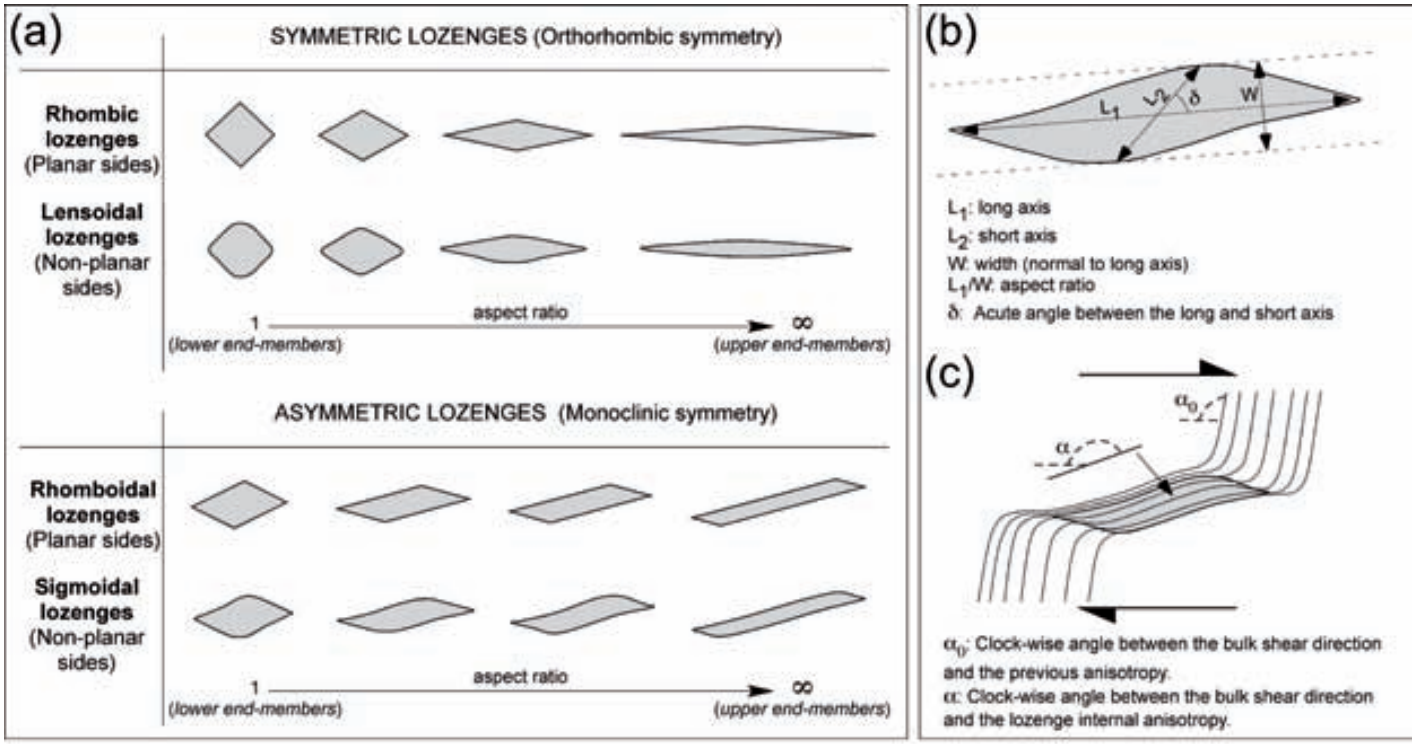

Fig. 4.1. Schematic representation of the diverse geometries and parameters that can be used to describe tectonic lozenges. (a) Different lozenge external shapes according to their symmetry, to their linear or curvilinear outline, and to aspect ratio. (b) Parameters used to geometrically define tectonic lozenges. (c) The angles α and α0 that are applied to lozenges in anisotropic rocks.

ranging from lensoidal (symmetric) to sigmoidal (asymmetric; Fig. 4.1). In general, interaction of dextral and sinistral conjugate shear zones leads to the development of lensoidal lozenges with orthorombic symmetry, while interaction of synthetic (dextral shears in the example) produces sigmoidal lozenges with monoclinic symmetry, although they are called assymmetric to differentiate from the formers.

This typology is only geometrical and thus not suitable to establish connections to formation mechanisms, neither from a mechanical nor from a kinematical sense. This is because the initial symmetry and shape parameters of lozenges (angle δ and aspect ratio L1/W; Fig. 4.1b) depend on many factors such as shear zone orientation (which in turn, depends on the orientation of the previous foliation), type of shear zone propagation and interconnection, distance and sense of offset between stepping shear zones, relative length and spacing between the conjugate pairs defining the lozenge, etc. All these variables make the lozenge geometry not unequivocally related neither to strain nor to kinematic types of deformation zones.

4.2. LOZENGE EVOLUTION AND INTERNAL DEFORMATION

Coalescence and interconnection of shear zones leads to isolation of elongated domains of undeformed or less deformed lozenge-shaped bodies, i.e. lozenges. Despite the initial angle at which shear zones interconnect, continuing shearing will gradually modify the angular relationships between shears (Fig. 4.2-4.4; Ramberg, 1975; Williams and Price, 1990; Carreras et al., 2010). While in networks of incipient conjugate shear zones the angle formed by individual shears can be close to 90°, in highly evolved shear zone networks this angle increases up to the extreme that shear zones with opposite shear sense may become parallel. It is generally assumed that anastomosed systems with coexisting nearly parallel shear zones with opposite shear sense is not an original feature but achieved as result of progressive deformation (Ramsay, 1980). This means that the external geometry of lozenges changes with increasing strain as well as the internal geometry: when the bounding shear zones rotate towards the extension direction, the foliation of the less deformed domain bounded by the shears rotates synthetically with the rotating, bounding shears causing the internal deformation of the lozenge (Fig 4.2).

The internal deformation may be achieved through folding, stretching and/or rotation of the foliation but also through new, minor shears. These secondary shears are antithetics to the main, bounding shears and can be traced from them to the interior of the lozenges, where they end. Simpson (1983) already documented these secondary shears in Roses granodiorite. With increasing strain these shears propagate through the interior of the lozenge until they connect to other main bounding shear thus the lozenge is compartmentalized (Fusseis et al., 2006). Once the propagating tip of the new, secondary shear zone is linked to a main, bounding shear zone the secondary shear would widens instead of propagating. In this way, lozenges are progressively compartmentalized and the resulting parts form smaller lozenges (Fusseis et al., 2006; Fig. 4.2).

This is illustrated in Figure 4.3, where three sigmoidal lozenges in foliated metasedimentary rocks from Cap de Creus surrounded by dextral shear zones are shown. In all three samples the foliation was initially at a hig angle (ca. 90°) to shear zones, as denoted by the country-non mylo-

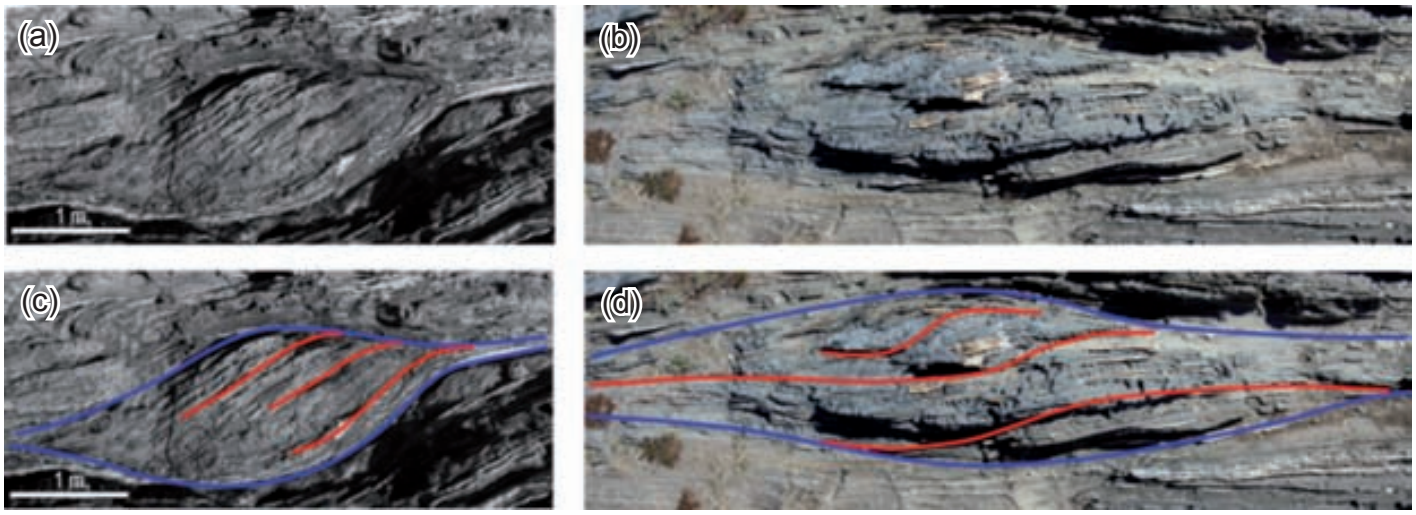

Fig. 4.2 Lozenge compartmentalization. Two lozenges showing secondary shear zones originated by the opening of the obtuse angle of the bounding shear zones. The incipient shears are antithetic to the main, enveloping shear zones and can be traced from the bounding shears to the interior of the lozenges where they end (c) or up to other or the same shear zone (d).

nitic foliation out from the lozenges. According to (i) the relative orientations between previous foliation and the trending of the shear belt giving rise to the bounding shears and (ii) the sigmoidal shapes, the three lozenges belong to model L2 or domino type. However, they show different (i) degree of rotation of the internal foliation (α value; Fig. 4.1c), (ii) external symmetry (acute angle between long axis and mean shear plane, δ; Fig. 4.1b) and (iii) aspect ratio (ratio of lozenge length to width normal to the long axis, L1/W; Fig. 4.1b). As said above, the outer geometry of the lozenge depends on many factors among them the distance and sense of offset between stepping shear zones that may originate different initial shapes, so the relative values of the two latters parameters should be taken as suggestives rather than conclusives. However, as the initial orientation of the previous foliation relative to the ISA's is the same for the three of them, the different angular relation between the mean shear plane and the lozenge domain foliation are ascribed to different evolution degrees. The degree of foliation rotation can be taken as a qualitative parameter of the lozenge evolution but not as a quantitative one.

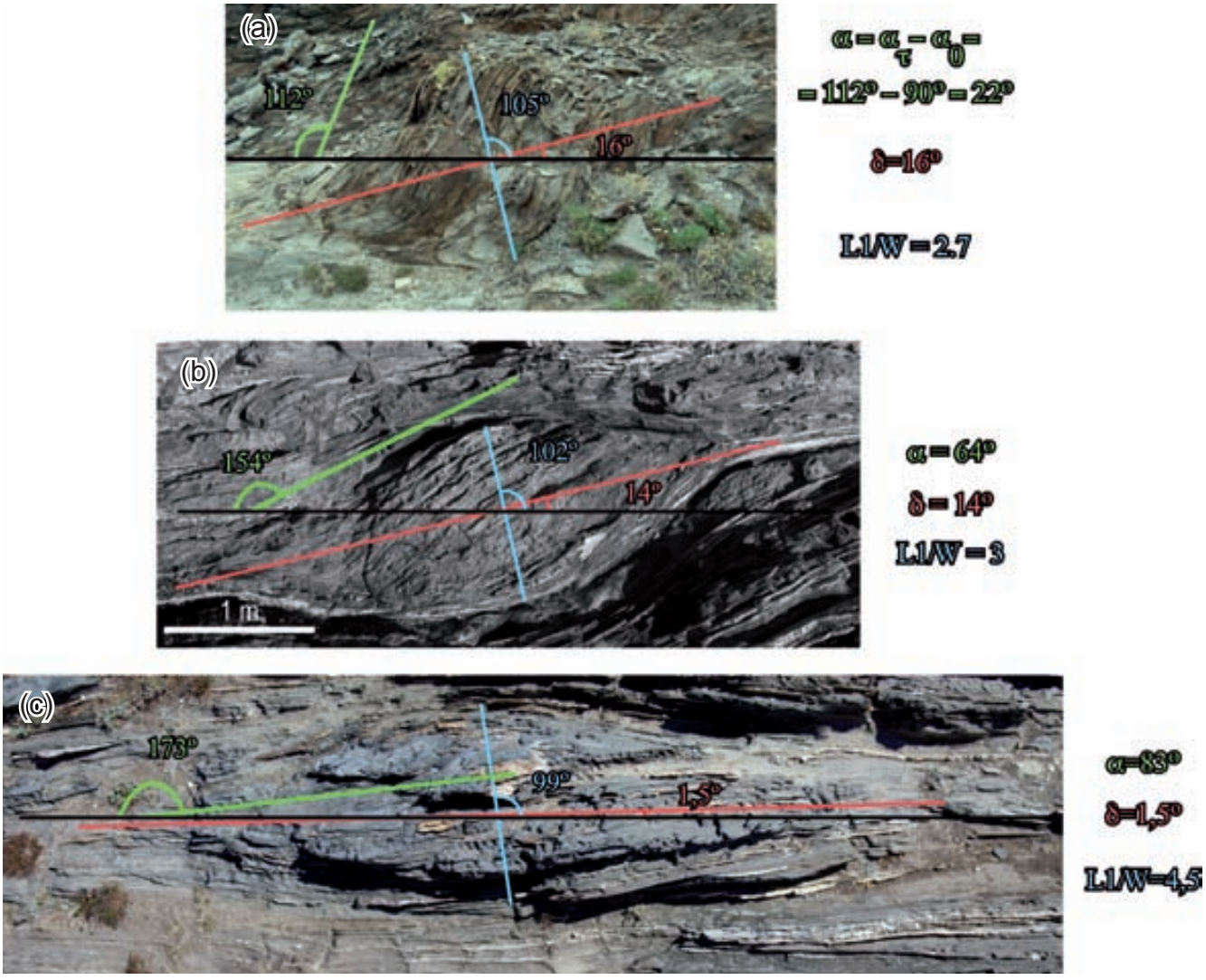

Fig. 4.3 Three examples of sigmoidal lozenges in metasedimentary rocks surrounded by dextral shear zones. Note the increasing degree of evolution (internal foliation rotation) from up to bottom. In all three samples the foliation was initially at a high angle (ca. 90°) to shear zones, as denoted by the country non-mylonitic foliation out from the lozenges. Also note the decreasing asymmetry with increasing evolution. With progressive deformation, the bounding shear zones tend to parallelize and this causes further lozenge elongation. The long and short axis rotates synthetically with the main shear sense and therefore there is a decrease in lozenge asymmetry with respect to the shear plane. Consequently, the lozenge can experience rigid body rotation (α and δ) and /or internal deformation. This internal deformation can be achieved either through folding and stretching, but also through foliation-parallel shearing, what implies that α and δ are not quantitative values of shear strain.

Thus, the internal foliation of the upper lozenge in Figure 4.3 has rotated 22°, the middle one has rotated 64° and the bottom one 83°. The tempting of calculating the tangent of those angles and relating the results to the shear strain underwent by the interior of each lozenge vanish when one remembers the total strain is accommodated through several mechanisms besides foliation rotation.

Hence, a newly formed lozenge would have small α and L1/W aspect ratio values and high δ values. As the lozenge is evolving, these parameters shifts, increasing the values of α and aspect ratio and decreasing the δ value. The foliation in a strongly evolved lozenge would rotate till closely parallelism to the stretching direction and finally, strain would became homogeneous at the lozenge scale and mylonitization of the lozenge would overprint the structure.

Thus, with progressive deformation the bounding shear zones tend to parallelize and this causes further lozenge elongation. It causes stretching and narrowing of the outer shape towards the stretching direction and the synthetic rotation of the long and short axis towards the shear sense. Therefore there may be a decrease in lozenge asymmetry with respect to the shear plane (Fig 4.3). Consequently, the internal foliation of the lozenge can experience rigid body rotation and/or internal deformation. This internal deformation can be achieved through folding and stretching, but also through foliation-parallel shearing in the case of foliated rocks (Fig. 4.1c). Accordingly, the rotation of the foliation cannot be taken as a measure of the shear strain underwent in the lozenge interior.

4.3. LOZENGE MODELLING

Lozenges have been modelled in both, rheologically heterogeneous and homogeneous anisotropic media (with slight competence contrast in the layering). Through *Elle* software heterogeneous anisotropic media was modelled and through the BCN-stage deformation machine both heterogeneous and homogeneous media were modelled. Graphical representations of the foliation orientation through lozenges were performed through SURGE.

4.3.1. Numerical modelling

Experiments of lozenges formed in heterogeneous anisotropic media were run in the Elle simulation platform under bulk simple shear conditions and without localization law. The results of the numerical modelling of such a media were showed in subchapter 3.1.1 and then they are discussed here:

(1) When the viscosity contrast between the softer layer and the hard phase is over several units of magnitude (1:5), the strain concentrates in the weaker matrix and at the soft/hard interface. Although only these two elements of the system are deformed (i.e., the multilayer and the rims of the initially elliptical hard phases), two types of lozenges are formed: (i) those outlined by the hard inclusions, whose rims are stretched adopting a lozenge shape. These types of lozenges are the analogous to the sigma structure; and (ii) the lozenge shapes achieved in the weaker media by the strain shadow effect beyond the hard phases. These are in accordance to lozenges observed in the field (Fig. 3.12). These lozenges rising up by strain shadow effect, are other (minor) type of lozenges formed by competence contrast.

(2) When the viscosity contrast between the softer layer and the hard phase is over several tens of magnitude (1:50), the strain in the weaker matrix is increased and the strain at the interface is almost undetectable; the hard inclusion rotates instead of deforming internally (although some insignificant internal deformation cannot be neglected). In this scenario, lozenges form exclusively in the multilayer by the strain shadow effect of the hard inclusions, what is enhanced by the rotation of them (Fig 3.11).

(3) Besides the competence contrast between weak multilayer and hard phase, small differences in the viscosity of the alternating multilayer have effect on the strain distribution through the whole system: for the same viscosity value of hard inclusion, the higher the competence contrast in the multilayer, the more heterogeneous the strain is distributed through the multilayer (Fig. 3.12).

(4) When the viscosity of all the elements in the model are set with same value, the experiment rheologically behaves as an isotropic media and the deformation is homogeneous throughout all the system. Hence, there is not neither strain localization, nor lozenge formation.

4.3.2. Analogue modelling

In the analogue modelling, experiments of homogeneous (experiment 14.01) and heterogeneous (experiments 15.01-15.05) anisotropic media were performed with plasticine and then subjected to pure shear in the BCN-stage machine. The discussion of the results is:

(1) The experiment performed with a small component of non-coaxial strain (the non-coaxiality is gotten by inclining the long axis of the model 15° (dextrally) relative to the shortening ISAs; Fig. 3.13) developed two sets of shear zones. The sinistral set is slightly dominant (i.e., more populated) over the dextral one. This might be due to the small non-coaxial dextral component of the deformation.

(2) However, when the induced strain in the model is coaxial, the population of both dextral and sinistral sets is similar.

(3) Lozenges form when shear zones start to propagate and then to interconnect. This leads to the fact that lozenges are related to anastomosing shear zone networks.

(4) The formation of lozenges takes place in both coaxial and non-coaxial deformation. When the models are shortened up to 50%, lozenges are formed only by synthetic pairs (Figs. 3.17 and 3.23b). When the models are shortened more than 60%, lozenges form by both synthetic pairs and conjugate pairs (Figs. 3.26).

(5) Lozenges start to abound when the shortening is around 60%-65%. They are formed by conjugated shears, but also by linkage of synthetic dextral and sinistral (Fig. 4.2).

(6) Shear zones end in the most ductile material, i.e. in the blue plasticine layers. (Figs. 3.17, 3.20, 3.23, 3.25).

(7) Small differences in the viscosity of the alternating multilayer have an effect on the strain distribution: the strain localizes in the softer layers nearby to the stiffer ones (Figs. 3.20 and 3.23). Up to 60% of shortening, the higher the viscosity contrast, the more shear zones developed (comparison of models 15.03 and 15.04 in experiment 15.05). Since 60% onwards, there is not difference in the shear zone concentration for such a small rheological difference between one and another model (Fig. 4.4).

(8) The obtuse angle of conjugate shear zones opens with increasing shear (Fig. 4.4).

(9) The cross-sections of the experiment giving rise to more deformation structures (experiment 15.05) show high variability in geometry and low continuity of the structures from one section to another, i.e., in the Y direction of the bulk imposed stress since the slices are XZ sections (Figs. 3.27 and 3.28). This evidence that any 3D interpretation from 2D outcrops would be highly tentative.

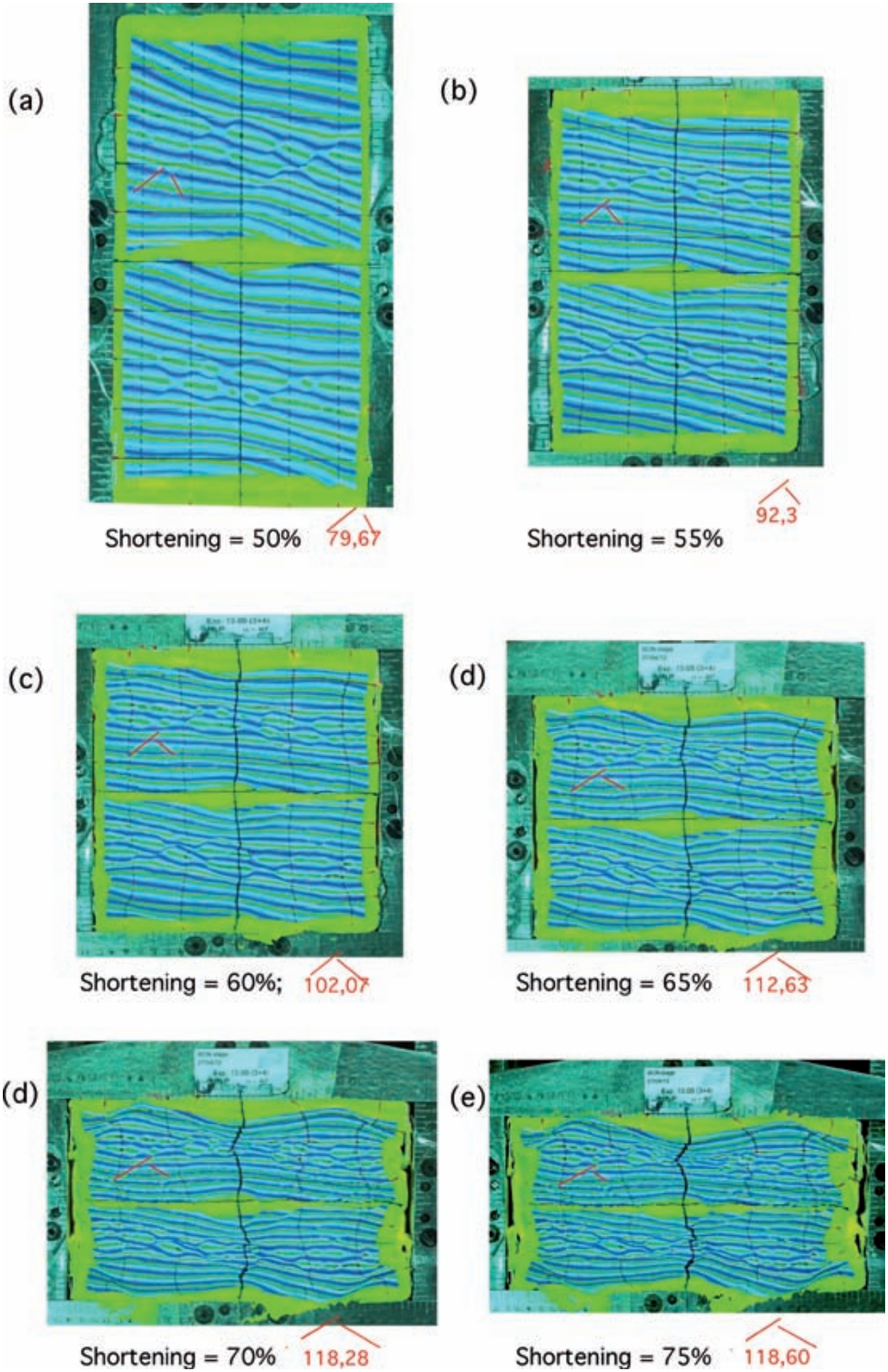

Fig. 4.4. Pictures of experiment 15.05 (models 15.03 and 15.04 shortened up to 75%) showing different deformation states at different degrees of shortenings. Two conjugate shear zones have been highlighted to show the opening of the obtuse angle with increasing shearing.

4.3.3. Graphical representation

2-D representations of the traces of the internal foliation in lozenges have been performed upon millipede-type and sigmoidal-type lozenges. Both types show that the higher foliation rotation takes place close to the borders. In the centre of the lozenge, there are even areas where the orientation of the previous foliation is well-preserved and shows no rotation (Figs. 3.27-3.29). Thus, the kinematics and the strain are localized at the rims and decrease towards the interior, where there may be areas with no appreciable effects of strain and kinematics change at the outcrop scale. However, while in the millipede-type this strain and kinematic gradation towards the interior happens in all borders, in the sigmoidal-type this occurr only next to the main border shear zones. The change in strain and kinematics from the secondary, antithetic, foliation parallel-shears to the lozenge interior is considerably smaller.

The general conclusion from the modeling is that lozenges develop in zones of high strains with high heterogeneous strain distribution, where the shear zones are interconnected and curved. High mechanical anisotropy and the associated different rheology of layering in anisotropic media enhance the anastomosing pattern, shear zone intercaction and, therefore, lozenge formation. Lozenges show higher strain close to the rims than in the centre.

4.4. DISPOSITION OF INTERNAL FOLIATION IN LOZENGES AND LOZENGE DEVELOPMENT IN FOLIATED ROCKS. RELATIONS TO THE KINEMATICS OF THE BOUNDING SHEAR ZONES

For foliated rocks, two typologies based on the orientation of the previous anisotropy and the kinematics of the bounding shear zones has been proposed. One typology is regarding the foliation as a passive marker (Kinematic typology, subchapter 3.2.1) and the other is regarding the foliation as playing an active role during deformation (Propagation typology, subchapter 3.2.2) and consequently controlling the orientation of the nucleation of shear zones and hence the shear zone pattern. Both typologies are defined in profiles normal to the mean shear plane and parallel to the shear direction.

The typology on the internal geometry of lozenges, i.e., on the internal foliation orientation of lozenges, is regarding the foliation as passive during deformation. It does not take into account the effect of anisotropy in the shear zone arrangements wich, although being a major control on the shear zone nucleation, may not be the dominant one for low mechanical anisotropies. Thus, the typology shows different lozenge internal geometries according to the relatives orientations between orientation of previous foliation and kinematics of the bounding shear zones for two end members of the kinematic of these: lozenges bounded by conjugate pairs of shear zones or by synthetic pairs of (dextral) shear zones (Fig. 3.32). It is assumed the shear zones make an acute angle to the long axis of the lozenge, being initially 90° for conjugate sets (Baumann, 1986; Baumann and Mancktelow, 1987; Ildefonse and Mancktelow, 1993; Mancktelow, 2002) and 30° for synthetic shear zones (Riedel, 1929). Although the typology neither takes into account whether the angular relationships of the wrapping shear zones is an original feature or achieved during deformation, Figure 3.32 is taken as the initial geometry of lozenges. With increasing strain the acute angle between shear zones narrows and the internal foliation rotates synthetically with the shear sense(s) (subchapter 4.5) what is shown in Figure 3.33.

The other typology (propagation typology) considers the pre-existing foliation as active planar mechanical anisotropy during deformation, thus it controls the nucleation of the shear zones (that would bound the lozenge) and therefore the orientation of these relative to the ISAs and in his turn, the kinematics of them. The typology does not take into account others factors that may control the shear zone nucleation. It has been settled up on the basis of the analysis of natural lozenges in foliated rocks, that were examined through detail mapping and analysis of shear zones from the Northern Cap de Creus area (Figs. 3.36-3.43). The models are drawn assuming bulk simple shear deformation (as D_3 shear zones in Cap de Creus), although the prevailing acting mechanism does not depend so much on the bulk kinematics (degree of non-coaxiality) but on the angular relationship between the pre- existing foliation and the bulk kinematic axes, as will be discussed in subchapter 4.5. Therefore, the different patterns depend on the initial orientation of the previous foliation with regard to the bulk shearing direction.

Figure 3.35 shows the initiation, propagation and linkage of the shear zones giving rise to lozenges for different foliation orientations. Any single mechanism is dominant within a range of orientations of the previous foliation with regard to the bulk shear direction. However, several mech-

anisms can be involved in a particular initial setting over which one generally prevails. This may be due to several factors which includes the unsteady relative orientation between previous foliation and stress axis (i.e., the changing orientation of previous foliation during the shear zones deformation event and the consequent different relative orientation between previous foliation and ISAs when new, younger shear zones are formed), different local stress axes, strain heterogeneities and others factors controlling the shear zone nucleation orientation. In fact, the orientation of the previous anisotropy is a major control on the initiation and evolution of shear zone patterns but not the unique. Although the models are in agreement with the results from modelling of shear zones in anisotropic materials under simple shear (Williams and Price, 1990) and with the field examples from Northern Cap de Creus (Figs. 3.36-3.43), where the orientation of the previous foliation seems to be the dominant control, the relative orientation between mechanical anisotropy and stress axis should not be directly correlated. I.e., a given initial orientation of the anisotropy with respect to the ISAs does not always imply a formation mechanism because of the reasons addressed above.

Finally, it has to be remarked that millipede-like geometries (Bell and Rubenach, 1980; Bell, 1981) are not exclusive of a particular bulk strain regime, because the presence of one or two sets and the prevalence of one over the other is the result of a complex relation between ISAs, anisotropy and progressive deformation.

4.5. ROLE OF ANISOTROPY IN FOLIATED LOZENGES

There are considerable differences between shear zone networks developed across previously anisotropic rocks (i.e. foliated/banded rocks) and those developed in low anisotropic or isotropic rocks. The difference lies in the effect of the anisotropy on the kinematics when that becomes active during deformation, what mainly causes two major circumstances: (i) the anisotropy, when it does not behave passively, governs the initial arrangement of shear zones, i.e., the pattern of the shear instabilities nucleation and (ii) when shearing a pre-existing foliation, the structures developed in each individual shear causes additional instabilities at shear zone margins.

The first situation has implications on the pattern of shear zone network, and the second has implications on the geometry/kinematics relationship of the deformation structures, thus they are explained by separate:

Bulk vorticity and shear zone network pattern in strongly foliated rocks

In isotropic rocks, the presence of two equally developed conjugate sets or the prevalence of one set (synthetic) over another (anthytetic) depends on the bulk vorticity (coaxial and non-coaxial flow respectively): in non-coaxial flow ductile shear zones initiate as a single set at 90° (Williams and Price, 1990) of the shortening ISAs (Passchier, 1988) and in coaxial flow as two conjugate sets, each one at an angle of about 45° with respect to the shortening ISAs (Baumann, 1986; Baumann and Mancktelow, 1987; Ildefonse and Mancktelow, 1993; Mancktelow, 2002). Recently, Zheng et al. (2011), based on the MMS criterion, stated the initial angle separating conjugate ductile shears in isotropic rocks is about 110° (i.e., each set at 55° with respect to the ISAs) and independent of rock properties. Such angular relationship can be achieved with progressive deformation as the strain affecting the shear bounded domains causes the gradual variation of angles (opening of the obtuse angle), enabling even the nearly parallelism of conjugate sets. However, to state that in isotropic rocks and under coaxial deformation ductile shear zones initiate at such angle and independently of the rock properties, contradicts experimental data (Cosgrove, 1976, Kidan and Cosgrove, 1996, Williams and Price, 1990) and field evidences that show how kink-like shears, shear bands or shear zones depend on rock properties.

Despite the contradiction about the initial angle at which conjugate sets form under bulk coaxial deformation, the fact is that when deforming isotropic media there is a correlation between the bulk vorticity (coaxial and non-coaxial) and the shear zone pattern (conjugate or synthetic shears), which cannot be applied to strongly foliated rocks due to the mechanical anisotropy induced by the foliation. When the foliation is strong enough as to become active during deformation, the initial arrangement of the shear zones (conjugate pairs or one dominant set) depends on the relative orientation of the previous foliation and the shortening ISAs rather than on the bulk vorticity. Thus, contrary to bulk coaxial flow, in bulk non-coaxial deformation equally developed conjugate sets may appear if the shortening ISAs are parallel (or closely parallel) to the anisotropy, and a prevalent set may develop if the shortening ISAs are oblique to the mechanical anisotropy, independently of the bulk vorticity (Fig. 4.5).

There are experiments (William and Price,

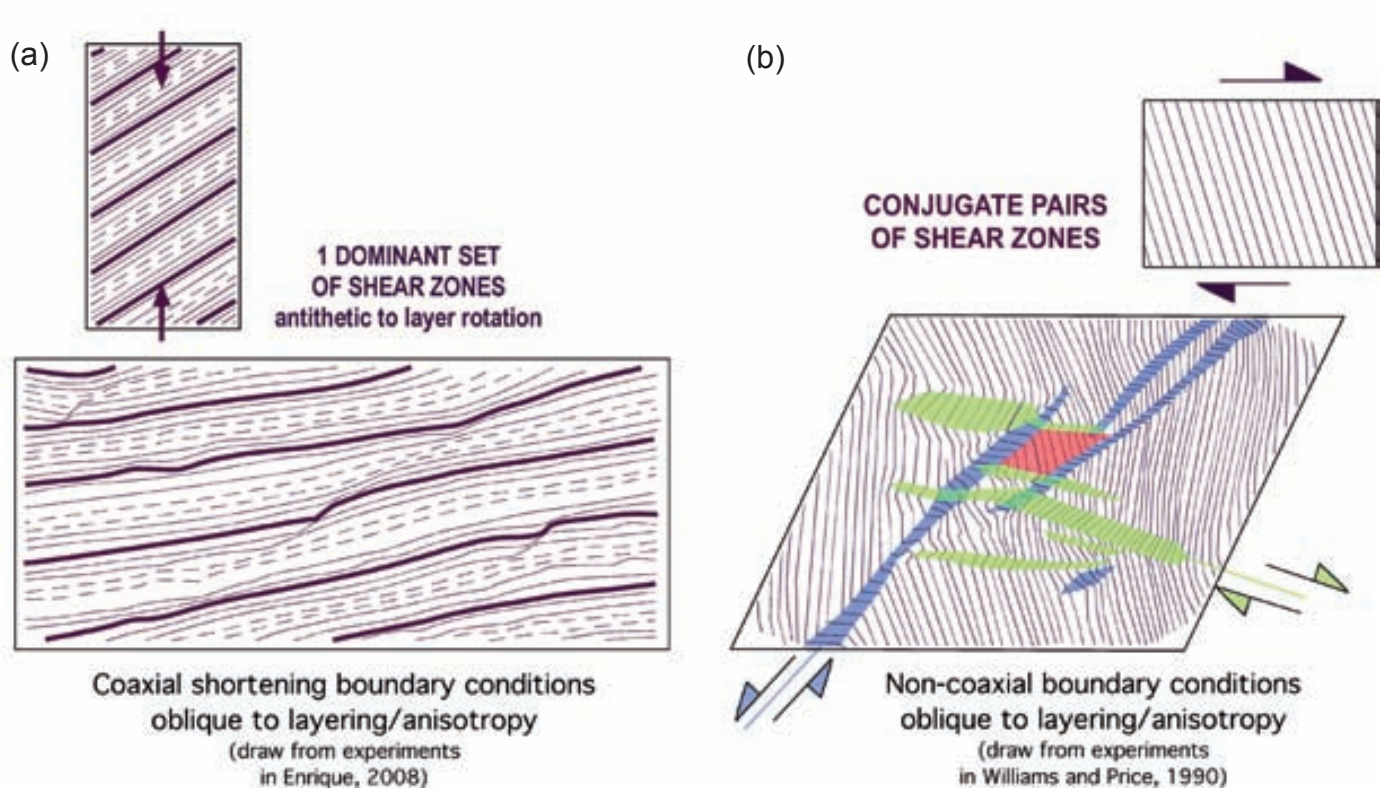

Fig. 4.5. Influence of the anisotropy/layering in the shear zone network independently of the bulk vorticity. (a) one dominant set of sinistral shear zones arises under coaxial deformation when layering is initially around 45º of the shortening ISAs (draw from Gomez-Rivas (2008)); (b) two conjugate systems of shear zones arise under non-coaxial deformation if the layering is normal to the shortening ISAs (draw from Williams and Price, 1990).

1990; Gómez-Rivas, 2008) and field examples (Figs. 4.9-4.11; Carreras et al., 2012) supporting this hypothesis. Gómez-Rivas (2005, 2008) performed a set of experiments under coaxial deformation in the same deformation machine (with similar materials and procedure) that the experiments performed for this study. Gómez-Rivas (2008) tested the different shear zone patterns originated after coaxial deformation of a multilayer media by changing the orientation of the anisotropy with respect to fixed ISAs. When the layering of the model was set at 50° dextrally rotated to the shortening axis (i.e., to the shortening ISAs), one dominant set of sinistral shears crosscutting the foliation at 30° was developed (Fig. 4.5a). Contrary, when the layering was at 90° to the shortening ISAs, two conjugate antithetic sets were formed. On the other hand, Williams and Price (1990) carried out similar experiments under non-coaxial deformation. They subjected specimens of artificial mica schist under simple shear with different initial orientations (intervals of 10° between 0° and 170°) of the anisotropy relative to the imposed simple shear plane. In those initial orientations oblique to the shear plane (i.e., closely parallel to the shortening axis), conjugate pairs of shear or kink bands were developed (Fig. 4.5b) while in those orientations closely parallel or orthogonal to the shear plane (i.e, oblique to the shortening ISAs), a single set was formed. This difference is due to strain partitioning: the strain within the specimens -prior to the development of the shears- can be partitioned into an anisotropy-parallel shear component and an anisotropy-normal shortening or extensional component. The relative magnitudes of the two strain components depend on the orientation of the mechanical anisotropy and it controls the shear zones pattern. Thus, when the layers are parallel to the shortening ISAs the flattening component is maximized

and the shear component is zero. Consequently, conjugate shears are formed. When they are parallel to the stretching ISAs, the anisotropy-parallel shear component is maximize and the flattening component is zero, so only a single set of shears is formed. For oblique orientations of the layers relative to the ISAs, a single orientation set would form when the shear component is high enough, and conjugate shears would form at lower ratios of shear strain to normal strain (Williams and Price, 1990).

In addition to the experiments, there are field examples supporting this fact. A very similar shear network pattern to that of the experiment of Williams and Price (1990) exists in Cap de Creus at the Lighthouse area (Fig. 4.6). Figure 4.6 is the drawing from picture of the area (map view) showing N-S trending foliation at the less deformed areas (slightly dextrally rotated at some domains). The wrench-dominated NW-SE

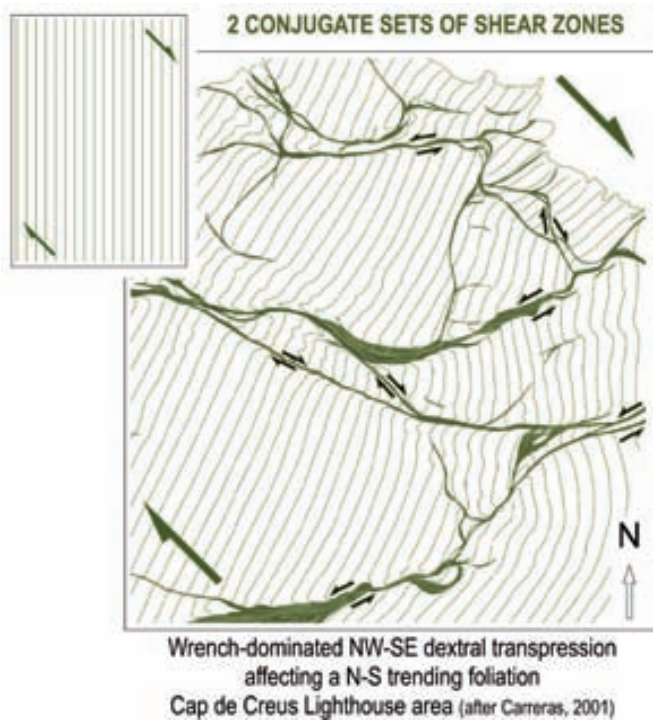

Fig. 4.6. Shear zone network of dextrally sheared anisotropic media with layering approximately parallel to the shortening ISAs in natural rocks (from Carreras (2001)). Note the similarity in the pattern to the experiments with artificial mica-schists from Williams and Price (1990) (Fig. 4.5b).

dextral transpression (Carreras, 2001) developed a conjugate set of ductile shear zones as the pre-existing foliation was initially closely parallel to the shortening ISAs. Actually, this role of the rock anisotropy on the initial arrangement of shear zones can be assessed through field analysis on the Northern Cap de Creus (NCC) shear belt. The NW-SE, D_3 NCC shear belt is formed by prevalent dextral with a minor reverse component D_3 shear zones and less abundant normal/sinistral shear zones producing a complex anastomosed network. The shear belt cut across domains with differently oriented dominant foliation (S_1, S_2 or $S_{1/2}$; Fig. 4.7). This variation in the foliation orientation allows to analyze the effect of the orientation of previous mechanical anisotropy on the shear zones pattern. Although there are different examples from the NCC shear belt evidencing the role of the previous foliation on the arrangement and kinematics of shear zones in shear belts, this can be best evidenced in the Culleró area. In there, the pre-shear foliation changes northward from E-W to N-S trends due to D_2 event (Figs. 4.7 and 4.8; Carreras and Druguet, 1994). In consequence, the NW-SE D_3 dextral shears cut across differently oriented mechanical anisotropies, and the shear belt displays a transversal variation. The southern domain essentially display synthetic (dextral) shear zones (shortening ISAs oblique to previous foliation) while in the northern part the presence of conjugate shear zones (dextral and sinistral) is common (shortening ISAs closely parallel to previous foliation). The former statement, summarized in Figure 4.10, is shown in detail in Figure 4.9 through two field examples from Culleró: Figure 4.9a is a domain belonging to the southern part. The stereoplot shows the orientation of the undeformed previous foliation ($S_{1/2}$) and the resulting shear zones orientation (one dextral set). Figure 4.9b is a drawing belonging to the northern part, and it shows different initial $S_{1/2}$ orientation and two pairs of conjugate shears.

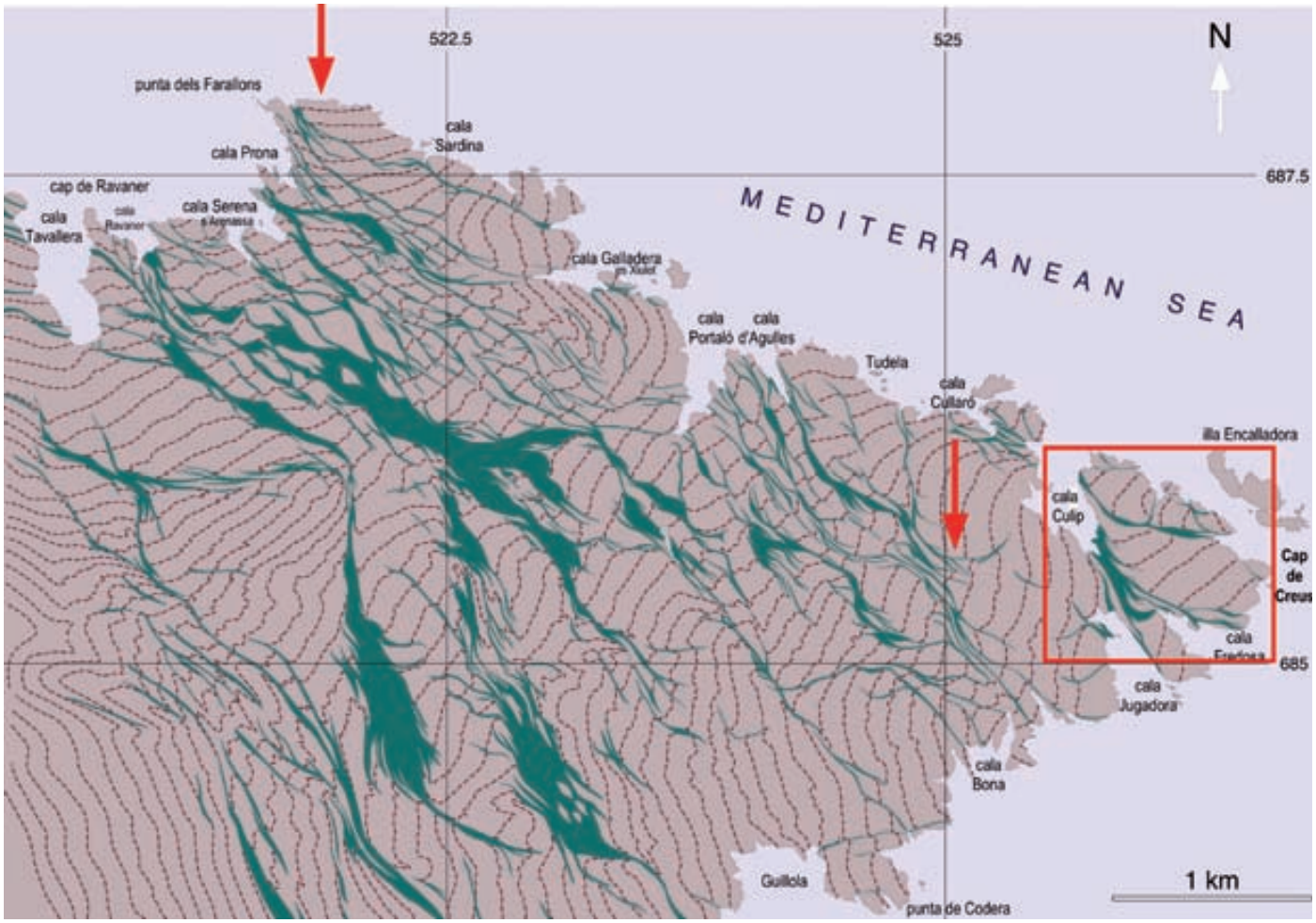

Fig. 4.7. Nothern Cap de Creus shear belt consisting on NW-SE trending shear zones. The belt is formed by dextral (with a slight reverse component) shear zones and less abundant sinistral (with a small normal component) shear zones and cross-cut the pre-existing foliation (S1, S2 and S1/S2) with different orientations (see arrows). Culleró area is highlighted through the red square.

Hence, the field case of NCC shear belt shows the key role of the anisotropy in strain partitioning and consequently in shear zone networks when it becomes active during deformation. Since lozenges are formed by shear zone interconnections, that role has also implications on the geometry of lozenges. Progression of shearing leads to interaction of shear zones (Ponce et al., 2013), and the NW-SE trending D_3, NCC shear belt consists on an anastomosed network of shear zones with coalescence and interaction of shears isolating lozenges. The structure of the lozenge differs if these are bounded by shear zones with the same kinematic sense or by conjugate shear zones (Fig. 3.32). Lozenges bounded by a single set of shears are sigmoidally-shaped and have a monoclinic symmetry (Fig. 4.10). Lozenges bounded by conjugate shear zones are millipede-shaped and ideally approximate the orthorhombic geometry, although the interaction of opposite shears can generate rather complex structures (Fig. 4.11d). The role of the mechanical anisotropy in the lozenge geometry is reflected in the Culleró area (Fig. 4.6). In the southern part of the shear belt, an anastomosed network of dextral shear zones bound sigmoidally-shaped lozenges (Fig. 4.11a and c). In the northern part of the shear belt, a network of conjugated shear zones occurs causing the development of complex orthorhombic, millipide-shaped lozenges (Figs. 4.11b and d). Therefore, the mechanical anisotropy leads to a situation in which the geometry of the lozenges have a complex relation with the bulk vorticity, being more related to the orientation of the previous foliation rather than to the bulk vorticity. In fact, the mechanical anisotropy control both the external

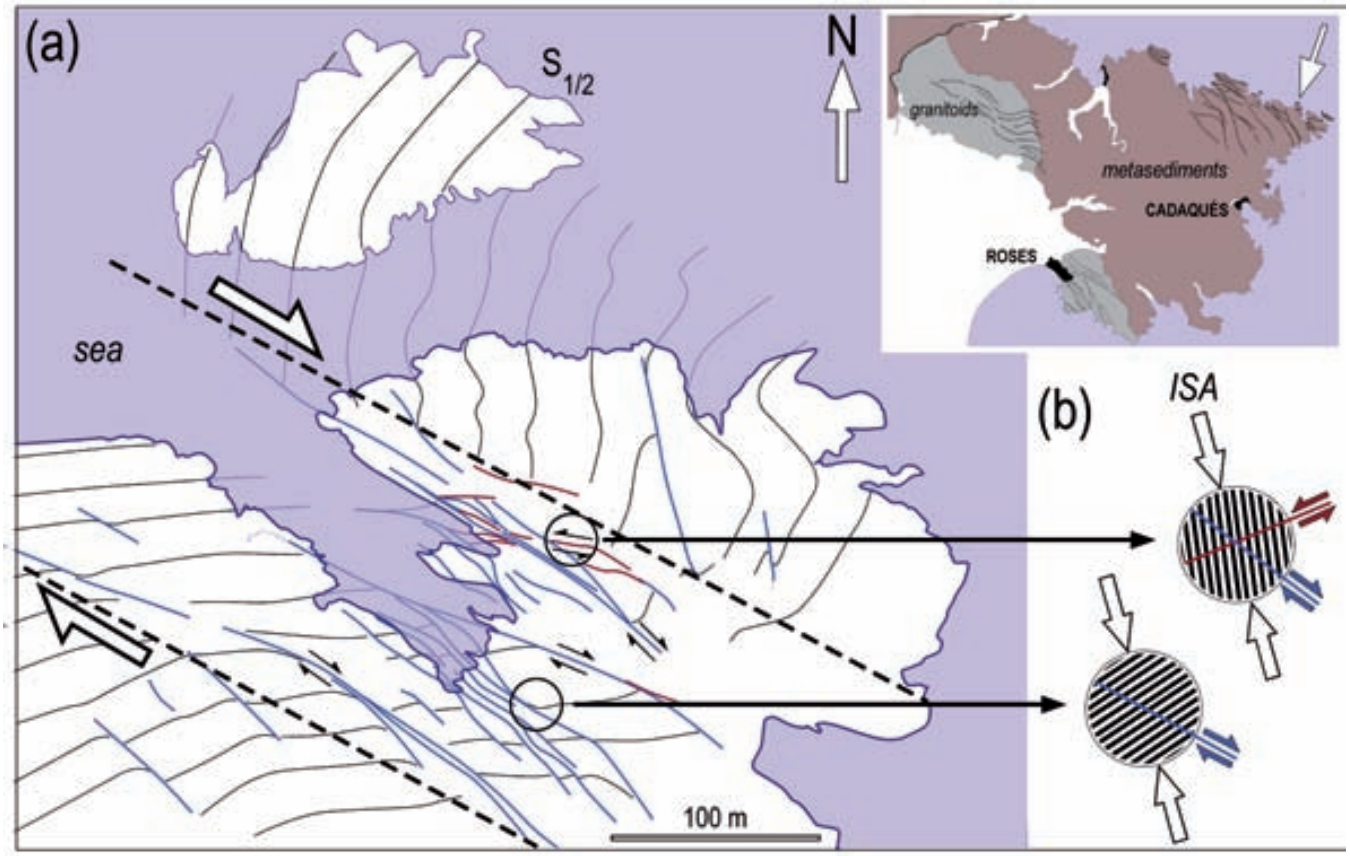

Fig. 4.8. (a) Sketch map of the Culleó area. The D3 shear belt cuts across a previous structure defined by the trend of S1/2 structure. (b) Circles showing the relation between previous anisotropy, instantaneous stretching areas and forming shears.

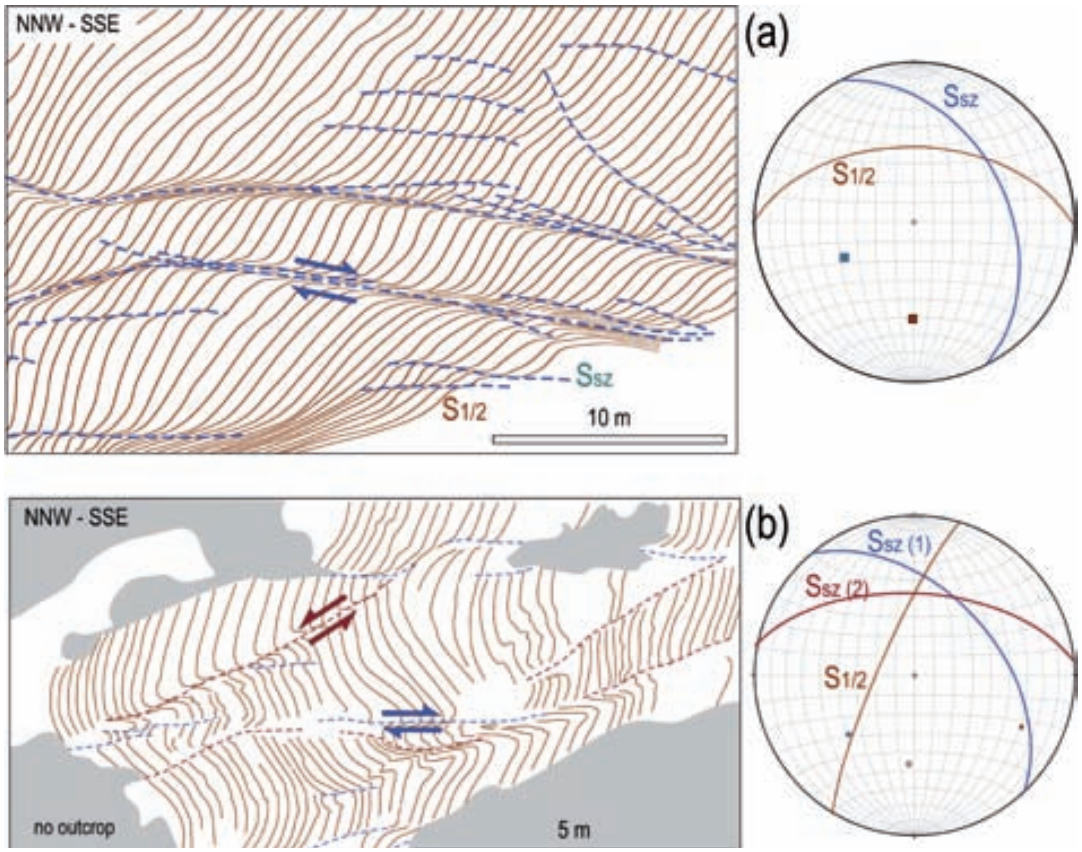

Fig. 4.9. Effects of the foliation on the development of shear zone sets evidenced by two examples from the NCC shear belt. (a) Obliquity of principal strain axes and pre-existing foliation (S1/2) leads to the development of a single set of dextral shear zones (Ssz). Cala d'Agulles area. (b) Close parallelism of the S1/2 foliation with the princiipal shortening direction lead to the development of two conjugate sets (dextral : Ssz(1) and sinistral Ssz(2)), (Punta dels Farallons).

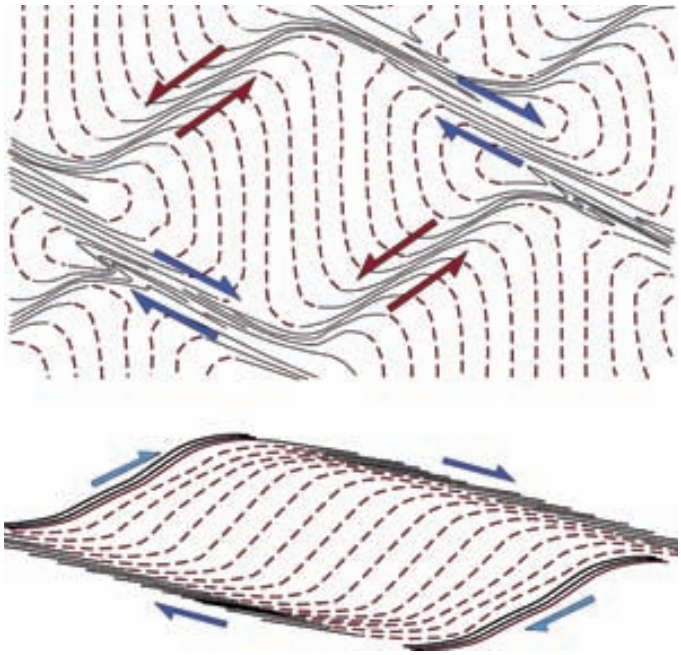

Fig. 4.10. Two types of lozenges arised from the coalescence of shears zones with oposite or same shear sense. (a). Lozenges are characterized by lower elongation in sections parallel to the shear sense , internal millipede-shaped structures and presence of complex folding at the tails of the lozenge. (b) Lozenges arosen from coalescence of shear zones with same kinematics are elongate and sigmoidally shaped and display a rather simple internal structure.

the internal geometry (millipede type –foliation rotated towards two senses- or sigmoidal type -foliation rotated towards one sense-). The field study shows that a single deformation event (D_3-related shear belt) involving deformations close to simple shear can generate both orthorhombic and monoclinic structures. Thus, the symmetry of the lozenge does not reflect the symmetry of the deformation and the formation of millipede-type (orthorhombic) or sigmoidal-type lozenges (Fig. 4.12) does not reflect the vorticity in a regional scale but the relative orientation between ISAs and previous anisotropy. This fact contradicts the common association of structural symmetry and deformation symmetry (Bell, 1981; Bell and Rubenach, 1983; Choukroune and Gapais, 1983; Gapais et al., 1987). This is shown in Figure 4.12, where the development of monoclinic and or

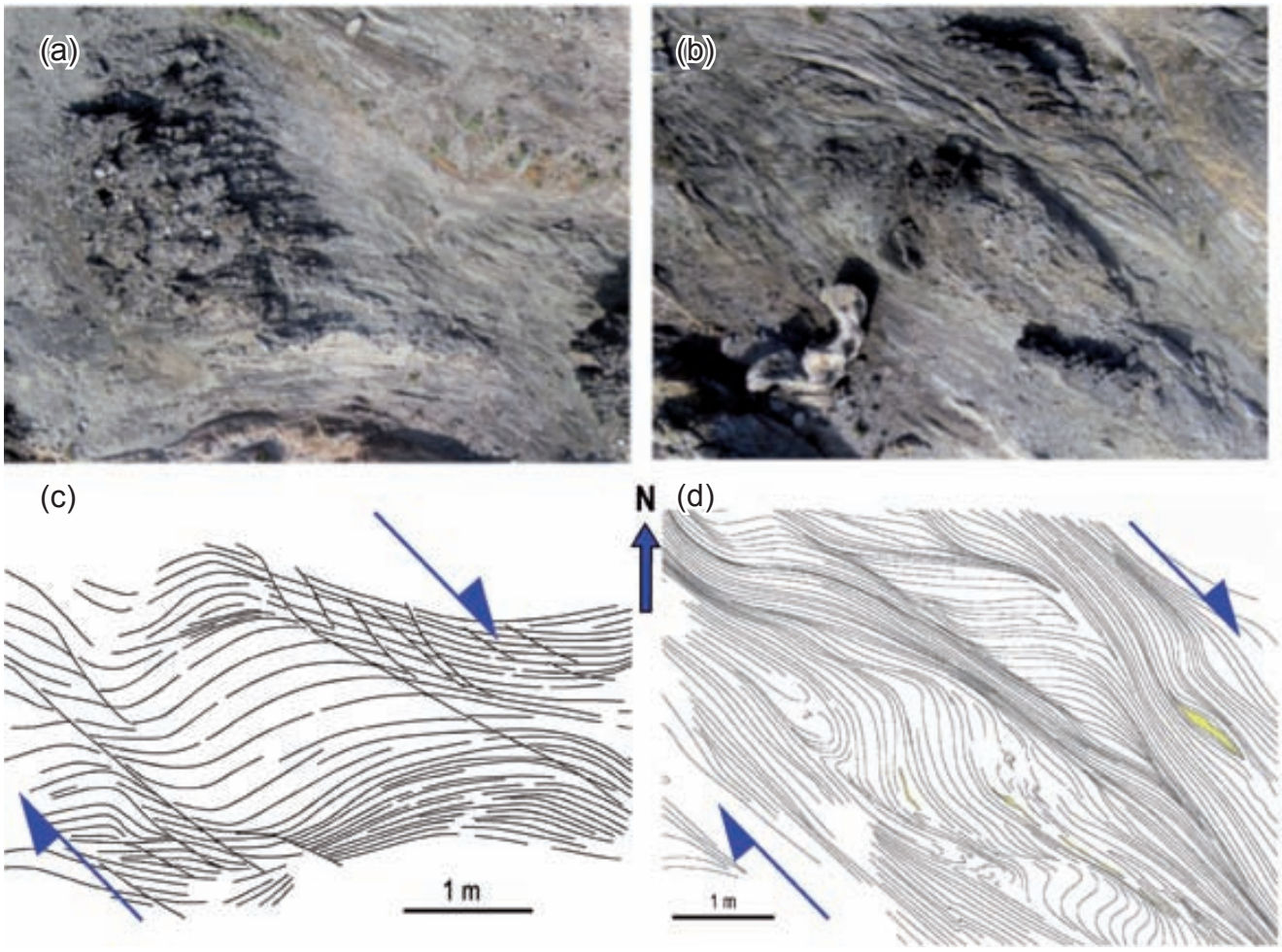

Fig. 4.11. Aerial picture from outcrop and drawing of two lozenges belonging to different domains in the NCC shear belt. (a) and (c) show a sigmoidal lozenge from the southern part where the previous foliation is W-E, and (b) and (d) show a millipede-type lozenge, bounded by conjugate pair of shear zones since the previous foliation was closely parallel to the shortening ISAs.

where the development of monoclinic and orthorhombic lozenges takes place under the same vorticity conditions in different foliation orientation domains .

Thus, the presented typologies (external geometry (Fig. 4.1), internal typology (Fig. 3.32) and development models (Fig 3.35)) are independent of the bulk vorticity of the flow, as the bounding shear zones can form in all bulk vorticity spectrum (0<Wk<1) and thus each individual type also.

Relations between geometry and kinematics in strongly foliated rocks.

The mechanical anisotropy has also implications in the kinematics of individual shear zones. Independently of the bulk strain regime (regional

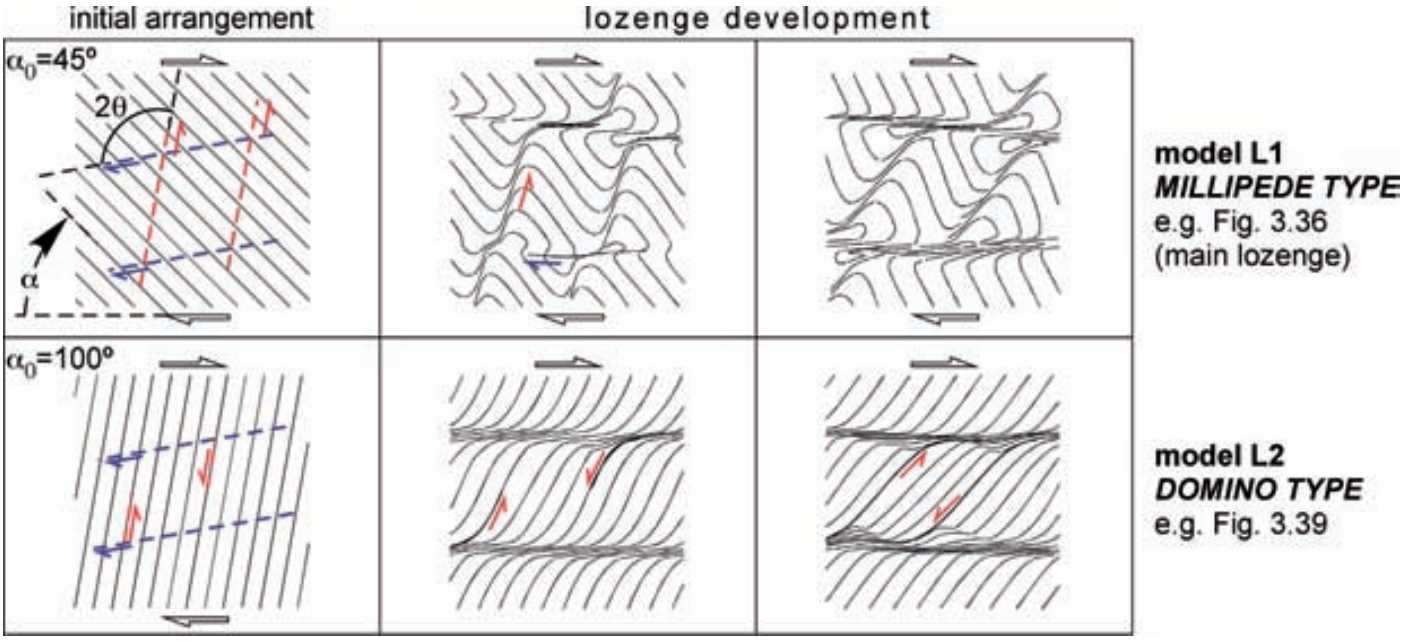

Fig. 4.12. Formation of lozenge with orthorombic geometry and foliation rotation towards two senses and formation of monoclinic, sigmoidal lozenge with foliation rotation towads one sense. The lozenges are generated under the same bulk strain regime, however one or another type is formed according to the anisotropy orientation.

vorticity), individual shear zones across strongly foliated rocks cause complex relationships between geometry and kinematics (Carreras, 1997; Ponce et al., 2013). The marginal deflection of the foliation (i.e, the drag of this at the shear zone margin) might give apparent displacements that contradict the real shear sense (Fig. 4.13).

This fact has implications on lozenges: It is assumed that lozenge asymmetries develop on sections parallel to the shear direction. However, when the host rock is anisotropic, the relation between 3-D lozenge geometry and shear kinematics is complex, as the structure depends on the relative orientation of pre-existing foliation and the shear plane, and it is independent of the shear direction. This is because the asymmetries of lozenges in foliated rocks caused by the marginal deformation of pre-existing foliation are controlled by the vorticity axis (i.e. the intersection line between foliation and shear plane; Fig. 2.4), which can form a variable angle with the shear direction (Figs. 2.4 and 2.5; Carreras, 1997). In consequence, some exposed asymmetries do not directly reflect the shear sense. This is illustrated with an example from Cala Culip (Cap de Creus, Fig. 4.13), where the vorticity axis is nearly paral-

lel to the mylonitic lineation.

In addition, the fact that the pre-existing foliation when sheared does not behave passively, causes the development of buckling instabilities at the initial stages or marginal domains of the shear zones that, as the result of progressive shearing, it would become sheared. This causes that shear related structures across pre-existing foliated rocks are far more complicated than ideal models, especially lozenges that may be bounded by several individual shear zones (Fig. 4.10a and 4.11b and d). Moreover, the fact that shear zones form anastomosed networks introduces an additional complexity of structural patterns.

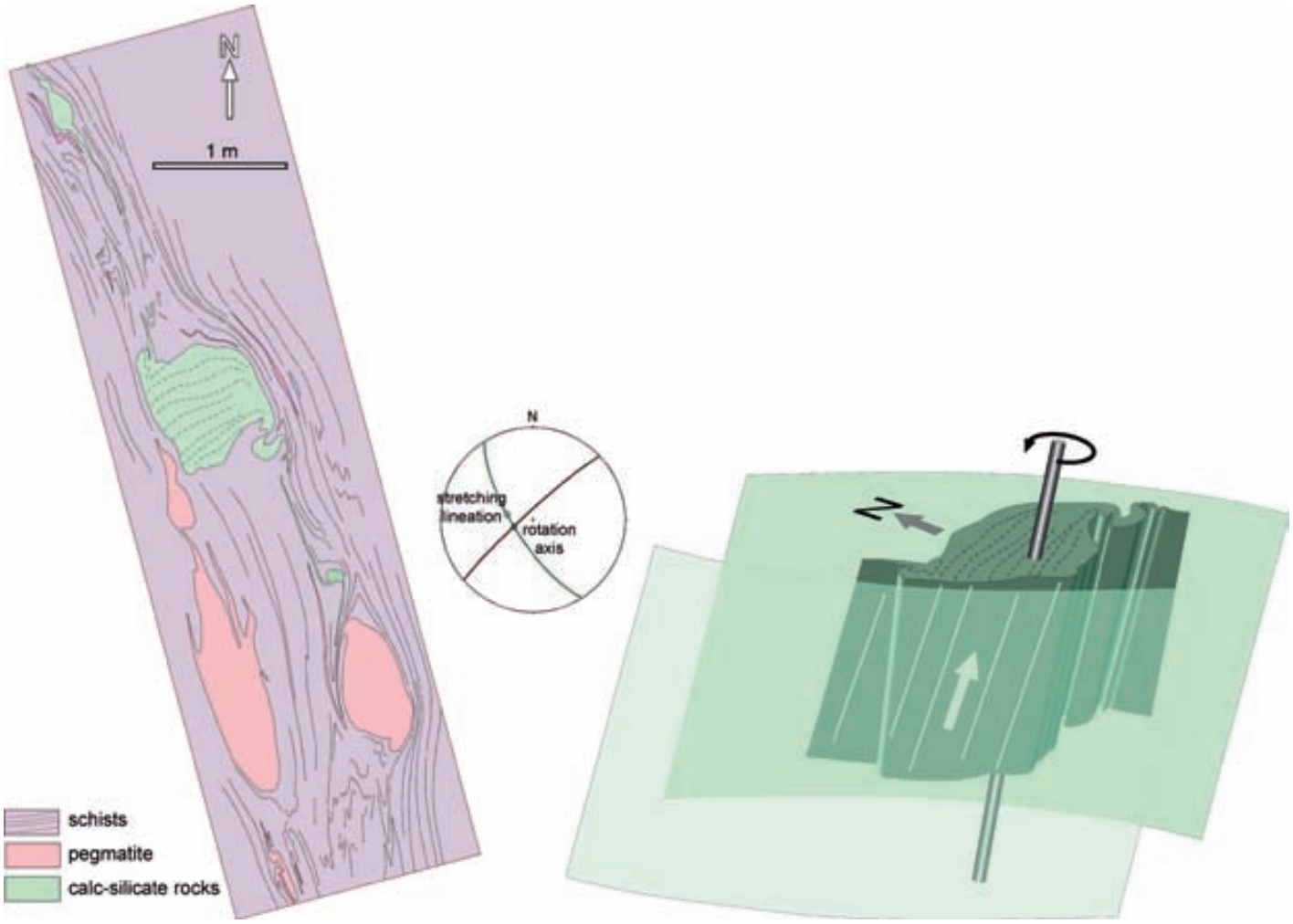

Fig. 4.13. Map view and three-dimensional sketch of a lozenge developed in a dip-slip shear zone. Note that the rotation axis (B) is closely parallel to the shear direction and thus the observed asymmetric delta-shaped structure is not kinematically indicative when observed on the shown section.

4.6. FINAL REMARKS

Tectonic lozenges are low deformed rock domains isolated by shear zones, showing an elliptical 2-D section in the plane perpendicular to the shear zone and containning the shear direction. Therefore, lozenges are associated to areas of high heterogeneous strain distribution where non-mylonitic rock is enclosed by mylonites. Two main types of lozenges are distinguised regarding the rheological composition of the enclosed, non-mylonitic rock relative to the wall/regional rock. If the lozenge is formed in a rock of different rheology than that of the walls, the lozenge is a sigma-like type (i). Strain partitioning amongst the phases leads to strain localization at the boundaries of the more competent material (Treagus and Sokoutis, 1992; Handy ,1994) causing stretching of its rims and oftenly giving rise to lozenge shape (Figs. 1.3 and 3.7). However, if the shear zones are enclosing the same rock than that of the wall/regional rock, they give rise to lozenges formed by interconnection of shear zones (ii). These are not related to rheological contrasts but to interaction of shear zones. This type of lozenges abounds in anastomosing shear zone networks and has been the focus of this research, especially those formed in anastomosing shear zone networks in foliated rocks, since the mechanical anisotropy exerted by the foliation gives more kinematical and geometrical complexities susceptible to study.

Therefore, anastomosing networks of shear zones have been also studied since they are the deformation structures defining lozenges. They have been analyzed from field cases from the nucleation of individual shears to their propagation and interconnection to give rise to shear zone networks in anisotropic media. The study has concerned the structural differences depending on the isotropy or foliation/bedding condition of the sheared rock and different shear zone networks with different relative orientation between ISAs and previous foliation are also analyzed to assess the effect of the anisotropy on the shear zone pattern. The main differences are:

(i) In isotropic rocks the presence of one or two sets is controlled by the bulk deformation regime: two conjugate sets are formed during coaxial flow and a dominant set is formed in non-coaxial flow. However, in anisotropic rocks, this correlation does not exist since two conjugate sets or a prevalent one may develop under any deformation regime. The field case of Culleró shows that strong foliations behave as mechanical anisotropy causing strain partitioning and controlling the shear zone pattern (Figs. 4.8 and 4.9). This is because the relative orientation between the ISAs and the previous foliation is an important factor in the shear zone nucleation pattern and consequently in the shear zone network pattern, and it is independently of the bulk vorticity. Therefore, contrary to isotropic rocks, equally developed conjugate sets may appear in non-coaxial deformation if the shortening ISAs are parallel or closely parallel to the anisotropy, and a prevalent set may develop in coaxial deformation if the shortening ISAs are oblique to the mechanical anisotropy (Fig. 4.5).

(ii) While in isotropic rocks the shear zones track the XY plane of the finite strain ellipsoid under simple shear, this is not the case of anisotropic rocks since the relative orientation between ISAs and foliation orientation controls the shear zone orientation. Thus the mechanical anisotropy, when behaving active during deformation, has a key role on strain partitioning and controls the local kinematics.

(iii) The vorticity axis (B axis, Fig. 2.4) in shear zones across isotropic rocks is contained in the

shear plane and normal to the shear direction, while in foliated rocks it is also contained in the shear plane but the angle with respect to the shear direction might vary between 0° and 90° (Figs. 2.4 and 2.5).

(iv) deflections at the shear zone margins in foliated rocks may show apparent deflections in contradiction with the real shear sense (Fig. 4.13; Carreras and Casas, 1987; Passchier and Trouw, 2005). Structures due to mechanical instabilities like crenulations and folds may also form at shear zone margins.

The debate about the rheology of the initiation and propagation of ductile shears zones (especially when the conditions are brittle-ductile) is also sought: the brittle tips of some ductile shear zones may lead to think they initiate as brittle shears and then evolve to ductile with increasing shearing. However, the tips are not an analogous to a shear zone initiation since they are propagation zones with likely differences with strain distribution, strain rate and stress trajectories. Isolated, incipient shear zones with relatively low shear values at the central domain are a better analogous to shear zone initiation. Analysis of this in Cap de Creus show that shear zones nucleate as buckling instabilities thus, at least in foliated rocks, shear zones nucleate ductilely (Fig. 2.7). The presence of brittle tips would be explained because both ductile and brittle deformation mechanisms may coexist in the same shear zone in low metamorphic grade conditions. The central part, achieving much finite strain than the tips develops a mylonitic fabric while at the propagating tips, the minerals susceptible of deforming by crystal-plastic deformation deform internally but have not undergone enough strain to recrystallize and only the microfractures are observed at the outcrop scale.

Experiments have been performed to reinforce the field analysis. Experiments on the effect of the anisotropy on the shear zone arrangement were already performed prior to this study through both, analogue and numerical modelling. The experiments performed in this study investigate into lozenges geometry, kinematics and formation. They shed some light on the debate about the rheology of shear zones nucleation: the analogue modelling suggest that different deformation mechanisms may coexist along a same shear zone.

The preliminar numerical modelling performed sought into sigma-type lozenges and the general conclusion is that lozenge shapes arise when the competence contrast between multilayer and hard inclusions is over several units of magnitude. In such scenario, the hard inclusions deform into lozenge shape. If the competence contrast is over several tens of magnitude, the hard inclusions rotate but do not deform into lozenge shapes. However, lozenge shapes generated by strain shadow effect may arise.

The analogue modelling was performed to look into lozenges formed by interconnection of shear zones. Analogue experiments of multilayer models has revealed that (i) shear zones end in the most ductile material, (ii) shear zones interconnection proliferates when the shortening is around 60%-65%. Therefore, lozenges start to abound at such shortening and they may form by conjugated shears and by linkage of synthetic dextral and sinistral (Fig. 4.4); and (iii) the obtuse angle of conjugate shear zones opens with increasing shear (Fig. 4.4), what is in agreement to field observations on the evolution of lozenges formed by shear zone interconnections (Fig. 4.3). Cross-sections of the experiments in the *Y* direction of the bulk imposed stress show high variability in geometry and low continuity of the structures from one section to another (Figs. 3.25 and 3.26). This evidence prevented any 3D interpretation from 2D outcrops.

The field observations and the experiments on shear zones in foliated rocks and related lozenges allow to deep into lozenge geometry, kinematics and developing models explaining the occurrence of them (main aims of Structural Geology; Davis and Reynolds, 1996). Three typologies have been ascertained:

(i) Geometrical typology. The variety of the external geometry of lozenges is displayed considering the symmetry, the aspect ratio and the straight vs. curvilinear character of the lozenge sides (Fig. 4.1). Four main types are depicted: rhombic, lensoidal, rhomboidal and sigmoidal lozenges. Although a wider geometric variety exists, the field study suggests that lensoidal and sigmoidal lozenges are the most common shapes. Generally, interaction of conjugate shear zones leads to the development of lensoidal lozenges with orthorombic symmetry while interaction of synthyetic shears produces sigmoidal lozenges with monoclinic symmetry (called assymmetric to differentiate from the formers; Figs. 4.10 and 4.12). These types can be taken as end-members thus lozenges can range in geometry from lensoidal to sigmoidal. The field study shows also that a single deformation event (D_3-related shear belt in Cap de Creus) involving deformations close to simple shear can generate both orthorhombic and monoclinic structures. This fact contradicts the common association of structural symmetry and deformation symmetry.

The external and the internal geometry of lozenges changes with increasing strain since with continuing shearing the angle between shears gradually opens towards the extension direction (Figs. 4.3 and 4.4) and this causes stretching and narrowing of the outer shape towards the stretching direction (aspect ratio (L1/W)) increases) and the synthetic rotation of the long and short axis towards the shear sense (symmetry (δ) decreases). Therefore there may be a decrease in lozenge asymmetry with respect to the shear plane.Furthermore, the foliation of the lozenge interior rotates synthetically (α increase) with the rotating, bounding shears causing the internal deformation of the lozenge. The internal deformation may be achieved through folding, stretching and/or rotation of the foliation but also through new, minor shears. With increasing strain, the minor shears propagate through the interior of the lozenge until they connect to other main bounding shear causing the compartimentalization of the lozenge.

The 3-D geometry of lozenges is very tentative to investigate through both field and experimental analysis. However, field observations of lozenges in sections oblique to the shear direction and the cross-sections of the analogue experiments suggest a spindle shape..

(ii) Kinematic typology. The internal geometry of lozenges in foliated rocks is depicted according to the relatives orientations between previous foliation and kinematics of the bounding shear zones for two end members of the kinematic of these: lozenges bounded by conjugate pairs of shear zones or by synthetic pairs of (dextral) shear zones (Fig. 3.32). The most important point of this typology is that the presence of millipede-like geometries (Bell, 1981) does not have any implication on the bulk strain regime (regional vorticity) because the presence of one or two sets and the prevalence of one over the other is the result of a complex relation between ISA, anisotropy and progressive deformation.

(iii) Propagation typology. The analysis of shear zone-related lozenges in foliated rocks from the northern Cap de Creus shear belt lead to infer five basic mechanisms for the origin and development of lozenges in foliated rocks. These mechanisms are based on the initial orientation of the previosu foliation with respect to the ISAs. Field observations indicate that local variations in foliation orientation at metric to centimetric scales can lead

to lozenges of different mechanisms coexist at the same outcrop. Indeed, more than one mechanism may operate in an individual lozenge over which one generally prevails. The prevailing acting mechanism does not depend so much on the bulk kinematics (degree of non-coaxiality) but on the angular relationship between the pre-existing foliation and the bulk kinematic axes. Only if the precise mechanism of lozenge initiation is determined, lozenges can be used as kinematic indicators. This is reliable for domino and for shear band type lozenges (models L2 and L5, respectively). Inferences from millipede and internal pinch-and-swell types lozenges (models L1 and L3, respectively) may be done if their shapes have been asymmetrized by non-coaxial progressive deformation. Reliability of the overstep type lozenges (model L4) is only warranted if contractional and extensional stepping can be discriminated from the lozenge internal and marginal structures.

The Cap de Creus case study shows the relevance of the orientation of the previous foliation in controlling the orientation and propagation of shear zones and, therefore, in the prevalent mechanism of lozenge formation. Where the foliation trends NW-SE to N-S, millipede-like lozenges (model L1) predominantly form by intersection of two sets of conjugate shear zones, while for the foliation progressively oriented towards NE-SW, E-W and WNW-ESE lozenges are mainly formed by models L2, L3 and L4 respectively (Fig. 3.35). Model L5 is typically restricted to domains where a mylonitic shear zone-related foliation is developed or where the previous foliation originally makes a very small angle (<5°) with the bulk shear direction. As the bulk kinematics is the same along the investigated areas (a simple shear-dominated dextral regime), it can be confirmed that foliation orientation plays an important role on the orientation of shear zones. This fact was already experimentally demonstrated by Williams and Price (1990) and it has been illustrated with field examples in this contribution.

The presented typologies (external geometry (Fig. 4.1), internal typology (Fig. 3.32) and development models (Fig 3.35)) are independent of the bulk vorticity of the flow as the bounding shear zones can form in all bulk vorticity spectrum ($0<Wk<1$) and thus each individual lozenge type also. The field study shows that a single deformation event (D_3-related shear belt in Cap de Creus) involving deformations close to simple shear can generate both orthorhombic and monoclinic structures. The mechanical anisotropy control both the external (orthorhombic or monoclinic symmetry) and the internal geometry (millipede type –foliation rotated towards two senses- or sigmoidal type -foliation rotated towards one sense-). Thus, the symmetry of the lozenge does not reflect the symmetry of the deformation and the formation of millipede-type (orthorombics) or sigmoidal-type lozenges (Figs. 4.10 and 4.12) does not reflect the vorticity in a regional scale but the relative orientation between ISAs and previous anisotropy. This fact contradicts the common association of structural symmetry and deformation symmetry (Bell, 1981; Bell and Rubenach, 1983; Choukroune and Gapais, 1983; Gapais et al., 1987). The geometry of lozenges is not univocally related neither to strain type (oblate/prolate) nor to the degree of non-coaxiality.

From this dissertation it can be concluded that an assessment of lozenge development mechanisms can be done through careful observation and detailed analysis of the bounding shear zones: their kinematics, their interconnections and their angular relations with the foliations in the host, less deformed rocks. It is clear that caution should be taken when analyzing lozenge shapes in terms of extracting general strain and kinematic inferences. A complete understanding of lozenges requires further investigation in 3-D.

Chapter 5

REFERENCES

5. REFERENCES

Aerden, D.G.A.M., Sayab, M., Bouybaouene, M.L., 2010. Conjugate-shear folding: A model for the relationships between foliations, folds and shear zones. Journal of Structural Geology 32, 1030-1045.

Agard P., Augier R., Monié P., 2011. Shear band formation and strain localization on a regional-scale: evidence from anisotropic rocks below a major detachment (Betic Cordilleras, Spain). Journal of Structural Geology 33, 114-131.

Ahlgren, S.G., 2001. The nucleation and evolution of Riedel shear zones as deformation bands in porous sandstone. Journal of Structural Geology 23, 1203-1214.

Alsop, G.I., Carreras, J., 2007. The structural evolution of sheath folds: a case study from Cap de Creus. Journal of Structural Geology 29, 1915-1930.

Alsop, G.I., Brown, J.P., Davison, I., Gibling, M.R., 2000. The geometry of drag zones adjacent to salt diapirs. Journal of the Geological Society 157, 1019-1029.

Aitchison, J.C., Bradshaw, M.A., Newman, J., 1988. Lithofacies and origin of the buckeye formation: Late paleozoic glacial and glaciomarine sediments, Ohio range, transantarctic mountains, Antarctica. Palaeogeography, Palaeoclimatology, Palaeoecology 64 , 93-104.

Arbaret, L., Fernández, A., Jezek, J., Ildefonse, B., Launeau, P., Diot, H., 2000. Analogue and numerical modeling of shape fabrics: application to strain and flow determination in magmas. Transactions of the Royal Society of Edinburgh—Earth Sciences 91, 97–109.

Arenas, R., Gil Ibarguchi, J.I., González Lodeiro, F., Klein, E., Martínez Catalán, J.R., Ortega Gironés, E., de Pablo Maciá, J.G., Peinado, M., 1986. Tectonostratigraphic units in the complexes with mafic and related rocks, NW of the Iberian Massif. Hercynica II, 87–110.

Astarita, G., 1979. Objective and generally applicable criteria for flow classification. Journal of Non-Newtonian Fluid Mechanics 6, 69-76.

Baird, G.B., Hudleston, P.J., 2007. Modeling the influence of tectonic extrusion and volume loss on the geometry, displacement, vorticity, and strain compatibility of ductile shear zones. Journal of Structural Geology 29, 1665–1678.

Bak, J., Korstgard, J., Sorensen, K., 1975. A major shear zone within the Nagssugtoquidian of West Greenland. Tectonophysics 27, 191-209.

Baldwin, J.A., Powell, R., Williams, M.L., Gonçalves, P., 2007. Formation of eclogite, and reaction during exhumation to mid-crustal levels, Snowbird tectonic zone, western Canadian Shield. Journal of Metamorphic Geology 25, 953-974.

Bard, J.P., Burg, J.P., Matte, Ph., Ribeiro, A., 1980. La Chaîne Hercynienne d'Europe occidentale en termes de Tectonique des Plaques. In: Géologie de l'Europe, du Précambrien aux basins sédimentaires post-Hercyniennes. Mémoires du Bureau de Recherches Géologiques et Minières 108, pp. 233-246.

Barr, T.D., Houseman, G.A., 1996. Deformation fields around a fault embedded in a non-linear ductile medium. Geophysical Journal International 125, 473-490.

Baumann, M. T., 1986. Verformungverstelung an Scherzonenenden: Analogmodelle und natuÈ rliche Beispile. Ph.D. thesis, ETH ZuÈ rich, Switzerland.

Baumann, M. T., Mancktelow, N. S. (1987) Initiation and propagation of ductile shear zones. Terra Cognita 7, 47.

Bastida, F., Marcos, A., Marquínez, J., Pérez-Estaún, A., Pulgar, A., 1984. Mapa geológico de España, 1:200000, Hoja No 1, La Coruña, Instituto Geológico y Minero de España, Madrid.

Beauchamp, W., Allmendinger, R.W., Barazangi, M., Demnati, A., El Alji, M., Dahmani, M., 1999. Inversion tectonics and the evolution of the High Atlas Mountains, Morocco, based on a geological-geophysical transect. Tectonics 18 (2), 163–184.

Bédard, J.H., Leclerc, F., Harris, L.B., Goulet, N.,2009. Intra-sill magmatic evolution in the Cummings Complex, Abitibi greenstone belt: Tholeiitic to calc-alkaline magmatism recorded in an Archaean subvolcanic conduit system. Lithos 111, 47-71.

Bell, T.H., 1981. Foliation development—the contribution, geometry and significance of progressive, bulk, inhomogeneous shortening. Tectonophysics 75, 273-296.

Bell, T. H. and Hammond, R. L., 1984. On the internal geometry of mylonite zones. Journal of Geology 92, 667-686.

Bell, T.H., Rubenach, M.J., 1980. Crenulation cleavage development-evidence of progressive bulk inhomogeneous shortening from the "millipede" microstructure in the Robertson River Metamorphics. Tectonophysics 68, T9–T15.

Bernet, M., Bassett, K., 2005. Provenance analysis by single-quartz-grain SEM-CL/optical microscopy. Journal of Sedimentary Research 75 (3), 492–500.

Berthé, D., Choukroune, P., Jegouzo, P., 1979. Orthogneiss, mylonite and non coaxial deformation of granites: the example of the south Amorican Shear Zone. Journal of Structural Geology 1, 31-42.

Bhattacharyya, P., Czech, D.M., 2008. Using network analyses within GIS technologies to quantify geometries of shear zone networks. Geosphere 4, 640-656.

Bhattacharyya, P., Hudleston, P., 2001. Strain in ductile shear zones in the Caledonides of northern Sweden: a three dimensional puzzle. Journal of Structural Geology 23, 1549-1565.

Bickford, M.E., Collerson, K.D., Lewry, J.F., 1994. Crustal history of the Rae and Hearne provinces, southwestern Canadian Shield, Saskatchewan: constraints from geochronologic and isotopic data. Precambrian Research 68, 1-21.

Bons, P.D., Koehn, D., Jessell, M.W. (Eds.), 2008. Microdynamics Modelling. Lecture Notes in Earth Sciences, vol. 106. Springer, Berlin, p. 405.

Bons, P.D., Druguet, E., Hamann, I., Carreras, J., Passchier, C.W., 2004. Apparent boudinage in dykes. Journal of Structural Geology 26, 625-636.

Boud, A., 1987. Potential application of remote sensing systems to the African rift system. Journal of Geodynamics 7, 373-394.

Bowden, P.B., 1970. A criterion for inhomogeneous plastic deformation. Philosophical Magazine 22, 455-462.

Boyer, S.E., Elliott, D., 1982. Thrust systems. American Association of Petroleum Geologist Bulletin 66, 1196-1230.

Brun, J.P., Cobbold, P.R., 1980. Strain heating and thermal softening in continental shear zones: a review. Journal of Structural Geology 2, 149-158.

Brum da Silveira, A., Cabral, J., Perea, H., Ribeiro, A., 2009. Evidence for coupled reverse and normal active faulting in W Iberia: The Vidigueira–Moura and Alqueva faults (SE Portugal). Tectonophysics 474, 184-199.

Butler, R.W.H., 1982. Terminology of structures in thrust belts. Journal of Structural Geology 4, 239-245.

Burg, J.P., Wilson, C.J.L., Mitchell, J.C., 1986. Dynamic recrystallization and fabric development during the simple shear deformation of ice. Journal of Structural Geology 8, 857–870.

Burg, J.P., 1986. Quartz shape fabrics variations and c-axis fabrics in a ribbon-mylonite: arguments for an oscillating foliation. Journal of Structural Geology 8, 123–131.

Carreras, J., 1997. Shear zones in foliated rocks: geometry and kinematics, in: Sengupta, S. (Ed.), Evolution of Geologic Structures in Micro- to Macro-scales. Chapman & Hall, London, pp. 185–201.

Carreras, J., 2001. Zooming on Northern Cap de Creus shear zones. Journal of Structural Geology 23, 1457-1486.

Carreras, J. 2013. Anastomosing network of shear zones across schists in Cap de Creus. Journal of Structural Geology 50, 5-6.

Carreras, J., Casas, J.M., 1987. On folding and shear zone-development: a mesoscale structural study on the transition between two different tectonic styles. Tectonophysics 135, 87-98.

Carreras, J., Losantos, M., 1982. Geological setting of the Roses granodiorite (E-Pyrenees, Spain). Acta Geologica Hispanica 17, 219-225.

Carreras, J., Ortuño, F., 1990. Fundamento geométrico y cinemático de la modelización teórica y experimental de deformaciones no-coaxiales. Acta Geológica Hispánica 25, 237–259.

Carreras, J., Julivert, M., Santanach, P., 1980. Hercynian mylonite belts in the eastern Pyrenees:

and example of shear zones associated with late folding. Journal of Structural Geology 2, 5-9.

Carreras, J., Druguet, E., Griera, A., 2000. Desarrollo de zonas de cizalla conjugadas por deformación coaxial de materiales analógicos anisótropos. Geotemas 1, 47-52.

Carreras, J., Druguet, E., Griera, A., 2005. Shear zone-related folds. Journal of Structural Geology 27, 1229-1251.

Carreras, J., Ponce, C., Druguet, E., 2012. Control of mechanical anisotropy on the initiation and development of shear zone-related lozenges: a field-based study. Geo-temas 13, 140.

Carreras, J., Cosgrove, J.W., Druguet, E., 2013. Strain partitioning in banded and/or anisotropic rocks: implications for inferring tectonic regimes. Journal of Structural Geology 50, 7-21.

Carreras, J., Druguet, E., Griera, A., Soldevila, J., 2004. Strain and deformation history in a syntectonic pluton. The case of the Roses granodiorite (Cap de Creus, Eastern Pyrenees). In:Alsop, G.I., Holdsworth, R.E., McCaffrey, K.J.W., Hand, W. (Eds.), Flow Processes in Faults and Shear Zones. Geological Society, London, Special Publications, vol. 224, pp. 307-319.

Carreras, J., Druguet, E., Rahimi, A., Castaño, L.M., Griera, A., Gómez-Rivas, E., 2006. Contribución del estudio estructural del enjambre de diques básicos del Precámbrico del Anti-Atlas al conocimientode su significación geotectónica en la orogenia panafricana. Geogaceta 40, 139-142

Carreras, J., Czech, D.M., Druguet, E., Hudleston, P.J., 2010. Structure and development of an anastomosing network of ductile shear zones. Journal of Structural Geology 32, 656-666.

Casey, M., 1980. Mechanics of shear zones in isotropic dilatant materials. Journal of Structural Geology 2, 143-147.

Castaño, L.M., 2010. Emplazamiento y deformación de venas y diques magmaticos en cinturones tectonometamórficos: análisis a partir de estudios de campo y modelización analogical. Ph.D. thesis, Universitat Autònoma de Barcelona.

Castiñeiras, P., Navidad, M., Liesa, M., Carreras, J., Casas, J.M., 2008. U–Pb zircon ages (SHRIMP) for Cadomian and Early Ordovician magmatism in the Eastern Pyrenees: New insights into the pre-Variscan evolution of the northern Gondwana margin. Tectonophysics 461, 228-239.

Chardon, D., Gapais, D., Cagnard, F., 2009. Flow of ultra-hot orogens: A view from the Precambrian, clues for the Phanerozoic. Tectonophysics 477, 105-118.

Childs, C., Nicol, A., Walsh, J.J., Watterson, J., 1996. Growth of vertically segmented normal faults. Journal of Structural Geology 18, 1389-1397.

Choukroune, P., Gapais, D., 1983. Strain pattern in the Aar Granite (Central Alps): Orthogneiss developed by bulk inhomogeneous flattening. Journal of Structural Geology 5, 411-418.

Cobbold, P.R., 1976. Mechanical effects of anisotropy during large finite deformations. Bulletin Société Géologique de France 28, 1497–1510.

Cobbold, P.R., 1983. Kinematic and mechanical discontinuity at a coherent interface. Journal of Structural Geology 5, 341-349.

Cobbold, P.R., Cosgrove, J.W., Summers, J.M., 1971. The development of internal structures in deformed anisotropic rocks. Tectonophysics 12, 23-53.

Corsini, M., Vauchez, A., Caby, R., 1996. Ductile duplexing at a bend of a continental-scale strike-slip shear zone: Example from Brazil. Journal of Structural Geology 18, 385-394.

Cosgrove, J.W., 1976. The formation of crenulation cleavage. Journal of the Geological Society London 132, 155-178.

Culshaw, N.G., Gerbi, C., Marsh, J.H., Plug, L., 2011. Heterogeneous amphibolite facies deformation of a granulite facies layered protolith: Matches Island Shear System, Parry Sound Domain, Grenville Province, Ontario, Canada. Journal of Structural Geology 33, 875-890.

Czeck, D.M., Fissler, D.A., Horsman, E., Tikoff, B., 2009. Strain analysis and rheology contrasts in polymictic conglomerates: an example from the Seine metaconglomerates, Superior Province, Canada. Journal of Structural Geology 31, 1365-1376.

Czeck, D.M., Hudleston, P.J., 2003. Testing models for obliquely plunging lineations in transpression: a natural example and theoretical discussion. Journal of Structural Geology 25, 959-

982.

Czeck, D.M., Hudleston, P.J., 2004. Physical experiment of vertical transpression with localized non vertical extrusion. Journal of Structural Geology 26, 573-581.

Dallmeyer. R.D. and Gil Ibarguchi, J.I., 1990. Age of amphibolitic metamorphism in the ophiolitic unit of the Morais allochthon (Portugal): implications for early Hercynian orogenesis in the Iberian Massif. Journal of Geological Society London, 147: 873-878.

Dallmeyer, R.D.. Ribeiro. A. and Marques, F., 1991. Polyphase Variscan emplacement of exotic terranes (Morais and Braganca Massifs) onto Iberian successions: Evidence from 40Ar/30Ar mineral ages. Lithos, 27: 133-144.

Davis, G.H., Bump, A.P., Garcia, P.E., Ahlgren, S.G., 1999. Conjugate Riedel deformation band shear zones. Journal of Structural Geology 22, 169-190.

Davis, G.H., Reynolds, S.J., 1996. Structural Geology of Rocks and Regions (2nd Edition): New York, John Wiley and Sons, Inc., 776 p

Delcaillau, B., Amrhar, M., Namous, M., Laville, E., Pedoja, K., Dugué, O., 2011. Transpressional tectonics in the Marrakech High Atlas: Insight by the geomorphic evolution of drainage basins. Geomorphology 134, 344-362.

Donath, F.A., 1961. Experimental study of shear failure in anisotropic rocks. Geological Society of America Bulletin 72, 985-989.

Donath, F.A., Parker, R.B., 1964. Folds and folding. Geological Society of America Bulletin 75, 45-62.

Druguet, E., 2001. Development of high thermal gradients by coeval transpression and magmatism during the Variscan orogeny: insights from the Cap de Creus (Eastern Pyrenees). Tectonophysics 332, 275-293.

Druguet E., Castaño L.M., 2010. Analysis of Syntectonic Magmatic Veins at the Mesoscale. Journal Geological Society of India 75, 65-73.

Druguet E, Carreras J. 2006. Analogue modelling of syntectonic leucosomes in migmatitic schists. Journal of Structural Geology 28, 1734-1747.

Druguet E, Czeck DM, Alsop IG, Bons PD. 2013. Preface: Deformation localization. Journal of Structural Geology, 50.

Druguet, E., Carreras, J., 2006. Analogue modeling of syntectonic leucosomes in migmatitic schists. Journal of Structural Geology 28, 1734-1747.

Druguet, E., Alsop, G.I., Carreras, J., 2009. Coeval brittle and ductile structures associated with extreme deformation partitioning in a multilayer sequence. Journal of Structural Geology 31, 498-511.

Duebendorfer, E.M., Christensen, C.H., 1998. Plastic-to-brittle deformation of microcline during deformation and cooling of a granitic pluton. In: Snoke, A.W., Tullis, J.A., Todd, V.R. (Eds.), Fault-related Rocks: a Photographic Atlas. Princeton University Press, pp. 176-179.

Duguet, M., Le Breton, N., Faure, M., 2007. P–T paths reconstruction of a collisional event: the example of the Thiviers–Payzac Unit in the Variscan French Massif Central. Lithos 98, 210-232.

Evans, B., Fredrich, J.T., Wong, T.F., 1990. The brittle-ductile transition in rocks: recent experimental and theoretical progress, in: Duba, A.G., Durham, W.B., Handin, J.W., Wang, H.F.(Eds.),The Brittle-Ductile Transition in Rocks, American Geophysical Union, Washington, D.C., monograph 56, pp. 1-20.

Fagereng, A., 2011. Frequency-size distribution of competent lenses in a block-in-matrix mélange: Imposed length scales of brittle deformation? Journal of Geophysical Research 116, B05302.

Fernández, F., 1993. La deformación de los gneisses de Chímparra en Punta Tarroiba (Cabo Ortegal, NW de España). Revista de la Sociedad Geológica de España 6, 77-91.

Fernández, F., 1993. Estructuras desarrolladas en Gneises bajo condiciones de alta P y T (Geneises de Chímparra, Cabo Ortegal). Universidad de Oviedo.

Fernandez, F.J., Marcos, A., 1996. Mylonitic foliation development by heterogeneous pure shear under high-grade conditions in quartzofeldspathic rocks (Chimparra Gneiss Formation, Cabo Ortegal Complex, NW Spain). In: Oncken, O., Janssen, C. (Eds.), Basement Tectonics, Europe and other Regions, vol. 11, pp. 17–34.

Fossen, H., 2010b. Structural Geology. Cambridge

University Press, Cambridge, p. 463.

Fossen, H., Schultz, R.A., Torabi, A., 2011. Conditions and implications for compaction band formation in the Navajo Sandstone, Utah. Journal of Structural Geology 33, 1477-1490.

Fressengeas, C., Molinari, A., 1987. Instability and localization of plastic flow in shear at high strain rates. Journal of the Mechanics and Physics of Solids 35, 185-211.

Froitzheim, N., Schmid, S.M., and Frey, M., 1996. Mesozoic paleogeography and the timing of eclogite-facies metamorphism in the Alps: A working hypothesis. Eclogae geol. Helv., 89, 81-110

Fusseis, F., Handy, M. R., Schrank, C., 2006. Networking of shear zones at the brittle-to-viscous transition (Cap de Creus, NE Spain). Journal of Structural Geology 28, 1228-1243.

Gapais, D., Bale, P., Choukroune, P., Cobbold, P.R., Mahjoub, Y., Marquer, D., 1987. Bulk kinematics from shear zone patterns: some field examples. Journal of Structural Geology 9, 635-646.

Garofalo, P., Matthäi, S.K., Heinrich, C.A., 2002. Three-dimensional geometry, ore distribution and time-integrated mass transfer through the quartz–tourmaline–gold vein network of the Sigma deposit (Abitibi belt, Canada). Geofluids 2, 217–232.

Gerbi, C., Culshaw, N.G., Marsh, J.H., 2010. Magnitude of weakening during crustal scale shear zone development. Journal of Structural Geology 32, 107-117.

Gil Ibarguchi, J. I., Mendia, M., Girardeau, J. and Peucat, J. J., 1990. Petrology of eclogites and clinopyroxene-garnet metabasites from the Cabo Ortegal Complex (northwestern Spain). Lithos 25, 133-162.

Gilotti, J.K., Kumpulanien, R.R., 1986. Strain-softening induced ductile flow in the Sarv thrust sheet, Scandinavian Caledonides; a description. Journal of Structural Geology 8, 441-455.

Gómez-Rivas, E., 2005. Shear bands in anisotropic materials: analogue modelling in coaxial deformation conditions. M.Sc. thesis, Univeristat Autònoma de Barcelona.

Gómez-Rivas, E., 2008. Localization of deformation in ductile and anisotropic materials: field, experimental and numerical study. Ph.D. thesis, Universitat Autònoma de Barcelona.

Gomez-Rivas, E., Griera, A. 2012. Shear fractures in anisotropic ductile materials: An experimental approach. Journal of Structural Geology 34, 61–76.

Goodwin, L.B., Earnest-Heckler, E., Tikoff, B., Blenkinsop, T., 2011. Evaluating controls on, and their rheologic significance of deformation localization. In: Druguet, E., Carreras, J., Alsop, G.I., Bons, P.D., Czeck, D.M., Hudleston, P.J., Siddoway, C.S. (Eds.), Deformation Localization in Rocks: New Advances (Keynote). Penrose Conferences, Geological Society of America, Cadaques and Cap de Creus, Catalonia, Spain.

Graham, R.H., 1980. The role of shear belts in the structural evolution of the South Harris igneous complex. Journal of Structural Geology 2, 29-37.

Grocott, J., 1977. The relationship between Precambrian shear belts and modern fault systems. Journal of Geological Society London 133, 257-262.

Groome, W.G., Johnson, S.E., Koons, P.O., 2006. The effects of porphyroblast growth on the effective viscosity of metapelitic rocks: implications for the strength of the middle crust. Journal of Metamorphic Geology 24, 389–407.

Grujic, D., Mancktelow, N.S., 1996. Structure of the Northern Maggia and Lebendun Nappes, Lepontine Alps, Switzerland. Eclogae geologicae Helvetiae 89, 461-504.

Guermani, A., Pennacchioni, G., 1998. Brittle precursors of plastic deformation in a granite: an example from the Mont Blanc massif (Helvetic western Alps). Journal of Structural Geology 20, 135-148.

Handy, M. R., 1994. Flow laws for rocks containing two non-linear viscous phases: a phenomenological approach. Journal of Structural Geology 16, 287-301.

Hanmer, S., 1986. Asymmetrical pull-aparts and foliation fish as kinematic indicators. Journal of Structural Geology 8, 111-122.

Hanmer, S., 1988. Great Slave Lake Shear Zone, Canadian Shield: reconstructed

vertical profile of a crustal-scale fault zone. Tectonophysics 176, 245-255.

Hanmer, S., Passchier, C.W., 1991. Shear-sense in-

dicators: a review. Geological Survey of Canada. Paper 90-17, p. 72.

Hansen, L.N., Zimmerman, M.E., Dillman, A.M., Kohlstedt, D.L., 2011. The influence of shear-zone Boundary conditions on strain localization: results from experimental investigations of olivine rheology. In: Druguet, E., Carreras, J., Alsop, G.I., Bons, P.D., Czeck, D.M., Hudleston, P.J., Siddoway, C.S. (Eds.), Deformation Localization in Rocks: New Advances (Keynote). Penrose Conferences, Geological Society of America, Cadaques and Cap de Creus, Catalonia, Spain.

Harris, L.B., 2003. Folding in high-grade rocks due to back-rotation between shear zones. Journal of Structural Geology 25, 223–240.

Hobbs, B., Means, W. and Williams, P., 1976. An Outline of Structural Geology. Wiley, New York, NY, 571 pp.

Hobbs, B. E., Mühlhaus, H-B, Ord, A., 1990. Instability, softening and localization of deformation. In Deformation Mechanisms, Rheology and Tectonics, eds R. J. Knipe and E. H. Rutter, pp. 143-165. Geological Society Special Publication, 54.

Hoeppener, R., Kalthoff, E., Schrader, P., 1969. Zur physikalischen Tektonik: Bruchbildung bei verschidenen affinen Defomartionen im Experiment. Geologisches Rundschau 59, 179-193.

Holzer, L., Frei, R., Barton Jr, J.M., Kramers, J.D., 1998. Unraveling the record of successive high grade events in the Central Zone of the Limpopo Belt using Pb single phase dating of metamorphic minerals. Precambrian Research 87, 87-115.

Hudleston, P., 1999. Strain compatibility and shear zones: is there a problem? Journal of Structural Geology 21, 923-932.

Iacopini, D., 2011. Exploring strain patterns within heterogeneous shear zones. In: Druguet, E., Carreras, J., Alsop, G.I., Bons, P.D., Czeck, D.M., Hudleston, P.J., Siddoway, C.S. (Eds.), Deformation Localization in Rocks: New Advances (Keynote). Penrose Conferences, Geological Society of America, Cadaques and Cap de Creus, Catalonia, Spain.

Ildefonse, B., Sokoutis, D., Mancktelow, N.S., 1992b. Mechanical interactions between rigid particles in a deforming ductile matrix. Analogue experiments in simple shear flow. Journal of Structural Geology 10, 1253–1266.

Ildefonse, B. and Mancktelow, N. S., 1993. Deformation around rigid particles: the influence of slip at the particle/matrix interface. Tectonophysics 221, 345-359.

Iglesias, M., Ribeiro, M.L., Ribeiro, A., 1983. La interpretación aloctonista de la estrutura del Noroeste Peninsular. In: Geología de España, Libro Jubilar J.M. Rios, IGME, pp. 459–467.

Jessell, M.W., Siebert, E., Bons, P.D., Evans, L., Piazolo, S., 2005. A new type of numerical experiment on the spatial and temporal patterns of localization of deformation in a material with a coupling of grain size and rheology. Earth and Planetary Science Letters 239, 309–326.

Jiang, D., Williams, P.F., 1999. When do dragfolds not develop into sheath folds in shear zones? Journal of Structural Geology 21, 577–583.

Jessell, M.W., Bons, P.D., Griera, A., Evans, L., Wilson, C.J.L., 2009. A tale of two viscosities. Journal of Structural Geology 31, 719-736.

Johnson, S.E., Moore, R.R., 1996. De-bugging the 'millipede' porphyroblast microstructure: a serial thin-section study and 3-D computer animation. Journal of Metamorphic Geology 14, 3-14.

Kaus, B.J.P., Podladchikov, Y.Y., 2006. Initiation of localized shear zones in viscoelastoplastic rocks. Journal of Geophysical Research 111, BO4412.

Kidan, T.W., Cosgrove, J.W., 1996. The deformation of multilayers by layer-normal compression; an experimental investigation. Journal of Structural Geology 18, 461-474.

Kim, J.W., Ree, J.H., Han, R., Shimamoto, T., 2010. Experimental evidence for the simultaneous formation of pseudotachylyte and mylonite in the brittle regime. Geology 38, 1143-1146.

Kirby, S.H., 1980. Tectonic stresses in the lithosphere: Constraints provided by the experimental deformation of rocks. Journal of Geophysical Research: Solid Earth 85, 6353–6363.

Kirby, S.H., 1985. Rock mechanics observations pertinent to the rheology of the continental lithosphere and the localization of strain along shear zones. Tectonophysics 119, 1-27.

Kuiper, Y.D., Lin, S., Böhm, C.O., 2011. Himalayan-type escape tectonics along the Superior Boundary Zone in Manitoba, Canada. Precambrian Research 187, 248-262.

Lacassin, R., 1988. Large-scale foliation boudinage in gneisses. Journal of Structural Geology 10, 643-647.

Lamouroux, C., Debat, P., Ingles, J., Guerrero, N., Sirieys, P., Soula, J.C., 1994. Rheological properties of rocks inferred from the geometry and microstructures in two natural shear zones. Mechanics of Materials 18, 79-87.

Le Pourhiet, L., Agard, P., Huet, B., Labrousse, L., Jolivet, L., 2010. Shear localization in foliated media: numerical experiments with application to the Bethique (Spain). In: Geophysical Research Abstracts (12), EGU 2010-10308. EGU General Assembly 2010.

Le Pourhiet, L., Huet, B., Agard, P., Labrousse, L., Jolivet, L., Yao, K., 2012. Strain localisation in mechanically Layered Rocks, insights from numerical modelling. Solid Earth Discussions, 4, 1165-1204.

Lamouroux, C., Ingles, J., Debat, P., 1991. Conjugate ductile shear zones. Tectonophysics 185, 309-323.

Lister, G.S., Williams, P.F., 1979. Fabric development in shear zones, theoretical controls and observed phenomena. Journal of Structural Geology 1, 283-297.

Logan, J. M., Higgs, N. G. and Friedman, M., 1981. Laboratory studies on natural gouge from the U.S. Geological Survey Dry Lake Valley No. 1 Well, San Andreas Fault Zone. In: Mechanical Behavior of Crustal Rocks (edited by Carter, N. L., Friedman, M., Logan, J. M. and Stearns, D. W.). Geophysical Monographs 24, 121-134.

Maeder, X., Passchier, C.W., Koehn, D., 2009. Modelling of segment structures: Boudins, bone-boudins, mullions and related single- and multiphase deformation features. Journal of Structural Geology 31, 817-830.

Mahan, K.H., Williams, M.L., 2005. Reconstruction of a large deep-crustal terrane: Implications for the Snowbird tectonics zone and early growth of Laurentia. Geology 33, 385-388.

Mancktelow, N.S., 2002. Finite-element modelling of shear zone development in viscoelastic materials and its implications for localisation of partial melting. Journal of Structural Geology 24, 1045-1053.

Mancktelow, N.S., 2006. How ductile are ductile shear zones? Geology 34, 345-348.

Mancktelow, N., Pennacchioni, G., 2005. The control of precursor brittle fracture and fluid-rock interaction on the development of single and paired dúctiles shear zones. Journal of Structural Geology 27, 645-661.

Mandl, G., 1984. Rotating parallel faults the "book shelf' mechanism. American Association of Petroleum Geologists Bulletin 68, 502-503.

Mandl, G., De Jong, L.N.J., Maltha, A., 1977. Shear zones in granular material. Rock Mechanics 9, 95-144.

Mann, P., 2007. Global catalogue, classification and tectonic origins of restraining- and releasing bends on active and ancient strike-slip fault systems. In: Cunningham, W.D., Mann, P. (Eds.) Tectonics of Strike-Slip Restraining and Releasing Bends. Geological Society, London, Special Publications, 290, 367-385.

Marcos, A., Farias, P., Galán, G., Fernández, F.J., Llana-Fúnez, S., 2002. The tectonic framework of the Cabo Ortegal Complex: A slab of lower crust exhumed in the Variscan orogen (northwestern Iberian Peninsula). In:Martínez Catalán, J.R., Hatcher Jr., R.D., Arenas, R., Díaz García, F. (Eds.), Variscan-Appalachian Dynamics: The Building of the Late Paleozoic Basement. Boulder, Colorado. Geological Society of America, Special Paper, vol. 364, pp. 143-162

Marquer, D., Challandes, N., Baudin, T., 1996. Shear zone patterns and strain distribution at the scale of a Penninic nappe: the Suretta nappe (Eastern Swiss Alps). Journal of structural Geology 18, 753-764.

Marques, F.O., Schmid, D.W., Andersen, T.B., 2007. Applications of inclusion behaviour models to a major shear zone system: The Nordfjord-Sogn Detachment Zone in western Norway. Journal of Structural Geology 29,1622-1631.

Martínez, F. J., Carreras, J., Arboleya, M. L., Dietsch, C., 1996. Structural and metamorphic evidence of local extension along the Vivero fault coeval with bulk crustal shortening in the Variscan chain (NW Spain). Journal of Structural Geology 18, 61-73.

Matte, P., 1991. Accretionary history and crustal

evolution of the Variscan belt in Western Europe. Tectonophysics 196, 309-337.

Means, W.D., Hobbs, B.E., Lister, G.S., Williams, P.F., 1980. Vorticity and non-coaxiality in progressive deformations. Journal of Structural Geology 2, 371-378.

McClay, K. R. 1976. The rheology of plasticine. Tectonophysics 33, 7-15.

McClay, K., Bonora, M., 2001. Analog models of restraining stepovers in strike-slip fault systems. AAPG Bulletin 85, 233–260.

Mitra. G., 1979. Ductile deformation zones in Blue Ridge Basement and estimation of finite strains. Geological Society of America Bulletin 90, 935-951.

Mitra, G.,1998. Anastomosing deformation zones. In: Snoke, A.W., Tullis, J., Todd, V. R. (Eds.), Fault-related Rocks: a Photographic Atlas. Princeton University Press, pp. 142-143.

Montési, L.G.J., 2011. Fabric development in ductiles shear zones as the key for plate tectonics. In: Druguet, E., Carreras, J., Alsop, G.I., Bons, P.D., Czeck, D.M., Hudleston, P.J., Siddoway, C.S. (Eds.), Deformation Localization in Rocks: New Advances (Keynote). Penrose Conferences, Geological Society of America, Cadaques and Cap de Creus, Catalonia, Spain.

Moores, E.M., Twiss, R.J., 1995. Tectonics. W.H. Freeman and Company, New York, 415 pp.

Müntener, O. & Hermann, J., 1996. The Val Malenco lower crust–upper mantle complex and its field relations (Italian Alps). Schweizerische Mineralogische und Petrographische Mitteilungen 76, 475–500.

Nabelek, P.I., Liu, M., Sirbescu, M.L., 2001. Thermo-rheological, shear heating model for leucogranite generation, metamorphism, and deformation during the Proterozoic Trans-Hudson orogeny, Black Hills, South Dakota. Tectonophysics 342, 371-388.

Naruk, S.J., 1986. Strain and displacement across the Pinaleño Mountains shear zone, Arizona, USA. Journal of Structural Geology 8, 35–46.

Nicol, A., Gillespie, P.A., Childs, C., Walsh, J.J., 2002. Relay zones between mesoscopic thrust faults in layered sedimentary sequences. Journal of Structural Geology 24, 709-727.

Ord, A., Hobbs, B.E., 1989. The strength of the continental crust, detachment zones and the development of plastic instabilities. Tectonophysics 158, 269–289.

Ordóñez Casado, B., Gebauer, D., Schafer, H.J., Ibarguchi, J.I., Peucat, J.J., 2001. A single Devonian subduction event for the HP/HT metamorphism of the Cabo Ortegal Complex within the Iberian massif. Tectonophysics 332, 359–385.

Passchier, C. W., 1990. Reconstruction of deformation and flow parameters from deformed vein sets. Tectonophysics 180, 185-199.

Passchier, C.W., 1997. The fabric attractor. Journal of Structural Geology 19, 113–127.

Passchier, C.W., 2011. Complex shear zones. In: Druguet, E., Carreras, J., Alsop, G.I., Bons, P.D., Czeck, D.M., Hudleston, P.J., Siddoway, C.S. (Eds.), Deformation Localization in Rocks: New Advances (Keynote). Penrose Conferences, Geological Society of America, Cadaques and Cap de Creus, Catalonia, Spain.

Passchier, C., Coelho, S., 2006. An outline of shear-sense analysis in high-grade rocks. Gondwana Research 10, 66-76.

Passchier, C.W., Trouw, R.A.J., 1996. Microtectonics. Springer-Verlag, Berlin, pp. 366.

Passchier, C.W., Trouw, R.A.J., 2005. Microtectonics, second edition. Springer-Verlag, Berlin, pp. 366.

Paterson, M.S., 2007. Localization in rate-dependent shearing deformation, with application to torsion testing. Tectonophysics 445, 273-280.

Peacock, D.C.P., Sanderson, D.J., 1992. Effects of layering and anisotropy on fault geometry. Journal of the Geological Society 149, 793-802.

Peacock, D.C.P., Knipe R.J., Sanderson, D.J., 2000. Glossary of normal faults. Journal of Structural Geology 22, 291-305.

Peucat, J.J., Bernard-Griffiths, J., Gil Ibarguchi, J.I., Dallmeyer, R.D., Menot, P., Cornichet, J. and Iglesias Ponce de León, M., 1990. Geochemical and geochronological cross-section of the deep Variscan crust: the Cabo Ortegal high-pressure nappe (Northwestern Spain). Tectonophysics 177, 263-292.

Pennacchioni, G., 2005. Control of the geometry of precursor brittle structures on the type of ductile shear zone in the Adamello tonalites,

Southern Alps (Italy). Journal of Structural Geology 27, 627-644.

Pennacchioni, G., Mancktelow, N.S., 2007. Nucleation and initial growth of a shear zone network within compositionally and structurally heterogeneous granitoids under amphibolite facies conditions. Journal of Structural Geology 29, 1757-1780.

Pini, G.A., 1999. Tectonosomes and olistostromes in the argille scagliose of the Northern Apennines, Italy. Geological Society of America Special Paper 335, pp. 70.

Platt, J.P., Vissers, R.L.M., 1980. Extensional structures in anisotropic rocks. Journal of Structural Geology 2, 397-410.

Poirier, J.P., 1980. Shear localization and shear instability in materials in the ductiles field. Journal of Structural Geology 2, 135-142.

Pollard, D.D., Aydin, A., 1984. Propagation linkage of Oceanic Ridge segments. Journal of Geophysical Research 89, 10017-10028.

Ponce, C., Carreras, J., Druguet, E., 2010. Development of "lozenges" in anastomosing shear zone networks in foliated rocks. Geogaceta 48, 207-210.

Ponce, C., Simancas, J.F., Azor, A., Martínez-Poyatos, D.J., Booth-Rea, G., Expósito, I., 2012. Metamorphism and kinematics of the early deformation in the Variscan suture of SW Iberia. Journal of Metamorphic Geology 30 (7), 625-638.

Ponce, C., Druguet, E., Carreras, J., 2013. Development of shear zone-related lozenges in foliated rocks. Journal of Structural Geology 50, 176-186.

Price, N.J., Cosgrove, J.W. 1990. Analysis of Geological Structures. Cambridge University Press, Cambridge, UK.

Priour, D. 1985. Genèse des zones de cisaillement. Application de la méthode des éléments finis à la simulation numerique de la deformation des roches. Mdm. Docums CAESS, Rennes, France 4, 1-157.

Ragan, D.M., 2009. Structural geology. An Introduction to Geometrical Techniques (4th Edition): Cambridge University Press. New York, 602 p.

Ramberg, H., 1981. Gravity, deformation and the earth's crust in theory, experiments and geological application (2nd Ed.): Academic Press, London .452 p.

Ramsay, J.G., 1980. Shear zone geometry: a review. Journal of Structural Geology 2, 83-99.

Ramsay, J.G., Allison, I., 1979. Structural analysis of shear zones in an Alpinised Hercynian granite, Maggia Nappen, Pennine Zone,Central Alps. Schweizerische Mineralogische und Petrographische Mitteilungen 59, 251-279.

Ramsay, J.G., Graham, R.H., 1970. Strain variation in shear belts. Canadian Journal of Earth Science 7, 786-813.

Ramsay, J.G., Huber, M.I., 1987. The Techniques of Modern Structural Geology, Vol. 1: Strain Analysis. Academic Press, London.

Ramsay, J. G. & Huber, M. I. 1987. The Techniques of Modern Structural Geology, Volume 2: Folds and Fractures. Academic Press, London.

Reston, T.J, 1989. Shear in the lower crust during extension: not so pure and simple. Tectonophysics 173, 175-183.

Rice, J.R., 1976. The localization of plastic deformation. In: Koiter, W.T. (Ed.), Theoretical and Applied Mechanics, Proceedings of the 14th International Congress on Theoretical and Applied Mechanics. North-Holland Publishing Company, Delft, The Netherlands, pp. 207–220.

Riedel, W., 1929. Zur Mechanik geologischer Brucherscheinungen. Zentralblatt für Mineralogie, Geologie und Paläontologie. B, 354-368.

Ries, A.C., Shackleton, R.M., 1971. Catazonal complexes of North-West Spain and North Portugal, remnants of a Hercynian Thrust Plate. Nature 234 (47), 65–79.

Robert, G., Andrews, G.D., Ye, J., Whittington, A.G., 2013. Rheological controls on the emplacement of extremely high-grade ignimbrites. Geology 41, 1031-1034.

Rosenberg, C.L., 2004. Shear zones and magma ascent: A model based on a review of the Tertiary magmatism in the Alps. Tectonics 23, TC3002.

Ross, J.V., Wilks, K.R., 1996. Microstructure development in an experimentally sheared orthopyroxene granulite. Tectonophysics 256, 83-100.

Rowe, P. W. 1962. The stress-dilitancy relation for static equilibrium of an assembly of particles

in contact. Proceedings, Royal Society of London, Ser. A, 269, pp. 500-527.

Santos Zalduegui, J.F., Schärer, U., Gil Ibarguchi, J.I., 1995. Isotope constraints on the age and origin of magmatism and metamorphism in the Malpica-Tuy allochthon, Galicia, NW-Spain. Chemical Geology 121, 91–103.

Scheuber, E., Andriessen, P.A., 1990. The kinematic and geodynamic significance of the Atacama fault zone, northern Chile. Journal of Structural Geology 12, 243-257.

Schöpfer, M.P.J., Zulauf, G., 2002. Strain dependent rheology and the memory of plasticine. Tectonophysics 354, 85–99.

Schrank, C.E., Handy, M.R., Fusseis, F., 2008. Multiscaling of shear zones and the evolution of the brittle-to-viscous transition in continental crust. Journal of Geophysical Research 113, B01407.

Schwarz, H.U., Kilfitt, F.W., 2008. Confluence and intersection of interacting conjugate faults: A new concept based on analogue experiments. Journal of Structural Geology 30, 1126-1137.

Segall, P., Simpson, C., 1986. Nucleation of ductile shear zones on dilatant fractures. Geology 14, 56-59.

Sengupta, A., Anbarasu, K., Gupta, S., 2008. Towards Understanding of Lanta Khola Landslide in Sikkim Himalayas

Segall, P., Simpson, C., 1986. Nucleation of ductile shear zones on dilatant fractures. Geology 14, 56-59.

Sibson, R.H., 1977. Fault rocks and fault mechanisms. Journal of the Geological Society, London 133, 191-213.

Simpson, C., 1983. Strain and shape-fabric variations associated with ductile shear zones. Journal Structural Geology 5, 61–72.

Simpson, C., 1985. Deformation of granitic rocks across the brittle-ductile transition. Journal of Structural Geology 7, 503-511.

Simpson, C., 1986. Fabric development in brittle-to-ductile shear zones. Pure and Applied Geophysics 124, 269-287.

Simpson, C., Carreras, J., Losantos, M., 1982. Inhomogeneous deformation in Roses granodiorite. Acta Geológica Hispánica 17, 219-226.

Simpson, C., Schmid, S.M., 1983. An evaluation of criteria to deduce the sense of movement in sheared rocks. Geological Society of America Bulletin 94, 1281-1288.

Sofuoglu, H., Rasty, J., 2000. Flow behavior of Plasticine used in physical modeling of metal forming processes. Tribology International 33, 523–529.

Swanson, M.T., 1990. Extensional duplexing in the York Cliffs strike-slip fault system, southern coastal Maine. Journal of Structural Geology 12, 499-512.

Swanson, M.T., 2005. Geometry and kinematics of adhesive wear in brittle strike-slip fault zones. Journal of Structural Geology 27, 871-887.

Swanson, M.T., 2006. Late Paleozoic strike-slip faults and related vein arrays of Cape Elizabeth, Maine. Journal of Structural Geology 28, 456-473.

Tchalenko, J.S., 1970. Similarities between shear zones of different magnitudes. Geological Society of America Bulletin 81, 1625-1640.

ten Grotenhuis, S.M., Trouw, R.A.J., Passchier, C.W., 2003. Evolution of mica fish in mylonitic rocks. Tectonophysics 372, 1-21.

Tentler, T., Amcoff, O., 2010. Interaction of microfractures: The mechanism of network building. Tectonophysics 485, 215-230.

Tilke, P. G., 1986. Caledonian structure, metamorphism, geochronology, and tectonics of the Sitas-Singis area, Sweden. Ph.D. thesis, Massachusetts Institute of Technology.

Tourigny, G., Tremblay, A., 1997. Origin and incremental evolution of brittle/ductile shear zones in granitic rocks: natural examples from the southern Abitibi Belt, Canada. Journal of Structural Geology 19, 15-27.

Treagus, S.H., 1988. Strain refraction in layered systems. Journal of Structural Geology 10, 517-27.

Treagus, S.H., Lan, L., 2000. Pure shear deformation of square objects, and applications to geological strain analysis. Journal of Structural Geology 22, 105-122.

Treagus, S.H., Sokoutis, D., 1992. Laboratory mod-

elling of strain variation across rheological boundaries. Journal of Structural Geology 14, 405-424.

Tremblay, A., Malo, M., 1991. Significance of brittle and plastic fabrics within the Massawippi Lake fault zone, southern Canadian Appalachians. Journal of Structural Geology 13, 1013–1023.

Trepmann, C.A., Stöckert, B., 2003. Quartz microstructures developed during non-steady state plastic flow at rapidly decaying stress and strain rate. Journal of Structural Geology 25, 2035–2051.

Truesdell, C., 1954. The Kinematics of Vorticity. Indiana University Press, Bloomington, Indiana.

Tullis, J., 1990. Experiment studies of deformation mechanisms and microstructures in quartzofeldspathic rocks. In: Barber, D.J., Meredith, P.G. (Eds.), Deformation Processes in Minerals, Ceramics and Rocks, Unwin Hyman, London, UK, 190–227.

Tullis, J., Snoke, A.W., Todd, V.R., 1982. Significance and petrogenesis of mylonitic rocks. Geology 10, 227-230.

Van Calsteren, P.W.C., Boelrijk, N.A.I.M., Hebeda, E.H., Priem, H.N.A., Den Tex, E., Verdurmen, E.A.T.H. and Verschure, R.H., 1979. Isotopic dating of older elements (including the Cabo Ortega1 mafic-ultramafic complex) in the Hercynian Orogen of NW Spain: manifestations of a presumed Early Paleozoic Mantle plume. Chemical Geology, 24: 35-56.

Van der Wal, D., Vissers, R.L.M., 1996. Structural petrology of the Ronda peridotite, SW Spain: deformation history. Journal of Petrology 37, 23–43.

Vitale, S., Mazzoli, S., 2010. Strain analysis of heterogeneous ductile shear zonesbased on planar markers. Journal of Structural Geology 32, 321–329.

Vogel, D.E., 1967. Petrology of an eclogite-and pyrigarnite-bearing polymetamorphic rock Complex at Cabo Ortega], NW Spain. Leidse Geologische Mededelingen, 40: 121-213.

Vogel, D.E., 1984. Cabo Ortegal, mantle plumeo r double klippe? In: Zwart, H.J., Hartman, P., Tobi, A.C. (Eds.), Ophiolites and ultramafic Rocks: a tribute to Emile den Tex. Geologisch Mijnbouwkundig Genootschap 63, 131-140.

Vollbrecht, A., Pawlowski, J., Leiss, B., Heinrichs, T., Seidel, M., Kronz, A., 2006. Ductile deformation of garnet in mylonitic gneisses from the Münchberg Massif (Germany). Tectonophysics 427, 153-170.

Wawersik, W.R., Brace, W.F., 1971. Post-failure behavior of a granite and diabase. Rock Mechanics 3, 61–85.

Walsh, J.J., Watterson, J., Bailey, W.R., Childs, C., 1999. Fault relays, bends and branch-lines. Journal of Structural Geology 21, 1019-1026.

Weijermars, R., 1987. The Palomares brittle–ductile Shear Zone of southern Spain. Journal of Structural Geology 9, 139–157.

Weijermars, R., 1992. Progressive deformation in anisotropic rocks. Journal of Structural Geology 14, 723-742.

Weinberg, R.F., Sial, A.N., Mariano, G., 2004. Close spatial relationship between plutons and shear zones. Geology 32, 377-380.

White, S., Burrows, S.E., Carreras, J., Shaw, N., Humphreys, J., 1980. On mylonites in ductile shear zones. Journal of Structural Geology 2, 175-187.

Williams, G., Dixon, J., 1982. Reaction and geometrical softening in granitoid mylonites. Texture, Stress and Microstructure 4, 223-239.

Williams, P.F., Price, G.P., 1990. Origin of kinkbands and shear-band cleavage in shear zones: an experimental study. Journal of Structural Geology 12, 145-164.

Woodcock, N.H., Fischer, M., 1986. Strike-slip duplexes. Journal of Structural Geology, 8, 725-735.

Zheng, Y., Zhang, J., Wang, T., 2011. Puzzles and the maximum-effective-moment (MEM) criterion in structural geology. Journal of Structural Geology 33, 1394-1405.